Dottorato di Ricerca in

"***Ambiente, Salute e Processi Ecosostenibili***"

Ciclo XXIV

Modeling Engineering Department
University of Calabria
In collaboration with
Institute on Membrane Technology of
National Research Council

Experimental & Simulation Analysis of Reforming Reactions of Bio-Fuels in Both Membrane and Fixed Bed Reactors for Hydrogen Production

Settore Scientifico-Disciplinare ING-IND/24

Ing Simona LIGUORI

Supervisori:

Prof. Vincenza Calabrò

Dr. Ing. Angelo BASILE

Coordinatore:

Prof. Bruno de Cindio

A.A. 2010-2011

Dottorato di Ricerca in

"*Ambiente, Salute e Processi Ecosostenibili*"

Ciclo XXIV

Modeling Engineering Department
University of Calabria
In collaboration with
Institute on Membrane Technology of
National Research Council

Experimental & Simulation Analysis of Reforming Reactions of Bio-Fuels in Both Membrane and Fixed Bed Reactors for Hydrogen Production

Settore Scientifico Disciplinare ING-IND/24

Ing Simona LIGUORI

Supervisori:

Prof. Vincenza Calabrò

Dr. Ing. Angelo BASILE

Coordinatore:

Prof. Bruno de Cindio

A.A. 2010-2011

A Vincenzo

&

Alla mia famiglia

Index

Introduction

The aim of the present thesis is to show the Pd-based membrane reactor (MR) potentialities for producing a pure or, at least, highly pure hydrogen stream by reforming reactions of bio-fuels.

In particular, the thesis consists of three key issues joined each other: (I) hydrogen production, (II) Pd-based MR and (III) bio-fuels reforming reactions. In detail, (I) the thesis starts with a discussion on the hydrogen production pointing out its importance as an energy carrier; (II) afterwards, the use of Pd-based MRs are introduced as alternative devices for producing hydrogen and their benefits are demonstrated by carrying out the reforming reactions as steam reforming of methane, glycerol and ethanol and steam oxidative reforming of ethanol and, (III) at the same time, the use of bio-fuels for these kind of reactions is dealt as a valid and alternative choice to fossil fuels.

In the following, an overview of what aforementioned is briefly illustrated.

Nowadays, the hydrogen is recognized as one of the most promising energy carriers and is gaining an important role in future energy systems such as Proton Exchange Membrane Fuel Cells (PEMFCs). It is well known that PEMFCs are fuelled by highly pure hydrogen. Indeed, the feed should not contain CH_4 (as it is a potential energy loss), CO (as it poisons the anode of the PEMFC), CO_2 (as it is a greenhouse gas) and N_2 (as it will reduce the efficiency of the PEMFC).
Currently, most of hydrogen production occurs by stem reforming reaction, although there are three types of processes:

- ✓ Steam Reforming;
- ✓ Partial Oxidation;
- ✓ Autothermal Reforming;

The advantage of partial oxidation and autothermal reforming is that these processes are self-sustaining and external provision of heat is not required. The main drawback: they are less efficient in hydrogen production with respect the steam reforming reaction.

In industrial applications, the most economical way for producing hydrogen is by methane steam reforming. The reaction is a catalytic process that typically takes place at high pressure and temperature around 15 atm and 800 °C, respectively.

The catalysts for hydrocarbons steam reforming reaction are mainly based on metals belong to group 8-10 with nickel as preferred metal owing to its activity, availability and low cost [Matar *et al* (2001)]. Indeed, although noble metals (Ru, Rh, Pt) are more effective than Ni and less subjected to coke formation, such catalysts are not usually used owing to their high cost [Garcia *et al* (2000)].

The pathway of hydrocarbons steam reforming reaction are very similar each other. Indeed, the steam reforming consists generally of two steps, in the first one the hydrocarbons reformation takes place, in the second step, known as water gas shift (WGS) reaction, the CO amount contained in the reformate stream is reduced. Nevertheless, keeping in mind to supply a PEMFCs, the residual CO, contained in the stream coming from the WGS reactor, has to be further reduced to ppm level by Pressure Swing Adsorption (PSA), cryogenic distillation or membrane separation techniques [Adhikari *et al* (2006)].

The main benefit of this process is that this is a mature technology, energetically efficient at large scale and it uses existing fuel infrastructures. The drawbacks are different such as the plant complexity, high size and high cost for hydrogen separation, as well as the pollution generated during this process.

For these reasons, the development of alternative technologies is necessary and the MRs seem to represent an alternative and valid solution to conventional reactors owing to their ability to combine distinct task as reaction and hydrogen separation in only one tool. So, over the years now, MRs have been widely studied and, in particular, a great scientific interest has been given to dense Pd-based MR owing to their full hydrogen perm-selectivity to permeation of this kind of membrane.

In particular, using a Pd-based MR in which the hydrogen is selectively removed from reaction zone, it is possible to achieve simultaneously two objectives:

- to maximize the MR performances in terms of hydrocarbon conversion, products selectivities and hydrogen yield;
- to produce high purity hydrogen (< 10 ppm CO) that can be directly supplied in PEMFCs.

As aforementioned, the most of hydrogen production comes from the fossil fuel steam reforming process. Nevertheless, owing to the depletion of fossil fuels, environmental concerns and stringent norms on emission, a growing attention is given to the use of renewable sources.

In theory, any hydrocarbon or alcohol, as ethanol, methanol, glycerol, etc. could be used as a feedstock for reforming process. Ethanol is the most important example of feedstock coming from renewable source, which could be used in steam reforming process. In particular, ethanol is produced from several biomass sources, including energy plants, waste materials form agro industries or forestry residue materials, organic fraction of solid waste and so on [Giunta *et al* (2007), Marino *et al* (1998), *et al* Marino (2001)]. Moreover, compared to methanol, ethanol is easier and safer to store and transport due to its low toxicity and volatility.

In addition, bio-ethanol, which is an aqueous solution containing between 8 and 12 wt% ethanol [Pfeffer *et al* (2007), Song *et al* (2007), Ni *et al* (2007)], can be directly supplied to a MR for carrying out steam reforming reaction, avoiding the expensive distillation operation required for producing pure ethanol [Vaidya *et al* (2006)].

Anyhow, also glycerol is available in large quantities and it could be used as feedstock for carrying out reforming reaction in MR. Indeed, glycerol is one of the by-products of transesterification of fatty acids for the production of biodiesel. Therefore, glycerol steam reforming could be considered as an interesting alternative for producing hydrogen and, in the meanwhile, to promote economically the transesterification process [Burnay *et al* (2005), Fernando *et al* (2007)].

Nevertheless, a complete transition from an economy based on fossil fuels to hydrogen economy, will require, at least, a few decades to be realized. In this interim period, alternative technologies can be developed and studied for minimizing emissions and optimizing the process performances.
Therefore, in this thesis, the study on the Pd-based MR performances, in terms of conversion, hydrogen recovery, yield and permeate purity, is done using two different types of Pd-based membranes, an unsupported Pd-Ag and a supported Pd/PSS ones, by varying the operative conditions, as catalyst, temperature, pressure, feed molar ratio and space velocity and utilizing different bio-fuels as feedstocks.
Moreover, a simulation analysis, carried out only for the methane steam reforming reaction, is used to predict the MR performances.

The structure of the thesis follows the so called "papers model dissertation" [Dunleavy (2003)], mainly consisting of an well-organized and articulated collection of papers written (no necessarily published) during the PhD course. In this context, the thesis is divided in four *Parts*:

i) *an overview on hydrogen economy and MR state-of-the-art*: literature information was collected in order to gain an appropriate knowledge and, based on it, the research program was organized;
ii) *methane steam reforming reaction in MR*: considered the starting point for the progressive understanding of reforming of complex hydrocarbons;
iii) *biofuels as bio-ethanol and bio-glycerol reforming reactions in MRs*: the core of this thesis, in which Pd-based MRs performances were studied carrying out steam reforming, oxidative steam reforming and partial oxidation reactions of ethanol, steam reforming reaction of bio-ethanol and glycerol and the influence of different operative conditions on the MR system were analyzed.

iv) *water gas shift reaction*: it takes places in many reforming reactions. Thus, the influence of some operative conditions on WGS reaction performed in a Pd-based MR was studied.

Each *Part* is usually constituted by an Introduction, some Chapters and final Conclusion; each Chapter is usually characterized by one or more papers, connected to each other by an Interconnection.

All the references cited in the text are reported at the end of each Part, except for those cited in the articles, which are reported at the end of each article.

All the experimental campaigns of this thesis were carried out at ITM-CNR laboratory and for three months at the Oulu University in Finland.

References

Adhikari S, Fernando S, "Hydrogen membrane separation techniques", *Ind Eng Chem Res*, 45 (2006) 875-881

Burnay L, Casanave D, Delfort B, Hillion G, Chordorge JA, "New heterogeneous process for biodiesel production: a way to improve the quality and the value of the crude glycerin produced by biodiesel plants", *Catal Today*, 106 (2005) 190-192

Dunleavy P, "Authoring a PhD. How to Plan, Draft, Write and Finish a Doctoral Thesis or Dissertation", New York: Palgrave Macmillan; 2003, ISBN 1-4039-0584-3

Fernando S, Adhikari S, Kota K, Bandi R, "Glycerol based auto motive fuels from future biorefineries", *Fuel*, 86 (2007) 2806-2809

Garcia L, French R, Czernik S, Chornet E, "Catalytic steam reforming of bio-oils for the production of hydrogen: effects of catalyst composition", *Appl Catal A : Gen*, 201 (2000) 225-239

Giunta P, Mosquerra C, Amadeo N, Laborde M, "Simulation of a hydrogen production and purification system for a PEM fuel –cell using bioethanol as raw material", *J Power Sou*, 164 (2007) 336-343

Marino F, Boveri M, Baronetti G, Laborde M, "Hydrogen production from steam reforming of bioethanol using Cu/Ni/K/γ-Al_2O_3 catalysts. Effect of Ni", *Int J Hydrogen En*, 26 (2001) 665-668

Marino F, Cerrella EG, Duhalde S, Jobbagy M, Laborde M, "Hydrogen from steam reforming of ethanol. Characterization and performance of copper-nickel supported catalysts", *Int J Hydrogen En*, 23 (1998) 1095-1101

Matar S, LF Hatch, "Chemistry of petrochemical processes" (2^{nd} ed.), USA: Gulf Professional Publishing, (2001), ISBN 0-88415-315-0

Ni M, Leung DYC, Leung MKH, "A review on reforming bioethanol for hydrogen production" *Int J Hydrogen En*, 32 (2007) 3238-3247

Pfeffer M, Wukovits W, Beckmann G, Friedl A, "Analysis and decrease of the energy demand of bioethanol-production by process integration", *Appl Therm Eng*, 27 (2007) 2657-2664

Song H, Zhang L, Watson RB, Braden D, Ozkan US, "Investigation of bio-ethanol steam reforming over cobalt based catalysts", *Catal Today*, 129 (2007) 346-354

Vaidya PD, Rodrigues AE, "Insight into steam reforming of ethanol to produce hydrogen for fuell cells" *Chem Eng J*, 117 (2006) 39-49

Part I

Hydrogen

&

Membrane Reactor

Introduction to *Part I*

The purpose of Part I is to show the benefits of Pd-based MRs for hydrogen production and their possible applications at industrial level. Before treating research aspects of this alternative device, two questions have to be firstly answered:

Why do we need a "hydrogen economy"?

Why is the worldwide attention focused on renewable sources and on the development of alternative technologies for hydrogen production?

The answers to these two questions are strictly related each other. Indeed, the dependence on fossil fuels as the main energy sources has led to serious energy crisis and environmental problems, i.e. fossil fuel depletion and pollutant emission [Ni *et al* (2006)]. In response to these two problems, continuous efforts have been made in exploration of clean, renewable alternatives for a sustainable development. In this contest, the hydrogen, produced by exploiting renewable resources, is recognized as one of the most promising energy carrier for the future.

It is essential to remember that hydrogen is not available on earth in elementary form. It is not a source of energy, but it has to be produced using other sources. So, in Figure 1.1, an overview of some feedstocks and process technologies is illustrated.

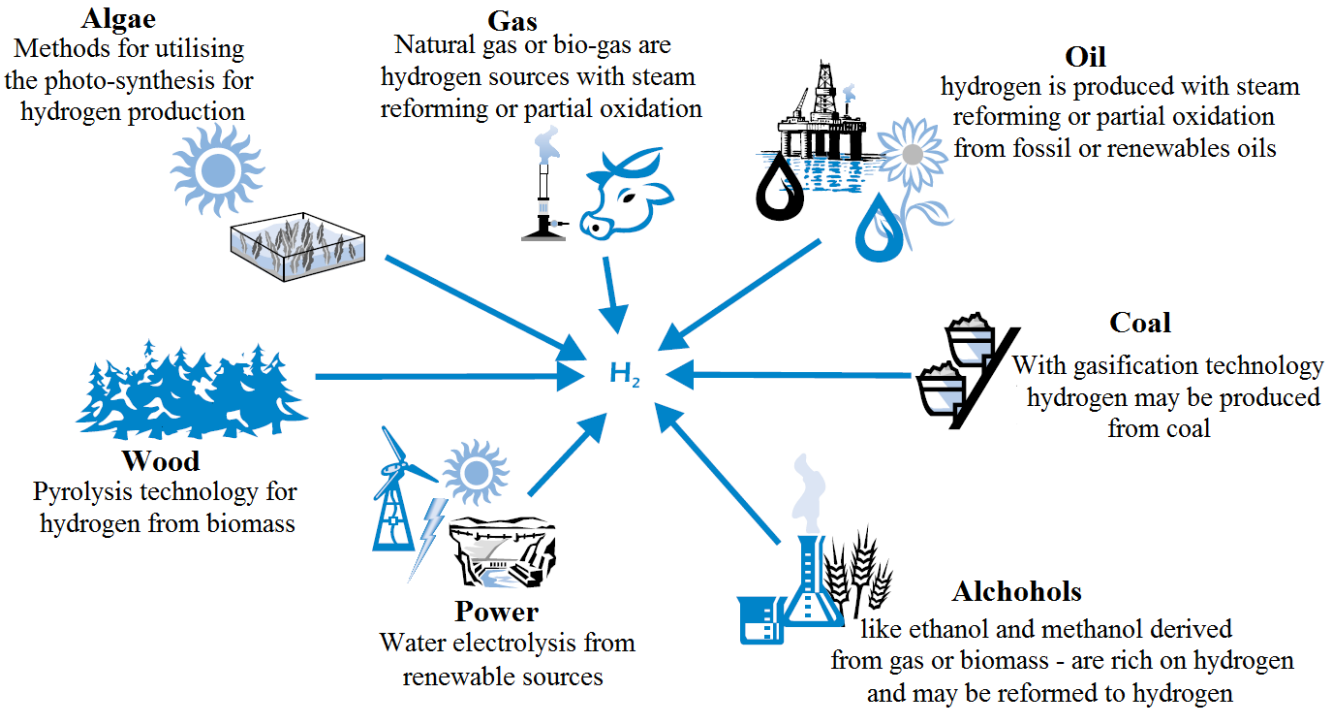

Figure 1.1. Several feedstocks and process technologies for hydrogen production

Nowadays, hydrogen is produced mainly from fossil fuels, accounting for 96% of the total volume (48% from natural gas, 30% from refinery/chemical off-gases, 18% from coal) [IEA (2005)]. The remaining 4% is obtained mainly from electrolysis. Based on its actual production, hydrogen is currently neither a solution for a shift from fossil fuels, nor it is possible to proclaim the hydrogen economy as a climate saver. Nevertheless, there is ongoing research for alternative methods and devices to produce hydrogen. In this contest, alcohols reforming reactions can cover an important role. Indeed, alcohols such as ethanol, but also glycerol, are largely available from renewable sources and they could be used as feedstocks for hydrogen generation. In particular, reforming reactions of alcohols are similar to hydrocarbons ones. As a consequence, the "bio-alcohols" can be considered as an alternative solution to fossil fuels and, furthermore, they could be exploited for hydrogen production.

In this way, the hydrogen could be used for supplying fuel cells, as the Proton Exchange Membrane Fuel Cells (PEMFCs). This latter can be considered as top candidates as an alternative technology to

the conventional processes owing to their zero pollution emissions and low operative temperature. Nevertheless, they are supplied by pure hydrogen owing to the low tolerance of the anodic Pt catalyst to CO (<10 ppm).

Therefore, hydrogen contained in the reformed stream needs to be purified by means of further processes like water gas shift (WGS) reaction, PSA and/or Pd membrane separation, etc.

As an alternative solution to the conventional systems, MR technology seems to represent a valid choice owing to its ability to combine distinct task as reaction and separation in only one tool [Mulder (1996)]. Currently, a great scientific interest is given to the dense Pd-based membranes owing to their full selectivity to hydrogen permeation [Lu *et al* (2007)].

Therefore, using a Pd-based MR, in which the hydrogen is selectively removed from reaction zone, it is possible to realize at the same time: better MR performances in terms of conversion, products yield and selectivities and to collect a highly pure hydrogen stream.

For a better understanding, a schematic representation of the Pd-based MR configuration is reported hereafter (Figure 1.2). As shown, the MR can consist of a tubular stainless steel module containing a tubular pin-hole free Pd–based membrane. In the case of Figure 1.2, it is joined to two stainless steel tube ends for the membrane housing, where one of them is closed. The graphite gasket is used to provide a gas-tight seal between lumen and shell sides. The catalyst is packed into lumen of the MR with glass spheres to avoid catalyst dispersion.

This typical tube-in-tube MR configuration was adopted in all experimental campaigns of this thesis.

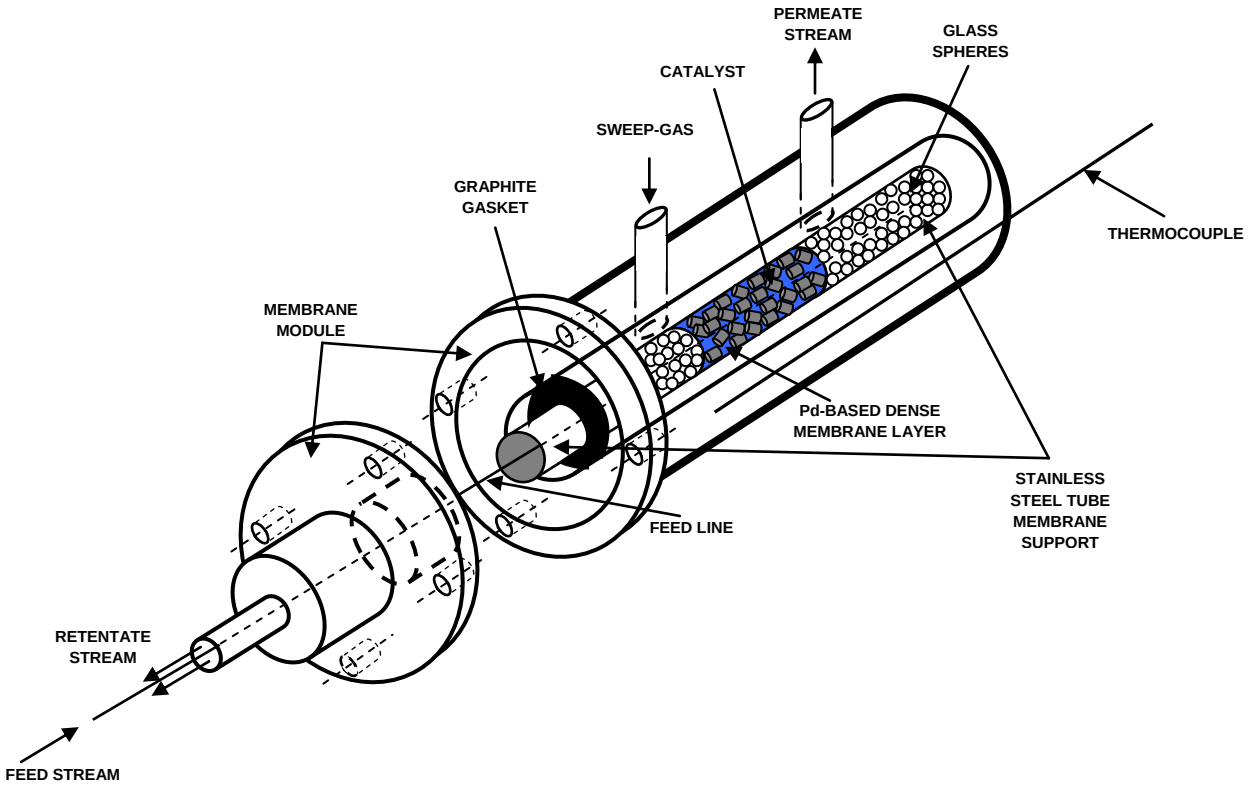

Figure 1.2. Scheme of the Pd-based membrane reactor

In the following, two papers, related to the two chapters of this part and prepared during the PhD course, will clarify each aforementioned aspects, highlighting the benefits in the use of MR compared to conventional reactors and the importance of hydrogen as future energetic carrier exploiting renewable sources.

The papers will follow this structure:

Paper 1: *Iulianelli A, **Liguori S**, Longo T, Basile A, Inorganic membrane and membrane reactor technologies for hydrogen production, Ch. 12 in "Hydrogen Production: Prospects and Processes", ed D.R. Honnery and P. Moriarty, Nova Sci. Pub., in press (2011).*

*Paper 2: Basile A, Iulianelli A, Longo T, **Liguori S**, De Falco M, Pd-based Selective Membrane State-of-the-Art, Ch. 2 pp. 21-55 in "Membrane Reactors for Hydrogen Production Processes", L. Marrelli, M. De Falco & G. Iaquaniello Editors, Springer London Dordrecht Heidelberg New York, 2011, ISBN 978-0-85729-150-9, DOI 10.1007/978-0-85729-151-6.*

Chapter 1

Overview on hydrogen economy

Introduction to paper 1

At the beginning of the work, the first need was to find basic information on the subject under study. This task was accomplished by means of a bibliographic research among international scientific journals. The result was that, for more than 30 years, the research has been worked to develop and demonstrate the potentialities of several alternative technologies for hydrogen production with the aim of accelerating widespread hydrogen use as a clean energy carrier.

As the papers 1 shows hereafter, hydrogen can be produced from a variety of feedstocks. These include fossil resources, such as natural gas and coal as well as renewable resources, such as biomass and renewable energy sources (e.g. sunlight, wind, wave or hydro-power). Each technology is clearly in a different stage of development and offers unique opportunities, benefits and challenges.

Concerning the alternative device as Pd-based MRs, most of the progress has happened in the last twenty years mainly owing to the development of new membrane materials. This significant progress is reflected in an increasing number of scientific publications, which has grown exponentially over the last few years.

Therefore, the purpose of this paper 1 is to present an overview on hydrogen production, pointing out the necessity to shift from fossil fuel to renewable sources and to show the benefits in the use of MR technology for producing hydrogen.

Paper 1, as in the form presented hereafter, has been accepted for publication on *Nova Sci. Pub*.

Inorganic membrane and membrane reactor technologies for hydrogen production

Adolfo Iulianelli*, Simona Liguori, Tiziana Longo, Angelo Basile

Institute on Membrane Technology of the National Research Council (ITM – CNR), Via P. Bucci c/o University of Calabria Cubo 17/C – 87030 - Rende (CS), Italy

ABSTRACT

Catalytic inorganic membrane reactor technology may be considered an opportunity as an application within petroleum refineries. Industrially, when the hydrogen content of the refinery gas overcomes 50% by volume, the hydrogen could be recovered exploiting inorganic membrane technology. Furthermore, inorganic membranes could be used for enhancing the hydrogen production in processes such as steam reforming, water gas shift reaction or the conversion of natural gas to syngas and/or exploiting the potentiality of biomass in the contest of environmental problems.

In the last decades, inorganic hydrogen selective membranes have gained a great attention in the field of the hydrogen economy development. In detail, dense self-supported palladium and palladium-based membranes are fully hydrogen perm-selective. When supplying a syngas stream to a dense palladium-based membrane reactor, combining both the hydrogen separation and the syngas conversion, for example via water gas shift reaction, only hydrogen can permeate through the membrane, which is collected as a high purity hydrogen stream to be used for further applications. Otherwise, supported inorganic palladium-based membranes are not fully hydrogen perm-selective, but they show a much higher resistance to mechanical stress and high temperature than the-self supported membranes and are more economical because constituted by a thin palladium/palladium-alloy layer deposited onto a porous support.

A further advantage makes competitive inorganic palladium-based membranes and membrane reactors not only for separating hydrogen but also for providing a stream rich in CO_2. In fact, when hydrogen is

selectively separated from the other gases, in the meanwhile the stream not permeated through the membrane is more concentrated in CO_2.

To resume, the main aim of this chapter is to give an extensive overview of the main reforming processes for producing hydrogen by using inorganic membranes. In particular, the description of the benefits and the principal drawbacks of inorganic membrane and membrane reactor technologies as well as the future trends in their application at industrial scale for producing hydrogen will be extensively proposed.

(*) Corresponding author: – Phone: +39 0984 492011, Fax: +39 0984 402103, e-mail: a.iulianelli@itm.cnr.it

Keyword: hydrogen production, renewable sources, inorganic membrane, palladium-based membrane reactors

1. INTRODUCTION: FROM OIL DEPLETION TO "HYDROGEN ECONOMY"

In the 21st century, over-population (the world population stands at 6.8 billion in 2009 [DESA, 2009] with respect to 5.2 billion in 1990 [CENSUS, 2010]) and over-consumption of energy (the predicted world-wide energy consumption is around 510 quadrillion BTU in 2010 with respect to 283 quadrillion BTU in 1980 [Anonimus 1, 2010; EIA, 2004]) represent two important problems to be solved. In particular, during the recent period of global industrialization, the level of population has been closely related to the amount of energy used. In the last four decades, the energy consumption per capita has averaged about 1.5 tonnes of oil equivalent (toe) per year [WRI, 2010]. Thus, this has adversely impacted the consumption of worldwide energy to develop several mathematical models for predicting the point of global peak of oil production and ensuing decline [Campbell, 1997; Laherrere, 1999], as shown, for example, in Figure 1.

Generally speaking, this kind of mathematical models are based on the following laws for describing the depletion of any finite resource such as oil:

- production starts at zero;
- production, then, rises to a peak, difficult to be overcome;
- once the peak is overcome, production declines until the resource depletion.

This scenario was firstly described in the 1950s by M.K. Hubbert and applied to any relevant system, including the depletion of the world's petroleum resources [Bardi, 2009; Mohr and Evans, 2008; Cavallo, 2004].

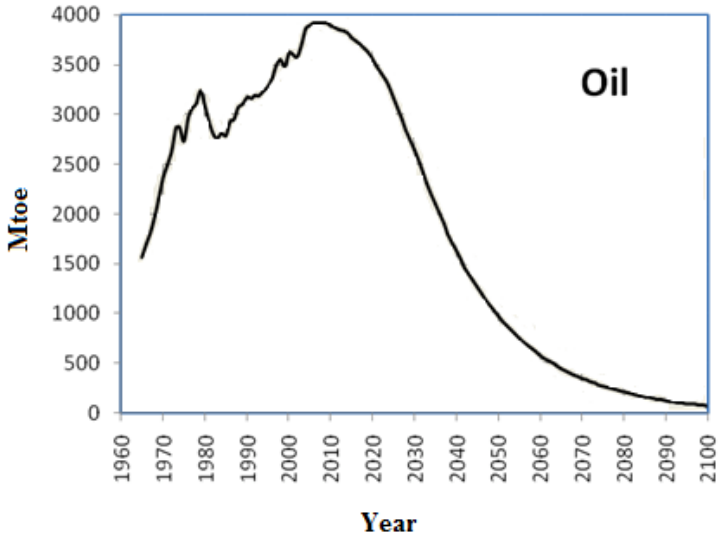

Figure 1. Global oil production, 1965 to 2100.

It is important to note that the point of maximum production, known as the "Hubbert peak", tends to coincide with the midpoint of depletion of the resource under consideration. In the case of oil, when the Hubbert peak will be reached, almost half of all the estimated recoverable oil on the planet will be consumed. This peak was also valued for other fossil fuels, such as natural gas and coal, as illustrated in Figure 2.

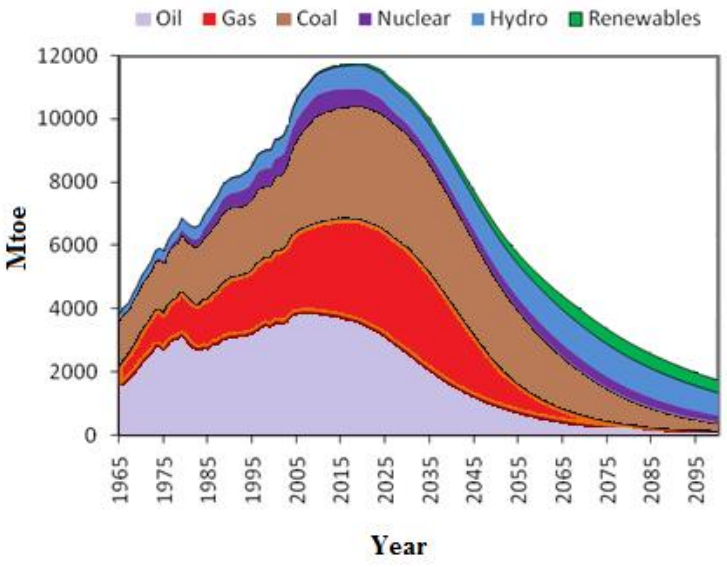

Figure 2: Total Energy Use, 1965 to 2100.

Nowadays, although fossil fuels are the most important contributors of energy, they are in rapid decline by the second half of the century, Figure 3. This figure shows a peak at about 2020, with a steepening decline out to 2100. The main reason for the decline is the loss of oil, gas and coal [BP, 2008]. Moreover, 90% of the oil produced today comes from feedstocks more than 30 years old [Campbell, 1998] and, despite exceptional advances in petroleum geology and the technologies employed in searching for petroleum deposits, discovery rates of new oil reserves are falling [Anonimus 2, 2010].

The mathematical models suggest a two-stages oil crisis:

1. **Increased Oil Prices:** The first crisis is predicted to occur in the near future, when the worldwide oil production share reaches 30% [Balat and Balat, 2009].
2. **Permanent Production Decline**: The second crisis is predicted occurring around 2015, when physical shortages begin to appear, Figure 3.

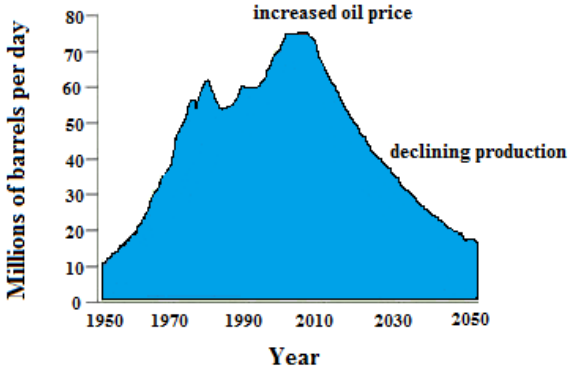

Figure 3. Projected worldwide oil production.

Furthermore, the exploitation of derived fossil fuels impacts a lot on the global environment owing to the greenhouse gas emissions. Therefore, in the last decades, different forms of renewable energies have been considered, which have lower carbon emissions than to conventional energy sources and are environmentally friend. In the following, a short list of renewable energies are summarized:

Solar: this form of energy relies on the nuclear fusion power from the core of the Sun. This energy can be collected and converted in a few different ways.

Wind Power: wind energy can be used to pump water or generate electricity, but requires extensive areal coverage to produce significant amounts of energy.

Geothermal power: in certain areas, the geothermal gradient is high enough to be exploited to generate electricity. Nevertheless, this possibility is limited to a few geographical locations and many technical problems exist, limiting its utility. Nevertheless, this form of energy cannot be used to produce electricity.

Hydroelectric energy: this form uses the gravitational potential of elevated water that is lifted from the oceans by sunlight. It is not strictly renewable since all reservoirs eventually fill up and require very expensive excavation to become useful again.

Biomass: it is a biological material from living or living organisms, such as wood, waste and alcohol fuels. The most conventional way to use the biomass relies on direct incineration of forest residues (such as dead trees, branches and tree stumps), yard clippings, wood chips and garbage. However, biomass also includes plant or animal matter used for production of fibers or chemicals. Biomass may also include biodegradable wastes that can be burned as fuel. However, around 1970s, the so called "hydrogen economy" took place with the intent to describe an energy infrastructure based on hydrogen produced from non-fossil energy sources. There is a non universally accepted definition of the "hydrogen economy", but it is generally viewed as the replacement of the vast majority of petroleum fuels used by transportation vehicles, with hydrogen burned in internal-combustion and external-combustion engines or, preferably, used in fuel cells to more efficiently generate power for transportation [14]. Hydrogen is a versatile molecule and can be used as a fuel for direct combustion or for producing electricity in fuel cells for stationary use (e.g. power plants, buildings and industry) [Cho, 2004]. This last aspect is important, mainly, for the economy of countries highly dependent on

imported petroleum products. In fact, as shown in Figure 4, the known reserves of fossil sources are geographically not equally distributed but concentrated in a few areas of the world [BP, 2010].

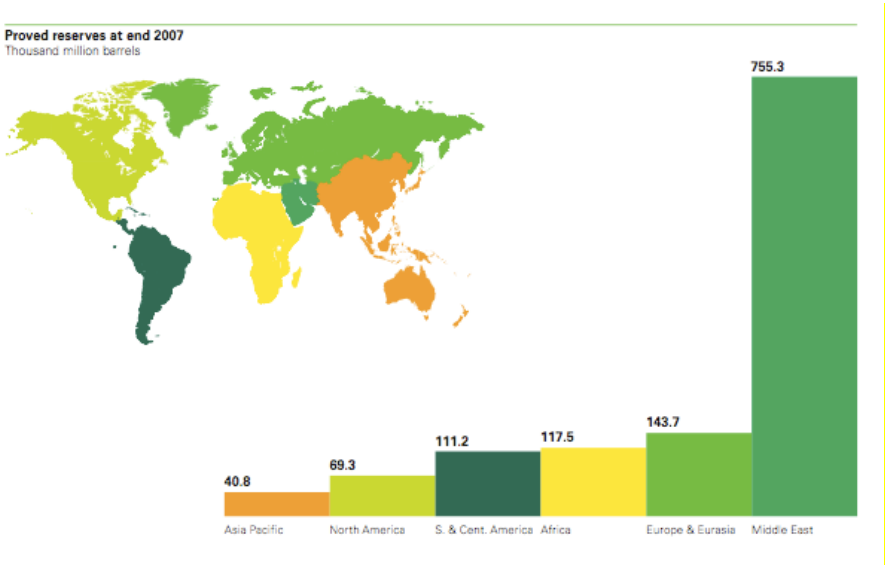

Figure 4. World distribution of known energy reserves. Source: BP Statistical Review of World Energy.

One of the most important aspects for promoting hydrogen as an energy carrier is its outstanding properties for environmental protection. The worldwide environmental pollution is mainly caused by the automotive industry and, in particular, by the combustion engines fuelled by derived fossil fuels. For this reason, in the last years, the "hydrogen economy" has taken place to solve the problematic concerning the climate change and air pollution owing to the emissions caused by the use of fossil fuels [Goltsov and Veziroglu, 2001]. The use of hydrogen for supplying fuel cells (PEMFC) completely eliminates all polluting emissions. The single byproduct resulting from the generation of electricity from hydrogen and air is demineralized water.

1.1 CONVENTIONAL PRODUCTION METHODS OF HYDROGEN

Currently, hydrogen is manufactured at industrial scale by steam reforming of natural gas, partial oxidation of heavy oil and coal gasification. In fact, as shown in Table 1, approximately 96% of the

worldwide hydrogen produced comes from fossil fuels conversion and only 4% is produced through water electrolysis. Nevertheless, owing to the global pollution caused by the greenhouse effect [Mohan et al., 2008], these industrial methods are considered to be not environmental friendly.

Source	**Share [%]**	**$m^3 \cdot 10^9/yr$**
Natural gas	48	240
Oil	30	150
Coal	18	90
Electrolysis	4	20

Table 1. Annual global hydrogen production share by source.

Therefore, renewable energy sources and alternative technologies to the conventional systems for hydrogen production will be necessary during coming decades. For example, hydrogen can be produced renewably from biomass. Two types of biomass feedstock are available to be converted into hydrogen: dedicated bio-energy crops, less expensive residues, such as organic waste from regular agricultural farming and wood processing (biomass residues).

Biomass in the form of organic waste offers an economical, environmental friendly way for renewable hydrogen production [Ni et al., 2006]. The production of hydrogen from biomass has several advantages compared to that from fossil fuels:

- use of biomass reduces CO_2 emissions,
- crop residues conversion increases the value of agricultural output,
- replacing fossil fuels with sustainable biomass fuel,
- costs of getting rid of municipal solid wastes.

However, conventionally hydrogen is produced almost exclusively via steam reforming of natural gas or partial oxidation of hydrocarbon fuels [Roh et al., 2010; Jaber et al., 2010; Ma et al., 2010].

Steam reforming of methane is currently the most used method and is responsible for more than 90% of worldwide hydrogen production [CENSUS, 2010]. It is an endothermic reaction as reported below:

$CH_4 + H_2O \Rightarrow CO + 3H_2$ $\Delta H^0_{298K} = +206$ kJ/mol (1)

It is usually coupled with the water gas shift (WGS) reaction:

$CO + H_2O \Rightarrow CO_2 + H_2$ $\Delta H^0_{298K} = -41$ kJ/mol (2)

Then, the overall reaction is :

$CH_4 + 2H_2O \Rightarrow CO_2 + 4H_2$ $\Delta H^0_{298K} = +165$ kJ/mol (3)

In the ***partial oxidation*** process, natural gas (or other liquid/gaseous hydrocarbons) and oxygen are injected into a high-pressure reactor. The oxygen to carbon ratio is optimally set for maximizing the yield of CO and hydrogen, and avoiding the formation of soot. Further steps and equipment remove the large amount of heat generated by the oxidation reaction, shift the CO with water to CO_2 and hydrogen, remove the CO_2 - which can be then captured - and purify the hydrogen produced. The partial oxidation of methane is reported in the following:

$CH_4 + ½\ O_2 \Rightarrow CO + 2H_2$ $\Delta H^0_{298K} = -36$ kJ/mol (4)

Partial oxidation is, however, typically less energy efficient than steam reforming.

Conventionally, in the ***auto-thermal reforming*** of natural gas or liquid hydrocarbons, steam and oxygen are reacted in a single vessel with a combustion zone and a reforming zone. The heat from the exothermic partial oxidation reaction balances that for the endothermic steam reforming reaction. Hydrogen can also be produced by the ***coal gasification***. Coal is a practical option for making hydrogen in large plants. Nevertheless, owing to the high carbon content of coal, the corresponding carbon dioxide emissions are larger than those from any other feedstock. Large-scale use of coal gasification implies that carbon capture and storage technologies have to be developed.

All these technologies produce a great amount of CO_2 needing to be concentrated and separated. The chemical and petrochemical industries have substantial experience to realize this purpose, mainly

through absorption and desorption of CO_2 in alkyl amines. In fact, absorption in solvents is, today, the most diffuse technique at industrial scale, in natural gas treatment and in experimental plants for CO_2 capture. In particular, the amine-based absorption with an aqueous monoethanolamine (MEA) solution is capable to achieve high level of CO_2 capture (more than 90%) from flue gas. Nevertheless, the ammines are corrosive, predisposed to degradation owing to the action of sulphur oxides and require considerable amount of energy, mainly, in the regeneration step [Choi et al., 2009; Maneeintr et al., 2010].

2. HYDROGEN PRODUCTION AND MEMBRANE TECHNOLOGY

As above introduced, in the viewpoint of the atmospheric pollution and greenhouse gas emissions reduction, the need of developing new technologies for realizing this intent constitutes a top priority. As an emergent technology, proton exchange membrane fuel cells (PEMFCs) could represent a viable solution for this purpose. It is well known that PEMFCs are fuelled by highly pure hydrogen and are able to transform the chemical energy produced by the electrochemical reaction between hydrogen and oxygen into electrical energy, in addition to the direct combustion of hydrogen and oxygen producing thermal energy at zero pollution. Furthermore, PEMFCs are conventionally exercised at $T < 100$ ºC. Therefore, what above reported is useful for describing PEMFCs as top candidates as an alternative technology to the conventional processes. Nevertheless, they are supplied by pure hydrogen owing to the low tolerance of the anodic Pt catalysts to CO (<10 ppm). As aforementioned, hydrogen is industrially produced via steam reforming reaction of derived fossil fuels (natural gas, gasoline, etc) in fixed bed reactors (FBRs), which produce a reformed stream containing besides hydrogen other byproducts such as CO, CH_4 and CO_2. Therefore, to supply a PEMFC, hydrogen needs to be purified by means of further processes like water gas shift (WGS) reaction, pressure swing adsorption (PSA) and/or Pd membrane separation, etc. As an alternative solution to the conventional systems, membrane

reactor (MR) technology seems to represent a valid choice because it offers the possibility to combine the reforming reaction for producing hydrogen and its separation in only one system [Mulder, 1996].

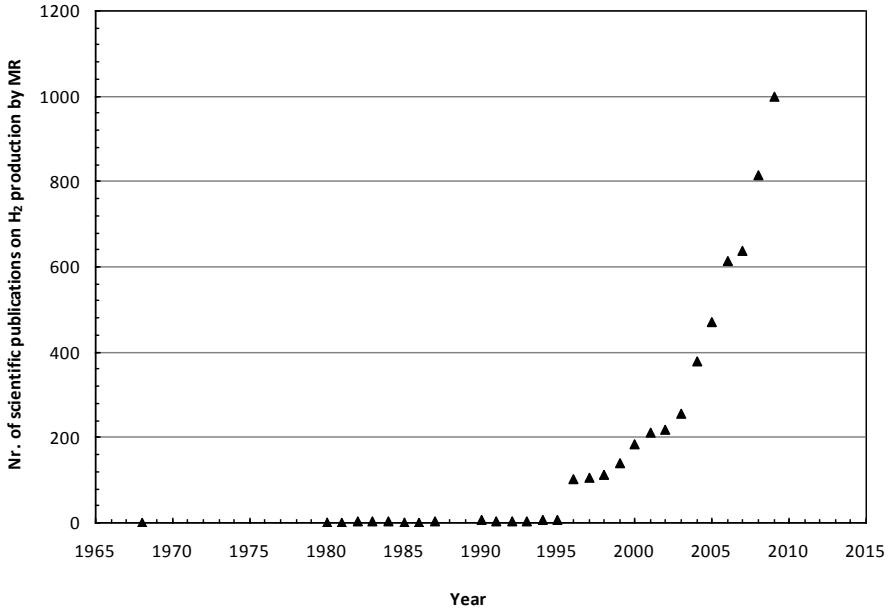

Figure 5. Scientific publications on H_2 production by MR technology vs year. Scopus database: www.scopus.com

In Figure 5, the number of scientific publications on hydrogen production by means of MR technology is illustrated. As shown, the increase of scientific contributions in the last decades confirms the growing attention of the scientific community towards the application of MR technology to hydrogen production with the purpose of proposing convincingly it at larger scale.

To resume the advantages related to the use of inorganic MRs over the conventional reactors [Saracco and Specchia, 1994; Shu et al., 1991], it should be considered that they:

1. perform the chemical reaction and hydrogen separation in the same device with a consequent reduction of the capital costs;
2. enhance the conversion of equilibrium limited reactions;
3. achieve higher conversions than FBRs (operated at the same MRs conditions) or the same conversion, but operating at milder conditions than FBRs;

4. improve both the hydrogen yield and hydrogen selectivity achievable in a FBR.
5. may produce directly a high purity (or CO_x-free) hydrogen stream (in the case of dense Pd-based MRs).

In particular, a great scientific interest is given to the dense palladium-based membranes because they show full hydrogen perm-selectivity to hydrogen permeation [Lu et al., 2007]. More in detail, hydrogen permeation through dense Pd-based membranes occurs via solution-diffusion transport mechanism [Ward and Dao, 1999]. As a main drawback, when dense palladium membranes are exposed to a hydrogen flow at T > 300 °C, the embrittlement phenomenon takes place after a few cycles of $\alpha \leftrightarrows \beta$ transitions of pure palladium [Grashoff et al., 1983; Hsieh, 1989; Lewis et al., 1988]. These transitions involve in a lattice dilatation instead of the change of the lattice structure. When palladium is alloyed with silver, copper or other metals, Pd-H phases are obtained with an improved reticular step and with the ability of anticipating the reticular expansion from hydrogen [Hou and Hughes, 2003].

However, the superiority of palladium membranes with respect to other materials is mainly due to the high solubility of hydrogen and the aforementioned full perm-selectivity to hydrogen permeation.

2.1 INORGANIC MEMBRANES AND MEMBRANE REACTORS

Following the definition of IUPAC [Koros et al., 1996], a membrane is a material having lateral dimensions much higher than its thickness, through which a mass transfer may occur owing to a driving force constituted by a gradient of concentration, pressure, temperature, electric potential, etc. Furthermore, membranes are categorized considering their nature, geometry and separation regime [Khulbe et al., 2008].

Biological membranes are manufactured easily, although they show limited operating temperature (below 100 °C), pH range, etc. [Xia et al., 2003]. Synthetic membranes can be further classified into organic (polymeric) and inorganic (ceramic, metallic), depending on their operating temperature limit.

Generally, polymeric membranes are exercised preferentially under 100-150 °C, making them ineffective for reforming processes in MRs. On the contrary, inorganic membranes operate above 250 °C and are stable between 300 - 800 ºC. Ceramic membranes, for example, may operate at temperatures higher than 1000 ºC [Van Veen et al., 1986].

Inorganic membranes may be further categorized into porous and metallic. Porous membranes are classified according to their pore diameter in microporous (d_p < 2nm), mesoporous (2nm < d_p < 50nm) and macroporous (d_p > 50nm) [Koros et al., 1996]. Metallic membranes can be subdivided into supported and unsupported. Another kind of membrane classification depends on the separation mechanisms, which are based on the specific material properties [EIA, 2004]. Therefore, depending on the dimension of the membrane pores, in the following some of the mechanisms occurring in both porous and dense membranes are summarized:

- Macroporous membranes (ϕ_{pore} > 50 nm): Poiseuille (Viscous flow) transport mechanism;
- Mesoporous membranes (ϕ_{pore} = 2 ÷ 50 nm) - Knudsen transport mechanism;
- Microporous membranes (ϕ_{pore} < 2 nm) - Activated process transport mechanism;
- Dense (Pd-based) membranes (ϕ_{pore} = -) - Fick transport mechanism.

Nevertheless, the choice of a membrane to be utilized in MRs depends on parameters such as the productivity, separation selectivity, membrane life time, mechanical and chemical integrity at the operating conditions and, particularly, the cost. For example, to produce pure hydrogen, it is preferred to use the inorganic membranes, in particular palladium-based membranes, which are characterized by the above mentioned full hydrogen perm-selectivity with respect to all other gases.

2.2 THE ROLE OF PALLADIUM MEMBRANES IN THE MR TECHNOLOGY

Owing to the well known in the membranologists area “shift effect”, which allows the thermodynamic equilibrium restrictions of a FBR to be overcome, the main MRs benefits for reforming reactions

concern the ability of improving the reaction conversion, hydrogen yield, etc. Depending on the type of inorganic MRs used for a such process, in the specialized literature it is reported that the MR conversions depend on the parameter "H", defined as permeation rate to reaction rate ratio [Keizer et al., 1994]. When H = 0, a FBR is represented because the permeation does not occur. In the case of low H values, low permeation to reaction rate takes place. In this region, microporous, dense and mesoporous MRs show the same behaviours [Keizer et al., 1994]. MRs with a finite separation factor (ratio between the permeability of a certain gas as hydrogen over that of referenced gas as a blank, generally an inert gas such as He, Ar, etc.) achieve an optimum in terms of H factor. Above the optimum, the reactant loss caused by permeation induces a detrimental effect on the conversion. On the contrary, at higher separation factors correspond higher conversions. MRs showing infinite separation factors, for example for hydrogen, do not give any drawback in terms of conversion because loss of reactants does not occur. Generally, at each H value, the MR performances are always superior over the FBRs. At least, MRs performances could be the same of a FBR working at the same MRs operating conditions.

However, in the field of the inorganic membranes, dense metallic membranes have attracted great interest of many researchers [Adhikari and Fernand, 2006]. However, between 0 – 700 °C such metals as niobium, vanadium and tantalum show higher hydrogen permeability than palladium, even though they possess a stronger surface resistance to hydrogen transport than palladium. Nevertheless, dense palladium membranes are more considered in the scientific community, although their commercialization is limited by some drawbacks such as the low hydrogen permeability and high costs. The hydrogen molecular transport in palladium membranes involves six different activated steps: dissociation of molecular hydrogen at the gas/metal interface, adsorption of the atomic hydrogen on the membrane surface, dissolution of atomic hydrogen into the palladium matrix, diffusion of atomic hydrogen through the membrane, re-combination of atomic hydrogen to form hydrogen molecules at

the gas/metal interface, desorption of hydrogen molecules. As a result, the hydrogen flux permeating through the membrane can be expressed as in the following [Gallucci et al., 2008]:

$$J_{H_2} = Pe_{H_2}(p^n_{H_2,retentate} - p^n_{H_2,permeate})/\delta \quad (5)$$

where J_{H2} is the hydrogen flux permeating through the membrane, Pe the hydrogen permeability, δ the membrane thickness, $p_{H2\text{-}retentate}$ and $p_{H2\text{-}permeate}$ the hydrogen partial pressures in the retentate (reaction side) and permeate (side in which hydrogen permeating through the membrane is collected) zones, respectively, n (variable in the range 0.5 - 1) the dependence factor of the hydrogen flux to the hydrogen partial pressure. At pressure relatively low and membrane thickness greater than 5 μm, the rate-limiting step of the hydrogen permeation through the membrane is assumed to be the diffusion [Dolan et al., 2006]. In this case, the equation (5) becomes Sieverts-Fick law:

$$J_{H_2,Sieverts\text{-}Fick} = Pe_{H_2} \cdot (p^{0.5}_{H_2,retentate} - p^{0.5}_{H_2,permeate})/\delta \quad (6)$$

At relatively high pressures, when the hydrogen-hydrogen interactions in the palladium bulk are not negligible, n becomes equal to 1:

$$J_{H_2} = Pe_{H_2} \cdot (p_{H_2,retentate} - p_{H_2,permeate})/\delta \quad (7)$$

The hydrogen permeability dependence on the temperature can be expressed by an Arrhenius like equation:

$$Pe_{H_2} = Pe^0_{H_2}\, exp\,(-E_a/RT) \quad (8)$$

where Pe_0 is the pre-exponential factor, E_a the apparent activation energy, R the universal gas constant and T the absolute temperature.

Therefore, when Sieverts-Fick law is valid, the hydrogen flux is expressed as indicated by the Richardson's equation :

$$J_{H_2} = Pe^0_{H_2}\,[exp\,(-E_a/RT)] \cdot (p^{0.5}_{H_2,retentate} - p^{0.5}_{H_2,permeate})/\delta \quad (9)$$

According to the scheme proposed in Figure 6, different researchers [Tosti et al., 2000; Wieland et al., 2002; Saracco et al., 1999; Basile, 2008] proposed as a more cost-effective solution the development of a single system combining both the reaction for hydrogen production and its purification as a pure stream. Therefore, the conventional systems for pure hydrogen production could be substituted by a dense palladium-based MR, contemporarily able to perform the reaction and to collect a high purity hydrogen stream.

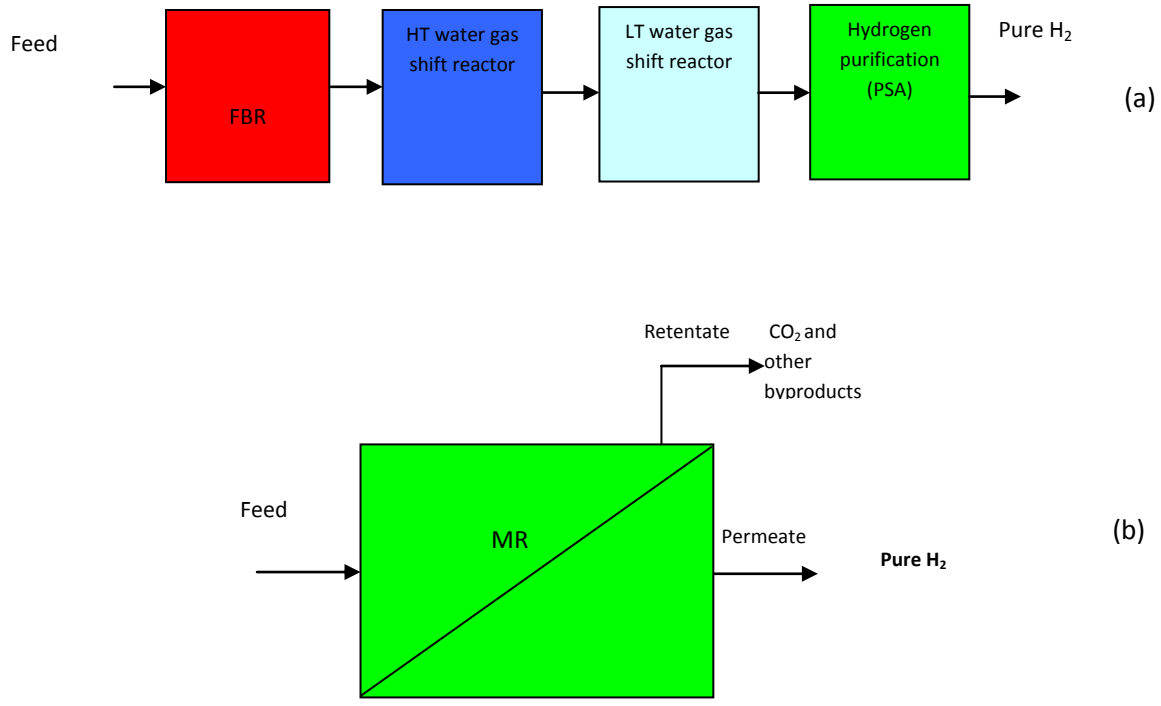

Figure 6. Conventional system (a) and dense Pd-based MR (b) for pure H_2 production from reforming reactions.

The first documented experience related to the separation of hydrogen from gaseous mixtures using foils of palladium as a membrane was performed in 1866 by Graham [Graham, 1866]. Only in 1956, Hunter patented the first Pd-alloy membranes as a new hydrogen purification system [Hunter, 1956; Hunter, 1960]. In fact, as reflected by the data of Figure 7, representing the scientific publications in the contest of palladium-based membranes applications [Scopus, 2010], the scientific interest towards

palladium-based membranes started appearing in the 1955s, increasing especially in the last two decades.

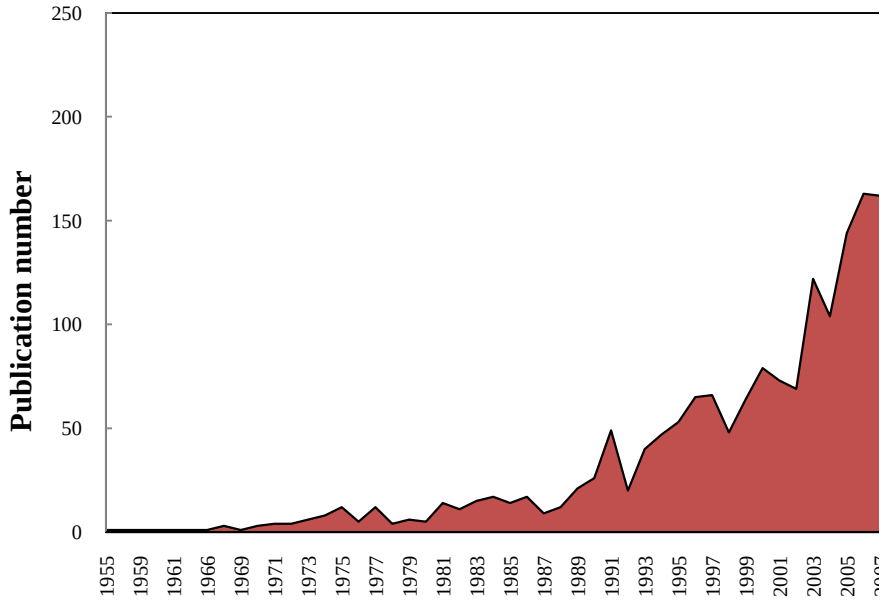

Figure 7. Number of published papers per year on palladium-based membrane applications.

The commercialization of pure palladium membranes is limited by several factors:

- pure palladium membranes undergo the embrittlement phenomenon when exposed to pure hydrogen at temperatures below 300 °C,
- pure palladium membranes are subject to deactivation by carbon compounds at temperature above 450 °C,
- pure palladium membranes are subject to irreversible poisoning by sulfur compounds,
- the cost of palladium is high.

However, as a general information, a representative summary of some reactions for producing hydrogen studied by membranologists via Pd-based MR technology is reported in Table 2.

On the contrary, as a special consideration, in the following paragraph a small overview on hydrogen production through dense Pd-based MRs from reforming reactions of different feedstocks produced

renewably is reported, paying particular attention to the performances in terms of conversion, hydrogen yield and CO_x-free hydrogen recovery.

Kind of reaction	**Membrane**	**Material**
Coupling of hydrogenation and dehydrogenation	dense	Pd
Dehydrogenation of cyclohexane to benzene	dense	Pd/Ag
Dehydrogenation of ethylbenzene to styrene	porous	Pd
Dehydrogenation of ethane to ethylene	dense	Pd/Ag
Dehydrogenation of isopropyl alcohol to acetone	dense	Pd
Dehydrogenation of n-heptane to toluene + benzene	dense	Pd/Rh
Dehydrogenation of butane to butadiene	dense	Pd
Dehydrogenation of 1,2-cyclohexanediol	dense	Pd/Cu
Dry reforming of methane	dense	Pd-alloy
Octane reforming	dense	Pd and Pd-al1oy
Partial oxidation of methane	porous	Pd-alloy
Steam reforming of ethanol	dense	Pd and Pd-al1oy
Oxidative steam reforming of ethanol	dense	Pd-al1oy
Steam reforming of ethanol	dense	Pd and Pd-al1oy
Partial oxidation of ethanol	dense	Pd-al1oy
Steam reforming of acetic acid	dense	Pd and Pd-al1oy
Steam reforming of glycerol	dense	Pd and Pd-al1oy
Steam reforming of methane	dense/porous	Pd-alloy/silica-alumina supported
Oxidative steam reforming of methanol	dense/porous	Pd-alloy/silica-alumina supported
Partial oxidation of methanol	dense/porous	Pd-alloy/silica-alumina supported
Steam reforming of methanol	dense	Pd and Pd-al1oy

Table 2. Representative list of chemical reactions for producing hydrogen by using Pd-based MRs.

2.3 REFORMING REACTIONS OF RENEWABLE FEEDSTOCKS FOR HYDROGEN PRODUCTION VIA PALLADIUM-BASED MEMBRANE REACTORS

2.3.1 METHANE STEAM REFORMING

Methane can be renewably produced from biogas, which is generated by fermentation of organic matter, including wastewater sludge, municipal solid waste or any other biodegradable feedstock, under anaerobic conditions [Martins das Neves et al., 2009]. Conventionally, methane steam reforming

(MSR) reaction is performed in FBRs at 800 - 900 °C because it is an endothermic reaction [Barelli et al., 2008].

$$CH_4 + 2H_2O = 4H_2 + CO_2 \qquad \Delta H^{\circ}_{298\,K} = 165.0\ kJ/mol \qquad (10)$$

In a FBR, the conversion is 100% only at elevated temperature, although the catalyst undergoes deactivation due to carbon formation. Otherwise, as summarized in Table 3, complete methane conversion is achieved at lower temperature (~ 500 °C) in Pd-based MRs. For example, Lin *et al.* [Lin et al., 2003], performed MSR reaction in a supported porous stainless steel (PSS) Pd-based MR with methane conversion > 80% at 500 °C and achieving a hydrogen recovery around 90%. Chen *et al.* [Chen et al., 2008] obtained almost complete methane conversion at 550 °C using an alumina supported Pd-based MR. Furthermore, the authors reached 95% pure hydrogen recovery, confirming that the selective removal of hydrogen from the reaction zone allows methane conversion greater than a FBR to be obtained.

Iulianelli et al. [Iulianelli et al. 2010a] using a dense self supported Pd-based MR obtained 50% methane conversion and 70% CO_x-free hydrogen recovery. The lower performance in terms of conversion was accounted for the relatively low temperature (450 °C) and for the low Ni phase concentration of the catalyst (0.5%).

Membrane	**Catalyst**	**Temp [°C]**	**Press [bar]**	**H_2O/CH_3OH molar ratio**	**HR [%]**	**Methane conversion [%]**	**Ref**
Pd supported onto PSS	Ni/Al_2O_3	500	20.0	3/1	90	86	[Lin et al., 2003]
Pd supported onto Al_2O_3	Ni-La/Mg-Al	550	9.0	3/1	95	99	[Chen et al., 2008]
Pd-Ag supported onto PSS	Cu/ZnO	500	6.0	2.9/1	-	50	[Jorgensen et al., 1995]
Pd supported on Vycor (*)	-	500	9.1	-	-	90	[Uemiya et al., 1991]
Pd-Ag supported onto PSS	Ni/Al_2O_3	500	1.36	3/1	-	55	[Shu et al., 1995]
Pd-based	Ni/Al_2O_3	500	1.0	3/1	-	100	[Kikuchi et al., 2000]

Flat Pd-Ag	Ru/Al_2O_3	300	1.0	-	-	16.5	[Basile et al., 2003]
Dense self-supported Pd-Ag	Ni/Al_2O_3	450	3.0	2/1	70	50	[Iulianelli et al., 2010a]
Pd supported onto PSS	Ni/Al_2O_3	527	3.0	3/1	-	100	[Tong and Matsumura, 2005]
Pd supported onto Inconel (**)	-	650	4.0	4/1	-	97	[Patil et al., 2007]
Pd-Ag supported onto Inconel (**)	Ni/Al_2O_3	500	2.0	3/1	-	80	[Shu et al., 1994]

(*) Vycor = glass support

(**) Inconel = referred to Ni-Cr based super alloy support

HR: hydrogen recovery

Table 3. A few experimental data from literature concerning MSR reaction in Pd-based MRs.

However, Table 3 confirms that Pd-based MRs use allows the operating conditions required for carrying out the MSR reaction in a FBR to be reduced and high methane conversion as well as high pure hydrogen recovery to be obtained.

2.3.2 ETHANOL STEAM REFORMING

In the last years, ethanol steam reforming (ESR) reaction (11) has been widely studied in FBRs for producing hydrogen. Indeed, ethanol can be produced renewably and represents an opportunity as an alterative to the derived fossil feedstocks. In particular, bioethanol is an aqueous solution containing between 8.0 and 12.0% wt of ethanol and other byproducts depending on the raw material used [Pfeffer et al., 2007]. Nevertheless, the bioethanol distillation is an expensive process, because of the azeotrope presence. For this reason, in the last years, bioethanol is directly used as fuel in steam reforming reaction. Moreover, an excess of water improves the palladium-based MR performances reducing also the CO content.

$$C_2H_5OH + 3H_2O = 2CO_2 + 6H_2 \qquad \Delta H°_{298\,K} = +157.0\ kJ/mol \qquad (11)$$

Table 4 shows some of the most relevant results on ESR performed in Pd-based MRs. In detail, Iulianelli et al. [Iulianelli et al., 2010b] studied from an experimental point of view the steam reforming reaction of a simulated bioethanol mixture (water/ethanol feed molar ratio = 18.7/1 mol/mol without other typical byproducts) to produce pure, or at least CO_x-free, hydrogen in a dense self-supported Pd-Ag MR. As a result, at 400 °C and 3.0 bar, the authors obtained a complete bioethanol conversion (~ 85.0% for the FBR working at the same MR operating conditions) and around 95.0% of CO_x-free hydrogen recovery. Nevertheless, in the case of Pd-based supported MRs, the performances in terms of conversion and hydrogen recovery are lower.

For example, Lin et al. [Lin et al., 2004] used a PSS supported Pd-Ag MR achieving at 450 °C and 10 bar a 70% of ethanol conversion and around 80% of hydrogen recovery.

Membrane	**Catalyst**	**Temp [°C]**	**Press [bar]**	**Feed molar ratio H_2O/C_2H_5OH**	**HR [%]**	**H_2 yield [%]**	**Ethanol conversion [%]**	**Ref**
Dense self-supported Pd-Ag	Co/Al_2O_3	400	3.0	18.7/1	95	60	100	[Iulianelli et al., 2010b]
Dense self-supported Pd-Ag	Ru/Al_2O_3	450	2.0	13/1	-	80	-	[Tosti et al., 2008]
Supported Pd-Ag	$Rh/LaAl_2O_3$	700	69	12/1	-	65	100	[Papadias et al., 2010]
Pd-Ag supported onto PSS	$Cu\text{-}Zn/Al_2O_3$	450	10	-	80	-	70	[Lin and Chang, 2004]
Laminated Pd-Ag	$Cu\text{-}Zn/Al_2O_3$	350	1.2	-	-	40	-	[Amandusson and Ekedahl, 2001]

HR: hydrogen recovery

Table 4. A few experimental data from literature concerning ESR reaction in Pd-based MRs.

However, both Iulianelli et al. [Iulianelli et al., 2009] and Lin et al. [Lin et al., 2008] performed the oxidative ethanol steam reforming (OESR) reaction in Pd-based MRs with the results shown in Table

5. In this case, Iulianelli et al. did not achieve great conversions and hydrogen recovery. This was due to the oxidation effect caused by the oxygen present in the reaction side that lowered the hydrogen content with a consequent reduction of the hydrogen permeation driving force. Therefore, the lower the hydrogen permeating flux the lower both the conversion and the hydrogen recovery.

On the contrary, Lin et al. [Lin et al., 2008] obtained a great conversion owing to a relatively high pressure and low oxygen supplying in the reaction side.

Membrane	Catalyst	Temp [°C]	Press [bar]	Feed molar ratio $H_2O/O_2/C_2H_5OH$	HR [%]	H_2 yield [%]	Ethanol conversion [%]	Ref
Dense self-supported Pd-Ag	Ru/Al_2O_3	400	2.5	11/0.6/1	30	18	40	[Iulianelli et al., 2009]
Pd-Ag supported onto PSS	-	450	9.0	1/0.2/1	-	40	90	[Lin et al., 2008]

HR: hydrogen recovery

Table 5. Experimental data from literature concerning OESR reaction in Pd-based MRs.

2.3.3 METHANOL STEAM REFORMING

Methanol is conventionally produced from natural gas. Otherwise, it may be produced from biomass, such as wood and agricultural waste. Renewable methanol shows some advantages as fuel because it is more easily transportable than methane or other fuel gases, it has high energy density without needing desulphurization. Methanol steam reforming (SRM) is an endothermic reaction, feasible at temperatures of 200 - 300 °C.

$$CH_3OH + H_2O = CO_2 + 3H_2 \qquad \Delta H°_{298\,K} = +49.7\ kJ/mol \qquad (12)$$

Table 6 illustrates a few experimental data from the specialized literature concerning this reaction performed in Pd-based MRs. For example, Lin et al. [Lin and Rei, 2000; Lin and Rei, 2001] utilized a double-jacketed supported palladium MR packed with a $Cu/ZnO/Al_2O_3$ catalyst at 350 °C and pressure ranging between 6.0 and 15.0 bar reaching a hydrogen recovery over 70.0% as well as 100% of

methanol conversion. Basile and coworkers [Basile et al., 2008a; Iulianelli et al., 2008a; Gallucci and Basile, 2006; Gallucci et al., 2007] studied extensively SRM in Pd-based MR, concluding that the combination of MR technology and steam reforming of methanol may represent a valid alternative solution to the conventional systems for hydrogen production.

Membrane	Catalyst	Temp [°C]	Press [bar]	Feed molar ratio H_2O/CH_3OH	HR [%]	H_2 yield [%]	Methanol conversion [%]	Ref
Pd supported onto PSS	$Cu/ZnO/Al_2O_3$	350	6.0	1.2/1	38	-	100	[Lin and Rei, 2001]
Pd supported onto PSS	$Cu/ZnO/Al_2O_3$	350	15.0	1.2/1	73	-	100	[Lin and Rei, 2000]
Dense self-supported Pd-Ag	$CuOAl_2O_3ZnO$ MgO	300	1.3	6/1	6	-	100	[Basile et al., 2008a]
Dense self-supported Pd-Ag	$CuOAl_2O_3ZnO$ MgO	300	3.0	3/1	93	77	-	[Iulianelli et al., 2008a]
Dense self-supported Pd-Ag	-	270	10.0	3/1	100	-	95	[Gallucci and Basile, 2006]
Dense self-supported Pd-Ag	Ru/Al_2O_3	350	1.3	4.5/1	40	-	100	[Gallucci et al., 2007]
Pd-Ag foil	Fe-Cr/based	450	5.2	1/1	15	-	76	[Damle, 2009]

HR: hydrogen recovery

Table 6. A few experimental data from literature concerning SRM reaction in Pd-based MRs.

In detail, as shown in Table 6, Basile obtained great results in terms of conversion (always higher than 95% working at 300 °C) and with a hydrogen recovery variation depending on the reaction pressure utilized. Furthermore, the authors pointed out that the low-thickness of palladium-based membrane may play an important role for the palladium-cost reduction.

2.3.4 BIOGLYCEROL STEAM REFORMING

Bioglycerol is a byproduct of biodiesel production, which is usually derived from the transesterification of vegetable oil with methanol or ethanol. During the process, the oil is mixed with a metallic base (sodium or potassium hydroxide) and alcohol (methanol or ethanol). The reaction produces methyl or ethyl ester (biodiesel) and glycerol as a byproduct, which can be used as a renewable source. From the open literature, at moment only Iulianelli et al. [Iulianelli et al., 2010c; Iulianelli et al., 2010d] studied glycerol steam reforming (GSR) reaction in a dense Pd-Ag MR, Table 7.

$$C_3H_8O_3 + 3H_2O = 3CO_2 + 7H_2 \qquad \Delta H°_{298\,K} = +346.4\ kJ/mol \qquad (13)$$

The authors studied the catalyst influence on the reactor performances (glycerol conversion and pure hydrogen recovery), using two commercial catalysts: Co/Al_2O_3 and Ru/Al_2O_3. At 4.0 bar and 400 °C, using a Co/Al_2O_3 catalyst, the authors obtained a glycerol conversion of 94.0% and a CO_x-free hydrogen recovery higher than 60.0%. On the contrary, using Ru/Al_2O_3 catalyst, the authors achieved around 20.0% glycerol conversion and 16.0% pure hydrogen recovery at 5.0 bar. The authors justified this poor performances with combination of ruthenium with an acid support as Al_2O_3, unfavorable for GSR reaction. Moreover, the authors observed that carbon formation taking place during the reaction affects negatively the performances of the Pd-Ag membrane in terms of a lower hydrogen permeating flux and catalyst deactivation.

Membrane	Catalyst	Temp [°C]	Press [bar]	Feed molar ratio H_2O/C_3H_8O	HR [%]	H_2 yield [%]	Glycerol conversion [%]	Ref
Dense self-supported Pd-Ag	Co/Al_2O_3	400	4.0	6/1	60	26	100	[Iulianelli et al., 2010c]
Dense self-supported Pd-Ag	Ru/Al_2O_3	400	5.0	6/1	60	28	57	[Iulianelli et al., 2010d]

HR: hydrogen recovery

Table 7. A few experimental data from literature concerning GSR reaction in Pd-based MRs.

2.3.5 ACETIC ACID STEAM REFORMING

Acetic acid is a renewable source and is produced by fermentation of biomass. Today, at scientific level, only a few studies concern the acetic acid steam reforming (AASR) reaction for producing hydrogen by means FBRs.

$CH_3COOH + 2H_2O = 2CO_2 + 4H_2$ $\Delta H°_{298\ K} = +134.9$ kJ/mol (14)

Nevertheless, as shown in Table 8, only two scientific papers were published dealing with the use of MR for performing the AASR reaction [Basile et al., 2008b; Iulianelli et al., 2008b]. In these studies, the AASR reaction was performed in a dense Pd-Ag MR packed with two different catalysts: on one hand only a Ni-based and in another hand with both Ru-based and Ni-based ones. In both cases, complete acetic acid conversion was reached, but in the study of Iulianelli et al. [Iulianelli et al., 2008b], 70% of hydrogen recovery was obtained.

Membrane	Catalyst	Temp [°C]	Press [bar]	Feed molar ratio H_2O/C_3H_8O	HR [%]	H_2 yield [%]	Acid acetic conversion [%]	Ref
Dense self-supported Pd-Ag	Ni/Al_2O_3-Ru/Al_2O_3	450	2.5	10/1	32	-	100	[Basile et al., 2008b]
Dense self-supported Pd-Ag	Ni/Al_2O_3	400	1.5	10/1	70	51	100	[Iulianelli et al., 2008b]

HR: hydrogen recovery

Table 8. A few experimental data from literature concerning AASR reaction in Pd-based MRs.

3. FUTURE TRENDS IN HYDROGEN PRODUCTION FROM REFORMING REACTIONS OF RENEWABLE SOURCES PERFORMED IN MEMBRANE REACTORS.

This chapter deals on the combination of two distinct sciences such as catalysis and membrane technology. At scientific level, it is difficult to consider which of them is more prevalent in MR development. Nevertheless, it is clear that the exploitation of renewable sources represents a key factor

for hydrogen production via reforming reactions by MR technology, particularly to improve the hydrogen production units. Rarely, in the open literature this concept is emphasized: while natural gas (and more in general derived fossil fuels) is preferentially used for stationary applications, it is expected that renewable feedstocks such as, for example, ethanol will play a more important role in the future non-stationary applications. Concerning the reforming reactions performed in MRs, a problem afflicting several studies present in the specialized literature consists of the impossibility to compare the performances in terms of conversion, hydrogen yield and hydrogen recovery because of the not equal operating conditions used in the experimental tests. Furthermore, there is a lack of information regarding the cost analysis for the MRs. This is because MR technology still presents some limits to be overcome before its implementation at larger scales.

Future efforts should be done for preparing defect-free inorganic membranes able to work for long periods at hard operating conditions as well as to develop membrane systems not based on palladium or with low palladium content. By solving these problems (i.e. synthesis of defect-free, stable and impurity-resistant membranes, no- and/or low-palladium content membranes development), the benefits resulting from the use of MRs at industrial scale rather than FBRs for performing reforming reactions to produce hydrogen could become more realistic. More consistent economic analyses based on the combination of renewable sources and MR technology would be necessary for stimulating improvements on this research contest.

CONCLUSIONS

Hydrogen is growing an important role as an energy carrier in future energy systems such as PEMFCs. Therefore, a great attention is paid by both the industrial and the scientific communities to produce hydrogen in a more technically, environmentally and economically attractive way. From a techno-economic point of view, today steam reforming of natural gas and the exploitation of derived fossil

fuels is the unique route for conventional hydrogen production. Hydrogen upgrading in industrial applications is achieved via PSA, membrane, or cryogenic separation processes. Nevertheless, inorganic membranes are excellent medium for hydrogen purification, especially when incorporated into MRs, combining the reaction/separation process in a single device. In this chapter, the state of the art on reforming processes of different renewable feedstocks performed in MRs has been proposed, paying special attention to the effect of palladium-based membranes applications. Indeed, Pd-based MRs seem to be the dominant applications in this field, particularly owing to the hydrogen perm-selectivity characteristics of Pd-based membranes.

In summary, the future perspectives on performing the reforming reactions of renewable sources via inorganic MRs are described as in the following:

• Scale-up of MRs for reforming reactions is one of the most important issues. The development of low-cost, defect-free, effective membranes could represent a chance for realistic application of MRs at industrial scale.

• Many efforts should be pursued for improving the membrane mechanical resistance during the reaction processes, both at relatively high reaction temperatures and pressures.

• More experimental analyses on the lifetime of MRs utilized to perform reforming reactions for hydrogen production should be realized to validate them as a possible alternative to the conventional systems at larger scales.

REFERENCES

- ✓ Adhikari S.; Fernand S. *Ind Eng Chem Res* 2006, *45*, 875-881.
- ✓ Amandusson H.; Ekedahl L. G.; Dannetun H. *Appl Catal A: Gen* 2001, *217*, 157-164.
- ✓ Anonimus 1 (2010). http://timeforchange.org/prediction-of-energy-consumption
- ✓ Anonimus 2 (2010). http://www.worldoil.com/about_us.aspx
- ✓ Balat M. *Int J Hydrogen En* 2008, *33*, 4013-4029.
- ✓ Balat M.; Balat M. *Int J Hydrogen En* 2009, *34*, 3589-3603.
- ✓ Bardi U. *Energy* 2009, *34*, 323-326.
- ✓ Barelli L.; Bidini G.; Gallorini F.; Servili S. *Energy* 2008, *33*, 554-570.
- ✓ Basile A.; Paturzo L.; Vazzana A. *Chem Eng J* 2003, *93*, 31-39.
- ✓ Basile A. *Top Catalysis* 2008, *51*, 107-122.
- ✓ Basile A.; Parmaliana A.; Tosti S.; Iulianelli A.; Gallucci F.; Espro C.; Spooren J. *Catal Today* 2008a, *137*, 17-22.
- ✓ Basile A.; Gallucci F.; Iulianelli A.; Borgognoni F.; Tosti S. *J Membrane Sci* 2008b, *311*, 46-52.
- ✓ BP (British petroleum company) (2008). BP statistical review of world energy 2008. http://www.bp.com/subsection.do?categoryId=4&contentId=2006741
- ✓ BP (British petroleum company) (2010). Statistical review of world energy 2010. http://www.bp.com/productlanding.do?categoryId=6929&contentId=7044622
- ✓ Campbell C. J. *Oil Gas J*. 1997, *95*, 33-37.
- ✓ Campbell C. J. *The National Interest* 1998, *51*, 47-55.
- ✓ Cavallo A. J. *Natural Resources Res* 2004, *13*, 211-221.
- ✓ CENSUS 2010. http://www.census.gov/ipc/www/idb/worldpop.php
- ✓ Chen Y.; Wang Y.; Xu H.; Xiong G. *Appl Catal B: Env* 2008, *80*, 283-294.
- ✓ Cho A. *Science* 2004, *305*, 964-965.

- ✓ Choi W. J.; Seo J. B.; Jang S. Y.; Jung J. H.; Oh K. J. *J Env Sci* 2009, *21*, 907-913.
- ✓ Damle A. S. *J Power Sou* 2009, *186*, 167-177.
- ✓ DESA (Department of Economic and Social Affairs) 2009. Population Newsletter, 87. http://www.un.org/esa/population/publications/popnews/Newsltr_87.pdf
- ✓ Dolan M. D.; Dave N. C.; Ilyushechkin A. Y.; Morpeth L. D.; McLennan K. G. *J Membrane Sci* 2006, *285*, 30-55.
- ✓ EIA (International Energy Annual) 2004. http://www.eia.doe.gov/iea
- ✓ Gallucci F.; Basile A. *Int J Hydrogen En* 2006, *31*, 2243-2249.
- ✓ Gallucci F.; Basile A.; Tosti S.; Iulianelli A.; Drioli E. *Int J Hydrogen En* 2007, *32*, 1201-1210.
- ✓ Gallucci F.; Tosti S.; Basile A. In *Inorganic membranes: synthesis, characterization and applications*; Malada, R.; Menendez, M.; Ed.; Membrane science and technology series, ISBN: 978-0-444-53070-7; Elsevier: GREAT BRETAIN (GB), 2008; pp 255-323.
- ✓ Goltsov V.; Veziroglu N. *Int J Hydrogen En* 2001, *26*, 909-915.
- ✓ Graham T. *Phil R Soc London* 1866, *156*, 399-439.
- ✓ Grashoff G. J.; Pilkington C. E.; Corti C. W. *Plat Met Rev* 1983, *27*, 157-168.
- ✓ Hou K.; Hughes R. *J Membrane Sci* 2003, *214*, 43-55.
- ✓ Hsieh H. P. *AIChE Symp Ser* 1989, *85*, 53-67.
- ✓ Hunter J. B. *Silver-palladium films for separation and purification of hydrogen*, US Patent No. 2773561, 1956.
- ✓ Hunter J. B. *Platinum Met Rev* 1960, *4*, 130-131.
- ✓ Iulianelli A.; Longo T.; Basile A. *Int J Hydrogen En* 2008a, *33*, 5583-5588.
- ✓ Iulianelli A.; Longo T.; Basile A. *Int J Hydrogen En* 2008b, *33*, 4091-4096.
- ✓ Iulianelli A.; Longo T.; Liguori S.; Seelam P.K.; Keiski R.L.; Basile A. *Int J Hydrogen En* 2009, *34*, 8558-8568.

- ✓ Iulianelli A.; Manzolini G.; De Falco M.; Campanari S.; Longo T.; Liguori S.; Basile A. *Int J Hydrogen En* 2010a, *35*, 11514-11524.
- ✓ Iulianelli A.; Liguori S.; Longo T.; Tosti S.; Pinacci P.; Basile A. *Int J Hydrogen En* 2010b, *35*, 3159-3164.
- ✓ Iulianelli A.; Longo T.; Liguori S.; Basile A. *Asia-Pac J Chem Eng* 2010c, *5*, 138-145.
- ✓ Iulianelli A.; Seelam P. K.; Liguori S.; Longo T.; Keiski R.; Calabrò V.; Basile A. *Int J Hydrogen En* 2010d, in press doi:10.1016/j.ijhydene.2010.02.079.
- ✓ Jaber O.; Naterer G. F.; Dincer I. *Int J Hydrogen En* 2010, *35*, 8569-8579.
- ✓ Jorgensen S.; Nielsen P. E. H.; Lehrmann P. *Catal Today* 1995, *25*, 303-307.
- ✓ Keizer K.; Zaspalis V. T.; De Lange R. S. A.; Harold M. P. In *Membrane processes in separation and purification*; Crespo, J. G.; Boddeker, K. W.; Ed.; ISBN: 0-7923-2929-5; Kluwer Academic Publishers: Dordrecht, NETHERLANDS (HB), 1994; pp 415-429.
- ✓ Khulbe K. C.; Feng C. Y.; Matsuura T. *Synthetic polymeric membranes, characterization by atomic force microscopy*; ISBN: 3540739939; Springer: Berlin, GERMANY (D), 2008; pp 1-197.
- ✓ Kikuchi E.; Nemoto Y.; Kajiwara M.; Uemiya S.; Kojima T. *Catal Today* 2000, *56*, 75-81.
- ✓ Koros W. J.; Ma Y. H.; Shimidzu T. *J Membrane Sci* 1996, *120*, 149-159.
- ✓ Laherrere J. H. *Oil Gas J.* 1999, *97*, 57-64.
- ✓ Lewis F. A.; Kandasamy K.; Baranowski B. *Plat Met Rev* 1988, *32*, 22-26.
- ✓ Lin W. H.; Chang H. F. *Cat Today* 2004, *97*, 181-188.
- ✓ Lin W. H.; Hsiao C. S.; Chang H. F. *J Membrane Sci* 2008, *322*, 360-367.
- ✓ Lin Y. M.; Rei M. H. *Int J Hydrogen En* 2000, *25*, 211-219.
- ✓ Lin Y. M.; Rei M. H. *Catal Today* 2001, *67*, 77-84.
- ✓ Lin Y. M.; Liu S. L.; Chuang C. H.; Chu Y. T. *Catal Today* 2003, *82*, 127-139.

- ✓ Lu G. Q.; Diniz de Costa J. C.; Duke M.; Giessler S.; Socolow R.; Williams R. H.; Kreutz T. *J Coll Interface Sci* 2007, *314*, 589-603.
- ✓ Ma P. Y.; Tang Z. G.; Li Y. L.; Nie C. H.; He X. Z.; Lin Q. Z. *Adv Materials Res* 2010, *105-106*, 701-705.
- ✓ Maneeintr K.; Idem R. O.; Tontiwachwuthikul P.; Wee A. G. H. *Ind Eng Chem Res* 2010, *49*, 2857-2863.
- ✓ Martins das Neves L. C.; Converti A.; Vessoni Penna T. C. *Chemical Eng Techn* 2009, *32*, 1147-1153.
- ✓ Mohan S. V.; Mohanakrishna G.; Ramanaiah S. V.; Sarma P. N. *Int J Hydrogen En* 2008, *33*, 550-558.
- ✓ Mohr S. H.; Evans G. M. *Natural Resources Res* 2008, *17*, 1-11.
- ✓ Mulder M. M. *Basic principles of membrane technology*; ISBN: 0-7923-4247-X; Kluwer Academic Publishers: Dordrecht, NETHERLANDS (HB), 1996**;** pp 1-564.
- ✓ Ni M.; Leung M. K. H.; Sumathy K.; Leung D. Y. C. *Int J Hydrogen En* 2006, *31*, 1401-1412.
- ✓ Papadias D. D.; Lee S. H. D.; Ferrandon M.; Ahmed S. *Int J Hydrogen En* 2010, *35*, 2004-2017.
- ✓ Patil C. S.; Annaland M. V. S.; Kuipers J. A. M. *Chem Eng Sci* 2007, *62*, 2989-3007.
- ✓ Pfeffer M.; Wukovits W.; Beckmann G.; Friedl A. *Appl Thermal Eng* 2007, *27*, 2657-2664.
- ✓ Roh H. S.; Koo K. Y.; Jung U. H.; Yoon W. L. *Current Appl Phys* 2010, *10*, S37-S39.
- ✓ Saracco G.; Specchia V. *Catal Rev Sci Eng* 1994, *36*, 305-384.
- ✓ Saracco G.; Neomagus H. W. J. P.; Versteeg G. F.; van Swaaij W. P. M. *Chem Eng Sci* 1999, *54*, 1997-2017.
- ✓ Scopus 2010. http://scopees.elsevier.com
- ✓ Shu J.; Grandjean B. P. A.; Van Neste A.; Kaliaguine S. *Can J Chem Eng* 1991, *69*, 1036-1060.
- ✓ Shu J.; Grandjean B. P. A.; Kaliaguine S. *Appl Catal A: Gen* 1994, *119*, 305-325.

- ✓ Shu J.; Grandjean B. P. A.; Kaliaguine S. *Catal Today* 1995, *25*, 327-332.
- ✓ Tong J.; Matsumura Y. *Appl Catal A: Gen* 2005, *286*, 226-231.
- ✓ Tosti S.; Bettinali L.; Violante V. *Int J Hydrogen En* 2000, *25*, 319-325.
- ✓ Tosti S.; Basile A.; Borgognoni F.; Capaldo V.; Cordiner S.; Di Cave S.; Gallucci F.; Rizzello C.; Cantucci A.; Traversa E. *J Membrane Sci* 2008, *308*, 250-257.
- ✓ Uemiya S.; Sato N.; Ando H.; Matsuda T.; Kikuchi E. *Appl Catal* 1991, *67*, 223-230.
- ✓ Van Veen H. M.; Bracht M.; Hamoen E.; Alderliesten P. T. In *Fundamentals of inorganic membrane science and technology*; Burggraaf, A. J.; Cot, L.; Ed.; ISBN: 0-444-81877-4; Elsevier: Amsterdam, NETHERLANDS (HB), 1996; Vol. 14, pp 641-681.
- ✓ Ward T. L.; Dao T. *J Membrane Sci* 1999, *153*, 211-231.
- ✓ Wieland S.; Melin T.; Lamm A. *Chem Eng Sci* 2002, *57*, 1571-1576.
- ✓ WRI (World Resources Institute) (2010). http://earthtrends.wri.org/
- ✓ Xia Y.; Lu Y.; Kamata K.; Gates B.; Yin Y. In *Chemistry of Nanostructured Materials;* Yang, P.; Ed.; ISBN: 981-238-405-7; World Scientific Publishing Co. Pte. Ltd.: SINGAPORE (SGP), 2003; pp 69-100.

Chapter 2

Membrane reactor technology: state of the art

Introduction to paper 2

At the beginning of the paper 1 it was explained how to shift from fossil fuel to renewable sources for solving both the problematic concerning the climate change and the depletion of fossil fuel. In particular, it was shown how the hydrogen, produced by exploiting bio-alcohols steam reforming reaction, can be recognized as one of the most promising energy carriers in the future.

As an innovative technology, a Pd-based MR has been proposed as an alternative solution to the conventional systems for producing high purity hydrogen. Therefore, in the Paper 2 the topic was to identify and to illustrate the progress and development obtained in Pd-based MRs area.

In particular, the methods for producing Pd-based membranes are illustrated as well as their benefits and drawbacks are, also, discussed. Moreover, their applications in the area of the MRs are illustrated and the reforming reactions performed in this kind of system for hydrogen production are considered.

Pd-based Selective Membrane State-of-the-Art

A. Basile, A. Iulianelli, T. Longo, S. Liguori and Marcello De Falco

Introduction

The first scientific study on palladium-based membranes was made in the 1955, when Juenker *et al.* [1955] analyzed the use of palladium membranes for the purification of hydrogen. Today, it is well known that the palladium membranes are, mainly, applied in the field of gas separation and, in particular, in the issue of the hydrogen rich-stream purification owing to their complete hydrogen perm-selectivity [Gao, 2004]. As reported in Figure 3.1, the scientific interest towards palladium-based membranes is increased especially in the last three decades. The data on the scientific publications in the contest of palladium membranes applications, reported in Figure 3.1, are made by Elsevier Scopus database [e-net 1], where more than 6.000 scientific journals are taken into account.

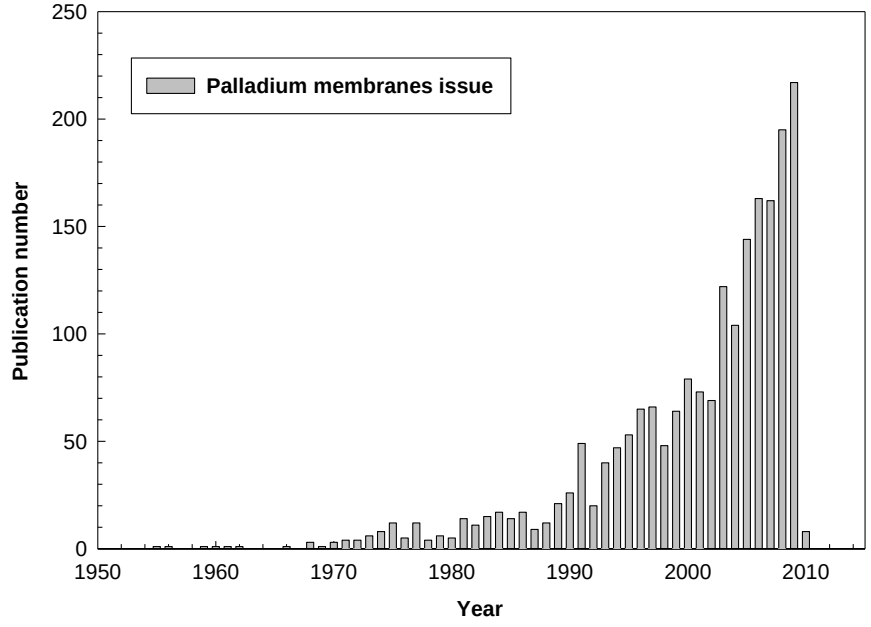

Figure 3.1. Number of published papers per year on palladium membrane applications.

Moreover, Figure 3.2 points out a further application of palladium membranes into membrane reactors (MRs), devices combining the separation properties of the membranes with the typical characteristics of catalytic reaction steps in only one unit. In particular, this figure reports the number of publications on palladium-based membranes reactors with respect to the total number of publications in the membrane reactors area.

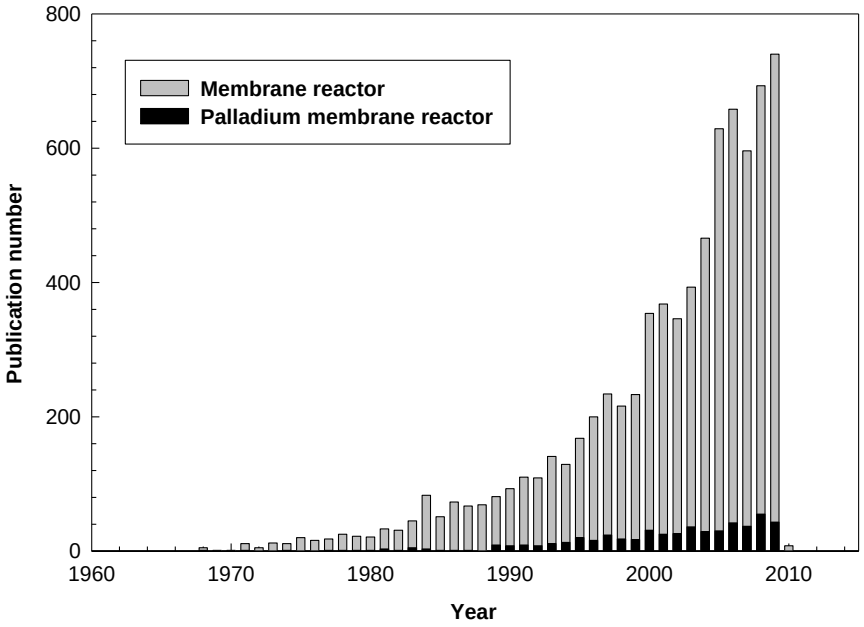

Figure 3.2. Number of publications per year on membrane reactors area and on restricted area on palladium-based membrane reactors.

The progress in the field of palladium-based MRs is due to their capacity to produce a pure hydrogen stream, owing to infinite hydrogen perm-selectivity with respect to all other gases. Moreover, in the last years, an "hydrogen economy" is developed to solve the negative effects such as climate change and air pollution, due to the emissions caused by the use of fossil fuels [Goltsov, 2001]. In particular, the "hydrogen economy" takes into consideration the use of hydrogen as energy carrier, produced by renewable sources with respect to fossil fuels, for using in alternative technologies such as, for example, the proton exchange membrane fuel cells (PEMFCs). A PEMFCs is a device capable to produce electricity directly from hydrogen and oxygen, without combustion, making the process clean and non-polluting.

Nevertheless, the commercialization of pure palladium membranes is still limited by several factors:

- pure palladium membranes undergo an embrittlement phenomenon when exposed to hydrogen at temperatures below 300 °C,
- pure palladium membranes are subject to deactivation by carbon compounds at temperature above 450 °C,
- pure palladium membranes are subject to irreversible poisoning by sulfur compounds,
- the cost of palladium is high.

In order to reduce the aforementioned drawbacks, palladium can be alloyed with a variety of other metals, even able to increase the hydrogen permeability of the palladium-based membranes with respect to the pure palladium membranes.

As main scope, the present chapter will give an overview on the general classification of the membranes, paying particular attention to palladium-based membranes, their use, applications, pointing out the most important benefits and the disadvantages. Finally, the application of palladium-based membranes in the area of membrane reactors will be discussed and such reactions process as reforming reactions will be given.

3.1. The membranes classification

As indicated by IUPAC definition [Koros, 1996], a *membrane* can be described as a structure having lateral dimensions much greater than its thickness through which mass transfer may occur under a variety of driving forces such as gradient of concentration, pressure, temperature, electric potential, etc. A schematic representation of a two-phase system separated by a membrane is given in Figure 3.3, where the Phase 1 is usually considered as the feed, while the Phase 2 as the permeate.

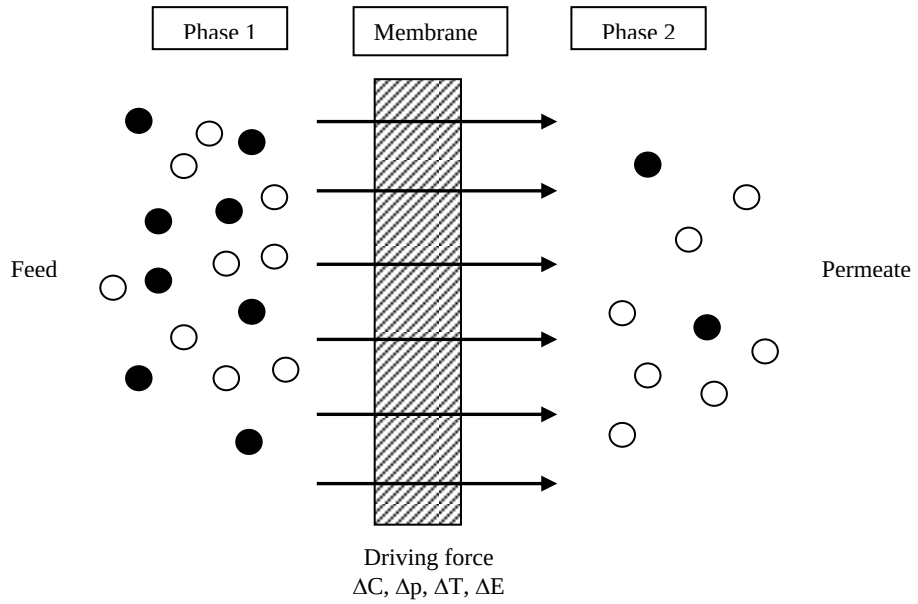

Figure 3.3. Schematic representation of a two-phase system separated by a membrane.

As schematically resumed in Figure 3.4, the membranes are classified on the base of their nature, geometry and separation regime [Khulbe, 2007].

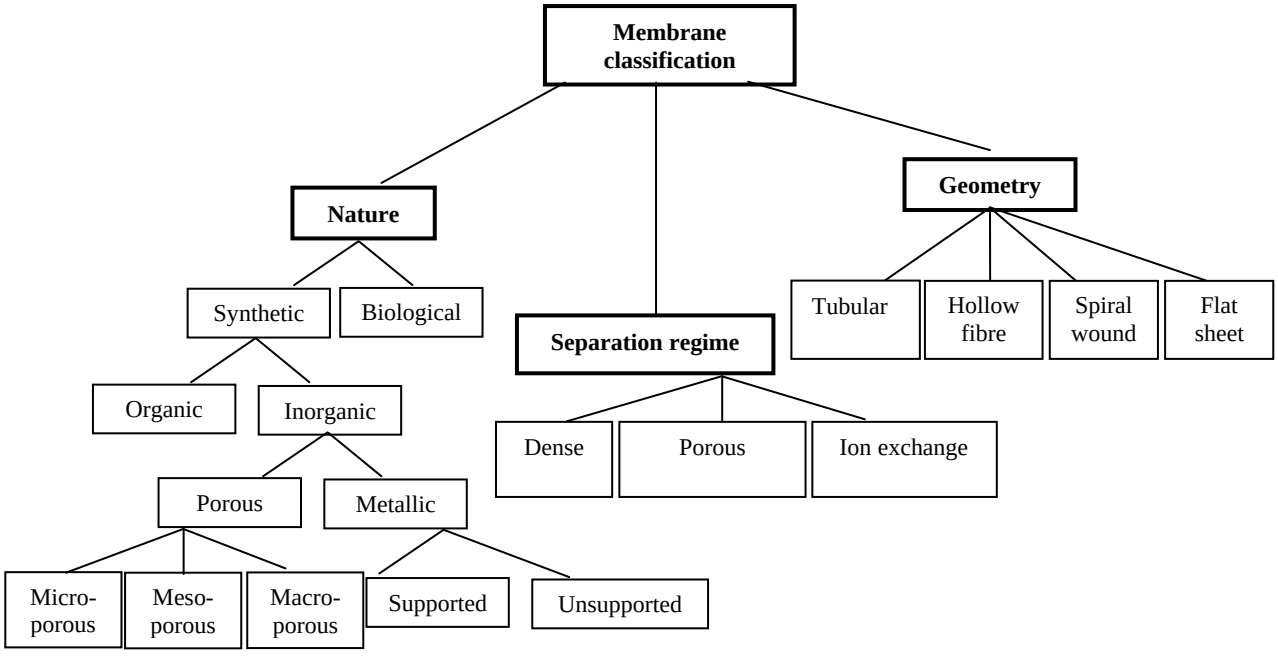

Figure 3.4. Scheme of a general membranes classification.

The classification by the nature distinguishes the membranes into biological and synthetic ones differing completely for functionality and structure [Xia, 2003].

Biological membranes are easy to be manufactured, but they present many drawbacks such as limited operating temperature (below 100 °C), limited pH range, problems related to the clean-up, susceptibility to microbial attack due to their natural origin [Xia, 2003].

Synthetic membranes can be subdivided into organic (polymeric) and inorganic (ceramic, metallic) ones according to the operative temperature limit: *polymeric membranes* commonly operate between 100 - 300 °C [Catalytica, 1988], *inorganic ones* above 250 °C. In the viewpoint of the morphology and/or membrane structure, the inorganic membranes can be subdivided into porous and metallic. In particular, *porous membranes* can be classified according to their pore diameter in microporous (d_p < 2nm), mesoporous (2nm < d_p < 50nm) and macroporous (d_p > 50nm) [Koros, 1996]. *Metallic membranes* can be categorized into supported and unsupported ones.

Generally, the inorganic membranes are stable between 300 - 800 ºC and in some cases they can operate at elevated temperatures (ceramic membranes) over 1000 ºC [Van Veen, 1996].

Depending on their geometry, the membranes can be subdivided in *tubular*, *hollow fiber*, *spiral wound* and *flat sheet* [Mallevialle, 1998]:

- *tubular membranes* are easy to clean and show good hydrodynamic control, but as important drawbacks they require relatively high volume per membrane area unit and present high costs.
- *Hollow fiber membranes* can be considered as practical and cheaper alternatives than conventional chemical and physical separation processes. They offer high packing densities and they can withstand relatively high pressure owing to their structural integrity. In this contest, they allow flexibility in system design and operation.
- *Spiral wound membranes* offer advantages such as compactness, good membrane surface/volume and low capital/operating cost ratios. Nevertheless, they are not suitable for viscous fluid and are difficult to clean.
- *Flat sheet membranes* offer moderate membrane surface/volume ratios. However, they are susceptible to plugging due to flow stagnation points, difficult to clean and expensive.

Finally, a further membrane classification is based on the separation mechanism. There are three separation mechanisms depending on specific properties of the components [Mulder, 1996]:

1) separation based on molecules/membrane surface interactions (e.g. multi-layer diffusion) and/or difference between the average pore diameter and the average free path of fluid molecules (e.g. Knudsen mechanism);
2) separation based on the difference of diffusivity and solubility of substances in the membrane: ***solution/diffusion mechanism***;
3) separation due to the difference in charge of the species to be separated: ***electrochemical effect***.

Based on these mechanisms, the membranes can be classified in *porous*, *dense* and *ion-exchange*. In Table 3.1, the different diffusion mechanisms are reported.

Membrane	**ϕ_{pore} (nm)**	**Diffusion mechanism**
Macroporous	>50	Poiseuille (Viscous flow)
Mesoporous	2-50	Knudsen
Microporous	<2	Activated process
Dense Pd	-	Fick

Table 3.1. Diffusion mechanisms in porous and dense membranes.

In the case of porous membranes:

- *Poiseuille (viscous flow) mechanism* occurs when the average pore diameter is bigger than the average free path of fluid molecules. In this case, the collisions among the different molecules are more frequent than those among the molecules and the porous wall, so no separation takes place [Saracco, 1994].
- *Knudsen mechanism* takes place when the average pore diameter is similar to the average free path of fluid molecules. In this case, the collisions of the molecules with the porous wall

are very frequent and the flux of the component permeating through the membrane is calculated by means of the following equation [Saracco, 1994]:

$$J_i = \frac{G}{\sqrt{2 \cdot M_i \cdot R \cdot T}} \cdot \frac{\Delta p_i}{\delta} \qquad (3.1)$$

where J_i is the flux of the i-species across the membrane, G the geometrical factor, which takes into account the membrane porosity and the pore tortuosity, M_i molecular weight of the i-species, R universal gas constant, T absolute temperature, Δp_i pressure difference of species and δ membrane thickness.

- *Surface diffusion* is achieved when one of the permeating molecules is adsorbed on the pore wall due to the active sites presented in the membrane [Knozinger, 1978]. This type of mechanism can reduce the effective pore dimensions not favouring the transfer of different molecular species [Kapoor, 1989]. However, this diffusion can take place also in the presence of a Knudsen transport. This mechanism is less significant by increasing the temperature owing to the progressive decrease of the bond strength between molecules and surface.
- *Capillary condensation* occurs when one of the components condenses within the pores due to capillary forces, which are sufficiently strong only at low temperature and in presence of small pores. If the pores dimension is small and homogeneous and the pores are uniformly distributed on the membrane, this mechanism can offer high selectivity [Falconer, 1995 - Sperry, 1991]. Generally, the capillary condensation favours the transfer of relatively large molecules [Lee, 1986].
- *Multi-layer diffusion* is developed when the molecule/surface interactions are strong. This mechanism is like to an intermediate flow regime between surface diffusion and capillary condensation [Ulhorn, 1992].
- *Molecular sieve* takes place when the pore diameters are very small, allowing the permeation of only smaller molecules.

In the case of dense membranes, the diffusion mechanism is a *solution-diffusion* mechanism, in which the dissociated molecules on the gas/membrane interface are adsorbed at the atomic level on the membrane surface. The atoms diffuse through the membrane and they are re-combined to form molecules at the gas/membrane interface. Afterwards, they desorb.

Among all type of membranes, the dense ones have attracted the interest of many researchers due to their capacity to separate completely a product from gaseous mixtures [Adhikari, 2006]. In particular, the dense palladium membranes are used owing to their complete hydrogen gas perm-selectivity. In the last years, the increasing interest towards this type of membranes is, also, due to hydrogen application as energy carrier (see 3.2).

For this reason, in the following, a general introduction to pure palladium membranes is given.

3.2. Hydrogen economy: palladium membranes

In the current fossil fuel economy, the fossil fuels burning causes the emission of greenhouse gases and other pollutants. In order to mitigate this air pollution and the climate change, the use of alternative technologies is became necessary. In this contest, great interest is paid to PEMFCs, which are capable to produce electricity directly from hydrogen and oxygen, without combustion, making the process non-polluting [Stambouli, 2002]. A PEMFC uses a permeable polymeric membrane as the electrolyte (Figure 3.5). The membrane is very small and light and in order to catalyze the reaction, platinum electrodes are used on either side of the membrane. Within the PEMFC unit, hydrogen molecules are supplied at the anode and split in to hydrogen protons and electrons. The protons pass across the polymeric membrane to the cathode while the electrons are pushed round an external circuit in order to produce electricity. Oxygen (in the form of air) is supplied to the cathode and combines with the hydrogen ions to produce water.

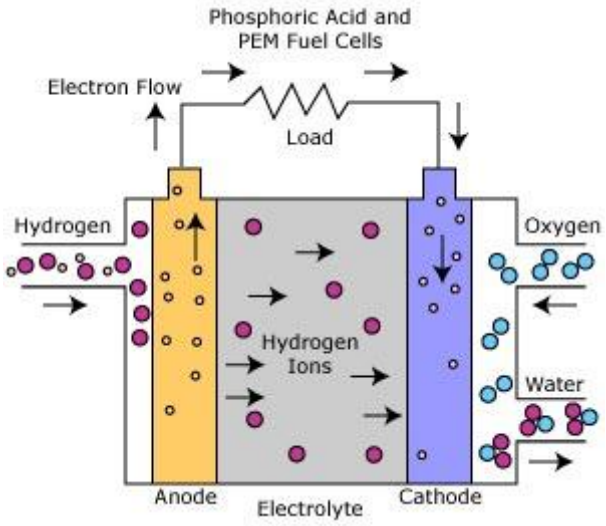

Figure 3.5. Diagram of a PEM fuel cell [e-net 2].

PEMFCs are characterized by low operative temperature (80 – 100 °C), high current density, compactness, fast start-ups and suitability for discontinuous operation [Mehta, 2003]. These features make PEMFCs the most promising and attractive candidate for a wide variety of power applications ranging from portable/micropower and transport to large-scale stationary power systems for buildings and distributed generation [Costamagna, 2001], as shown in Figure 3.6.

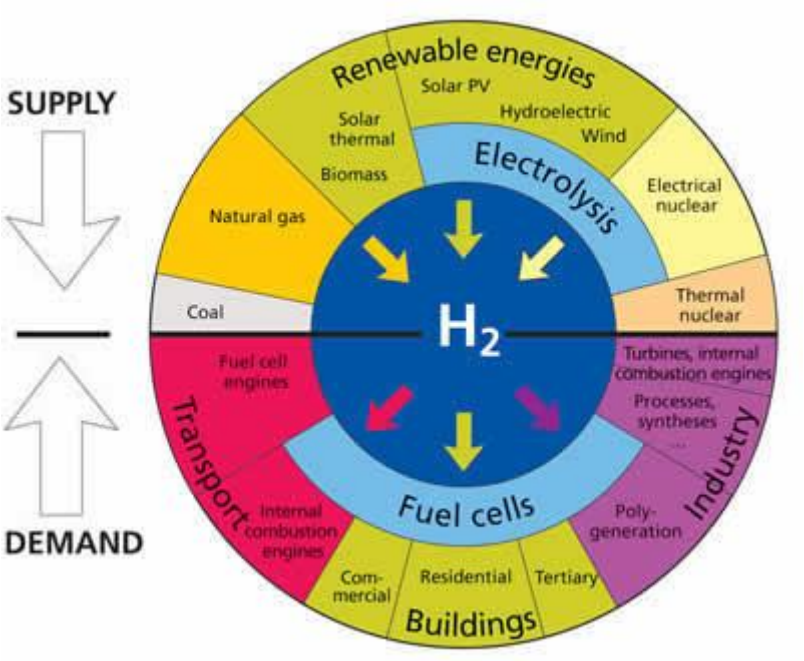

Figure 3.6. Summary of the hydrogen economy. Upper part: production – Lower part: uses. [e-net 3]

Today, the hydrogen for feeding to the PEMFCs comes, principally, from fossil fuels (48% from natural gas, 30% from oil, and 18% from coal) [e-net 4]. Nevertheless, owing to the climate change as well as the cost increase of oil and gas, the development of a strategy for exploiting alternative and renewable sources represent a top priority in which hydrogen could be an inexhaustible energy carrier [Rifkin, 2002].

Nevertheless, the full commercialization of PEMFC systems needs a stable supply of hydrogen, which must be characterized by high-purity for avoiding the CO poisoning of the anodic catalyst [Cheng, 2007].

Nowadays, the dominant technology for direct hydrogen production is steam reforming from hydrocarbons. Generally, the steam reforming reaction, carried out in conventional fixed bed reactors (FBRs), produces a hydrogen rich gas mixture containing carbon oxides and other by-products as well as the unreacted reactants. Therefore, in the viewpoint of feeding a PEMFC, which can tolerate only few ppm of CO, the hydrogen going out from a reformer needs to be purified by means of the following processes: two-steps water gas shift reactor followed by a separation/purification unit (PSA, Pd-membrane, etc.), as reported in Figure 3.7 (a) [Barelli, 2008].

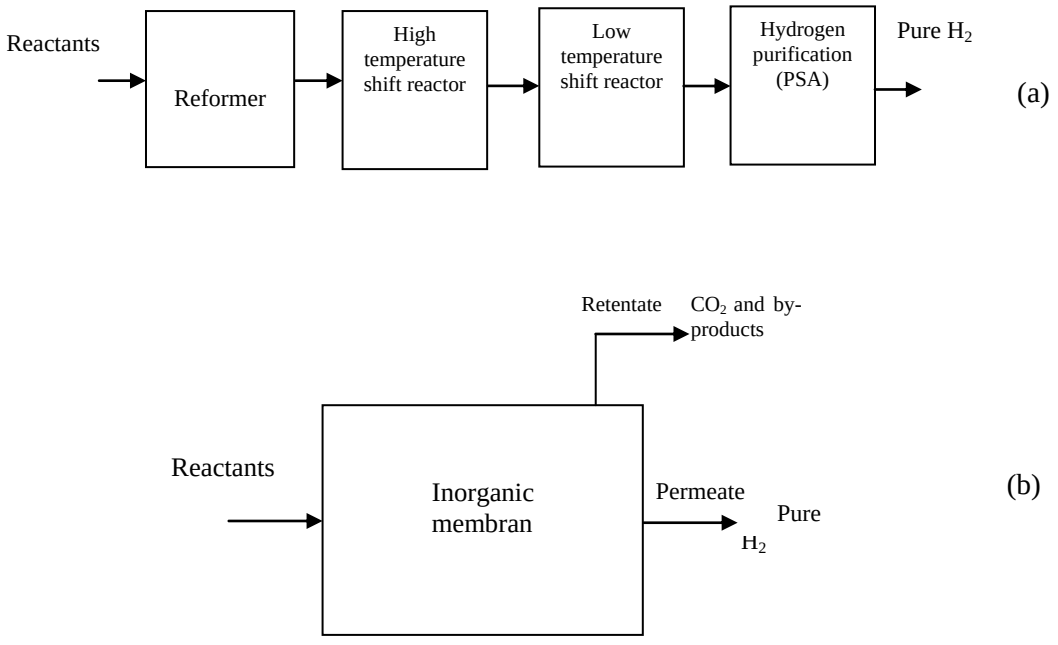

Figure 3.7. Scheme of pure hydrogen production by hydrocarbons compounds steam reforming: traditional scheme (a) and inorganic membrane reactor (b) [Basile, 2008].

Many researchers have proposed, as economically more advantageous method, the use of a process able to produce a pure hydrogen stream in only one system [Tosti, 2000 – Cheng, 2002 –Wieland, 2002 – Basile, 2008 – Valenti, 2008 – Damle, 2009]. In this contest, dense palladium MRs are able to both carry out the reaction and separate pure hydrogen stream in the same device (Figure 3.7 (b)). Among the different metals, niobium (Nb), vanadium (V) and tantalum (Ta) offer higher hydrogen permeability than palladium in a temperature range between 0 – 700 °C, as shown in Figure 3.8.

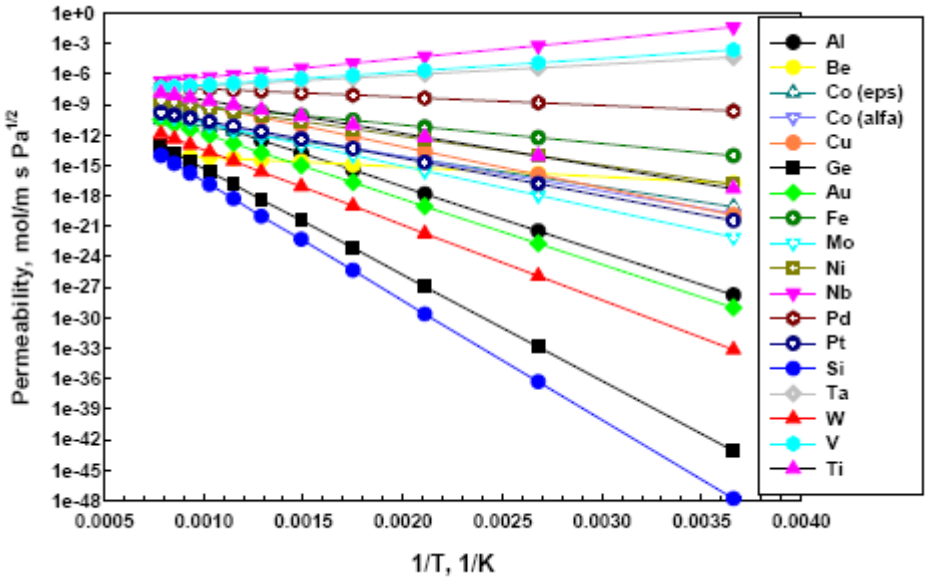

Figure 3.8. Hydrogen permeability through different metals [Gallucci, 2007].

Nevertheless, these metals have a stronger surface resistance to hydrogen transport than the palladium (Pd). For this reason, dense palladium membranes are most used.

Palladium is able to absorb about 600 times its volume of hydrogen at room temperature [Hughes, 2001], showing an infinite perm-selectivity to this gas [Tosti, 2004].

The hydrogen molecular transport in the palladium membranes occurs through a solution/diffusion mechanism, which follows six different activated steps [Koros, 1993]:

- ✓ dissociation of molecular hydrogen at the gas/metal interface,
- ✓ adsorption of the atomic hydrogen on membrane surface;
- ✓ dissolution of atomic hydrogen into the palladium matrix;
- ✓ diffusion of atomic hydrogen through the membrane;

- ✓ re-combination of atomic hydrogen to form hydrogen molecules at the gas/metal interface;
- ✓ desorbtion of hydrogen molecules.

Depending on temperature, pressure, gas mixture composition and thickness of the membrane, each one of these steps may control hydrogen permeation through the dense film [Basile, 2008]. As a result, the hydrogen permeating flux can be expressed by means of the following equation:

$$J_{H_2} = Pe_{H_2}(p^n{}_{H_2,ret} - p^n{}_{H_2,perm})/\delta \qquad (3.2)$$

where *n* (variable in the range 0.5 - 1) is the dependence factor of the hydrogen flux to the hydrogen partial pressure, J_{H2} is the hydrogen flux permeating through the membrane, *Pe* the hydrogen permeability, δ the membrane thickness, $p_{H2\text{-}ret}$ and $p_{H2\text{-}perm}$ the hydrogen partial pressures in the retentate (the reaction side) and permeate (side in which hydrogen permeating through the membrane is collected) sides, respectively.

This equation even points out the inverse proportionality to the membrane thickness. The role of the membrane thickness is very important. On one hand, a thinner membrane offers a higher permeability; on the other hand, thicker membranes are necessary in order to ensure the mechanical resistance and strength.

When the pressure is relatively low, the diffusion step is assumed to be the rate-limiting one and the factor *n* is equal to 0.5. In this case, the equation (3.2) becomes Sieverts-Fick law [Dolan, 2006]:

$$J_{H_2,Sieverts\text{-}Fick} = Pe_{H_2} \cdot (p^{0.5}{}_{H_2,ret} - p^{0.5}{}_{H_2,perm})/\delta \qquad (3.3)$$

On the contrary, at high pressures the hydrogen-hydrogen interactions in the palladium bulk are not negligible. In this case, n becomes equal to 1:

$$J_{H_2} = Pe_{H_2} \cdot (p_{H_2,ret} - p_{H_2,perm})/\delta \qquad (3.4)$$

The relationship between hydrogen permeability and temperature follows an Arrhenius behaviour (eq. 3.5), while the hydrogen partial pressure exponent not depends on the temperature:

$$Pe_{H_2} = Pe^0{}_{H_2}\, exp\,(-E_a/RT) \qquad (3.5)$$

where Pe_0 is the pre-exponential factor, E_a the apparent activation energy, R the universal gas constant and T the absolute temperature.

As a consequence, when Sieverts-Fick law is valid, the hydrogen flux is written in terms of the so-called Richardson's equation:

$$J_{H_2} = Pe^0_{H_2} [exp (-E_a /RT)] \cdot (p^{0.5}_{H_2,ret} - p^{0.5}_{H_2,perm})/\delta \quad (3.6)$$

Nevertheless, although the pure palladium membranes are characterized by a complete hydrogen perm-selectivity, their commercialization is limited by some drawbacks such as relatively low hydrogen permeability and high cost [Gallucci, 2007b].

3.2.1. Problems associated with the pure palladium membranes

The most important problem associated with the pure palladium membranes is the "hydrogen embrittlement" phenomenon. When the temperature is below 300 °C and the pressure below 2.0 MPa, the β–hydride phase may nucleate from the α-phase, resulting in severe lattice strains (see Figure 3.9), so that the pure palladium membrane becomes brittle after a few cycles of α⇆β□ transitions [Grashoff, 1983 – Lewis, 1988 – Hsieh, 1989].

These transitions do not take place as a change of the lattice structure, but as a lattice dilatation. The β-hydride phase formation isrepresented as a clustering of hydrogen atoms, whose energy of attraction, being associated with the lattice, strains around the dissolved hydrogen atom [Brodowsky, 1972].

A possible solution to avoid this phenomenon is represented by the use of a Pd-alloy containing an other metal, such as silver. The role of silver is explained by its electron donating behaviour, being largely similar to the one of the hydrogen atom in palladium. Silver and hydrogen atoms would compete for the filling of electron holes [Shu, 1991].

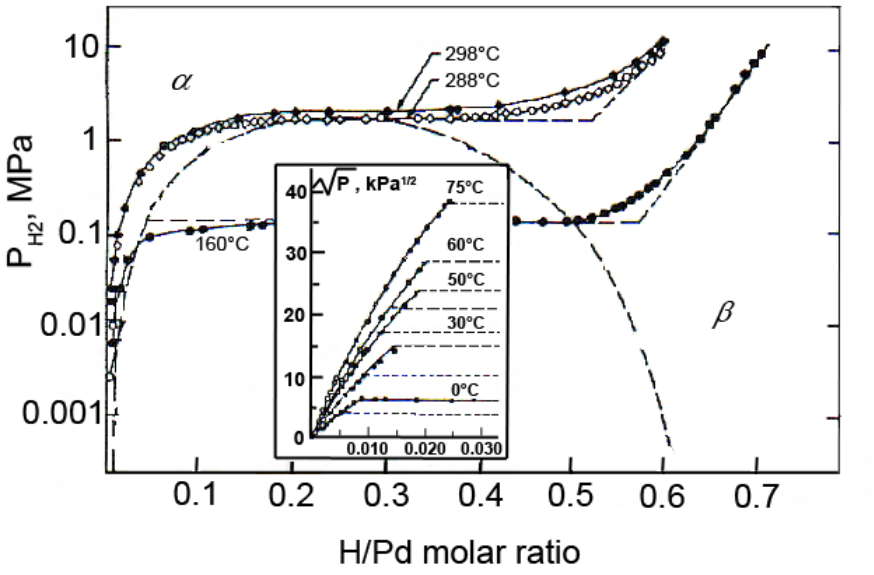

Figure 3.9. Equilibrium solubility isotherms of PdH_n for bulk Pd at different temperatures [Shu, 1991].

An other critical problem is represented by the palladium surface contamination of Hg vapour, hydrogen sulfide, SO_2, thiophene, arsenic, unsaturated hydrocarbons, chlorine carbon from organic materials. In particular:

- *Poisoning of sulphur compounds*: Pd-coated membranes could rapidly be destroyed after exposure to a gas stream containing hydrogen sulphide and the poisoning effects are irreversible [Edlund, 1993 – 1994]. Palladium becomes palladium sulphide, whose lattice constant is twice than of pure Pd and, thus, the structural stress leads to the formation of cracks.
- *Poisoning of CO*: the presence of CO in a feed gas stream could cause a decrease in the hydrogen permeation flux, because the adsorbed CO displaces the adsorbed hydrogen and further blocks hydrogen adsorption sites [Noordermeer, 1986]. Moreover, this reduction becomes more significant at low temperature (below 150 °C) or high CO concentration [Li, 2000]. CO is adsorbed on the palladium surface blocking available dissociation sites for hydrogen. For improving the chemical stability of the metal membranes it is possible:
  - ✓ to use different types of Pd alloys constituted by other metals such as Cu, Ni, Fe, Pt, and Ag,

- ✓ to prepare nanostructured or amorphous thin alloy membranes.

- *Poisoning of H_2O*: the presence of water vapour has a more negative effect on hydrogen permeability than the presence of CO [Amandusson, 2000]. The adsorbed water molecules dissociate on the surface of the Pd film:

$$H_2O_{ads} \rightarrow OH_{ads} + H_{ads} \quad \text{and/or} \quad H_2O_{ads} \rightarrow O_{ads} + 2H_{ads} \tag{3.9}$$

  where the H_{ads} may permeate into the bulk of the Pd film [Heras, 1997]. H_2O is recombined through these reactions:

$$2OH_{ads} \rightarrow H_2O_{gas} + O_{ads} \quad \text{and/or} \quad O_{ads} + 2H_{ads} \rightarrow H_2O_{gas} \tag{3.10}$$

  Therefore, the process of H_2O dissociation/recombinative desorption contaminates the palladium surface with adsorbed O.

- *Poisoning of coke*: both hydrogen permeance and perm-selectivity for a thin palladium membrane decrease after it is brought in contact with coke at elevated temperature [McCool, 2001]. This phenomenon can be addressed for the fact that carbon atoms penetrate into the palladium lattice and cause the failure of the membrane owing to the expansion of the palladium lattice.

Moreover, the palladium membranes are most expensive. In order to reduce their cost, it is possible develop non-palladium based or, at least, a low palladium content based alloys [Nishimura, 2002 – Luo, 2006 – Adams, 2007].

3.3. Palladium-based membranes

Generally, the palladium-based membranes can be supported and laminated ones. In the *supported membranes*, a thin dense layer of a palladium alloy is deposited on a porous support such as porous Vycor glass (silica gel). Nevertheless, using this kind of support, the fabricated metal film is easily stripped off owing to the loss of an anchor effect [Mallada, 2008].

Other type of porous glass materials are, thus, represented by SiO_2, Al_2O_3, and B_2O_3, giving excellent anchor effect and adherence [Mallada, 2008]. Also porous stainless steel (PSS) can be

considered as a valid support due to its mechanical durability, its thermal expansion coefficient close to that of palladium and the ease of gas sealing [Mallada, 2008]. Unfortunately, PSS support forms an alloy with the palladium at relatively high temperatures, leading to lower the hydrogen permeability. However, the upper temperature limits of the supported membranes depend on: the material, the chemical atmosphere and the support characteristics such as porosity and pore diameter [Uemiya, 1999].

In the *laminated membranes*, thin palladium (or palladium alloys) layer avoids the formation of oxides on the metallic surfaces resulting in a reduction of the hydrogen adsorption activation energy and consequently in an increase of the hydrogen permeation flux.

Generally, the palladium alloys have some advantages with respect to the pure palladium membranes such as a reduced critical temperature for the α-β phase transition. For example, Pd-Ag membranes can operate in hydrogen presence at temperatures below 300 ºC without the hydrogen embrittlement observed for pure palladium membranes [Shu, 1991]. Moreover, in some cases, the hydrogen permeability of palladium alloys is higher than pure palladium, as reported in Table 3.2. In fact, as shown also in Figure 3.10, the hydrogen flux through the Pd-Ag membranes reaches maximum value at 350 °C and 2.2 MPa with a 23% Ag content. In this case, the permeability is 1.7 times higher than one of a pure Pd membrane. The Pd-Cu alloy even shows a maximum value of hydrogen flux with 40% Cu content, although these membranes suffer a permeation decrease when exposed at 900 °C for a long time [Howard, 2004].

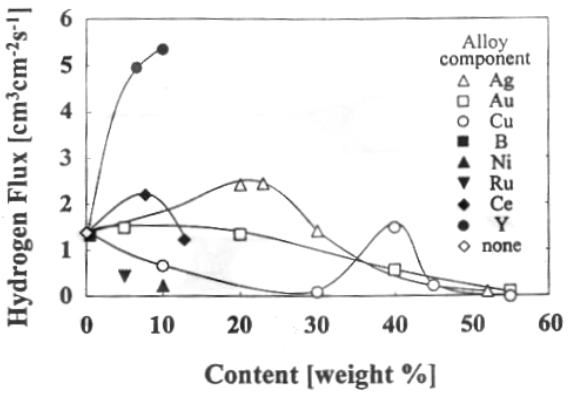

Figure 3.10. Hydrogen flux through palladium alloy membranes against metal content [Hwang, 1975].

Alloy metal	wt % for maximum permeability	Normalized permeability (Pe_{alloy}/Pe_{Pd})
Y	10.0	3.8
Ag	23.0	1.7
Ce	7.7	1.6
Cu	40.0	1.1
Au	5.0	1.1
Ru, In	0.5 - 6.0	2.8
Ag, Ru	30.2	2.2
Ag, Rh	19.1	2.6
Pure Pd	-	1.0

Table 3.2. Improvement in hydrogen permeability of various binary and tertiary palladium alloys at 350 ºC [Gryaznov, 2000].

Moreover, the palladium alloys improve chemical resistance of membrane. For example, Pd-Cu and Pd-Au increase the resistance to H_2S [McKinley, 1967], as well as palladium-coated amorphous Zr–M–Ni (M = Ti, Hf) alloy membranes are resistant enough in a hydrogen atmosphere and have stable hydrogen permeability in the range of 200 – 300 °C [Hara, 2002].

In order to reduce the further membrane cost, low palladium content based alloys can be produced [Adams, 2007]. In fact, Basile et al. [2008b] demonstrated that thin dense Ti–Ni–Pd membrane with a low palladium content (4.17% vs 77.0% of the Pd-Ag and 60.0% of the Pd-Cu) make this membrane still competitive from an economical point of view.

3.3.1. Palladium-based membranes production methods

Palladium-based membranes can be produced by several methods, depending on some factors such as the nature of the metal itself, the manufacturing facilities, required thickness, surface area, shape, purity, etc. Nevertheless, no one method can produce a membrane, which combine advantageously all these factors. Therefore, the choice of the production method becomes a compromise between these factors [Shu, 1991]. In lab-scale, the thickness as well as the continuity and imperviousness of the film are considered the more important factors [Shu, 1991]. In particular, in the last few years, the main aim has been to reduce the thickness of the palladium-based films. The most important production methods of palladium-based membranes are described in the following.

The ***conventional cold rolling*** is the most diffuse technique for producing metallic plates or sheets at laboratory scale [Wilde, 2005]. It involves:

- melting the raw materials with chosen composition at very high temperature,
- ingot casting,
- high temperature homogenization,
- hot and cold forging or pressing, followed by repeated sequences of alternate cold rolling and anneals, down to the required thickness.

If the cooling speed of melts is fast, amorphous materials (*metallic glasses*) can be realized obtaining good characteristics such as high mechanical toughness, considerable corrosion resistance, good electronic properties, high catalytic activities, reversible hydrogen storage, etc. [Smith, 1981 – Molnar, 1989]. The cold rolling treatment can enhance the hydrogen solubility in palladium and its alloys owing to the accumulation of hydrogen excess in the stress field around dislocations, formed during the process. This effect can be gradually eliminated during annealing of the deformed membranes by increasing the temperature [Kishimoto, 1990].

In ***physical vapour deposition*** (PVD) method, the solid material to be deposited is evaporated in a vacuum system through physical techniques, followed by condensation and deposition as a thin film on a cooler substrate. PVD is a very versatile method for manufacturing of pure metal films, alloys or compounds of thickness up to 50 μm [Reichelt, 1990]. At relatively high temperature, thermal treatment is generally necessary to homogenize the composition of a multilayer deposit [Mattox, 1998].

Sputtering and magnetron sputtering (MS) is an evaporation technique used for PVD under vacuum. A sputtering system consists of a vacuum chamber containing a target (a plate of the material to be deposited) and the substrate (*i.e.* the membrane), in which a sputtering gas (an inert gas such as argon) is introduced to provide the medium in which a glow discharge, or plasma, may be initiated and maintained. Afterwards, positive ions strike the target and remove target atoms and ions by momentum exchange. The condensation of these species over the support produces a thin

film. Before sputtering the metal, the ion bombardment of the support is carried out for cleaning its surface and improving the film adherence.

Spray pyrolysis is very simple technique in which a metal salt solution is sprayed into a heated gas stream and, then, pyrolysed. It could be useful in the case of not requiring very high purity of hydrogen due to the relatively low H_2/other gases perm-selectivity showed by using this technique. Compared to the other deposition techniques, the spray pyrolysis method shows quite low separation factor, indicating that the technique needs some improvements, especially for producing dense films.

Solvated metal atom deposition method (or co-condensation technique) allows the easy introduction of the metal phase on the inner surface of a tubular membrane. Palladium vapour obtained by the resistive heating of a crucible loaded with Pd shots is co-condensed in a typical glass reactor. At the end of the reaction, the flask is allowed to warm up to – 40 °C and the resulting yellow-brown solution siphoned under argon and handled at low temperature, using the Schlenk tube technique. The amount of palladium in the isolated solution is determined by X-ray fluorescence. Palladium particles are deposited on the inner surface of a tubular membrane by filling the membrane tube (fitted with Teflon stoppers at the ends) with the above solution and heating up to room temperature.

In ***chemical vapour deposition*** (CVD) process, a chemical reaction involving a metal complex in the gas phase is performed at a controlled temperature and the produced metal deposits as a thin film by nucleation and growth on the substrate [Jones, 2008]. The deposition takes place on the hot substrate positioned in the CVD reactor. As in the case of PVD technique, the reaction temperature can be reached either by resistive heating of the substrate or by other heating sources [Biswas, 1986].

Electrochemical vapour deposition (EVD) is, essentially, a variation of the CVD technique. In the EVD process, for example, a porous substrate separates a mixture of chlorine vapours (ZCl_3, YCl_3, etc.) and an oxygen source (water vapour or oxygen) [Mulder, 1996]. Initially, the reactants from

both sides of the support inter-diffuse into the pores and form solid oxides, as in the CVD process. When the pores are closed, oxygen ions are conducted across the solid oxide and the oxide film grows on the chlorine side.

In the ***electroplating*** (EP) method, a substrate, used as a cathode, is coated with a metal or an alloy in a plating bath [Mohler, 1969]. Palladium can be easily deposited in thick and ductile deposits, providing a good control on the composition of the bath, its temperature and current density [Wise, 1968]. The thickness of deposited films can be mastered by controlling electroplating time and current density [Sturzenegger, 1984 – Reid, 1985] and film values from a few microns up to millimetres can be obtained. However, the large domains of alloy composition is not easy to control since the relative deposition of two metals simultaneously from the same solution depends on the simplicity of controlling chemical complexing in the bath [Mulder, 1996].

The ***electroless plating deposition*** (ELP) technique is based upon the controlled auto-catalyzed decomposition or reduction of meta-stable metallic salt complexes on target surfaces [Loweheim, 1974]. In the case of palladium, usually, the substrate should be pre-seeded with palladium nuclei in an activation solution in order to reduce the induction period of the autocatalytic plating reaction. For some applications, this technique provides strong benefits such as uniformity of deposits on complex shapes and hardness. Palladium and some of its alloys are among the few metals that can be deposited in this way [Mulder, 1996]. However, this method presents some drawbacks such as difficult thickness control, costly losses of palladium in the bath, non guaranteed purity of the deposit and so on [Loweheim, 1974].

Sol-gel technique is a technique adopted for the preparation of thin materials on which the morphological characteristics (*e.g.* thickness and porosity) must be accurately controlled. Composite membranes resulting from this process are usually microporous and mesoporous, on which permeation of gases is mainly controlled by surface transport and/or the Knudsen flow mechanism [Mulder, 1996].

Molecular layering (ML) technique is one of the most promising methods of membrane modification at the atomic level [Malygin, 2006 – Tereshchenko, 2006]. The ML method is based on the chemisorptions of reagents on a solid substrate surface and consists of the irreversible interaction of low-molecular reagents and functional groups of a solid substrate surface under the conditions of continuous reagent feed and the subsequent removal of the formed gaseous products.

However, each aforementioned method presents advantages and drawbacks. For example, both CVD and ELP techniques are able to coat a complex-shaped component with a uniform thickness layer. Unfortunately, non desired compounds and impurities can be formed and incorporated in the Pd layer, reducing the flux of hydrogen through the film. Moreover, by ELP method, it is not easy to control the thickness of the film. On the contrary, an important benefit of electroless coating is that it is well suited to applications on available commercial tubular membranes. CVD is not an economic process due to the strict conditions required for the process.

In conclusion, Table 3.3 reports the permeation data of different palladium-based composite membranes, produced, principally, by ELP or CVD techniques. Many parameters are reported in the table: membrane type and thickness, temperature and pressure ranges of the permeation experiments, hydrogen flux, hydrogen permeance, ideal separation factor, preparation method of the metallic thin layer and relative bibliography. Generally, it is possible to state that the porous palladium-based membranes have high gas fluxes and low selectivities, while dense palladium-based membranes show low hydrogen flux and high hydrogen selectivity.

Membrane type	T [°C]	Δp [bar]	δ [μm]	J_{H2} [mol/m^{2}s]	$\alpha_{H2/N2}$	Preparation method	References
Pd/PSS-YSZ	400	-	7-10	$2.5\cdot10^{-2}$	800-900	ELP	Huang, 2007
Pd/Al_2O_3	200	0.1	15	$2.2\cdot10^{-1}$	7	ELP	Altinisik, 2005
Pd/glass	350-500	4.0	2	-	1140-12900	ELP	Wang, 2004
Pd/Al_2O_3	450	-	4.8	-	60	ELP	Van Dyk, 2003
Pd/Al_2O_3	300	0.3	2-4	$1.0\text{-}2.0\cdot10^{-1}$	5000	CVD	Itoh, 2005
Pd/Al_2O_3	528	-	2-3	-	<18	ELP	Kleinert, 2005
Pd/Al_2O_3	400	1.0	5	$1.6\cdot10^{-1}$	100-200	ELP	Liang, 2005
Pd/$BaZrO_3$	600	-	41	-	5.7	CVD	Okada, 2007
Pd/MPSS	500	1.0	6	$3.0\cdot10^{-1}$	-	ELP	Tong, 2005b
Pd/PNS	500	3.6	-	$8.3\cdot10^{-2}$	3.7	MS	Ryi, 2006
Pd/PSS	520	1.5	10	$1.8\cdot10^{-1}$	-	ELP	Basile, 2008b
Pd/ZrO_2/PSS	500	1.0	10	$8.3\cdot10^{-2}$	-	ELP	Wang, 2004b
Pd/αAl_2O_3	370	2.9	1	$4.0\cdot10^{-1}$	3000-8000	ELP	Nair, 2007
Pd_{84}–Cu_{16}/ZrO_2-PSS	480	2.5	5	$6.0\cdot10^{-1}$	∞	ELP	Gao, 2005
Pd_{90}–Ag_{10}/αAl_2O_3	200-343	0.8– 2.5	20	$1.4\cdot10^{-1}$	30-178	ELP	Huang, 2003
Pd–Ag/Al_2O_3	-	1.4	10	$1.0\cdot10^{-1}$	1500	ELP	Liang, 2005b
Pd–Ag/PSS	400-500	1.0	2-3	$3.0\cdot10^{-1}$	-	ELP	Tong, 2005c
Pd/αAl_2O_3	550	4.0	11	$7.0\cdot10^{-2}$	~1000	ELP	Nair, 2007b
Pd-Cu/αAl_2O_3	450	3.5	11	$8.0\cdot10^{-1}$	1150	ELP	Roa, 2003
Pd-PSS	320-500	-	20	-	-	ELP	Aspen Systems, 1999
Ti-Ni-Pd	450	3.0	45	$\sim3.3\cdot10^{-3}$	∞	Cold rolling	Basile, 2008b

Table 3.3. Permeation data of different palladium-based membranes reported in the literature.

3.4. Reaction processes using palladium-based membranes

The first use of palladium membranes was registered in the 1866, when Graham used a palladium membrane to separate hydrogen from gases mixtures [Graham, 1866]. In 1915, Snelling patented the hydrogen removal through palladium or platinum tubes from a reactor using a granular catalyst for dehydrogenation reactions [Mallada, 2008]. In 1964, Gryaznov proposed as a novel application of palladium-based membranes a method for carrying out simultaneously the evolution and the consumption of hydrogen in a dense tubular palladium reactor, where palladium is permeable only to hydrogen and also serves as a catalyst.

The first commercial application of a dense 23 wt% Pd-Ag membrane happened in the 1964, when Johnson Matthey used this membrane for purifying a hydrogen reach stream [Booth, 1996]. Successively, Johnson Matthey also developed a hydrogen generator constituted by a palladium MR fed with a methanol/water mixture. This plant was used in small scale by British Antarctic Survey in 1975 [Cole, 1981 – Philpott, 1985].

Moreover, the first pilot-scale composite palladium MR for direct ultra-pure hydrogen production has been realized by the largest gas company in Tokyo (Tokyo Gas Company Ltd.).

Actually, the palladium-based MR represents an alternative solution to conventional systems for pure hydrogen production to be feed a PEMFC.

In fact, the palladium-based MR, combining in only one unit the separation phase with the reaction steps, offers the following advantages with respect to a FBR:

- to combine the chemical reaction and the gas separation in only one system reducing the capital costs,
- to enhance the conversion of equilibrium limited reactions. In fact, by the selective removal of one or more products from the reaction side, the thermodynamics equilibrium restrictions can be overcome, due to the so called “shift effect”,
- to achieve higher conversions than FBRs, operating at the same MR conditions, or, on the contrary, the same conversion, but operating at milder conditions,
- to improve products yield and selectivity,
- and, especially, to produce a pure hydrogen stream.

In order to produce pure hydrogen stream by using a palladium-based MR, many chemical reactions can be used, as reported in Table 3.4.

Kind of reaction	**Membrane**	**Material**
Coupling of hydrogenation and dehydrogenation reactions	dense	Pd
Decomposition of RuO_4 to $RuO_2 + O_2$	dense	Pd/Ag
Decomposition of ammonia	dense	Pd
Dehydrogenation of cyclohexane to benzene	dense	Pd/Ag
Dehydrogenation of ethylbenzene to styrene	porous	Pd
Dehydrogenation of ethane to ethylene	dense	Pd/Ag
Dehydrogenation of isopropyl alcohol to acetone	dense	Pd
Dehydrogenation of water-gas shift reaction	dense porous	Pd, Pd/Ag Pd
Dehydrogenation of n-heptane to toluene + benzene	dense	Pd/Rh
Dehydrogenation of butane to butadiene	dense	Pd
Dehydrogenation of 1,2-cyclohexanediol	dense	Pd/Cu
Dry reforming of methane	dense	Pd-alloy
Hydrogenation of ethylene to ethane	dense	Pd
Hydrogenation of butadiene	dense	Pd
Hydrogenation of acetylene	dense	Pd/Ag
Hydrogenation of butenes	dense	Pd/Sb
Hydrogenation of diene hydrocarbons	dense	Pd/Ru
Hydrogenation of phenol to cyclohexanone	dense	Pd; $Pd_{93}Ni_7$; $Pd_{93}Ru_7$; $Pd_{77}Ag_{23}$
Hydrodealkylation of dimethylnapthalenes	dense	Pd/Ni
Methane conversion into hydrogen and higher hydrocarbons	porous	Pd-al1oy
Octane reforming	dense	Pd and Pd-al1oy
Partial oxidation of methane	porous	Pd-alloy
Steam reforming of ethanol	dense	Pd and Pd-al1oy
Steam reforming of methane	dense	Pd-alloy
Steam reforming of methanol	dense	Pd and Pd-al1oy

Table 3.4. Chemical reactions for producing pure hydrogen by using a palladium-based MR.

In this chapter, a particular attention will be address to the following reactions:

- methane steam reforming
- dry reforming of methane
- water gas shift
- ethanol steam reforming
- methanol steam reforming
- bioglycerol steam reforming
- acetic acid steam reforming.

Moreover, in order to solve the problems related to the environmental pollution, previously mentioned, it will be interest to investigate the hydrogen production via reforming reaction of

biofuels, such as methanol, glycerol, ethanol, biogas, etc., which can be produced by renewable sources such as biomass, as reported in Figure 3.11.

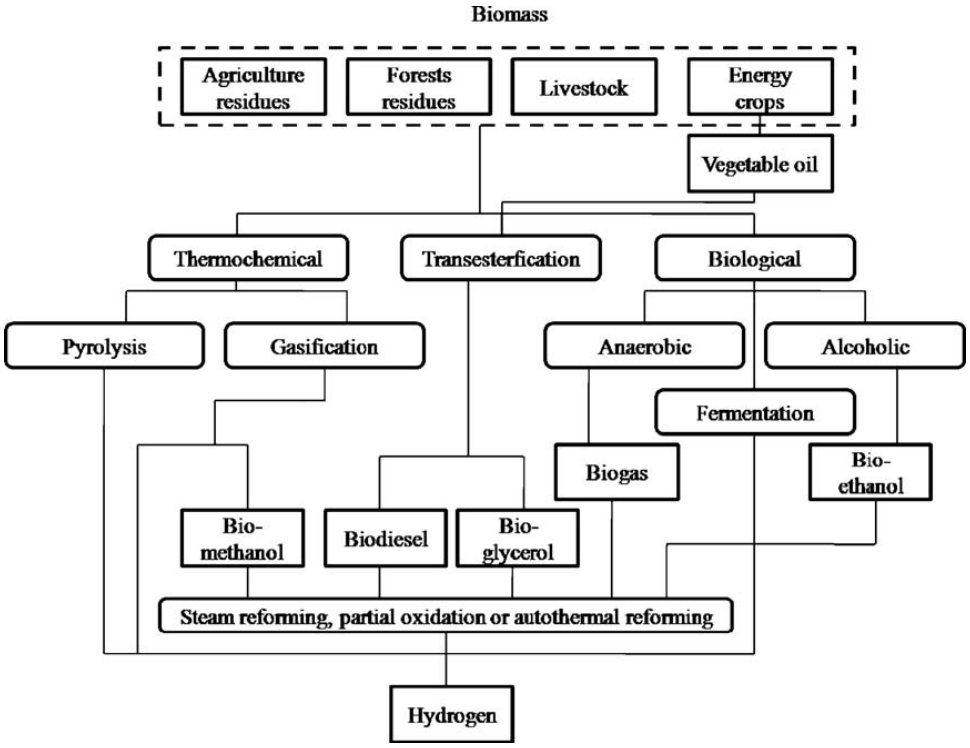

Figure 3.11. Selected hydrogen production technologies from various renewable sources [Xuan, 2009].

3.4.1. Methane steam reforming

The methane can be renewably obtained via biogas generated by the fermentation of organic matter including wastewater sludge, municipal solid waste (including landfills) or any other biodegradable feedstock, under anaerobic conditions [Martins das Neves, 2009]. Generally, the methane steam reforming (MSR) reaction is carried out in a FBR at 800 - 900 °C due to the endothermicity of the reaction [Barelli, 2008].

$$CH_4 + 2H_2O \leftrightarrows 4H_2 + CO_2 \qquad \Delta H^{\circ}_{298\,K} = 165.0\ kJ/mol \qquad (3.11)$$

Only at this elevated temperature, the methane conversion in a FBR is complete. Furthermore, in these conditions, the catalyst undergoes deactivation due to carbon formation. On the contrary, in Pd-based MRs it is possible to reach the complete methane conversion at lower temperature (~500 °C) as summarized in Table 3.5. For example, Lin *et al.* [2003], carried out the MSR reaction in palladium-based MR, obtaining a methane conversion exceeding 80% at 500 °C with respect to 850

°C necessary in a FBR. Chen *et al.* [2008] obtained almost 100% methane conversion at 550 °C with respect to 27% obtained in a FBR. In particular, the authors reached 95% pure hydrogen recovery, confirming that the selective removal of hydrogen from the reaction zone allows to obtain methane conversion significantly higher than a FBR.

Membrane	**T [°C]**	**$p_{reaction}$ [bar]**	**MR conversion [%]**	**FBR conversion [%]**	**Pure hydrogen recovery [%]**	**Authors**
Pd	727	19.6	94	-	-	Nazarkina, 1979
Pd	800	-	96	-	-	Oertel, 1987
Pd/Vycor	500	1.0-9.1	90	-	-	Uemiya, 1991
Pd/ 5.1%Ag	500	1.4	50	35	-	Shu, 1995
Pd-23% Ag	500	6.1 10.0	50 60	~20 (equilibrium)	- -	Jorgensen, 1995
Pd-based	500	1.0	100	-	-	Kikuchi, 2000
Pd-25%Ag	150 300	1.0	15.4 16.5	12.7 16.5	- -	Basile, 2003
Pd-SS	500	20.0 9.0	85 40	- 20	90 30	Lin, 2003
Pd-PSS	527	3.0	100	~50	-	Tong, 2005
Pd-based	650	2.0- 4.0	97	-	-	Patil, 2007
Pd/Al_2O_3	550	9.0	99	27	95	Chen, 2008

Table 3.5. Methane conversion and pure hydrogen recovery data for methane steam reforming reaction.

Generally, the Table 3.5 shows that the palladium-based MRs use permits to reduce the operative conditions required for carrying out the MSR reaction in a FBR and to obtain high methane conversion as well as high pure hydrogen recovery.

3.4.2. Dry reforming of methane

One of the most important problem in the methane dry reforming reaction is the carbon deposition.

$$CH_4 + CO_2 = 2CO + 2H_2 \qquad \Delta H°_{298\,K} = +247.0\ kJ/mol \qquad (3.12)$$

In fact, Galuszka *et al.* [1998] observed carbon formation carrying out the reaction (3.12) at 550 - 600 °C in both FBR and MR (housing dense palladium membrane prepared by electroless-plating).

Gallucci *et al.* [2008] performed the methane dry reforming reaction in FBR and both a porous and a dense Pd–Ag MRs at 400 and 450 °C. The authors demonstrated that the MRs give lower deposited carbon with respect to the FBR and, in particular, the lower carbon deposition is obtained when the dense membrane is used.

Membrane	**T [°C]**	**MR conversion [%]**	**FBR conversion [%]**	**Authors**
Pd-based	550	37.5	17.2	Galuszka, 1998
	600	48.6	40.9	
Porous Pd-Ag	400	2.1	5.6	Gallucci, 2008
	450	8.4	17.4	
Dense Pd-Ag	400	7.9	5.6	Gallucci, 2008
	450	17.8	17.4	
Pd/ceramic composite	500	54	-	Kikuchi, 1995

Table 3.6. Methane conversion data for methane dry reforming reaction.

In this case, the palladium-based MR advantages result in higher methane conversion than FBR, as reported in Table 3.6 and a reduction of the carbon deposition with respect to a conventional reformer.

3.4.3. Water gas shift reaction

The water gas shift (WGS) reaction is one of the most important industrial reactions used to produce hydrogen.

$$CO + H_2O = CO_2 + H_2 \qquad \Delta H°_{298\ K} = -41.1\ kJ/mol \qquad (3.13)$$

CO conversion values obtained in MR and compared with the thermodynamic equilibrium ones of some scientific works are resumed in Table 3.7. In particular, among these works, Kikuchi *et al.* [1989] demonstrated that, using a 20 μm layer of palladium coated onto a porous glass tube, permitted to reduce the amount of steam needed to achieve reasonable levels of CO conversion. Basile *et al.* [2001] studied the WGS reaction using a MR consisting of a composite membrane realized with an ultrathin palladium film (~ 0.1 μm) coated on the inner surface of a porous ceramic

support (γ-Al_2O_3) by the co-condensation technique. The authors obtained 96% CO conversion with respect to 70% the thermodynamic equilibrium working at 320 °C and 1.1 bar. Moreover, they illustrated that a 98% CO conversion could be reached by using a composite membrane with a 10 μm Pd film coated on a ceramic support [Basile, 1995]. Moreover, Iyoha *et al.* [2007] observed that the conversion decreased from 93% to 66% once the Pd-based MR was replaced with another MR containing a $Pd_{80}Cu_{20}$ membrane, due to the lower hydrogen permeance of the Pd/Cu membrane.

Membrane	**T [°C]**	**$p_{reaction}$ [bar]**	**MR conversion [%]**	**Equilibrium conversion [%]**	**Authors**
Pd/Vycor	400	1.0	92	76	Kikuchi, 1989
Pd on porous glass	400	1.0	98	75	Uemiya, 1991b
Pd on ceramic	320	1.0	98	83	Basile, 1995
Pd-composite	322	1.1 1.2	99.2 99.9	99.1	Basile, 1996
Pd/γ- Al_2O_3	320	1.1	100	84	Basile, 2001
Pd Pd_{80}-Cu_{20}	900	2.4	93 66	-	Iyoha, 2007
Pd-Ag	325	1.0	100	84	Tosti, 2000b
Pd Mesoporous Pd	320	1.3-1.5	100 78	<50	Criscuoli, 2000
Pd(60%)-Cu	350	-	94	93	Flytzani-Stephanopoulos, 2004

Table 3.7. CO conversion data for water gas shift reaction.

In the Table 3.7, the comparison between the CO conversion values obtained in different palladium-based MRs and the equilibrium ones is reported, demonstrating the capacity of palladium-based MRs to overcome the thermodynamic limits and to obtain high CO conversion.

3.4.4. Ethanol steam reforming

Ethanol can be produced by renewable sources via bioethanol distillation. Bioethanol is an aqueous solution containing between 8.0 and 12.0% wt of ethanol and some by-products depending on the raw material used [Pfeffer, 2007]. Nevertheless, the bioethanol distillation is an expensive process,

because of the azeotrope presence. For this reason, in the last years, bioethanol is directly used as fuel in steam reforming reaction. Moreover, an excess of water improves the palladium-based MR performances reducing also the CO content as by-products.

$C_2H_5OH + 3H_2O = 2CO_2 + 6H_2$ $\Delta H°_{298\,K} = +157.0$ kJ/mol (3.14)

Most part of scientific literature is focused on carrying out this reaction using ethanol produced by no-renewable sources. Concerning the bioethanol steam reforming (BESR) reaction, only few studies are carried out in a FBR [Dolgykh, 2006 – Frusteri, 2006 – Benito, 2005] and MR [Gernot, 2006 – Iulianelli, in press – press b], as reported in Table 3.8.

In particular, Gernot *et al.* [2006] used a composite Pd-based MR, whose structure consists of a three layers stacking. This membrane structure reduces the thermal expansion stresses between the membrane and the support. As best results, a complete bioethanol conversion and a pure hydrogen stream were obtained with an impurity content < 1.0 % at 600 °C and for 500 h of work.

Iulianelli *et al.* [in press – in press b] studied from an experimental point of view the steam reforming reaction of a simulated bioethanol mixture (water/ethanol feed molar ratio = 18.7/1 mol/mol without other typical byproducts) in order to produce pure hydrogen in a dense Pd-Ag MR. The dense Pd-Ag membrane was prepared by cold-rolling and diffusion welding technique [Tosti, 2004]. Working at 400 °C and 3.0 bar, the authors obtained a complete bioethanol conversion (~ 85.0% for the FBR working at the same MR operating conditions) and around 95.0 % pure hydrogen recovery.

Membrane	**T [°C]**	**$p_{reaction}$ [bar]**	**MR conversion [%]**	**FBR conversion [%]**	**Pure hydrogen recovery [%]**	**Authors**
Dense Pd-Ag	400	1.3	99	-	-	Basile, 2006 – 2008c
Pd-based	600	-	100	-	-	Gernot, 2006
Dense Pd-Ag	400	1.5	95	60	30	Iulianelli, in press
Dense Pd-Ag	400	3.0	100	65	95	Iulianelli, submitted

Table 3.8. Ethanol conversion and pure hydrogen recovery data for ethanol steam reforming reaction.

The Table 3.8 shows the capacity of palladium-based MRs to obtain higher ethanol conversions than FBR.

3.4.5. Methanol steam reforming

Methanol is produced from natural gas [Cifre, 2007]. Alternatively, methanol can be produced from biomass, such as wood and agricultural waste [Cifre, 2007]. Renewable methanol presents different advantages as fuel and raw material. For example, it is more easily transportable than methane or other fuel gases, it has high energy density and does not require desulphurization.

Methanol steam reforming (SRM) is an endothermic reaction, feasible at temperatures of 200 - 300 °C [Wieland, 2002].

$$CH_3OH + H_2O = CO_2 + 3H_2 \qquad \Delta H°_{298\,K} = +49.7\ kJ/mol \qquad (3.15)$$

Wieland *et al.* [2002] carried out the SRM reaction using three different palladium-based MRs (Pd_{75}-Ag_{25}, Pd_{60}-Cu_{40} and Pd-V-Pd). Since the coated vanadium membrane was not stable at pressures above 4.2 bar, the authors compared only the Pd-Ag membrane with the Pd-Cu one, as reported in Table 3.9. The authors showed that the higher pure hydrogen recovery is obtained using the Pd-Ag MR (at 25.0 bar, 300 °C, the hydrogen recovery of Pd-Ag MR is 96.0%, while 78.0% for Pd-Cu MR). Lin *et al.* [2000 – 2001] used a double-jacketed supported palladium MR packed with $Cu/ZnO/Al_2O_3$ catalyst. The authors obtained a pure hydrogen recovery over 70.0%, concluding that this process can be an alternative solution of on-board hydrogen generation for electric vehicle fuel cells. Basile *et al.* [2005], compared the performances in terms of methanol conversion and pure hydrogen production with respect to the ones of a FBR. The authors demonstrated that the MR gives a higher methanol conversion at each operating condition investigated. As best results, a 80.0% methanol conversion is reached working at 250 °C and 1.3 bar, as reported in Table 3.9. Arstad *et al.* [2006] used a self-supported, Pd/(23 wt.%) Ag-based MR (with a thickness of 1.6 μm) achieving 100.0% the production of pure hydrogen. Hence, the authors concluded that the low-thickness palladium-based membrane use can represent a fundamental step for reducing the

palladium-cost and making competitive the hydrogen separation technologies by palladium-based membrane.

Membrane	T [°C]	$p_{reaction}$ [bar]	MR conversion [%]	FBR conversion [%]	Pure hydrogen recovery [%]	Authors
Pd-Ag	300	25.0	-	-	96	Wieland, 2002
Pd-Cu					78	
Dense Pd-Ag	250	1.3	80	40	-	Basile, 2005
MR1	350	1.3	30	86	-	Basile, 2006b
	600		100		-	
MR2	350		45		-	
	550		65		-	
MR3	350		87		-	
	450		100		-	
Dense Pd-Ag	300	1.3	100	55	-	Basile, 2008d
Dense Pd-Ag	300	3.0	-	-	93	Iulianelli, 2008 – 2008b
Pd-Ag	450	5.2	76	-	15	Damle, 2009
	550	5.2	73		45	
		7.9	72		50	
		11.4	71		53	
	600	11.4	75		60	

Table 3.9. Methanol conversion and pure hydrogen recovery data for methanol steam reforming reaction.

3.4.6. Bioglycerol steam reforming

Bioglycerol is a byproduct of biodiesel production [Valliyappan, 2008]. Biodiesel is usually derived from the transesterification of vegetable oil with methanol or ethanol. During the process, the oil is mixed with a metallic base (sodium or potassium hydroxide) and an alcohol (methanol or ethanol). The reaction produces methyl or ethyl ester (biodiesel) and glycerol as a byproduct, which can be used as a renewable source [Adams, 2004]. To the best of our knowledge, at moment, only Iulianelli *et al.* [in press c – submitted] studied glycerol steam reforming (GSR) reaction in a dense Pd-Ag MR, as reported in Table 3.10.

$$C_3H_8O_3 + 3H_2O = 3CO_2 + 7H_2 \qquad \Delta H°_{298\,K} = +346.4\ kJ/mol \qquad (3.16)$$

The authors studied the catalyst influence on the reactor performances (glycerol conversion and pure hydrogen recovery), using two commercial catalysts: Co/Al_2O_3 and Ru/Al_2O_3. Using Co/Al_2O_3 catalyst, the authors obtained as best result at 4.0 bar and 400 °C, a glycerol conversion of 94.0%

and a pure hydrogen recovery higher than 60.0%. Vice versa, using Ru/Al_2O_3 catalyst, the authors achieved around 20.0% glycerol conversion and 16.0% pure hydrogen recovery at 5.0 bar. Iulianelli justified these low performances as the main drawback due to the combination of ruthenium with an acid support as Al_2O_3, unfavorable for GSR reaction. Moreover, the authors observed that carbon formation, taking place during the reaction, affects negatively the performances of the Pd-Ag membrane in terms of a lower hydrogen permeated flux and catalyst deactivation.

Membrane	T [°C]	$p_{reaction}$ [bar]	MR conversion [%]	FBR conversion [%]	Pure hydrogen recovery [%]	Authors
Dense Pd-Ag	400	4.0	94	40	60	Iulianelli, in press c
Dense Pd-Ag	400	5.0	60	42	58	Iulianelli, submitted

Table 3.10. Glycerol conversion and pure hydrogen recovery data for glycerol steam reforming reaction.

3.4.7. Acetic acid steam reforming

Acetic acid is a renewable source and can be easily obtained by fermentation of biomass [Liu, in press]. Few studies [Takanabe, 2004 - Hu, 2007 – Bimbela, 2007, Basagiannis, 2007] concerned the acetic acid steam reforming (AASR) reaction for producing hydrogen by means only FBRs.

$$CH_3COOH + 2H_2O = 2CO_2 + 4H_2 \qquad \Delta H°_{298\,K} = +134.9\ kJ/mol \qquad (3.17)$$

Only two scientific papers were published dealing with the use of MR for carrying out the AASR reaction [Basile, 2008e – Iulianelli, 2008c], as shown in Table 3.11. In these studies, the AASR reaction was performed in a dense Pd-Ag MR packed with two kinds of catalyst: a Ni-based commercial catalyst in the first case and both Ru-based and a Ni-based commercial catalysts in the second case. In both experiments, a complete acetic acid conversion was obtained.

Membrane	T [°C]	$p_{reaction}$ [bar]	MR conversion [%]	FBR conversion [%]	Pure hydrogen recovery [%]	Authors
Dense Pd-Ag (MR1)	400	2.5	100	85	32	Basile, 2008e
	450		100	75	36	
Dense Pd-Ag (MR2)	400		100	92	26	
	450		100	87	32	
Dense Pd-Ag	400	4.0	100	-	70	Iulianelli, 2008c

Table 3.11. Acid acetic conversion and pure hydrogen recovery data for acetic acid steam reforming reaction.

Conclusions

An extensive overview concerning palladium-based membranes was presented, subsequently to a general classification of the membranes. In particular, an assessment of the problems associated with the pure palladium membranes was presented, which was followed by a description of the preparation methods of palladium-based membranes and their industrial applications.

In particular, this chapter highlighted the importance of palladium-based membranes for producing pure hydrogen. Applicability of these membranes is limited by sensitivity towards certain species and cost. When these membranes are applied to the reactor system, the MR constitute an interesting alternative approach to the FBRs, owing to the ability of the palladium-based MRs in performing simultaneously the reaction process and the selective hydrogen separation. In this way, the continuous hydrogen removal permits to obtain reaction conversions higher than the thermodynamic equilibrium, which is the upper limit to be considered in a FBR and a pure hydrogen stream for directly feeding a PEMFC without needing any other purification process.

Nomenclature

AASR: acetic acid steam reforming

BESR: bioethanol steam reforming

CVD: chemical vapour deposition

D: diffusion coefficient

d_p: pore diameter

E_a: apparent activation energy

ELP: electroless plating deposition

EP: electroplating

ESR: ethanol steam reforming

EVD: electrochemical vapour deposition

FBR: fixed bed reactor

G:geometrical factor

GSR: glycerol steam reforming

HTR: high temperature reactor

IUPAC: International Union of Pure and Applied Chemistry

J: flux or permeation rate

$J_{H2,Sieverts\text{-}Fick}$*:* hydrogen flux through the membrane according to Sieverts-Fick law

J_{H2}*:* hydrogen flux through the membrane

J_i: flux of the i-species across the membrane

J_m: mass flux

LTR: low temperature reactor

M_i: molecular weight of the i-species

ML: molecular layering

MR: membrane reactor

MS: magnetron sputtering

MSR: methane steam reforming

n: dependence factor of the hydrogen flux on the hydrogen partial pressure

p: pressure

Pe^0_{H2}: the pre-exponential factor

Pe_{H2}: the hydrogen permeability

PEMFC: proton exchange membrane fuel cell

$p_{H2,perm}$: hydrogen partial pressures at the permeate side

$p_{H2,ret}$: hydrogen partial pressures at the retentate side

POM: partial oxidation of methane

PSA: pressure swing adsorption

PVD: physical vapour deposition

R: universal gas constant

SRM: methanol steam reforming

T: absolute temperature

WGS: water gas shift

WHSV: weight hourly space velocity

x: coordinate perpendicular to the transport barrier

$\Delta H°_{298\ K}$: enthalpy variation in standard conditions

Δp_i: pressure difference of species

α: ideal separation factor or selectivity

δ: membrane thickness

ϕ_{pore}: pore diameter

References

- Adams J., Cassarino C., Lindstrom J., Spangler L., Binder M.J., Holcomb F.H., "Canola oil fuel cell demonstration I", *US Army Corps of Engineer* (**2004**).
- Adams T.M., Mickalonis J., "Hydrogen permeability of multiphase V–Ti–Ni metallic membranes", *Mater. Lett.,* 61 (**2007**) 817-820.
- Adhikari S., Fernand S., "Hydrogen Membrane Separation Techniques", *Ind. Eng. Chem. Res.*, 45 (**2006**) 875-881.
- Altinisik O., Dogan M., Dogu G., "Preparation and characterization of palladium-plated porous glass for hydrogen enrichment", *Catal. Today*, 105 (**2005**) 641-646.
- Amandusson H., Ekedahl L.G., Dannetun H., "The effect of CO and O_2 on hydrogen permeation through a palladium membrane", *Appl. Surf. Sci*., 153 (**2000**) 259-267.
- Arstad B., Venvik H., Klette H., Walmsley J.C., Tucho W.M., Holmestad R., Holmen A., Bredesen R., "Studies of self-supported 1.6 μm Pd/23 wt.% Ag membranes during and after hydrogen production in a catalytic membrane reactor", *Catal. Today,* 118 (**2006**) 63-72.

- Aspen Systems, "Compact Single Stage Fuel Reformer for PEM Fuel Cells,", *Proceedings of the USDOE CARAT program review,* Troy (Michigan) (**1999**).
- Barelli L., Bidini G., Gallorini F., Servili S., "Hydrogen production through sorption-enhanced steam methane reforming and membrane technology: A review", *Energy,* 33 (**2008**) 554-570.
- Basagiannis A.C., Verykios X.E., "Catalytic steam reforming of acetic acid for hydrogen production", *Int. J. Hydrogen En.,* 32 (**2007**) 3343-3355.
- Basile A., Violante V., Santella F., Drioli E., "Membrane integrated system in the fusion reactor fuel cycle", *Catal. Today*, 25 (3-4) (**1995)** 321-326.
- Basile A., Criscuoli A., Santella F., Drioli E., "Membrane reactor for water gas shift reaction", *Gas Sep. Purif.*, 10 (4) (**1996)** 243-254.
- Basile A., Chiappetta G., Tosti S., Violante V., "Experimental and simulation of both Pd and Pd/Ag for a water gas shift membrane reactor", *Sep. Pur. Techn.*, 25 (**2001)** 549-571.
- Basile A., Paturzo L., Bazzana A., "Membrane reactor for the production of hydrogen and higher hydrocarbons from methane over Ru/Al_2O_3 catalyst", *Chem. Eng. J.*, 93 (**2003**) 31-39.
- Basile A., Gallucci F., Paturzo L., "A dense Pd/Ag membrane reactor for methanol steam reforming: Experimental study", *Catal. Today*, 104 (**2005**) 244-250.
- Basile A., Gallucci F., Iulianelli A., Tosti S., Drioli E., "The pressure effect on ethanol steam reforming in membrane reactor: experimental study", *Desalination*, 200 (**2006**) 671-672.
- Basile A., Tosti S., Capannelli G., Vitulli G., Iulianelli A., Gallucci F., Drioli E., "Co-current and counter-current modes for methanol steam reforming membrane reactor: Experimental study", *Catal. Today*, 118 (**2006b**) 237-245.
- Basile A., "Hydrogen Production Using Pd-based Membrane Reactors for Fuel Cells", *Top. Catal.,* 51 (**2008**) 107-122.
- Basile A., Gallucci F., Iulianelli A., Tereschenko G.F., Ermilova M.M., Orekhova N.V., "Ti-Ni-Pd dense membranes - The effect of the gas mixtures on the hydrogen permeation", *J. Membrane Sci.*, 310 (**2008b**) 44-50.

- Basile A., Gallucci F., Iulianelli A., Tosti S., "CO-free hydrogen production by ethanol steam reforming in a Pd-Ag membrane reactor", *Fuel Cells*, 1 (**2008c**) 62-68.
- Basile A., Parmaliana A., Tosti S., Iulianelli A., Gallucci F., Espro C., Spooren J., "Hydrogen production by methanol steam reforming carried out in membrane reactor on Cu/Zn/Mg-based catalyst", *Catal. Today*, 137 (**2008d**) 17-22.
- Basile A., Gallucci F., Iulianelli A., Borgognoni F., Tosti S., "Acetic acid steam reforming in a Pd–Ag membrane reactor: The effect of the catalytic bed pattern", *J. Membrane Sci.*, 311 (**2008e**) 46-52.
- Benito M., Sanz J.L., Isabel R., Padilla R., Arjona R., Daza L., "Bio-ethanol steam reforming: Insights on the mechanism for hydrogen production", *J. Power Sou.*, 151 (**2005**) 11-17.
- Bimbela F., Oliva M., Ruiz J., Garc´ıa L., Arauzo J., "Hydrogen production by catalytic steam reforming of acetic acid, a model compound of biomass pyrolysis liquids", *J. Anal. Appl. Pyrolysis*, 79 (**2007**) 112-120.
- Biswas D.R., "Review: Deposition processes for films and coatings", *J. Mater. Sci.*, 21 (**1986**) 2217-2223.
- Booth J.C.S., Doyle M.L., Jee S.M., Miller J., Scholtz L.A., Walker P.A., *Proc. of the 11th World Hydrogen Energy Conf*., Stuttgart (**1996)** 867.
- Brodowsky H., "On the non-ideal solution behavior of hydrogen in metals", *Ber. Bunsenges Physik. Chem.*, 76 (**1972**) 740-749.
- Catalytica®, Catalytic membrane reactors: concepts and applications, Catalytica Study N. 4187 MR (**1988**).
- Chen Y., Wang Y., Xu H., Xiong G., "Efficient production of hydrogen from natural gas steam reforming in palladium membrane reactor", *Appl. Catal. B: Env*., 80 (**2008**) 283-294.
- Cheng Y.S., Pena M.A., Fierro J.L., Hui D.C.W., Yeung K.L., "Performance of alumina, zeolite, palladium, Pd-Ag alloy membranes for hydrogen separation from Towngas mixture", *J. Membrane Sci.*, 204 (**2002**) 329-340.

- Cheng X., Shi Z., Glass N., Zhang L., Zhang J., Song D., Liu Z.S., Wang H., Shen J., "A review of PEM hydrogen fuel cell contamination: Impacts, mechanisms, and mitigation", *J. Power Sou*, 165 (**2007**) 739-756.
- Cifre G.P., Badr O., "Renewable hydrogen utilization for the production of methanol", *En. Conver. & Manag.*, 48 (**2007**) 519-527.
- Cole M. J., "The generator of pure hydrogen for industrial applications", *Plat. Met. Rev.*, 25 (**1981**) 12-13.
- Costamagna P., Srinivasan S., "Quantum jumps in the PEMFC science and technology from the 1960s to the year 2000 Part II. Engineering, technology, development and application aspects", *J. Power Sou.*, 102 (**2001**) 253-269.
- Criscuoli A., Basile A., Drioli E., "An analysis of the performance of membrane reactors for the water-gas shift reaction using gas feed mixtures", *Catal. Today*, 56 (**2000**) 53-64.
- Damle A.S., "Hydrogen production by reforming of liquid hydrocarbons in a membrane reactor for portable power generation – Experimental studies", *J. Power Sou.*, 186 (**2009**) 167-177.
- Dolan M.D., Dave N.C., Ilyushechkin A.Y., Morpeth L.D., McLennan K.G., "Composition and operation of hydrogen-selective amorphous alloy membranes", *J. Membrane Sci.*, 285 (**2006**) 30-55.
- Dolgykh L., Stolyarchuk I., Denyega I., Strizhak P., "The use of industrial dehydrogenation catalyst for hydrogen production from bioethanol", *Int. J. Hydrogen En.*, 31 (**2006**) 1607-1610.
- Edlund D.J., Pledger W.A., "Thermolysis of hydrogen sulfide in a metal-membrane reactor", *J. Membrane Sci.* 77 (**1993)** 255-264.
- Edlund D.J., Pledger W.A., "Catalytic platinum-based membrane reactor for removal of H2S from natural gas streams", *J. Membrane Sci., 94* (**1994)** 111-119.
- Falconer J.L., Noble R.D., Sperry D.P., "Catalytic Membrane Reactors", *Membrane Separations Technology: Principles and Applications*, pp. 669-712, Elsevier (R.D. Noble and S.A. Stern, ed.) (**1995**).

- Flytzani-Stephanopoulos M., X. Qi, Kronewitter S., "Water-gas shift with integrated hydrogen separation process", *Final report to DOE,* Grant # DEFG2600-NT40819 (**2004**) 1-38.
- Frusteri F., Freni S., Chiodo V., Donato S., Bonura G., Cavallaro S., "Steam and auto-thermal reforming of bio-ethanol over MgO and CeO_2 Ni supported catalysts", *Int. J. Hydrogen En.,* 31 (**2006**) 2193-2199.
- Gallucci F., De Falco M., Tosti S., Marrelli L., Basile A., "The effect of the hydrogen flux pressure and temperature dependence factors on the membrane reactor performances", *Int. J. Hydrogen En.*, 32 (**2007**) 4052-4058.
- Gallucci F., Tosti S., Basile A., *Synthesis, Characterization and Applications of Palladium Membranes*, Eds. R. Malada, M. Menendez, Elsevier, cap.8 (**2007b**).
- Gallucci F., Tosti S., Basile A., "Pd–Ag tubular membrane reactors for methane dry reforming: A reactive method for CO_2 consumption and H_2 production", *J. Membrane Sci.*, 317 (**2008**) 96-105.
- Galuszka J., Pandey R.N., Ahmed S., "Methane conversion to syngas in a palladium membrane reactor", *Catal. Today,* 46 (**1998**) 83-89.
- Gao H., Lin Y.S., Li Y., Zhang B., "Chemical stability and its improvement of palladium-based metallic membranes", *Ind. Eng. Chem. Res.*, 43 (**2004**) 6920-6930.
- Gao H., Lin J.Y.S., Li Y., Zhang B., "Electroless plating synthesis, characterization and permeation properties of Pd-Cu membranes supported on ZrO_2 modified porous stainless steel", *J. Membrane Sci.*, 265 (**2005**) 142-152.
- Gernot E., Aupretre F., Deschamps A., Epron F., Merecot P., Duprez D., Etievant C., "Production of hydrogen from bioethanol in catalytic membrane reactor", 16th Confèrence Mondiale de l'Hydrogène Energie (WHEC16), Lyon (France), (**2006**) http://www.ceth.fr/download/presse/art_ceth_3.pdf
- Goltsov V., Veziroglu N., "From hydrogen economy to hydrogen civilization", *Int. J. Hydrogen En.*, 26 (**2001**) 909-915.

- Graham T., *Proc. Roy. Soc.* (London), 156 (**1866**) 399.
- Grashoff G.J., Pilkington C.E., Corti C.W., "The purification of hydrogen – A review of the technology emphasing, the current status of palladium membrane diffusion", *Plat. Met. Rev.*, 27 (**1983**) 157-168.
- Gryaznov V., *Sov. Patent n*. 274 092 (**1964**).
- Gryaznov V.M., *Separation and Purification Methods*, 29 (**2000**) 171-187.
- Hara S., Hatakeyama N., Itoh N., Kimura H.M., Inoue A., "Hydrogen permeation through palladium-coated amorphous Zr–M–Ni (M = Ti, Hf) alloy membranes", *Desalination* 144 (**2002**) 115-120.
- Howard B.H., Killmeyer R.P., Rothenberger K.S., Cugini A.V., Morreale B.D., Enick R.M., Bustamante F., "Hydrogen permeance of palladium–copper alloy membranes over a wide range of temperatures and pressures", *J. Membrane Sci.*, 241 (**2004**) 207-218.
- Hsieh H.P., "Inorganic membrane reactors – A review", *AIChE Symp. Ser*., 85 (**1989**) 53-67.
- Hu X., Lu G., "Investigation of steam reforming of acetic acid to hydrogen over Ni–Co metal catalyst", *J. Mol. Catal. A: Chem.*, 261 (**2007**) 43-48.
- Huang T.C., Wei M.C., Chen H.I., "Preparation of hydrogen-permselective palladium-silver alloy composite membranes by electroless co-deposition", *Sep. Purif. Techn.*, 32 (**2003**) 239-245.
- Huang Y., Dittmeyer R., "Preparation of thin palladium membranes on a porous support with rough surface", *J. Membrane Sci.*, 302 (**2007**) 160-170.
- Hughes R., "Composite palladium membranes for catalytic membrane reactors", *Membr. Tech*., 131 (**2001**) 9-13.
- Hwang S.T., Kammermeyer K., "Techniques in chemistry: membranes in separation", *Wiley Interscience*, New York (**1975**).
- e-net 1:http://scopees.elsevier.com
- e-net 2: http://www.fctec.com/fctec_types_pem.asp

- e-net 3: http://ec.europa.eu/research/rtdinfo/42/01/article_1315_en.html
- e-net 4: http://www.hydrogenassociation.org/general
- Itoh N., Akiha T., Sato T., "Preparation of thin palladium composite membrane tube by a CVD technique and its hydrogen permselectivity", *Catal. Today,* 104 (**2005**) 231-237.
- Iulianelli A., Longo T., Basile A., "Methanol steam reforming in a dense Pd–Ag membrane reactor: The pressure and WHSV effects on CO-free H_2 production", *J. Membrane Sci.*, 323 (**2008**) 235-240.
- Iulianelli A., Longo T., Basile A., "Methanol steam reforming reaction in a Pd–Ag membrane reactor for CO-free hydrogen production", *Int. J. Hydrogen En.*, 33 (**2008b**) 5583-5588.
- Iulianelli A., Longo T., Basile A., "CO-free hydrogen production by steam reforming of acetic acid carried out in a Pd–Ag membrane reactor: The effect of co-current and counter-current mode", *Int. J. Hydrogen En.*, 33 (**2008c**) 4091-4096.
- Iulianelli A., Liguori S., Longo T., Tosti S., Pinacci P., Basile A., "An experimental study on bio-ethanol steam reforming in a catalytic membrane reactor. Part II: reaction pressure, sweep factor and WHSV effects", *Int. J. Hydrogen En.*, Article in press, doi:10.1016/j.ijhydene.2009.11.034.
- Iulianelli A., Basile A., "An experimental study on bio-ethanol steam reforming in a catalytic membrane reactor. Part I: temperature and sweep-gas flow configuration effects", *Int. J. Hydrogen En.*, Article in press b, doi: 10.1016/j.ijhydene.2009.11.076.
- Iulianelli A., Longo T., Liguori S., Basile A., "Production of hydrogen via glycerol steam reforming in a Pd-Ag membrane reactor over Co-Al_2O_3 catalyst", *Asia-Pac. J. Chem. Eng.*, Article in press c, doi:10.1002/apj.365.
- Iulianelli A., Seelam P.K., Liguori S., Longo T., Keiski R., Calabrò V., Basile A., "Hydrogen production for PEM fuel cell by gas phase reforming of glycerol as byproduct of bio-diesel. The use of a Pd-Ag membrane reactor at middle reaction temperature", submitted.

- Iyoha O., Enick R., Killmeyer R., Howard B., Morreale B., Ciocco M., "Wall-catalyzed water-gas shift reaction in multi-tubular Pd and 80 wt%Pd–20 wt%Cu membrane reactors at 1173 K", *J. Membrane Sci.*, 298 (**2007**) 14-23.
- Jones A.C., Hitchman M.L., "Chemical Vapour Deposition Precursors, Processes and Applications", *RSC Publishing* (**2008**) doi: 10.1039/9781847558794.
- Jorgensen S., Nielsen P.E.H., Lehrmann P., "Steam reforming of methane in membrane reactor", *Catal. Today*, 25 (**1995**) 303-307.
- Juenker, D.W., Van Swaay M., Birchenall C.E, "On the use of palladium diffusion membranes for the purification of hydrogen", *Review of Scientific Instruments,* 26 (**1955**) 888.
- Kapoor A., Yang R.T., Wong C., "Surface diffusion", *Catal. Rev.*, 31 (**1989**) 129-214.
- Khulbe K.C., Feng C.Y., Matsuura T., "Synthetic polymeric membranes, characterization by atomic force microscopy", *Springer* ISBN:3540739939 (**2007**) pp. 216.
- Kikuchi E., Uemiya S., Sato N., Inoue H., Ando H., Matsuda T., "Membrane reactor using microporous glass supported thin film of palladium. Application to the water gas shift reaction", *Chem. Lett*., 18 (**1989**) 489-492.
- Kikuchi E., "Palladium/ceramic membranes for selective hydrogen permeation and their application to membrane reactor", *Catal. Today*, 25 (**1995**) 333-337.
- Kikuchi E., Nemoto Y., Kajiwara M., Uemiya S., Kojima T., "Steam reforming of methane in membrane reactors: comparison of electroless-plating and CVD membranes and catalyst packing modes", *Catal. Today*, 56 (**2000**) 75-81.
- Kishimoto S., Yoshida N., Arita Y., Flanagan T.B., "Solution of hydrogen in cold-worked and annuale $Pd_{95}Ag_5$ alloys", *Ber. Bunsenges Physik. Chem.*, 94 (**1990**) 612-615.
- Kleinert A., Grubert G., Pan X., Hamel C., Seidel-Morgenstern A., Caro J., "Compatibility of hydrogen transfer via Pd-membranes with the rates of heterogeneously catalysed steam reforming", *Catal. Today*, 104 (**2005**) 267-273.

- Knozinger H., Ratnasamy P., "Catalytic aluminas: surface models and characterization of surface sites", *Catal. Rev. Sci. Eng.*, 17 (**1978**) 31-70.
- Koros W.J., Fleming G.K., "Membrane-based gas separation", *J. Membrane Sci.*, 83 (**1993**) 1-80.
- Koros W.J., Ma Y.H., Shimidzu T., "Terminology for membranes and membrane processes", *J. Membrane Sci.*, 120 (**1996**) 149-159.
- Lee K.H., Hwang S.T., "Transport of condensible vapors through a microporous vycor glass membrane", *J. Coll. Int. Sci.*, 110 (**1986**) 544-555.
- Lewis F.A., Kandasamy K., Baranowski B., "The "Uphill" diffusion of hydrogen – Strain-gradient-induced effects in palladium alloy membranes", *Plat. Met. Rev.*, 32 (**1988**) 22-26.
- Li A., Liang W., Hughes R., "The effect of carbon monoxide and steam on the hydrogen permeability of a Pd/stainless steel membrane", *J. Membrane Sci.*, 165 (**2000)** 135-141.
- Liang W., Hughes R., "The effect of diffusion direction on the permeation rate of hydrogen in palladium composite membranes", *Chem. Eng. J.*, 112 (**2005**) 81-86.
- Liang W., Hughes R., "The catalytic dehydrogenation of isobutane to isobutene in a palladium/silver composite membrane reactor", *Catal. Today.*, 104 (**2005b**) 238-243.
- Lin Y.M., Rei M.H., "Process development for generating high purity hydrogen by using supported palladium membrane reactor as steam reformer", *Int. J. Hydrogen En.*, 25 (**2000**) 211-219.
- Lin Y.M., Rei M.H., "Study on the hydrogen production from methanol steam reforming in supported palladium membrane reactor", *Catal. Today*, 67 (**2001**) 77-84.
- Lin Y.M., Liu S.L., Chuang C.H., Chu Y.T., "Effect of incipient removal of hydrogen through palladium membrane on the conversion of methane steam reforming. Experimental and modeling", *Catal. Today*, 82 (**2003**) 127-139.

- Liu B.F., Ren N.Q., Tang J., Ding J., Liu W.Z., Xu J.F., Cao G.L., Guo W.Q., Xie G.J., "Bio-hydrogen production by mixed culture of photo- and dark-fermentation bacteria", *Int. J. Hydrogen En.*, Article in press, doi:10.1016/j.ijhydene.2009.05.005.
- Loweheim F.A., "Modern electroplating", *John Wiley & Sons,* New York (**1974**) 342-357 and 739-747.
- Luo W., Ishikawa K., Aoki K., "High hydrogen permeability in the Nb-rich Nb–Ti–Ni alloy", *J. Alloys Compd.,* 407 (**2006**) 115-117.
- Mallada R., Menéndez M., "Inorganic Membranes: Synthesis, Characterization and Applications", *Technology & Engineering,* (**2008**) pp. 460.
- Mallevialle J., Odendaal P.E., Wiesner M.R., "Water Treatment Membrane Processes", *ed. McGraw-Hill Publishers* New York (**1998**).
- Malygin A.A.**,** "The Molecular Layering Nanotechnology: Basis and Application", *J. Ind. Eng. Chem.*, 12 (**2006**) 1-11.
- Martins das Neves L.C., Converti A., Vessoni Penna T.C., "Biogas Production: New Trends for Alternative Energy Sources in Rural and Urban Zones", *Chemical Engineering & Technology,* 32 (**2009**) 1147-1153.
- Mattox D.M., "Handbook of Physical Vapor Deposition (PVD) Processing: Film Formation, Adhesion, Surface Preparation and Contamination Control", *Westwood, N.J.: Noyes Publications* (**1998**) ISBN 0815514220.
- McCool B.A., Lin Y.S., "Nanostructured thin palladium-silver membranes: Effects of grain size on gas permeation properties.", *J. Mater. Sci.,* 36 (**2001**) 3221-3227.
- McKinley D.L., Nitro W.V., US patent 3.350.845 (**1967**).
- Mehta V., Cooper J.S., "Review and analysis of PEM fuel cell design and manufacturing", *J. Power Sou.,* 114 (**2003**) 32-53.
- Mohler J.B., "Electroplating and Related Processes", *Chemical Publishing Co.,* (**1969**) ISBN 0-8206-0037-7.

- Molnar A., Smith G.V., Bartok M., "New catalytic materials from amorphous metal alloys", *Adv. Catal.,* 36 (**1989**) 329-383.
- Mulder M., "Basic Principles of Membrane Technology", *Kluwer Academic: Dordrecht* (**1996**) pp. 564.
- Nair B.K.R., Harold M.P., "Pd encapsulated and nanopore hollow fiber membranes: Synthesis and permeation studies", *J. Membrane Sci.,* 290 (**2007**) 182-195.
- Nair B.K.R., Choi J., Harold M.P., "Electroless plating and permeation features of Pd and Pd/Ag hollow fiber composite membranes", *J. Membrane Sci.*, 288 **(2007b**) 67-84.
- Nazarkina E.B., Kirichenko N.A., "Improvement in the steam catalytic conversion of methane by hydrogen liberation via palladium membranes", *Khim. Technol. Topl. Masel,* 3 (**1979**) 5-7.
- Nishimura C., Komaki M., Hwang S.,Amano M., "V–Ni alloy membranes for hydrogen purification", *J. Alloys Compd.,* 330-332 (**2002**) 902-906.
- Noordermeer A., Kok G.A., Nieuwenhuys B.E., "Comparison between the adsorption properties of Pd (111) and PdCu (111) surfaces for carbon monoxide and hydrogen", *Surf. Sci.,* 172 (**1986**) 349-362.
- Oertel M., Schmitz J., Weirich W., Jendryssek-Neumann D., Schulten R., "Steam reforming of natural gas with integrated hydrogen separation for hydrogen production", *Chem. Eng. Technol*., 10 (**1987**) 248-255.
- Okada S., Mineshige A., Kikuchi T., Kobune M., Yazawa T., "Cermet-type hydrogen separation membrane obtained from fine particles of high temperature proton-conductive oxide and palladium", *Thin Solid Films,* 515 (**2007**) 7342-7346.
- Patil C.S., Annaland M.V.S., Kuipers J.A.M., "Fluidised bed membrane reactor for ultrapure hydrogen production via methane steam reforming: Experimental demonstration and model validation", *Chem. Eng. Sci.,* 62 (**2007**) 2989-3007.

- Pfeffer M., Wukovits W., Beckmann G., Friedl A., "Analysis and decrease of the energy demand of bioethanol-production by process integration", *Appl. Thermal Eng.*, 27 (**2007**) 2657-2664.
- Philpott J., "Hydrogen diffusion technology. Commercial applications of palladium membrane", *Plat. Met. Rev*., 29 (**1985**) 12-16.
- Reichelt K., Jiang X., "The preparation of thin films by physical vapor deposition methods", *Thin Solid Films,* 191 (**1990**) 91-126.
- Reid H.R., "Palladium-nickel electroplating. Effects of solution parameters on alloy properties", *Plat. Met. Rev.*, 29 (**1985**) 61-62.
- Rifkin J., "The Hydrogen Economy: The Creation of the Worldwide Energy Web and the Redistribution of Power on Earth", *Jeremy P. Tarcher*, ISBN 1-58542-193-6 (**2002**).
- Roa F., Douglas Way J., Mc Cormik R.L., Paglieri S.N., "Preparation and characterization of Pd-Cu composite membranes for hydrogen separation", *Chem. Eng. J.*, 93 (**2003**) 11-22.
- Ryi S.K., Park J.S., Kim S.H., Cho S.H., Park J.S., Kim D.W.," Development of a new porous metal support of metallic dense membrane for hydrogen separation", *J. Membrane Sci*., 279 (**2006**) 439-445.
- Saracco G., Specchia V., "Catalytic inorganic membrane reactors: present experience and future opportunities", *Catal. Rev. Sci. Eng.*, 36 (**1994**) 305-384.
- Shu J., Grandjean B.P.A., Van Neste A., Kaliaguine S., "Catalytic palladium-based membrane reactors: a review", *Can. J. Chem Eng.*, 69 (**1991**) 1036-1060.
- Shu J., Grandjean B.P.A., Kaliaguine S., "Asymmetric Pd-Ag/stainless steel catalytic membranes for methane steam reforming", *Catal. Today*, 25 (**1995**) 327-332.
- Smith G.V., Brower W.E., Matyjaszezyk M.S., Pettit T.L., *Proc. 7th Int. Congr. Catal., Part A,* T. Seiyama and K. Tanabe, Eds., Elsevier, Amsterdam (**1981**) 355-366.
- Sperry D. P., J. L. Falconer, R. D. Noble, "Methanol—hydrogen separation by capillary condensation in inorganic membranes", *J. Membrane Sci.*, 60 (**1991**) 185-193.

- Stambouli A., Traversa E., "Fuel cells, an alternative to standard sources of energy", *Renew. Sust. Energy Rev.*, 6 (**2002**) 295-304.
- Sturzenegger B., Puippe J.C., "Electrodeposition of palladium-silver alloys from ammoniacal electrolytes", *Plat. Met. Rev.,* 20 (**1984**) 117-124.
- Takanabe K., Aika K., Seshanb K., Lefferts L., "Sustainable hydrogen from bio-oil-steam reforming of acetic acid as a model oxygenate", *J. Catal*., 227 (**2004**) 101-108.
- Tereshchenko G.F., Orekhova N.V., Ermilova M.M., Malygin A.A., Orlova A.I., "Nanostructured phosphorus–oxide-containing composite membrane catalysts", *Cat. Today*, 118 (**2006**) 85-89.
- Tong J., Matsumura Y., "Effect of catalytic activity on methane steam reforming in hydrogen-permeable membrane reactor", *Appl. Catal. A: Gen*., 286 (**2005**) 226-231.
- Tong J., Suda H., Haraya K., Matsumura Y., "A novel method for the preparation of thin dense Pd membrane on macroporous stainless steel tube filter", *J. Membrane Sci.*, 260 (**2005b**) 10-18.
- Tong J., Shirai R., Kashima Y., Matsumura Y., "Preparation of a pinhole-free Pd-Ag membrane on a porous metal support for pure hydrogen separation", *J. Membrane Sci*., 260 (**2005c**) 84-89.
- Tosti S., Bettinali L., Violante V., "Rolled thin Pd and Pd–Ag membranes for hydrogen separation and production", *Int. J. Hydrogen En.,* 25 (**2000**) 319-325.
- Tosti S., Violante V., Basile A., Chiappetta G., Castelli S., De Francesco M., Scaglione S., Sarto F., "Catalytic membrane reactors for tritium recovery from tritiated water in the ITER fuel cycle", *Fusion Eng. Des*., 49-50 (**2000b)** 953-958.
- Tosti S., Bettinali L., "Diffusion bonding of Pd-Ag rolled membranes", *J.Mat. Sci.*, 39 (**2004**) 3041-3046.
- Uemiya S., Sato N., Ando H., Matsuda T., Kikuchi E., "Steam reforming of methane in a hydrogen-permeable membrane reactor", *Appl. Catal.*, 67 (**1991**) 223-230.

- Uemiya S., Sato N., Ando H., Kikuchi E., "The water gas shift reaction assisted by a palladium membrane reactor", *Ind. Eng. Chem. Res.*, 30 (**1991b)** 585-589.
- Uemiya S., "State-of-art-the-art of supported metal membranes for gas separation", *Sep. Pur. Methods*, 28 (**1999**) 51-85.
- Ulhorn R.J.R., Keizer K., Burggraaf A.J., "Gas transport and separation with ceramic membranes. Part I. Multilayer diffusion and capillary condensation", *J. Membrane Sci.*, 66 (**1992**) 259-269.
- Valenti G., Macchi F., "Proposal of an innovative, high efficiency, large-scale hydrogen liquefier", *Int. J. Hydrogen En.*, 33 (**2008**) 3116-3121.
- Valliyappan T., Ferdous D., Bakhshi N.N., Dalai A.K., "Production of hydrogen and syngas via steam gasification of glycerol in a fixed-bed reactor", *Top. Catal.*, 49 (**2008**) 59-67.
- Van Dyk L., Miachon S., Lorenzen L., Torres M., Fiaty K., Dalmon J.A., "Comparison of microporous MFI and dense Pd membrane performances in an extractor-type CMR", *Catal. Today*, 82 (**2003**) 167-177.
- Van Veen H.M., Bracht M., Hamoen E., Alderliesten P.T., "Feasibility of the application of porous inorganic gas separation membranes in some large-scale chemical processes", *Fundamentals of inorganic membrane science and technology*, edited A.J. Burggraaf, L. Cot, Elsevier, 14 (**1996**) 641-681.
- Wang D., Flanagan T.B., Shanahan K.L., "Permeation of Hydrogen through Pre-oxidized Membranes in Presence and Absence of CO*", J. Alloys Compd.*, 372 (**2004**) 158-164.
- Wang D., Tong J., Xu H., Matsamura Y., "Preparation of palladium membrane over porous stainless steel tube modified with zirconium oxide*", Catal. Today*, 93-95 (**2004b**) 689-693.
- Wieland S., Melin T., Lamm A., "Membrane reactors for hydrogen production", *Chem. Eng. Sci.*, 57 (**2002**) 1571-1576.
- Wilde G., Dinda G.P., Rösner H., "Synthesis of bulk nanocrystalline materials by repeated cold rolling", *Adv. Eng. Mat.*, 7 (**2005**) 11-15.

- Wise E.M., "Palladium-recovery, properties and uses", *Academic Press,* New York (**1968**).
- Xia Y., Lu Y., Kamata K., Gates B., Yin Y., "Macroporous materials containing three-dimensionally periodic structures", *Chemistry of Nanostructured Materials* (Ed.: Yang, P.), World Scientific (**2003**) 69-100.
- Xuan J., Leung M.K.H., Leung D.Y.C., M. Ni, "A review of biomass-derived fuel processors for fuel cell systems", *Renew. Sust. Energy Rev.*, 13 (**2009**) 1301-1313.

Conclusion Part I

The paper 1 illustrated the great attention paid by both the industrial and the scientific communities to produce hydrogen in a more technically, environmentally and economically attractive way.

From a techno-economic point of view, today hydrogen is mainly produced from natural gas via methane steam reforming, a process characterized by several limits, such as the thermodynamic equilibrium restrictions, high energy demand, catalyst deactivation due to carbon deposition and increased CO_2 emission. Nevertheless, this process is the most economical way for producing hydrogen with respect to other ones such as electrolysis.

On this route, the research of new alternative and economical device is continuously in progress.

MR could be considered as a valid and alternative solution to conventional systems owing to its ability to combine reaction and separation in only one device. In particular, the dense Pd-based MR covers an important role in this sense owing to the full hydrogen perm-selectivity of this kind of membrane.

Therefore, in the Paper 2, a comprehensive review of Pd-based MRs state of the art showed their potentialities and drawbacks. Moreover, this chapter illustrated the possibility to exploit the renewable sources as a substitute of fossil fuels by using the bio-fuels as feedstocks for performing reforming reaction and producing hydrogen.

From the analysis of current information, some main aspects appear to need close examinations in the MR use:

- the utilization of bio-alcohols as feedstocks for carrying out the reforming reactions;
- to find most favourable operative conditions in which the MR realizes the best performances in terms of reactants conversion, hydrogen recovery and yield.

Therefore, in the following, the bio-fuel reforming reactions, (such as ethanol and glycerol steam reforming, oxidative steam reforming and partial oxidation of ethanol), performed in Pd-based MR

will be widely and deeply studied varying several operating conditions (as reaction temperature and pressure, catalyst, space velocity, feed molar ratio and sweep gas flow rate).

Nevertheless, as a starting point an experimental and simulation analysis of methane steam reforming performed in Pd-Ag MR is realized.

References

Mulder M M, "Basic principles of membrane technology"; ISBN: 0-7923-4247-X; Kluwer Academic Publishers: Dordrecht, NETHERLANDS (HB), (1996), 1-564.

Ni M, Leung MKH, Sumathy K, Leung DYC, "Potential of renewable hydrogen production for energy supply in Hong Kong", *Int J Hydrogen En*, 31 (2006) 1401-1412.

Lu GQ, Diniz de Costa JC, Duke M, Giessler S, Socolow R, Williams RH, Kreutz T, "Inorganic membranes for hydrogen production and purification: a critical review and perspective", *J Coll Interface Sci*, 314 (2007) 589-603.

International Energy Agency (IEA), "Prospects for hydrogen and fuel cells", © OEDC/IEA, 2005 www.iea.org/books/

Part II

Methane Steam Reforming Reaction

Introduction to *Part II*

Methane steam reforming (MSR) is used in this thesis as the starting point for building block of progressive understanding of reforming reactions of complex hydrocarbons.

The MSR is the most important process for hydrogen and syngas production necessary in different chemical and petrochemical processes [Rostrup-Nielsen (1984), Wagner *et al* (1992), Fernandes *et al* (2006)]. The MSR is a catalytic process that involves a reaction between methane and steam and is characterized by multi-steps as steam reforming, water-gas shift and PROX, PSA for H_2 purification. The MSR reaction is performed by using hard operating conditions. In particular, the reaction temperature and pressure have to be in the range of 800 – 1000 °C, 14 – 20 atm, respectively, over Ni-based catalyst [Barelli *et al* (2008)]. At this elevated temperature, the catalyst could undergo deactivation due to carbon formation, also resulting in blockage of reformer tubes and increasing pressure drops [Trimm (1997)].

In order to avoid the problems associated with catalyst fouling and high process energy requirements, the MSR reaction can be carried out in MR. In particular, the use of hydrogen perm-selective MRs allow to perform this reaction at milder operative conditions with respect to the conventional reactor, to combine the chemical reaction and hydrogen separation in only one system and, as a consequence, to enhance methane conversion and both hydrogen yield and selectivity.

Over the last 20 years now, many scientific studies are focused on hydrogen production by MSR reaction carried out in Pd-based MRs confirming the aforementioned benefits [Chen *et al* (2008), Gallucci *et al* (2008), Haag *et al* (2007), Kikuchi (2000a), Kikuchi *et al* (2000b), Lin *et al* (2003), Paturzo *et al* (2003), Tong *et al* (2005), Tong *et al* (2005), Tong *et al* (2006), Tsuru *et al* (2004), Tsuru *et al* (2006)].

In this contest, mathematical models and process simulations have been a very strong tool for academic and industrial research and the development of a complex modeling system, which can simulate the overall SRM process. This research field is still ongoing.

The preparation of the mathematical model for a gas-solid reactive system as MRS reaction, depends on the knowledge of the physical and chemical laws governing the process. In particular, it includes the mechanism and kinetic rates of the reaction, the thermodynamic limitations and also includes heat production as well as heat transfer rates. It is important to recognize that most of the mathematical models is not completely rigorous owing to the complexity of the system.

Therefore, in the academic literature various mathematical models on MSR reaction, different in the simplifying assumptions and in the reactor configuration, are ongoing.

In this Part II, two papers are presented on MSR reaction carried out in Pd-Ag MR. The first is an experimental study on the influence of reaction pressure and catalyst support. In the second, both simulation and experimental studies are presented analyzing the influence of pressure on the reaction system.

The papers are reported hereunder:

Paper 1: A. Basile, S. Campanari, G. Manzolini, A. Iulianelli, T. Longo, ***S. Liguori****, M. De Falco, V. Piemonte, "Methane steam reforming in a Pd-Ag membrane reformer: An experimental study on reaction pressure influence at middle temperature", Int J Hydrogen En, 36 (2011) 1531-1539*

Paper 2: A. Iulianelli, G. Manzolini, M. De Falco, S. Campanari, T. Longo, ***S. Liguori,*** *A. Basile, "H_2 production by low pressure methane steam reforming in a Pd-Ag membrane reactor over a Ni-based catalyst: Experimental and modeling", Int J Hydrogen En, 35 (2011) 11514-11524;*

Chapter 1

Methane steam reforming reaction: experimental analysis

Introduction to paper 1

As aforementioned several times, MSR reaction is carried out in harsh operative conditions in conventional reactor, i.e. high reaction temperature and pressure owing to the serious thermodynamics constraints.

The main advantage to perform this reaction in a Pd-based MR is the possibility to operate at lower temperatures and pressure, still maintaining high conversion. This benefit is due to the so-called "shift effect". In particular, owing to the selective removal of one or more products from the reaction side, the reaction shifts towards further products formation with a consequent enhancement of conversion. So, in Paper 1, MSR reaction is carried out in dense unsupported Pd-Ag MR, packed with Ni/ZrO catalyst, at middle temperature (450°C). The influence of pressure on MR performances in terms of methane conversion, hydrogen recovery, products selectivities is analyzed and discussed. In particular, in the first part of reaction tests, the pressure is varied from 3.0 to 9.0 bar in both retentate and permeate stream, whereas in the second, the retentate pressure is kept constant at 9.0 bar and the permeate pressure is varied in the range of 5.0 – 9.0 bar.

Moreover, permeation tests to pure gas and different H_2-rich gaseous mixtures are realized for characterizing the permeative behaviour of Pd-based membrane.

Hence, the aim of this paper is:

- to study the hydrogen permeation behaviour of a dense and self-supported Pd-Ag membrane, paying particular attention to the influence of hydrogen-rich gas mixture on the hydrogen permeation through the membrane;

- to analyze the MR performances increasing firstly both retentate and permeate pressure and afterwards only permeate one.

INTERNATIONAL JOURNAL OF HYDROGEN ENERGY 36 (2011) 1531–1539

Available at www.sciencedirect.com

ScienceDirect

journal homepage: www.elsevier.com/locate/he

Methane steam reforming in a Pd–Ag membrane reformer: An experimental study on reaction pressure influence at middle temperature

Angelo Basile [a,*], *Stefano Campanari* [b], *Giampaolo Manzolini* [b], *Adolfo Iulianelli* [a], *Tiziana Longo* [a], *Simona Liguori* [a,c], *Marcello De Falco* [d], *Vincenzo Piemonte* [e]

[a] *Institute on Membrane Technology of National Research Council (ITM-CNR), Via P. Bucci, Cubo 17/C, c/o University of Calabria, Rende (CS) 87036, Italy*

[b] *Politecnico di Milano, Department of Energy, via Lambruschini 4, Milano (MI) 20156, Italy*

[c] *University of Calabria, Department of Engineering Modeling, University of Calabria, via Pietro Bucci, Cubo 39/C, 87030 Rende (CS), Italy*

[d] *University Campus Bio-Medico of Rome, Faculty of Engineering, via Alvaro del Portillo 21, 00128 Rome, Italy*

[e] *University of Rome "La Sapienza", Department of Chemical Eng. Materials & Environment, via Eudossiana 18, 00184 Rome, Italy*

ARTICLE INFO

Article history:
Received 15 July 2010
Received in revised form
29 October 2010
Accepted 30 October 2010
Available online 3 December 2010

Keywords:
Methane steam reforming
Membrane reactor
Pd–Ag membrane
Pressure effect
Hydrogen production

ABSTRACT

In this experimental work, methane steam reforming (MSR) reaction is performed in a dense Pd–Ag membrane reactor and the influence of pressure on methane conversion, CO_x-free hydrogen recovery and CO_x-free hydrogen production is investigated. The reaction is conducted at 450 °C by supplying nitrogen as a sweep gas in co-current flow configuration with respect to the reactants. Three experimental campaigns are realized in the MR packed with Ni–ZrO catalyst, which showed better performances than Ni–Al_2O_3 used in a previous paper dealing with the same MR system. The first one is directed to keep constant the total pressure in both retentate and permeate sides of the membrane reactor. In the second case study, the total retentate pressure is kept constant at 9.0 bar, while the total permeate pressure is varied between 5.0 and 9.0 bar. As the best result of this work, at 450 °C and 4.0 bar of total pressure difference between retentate and permeate sides, around 65% methane conversion and 1.2 l/h of CO_x-free hydrogen are reached, further recovering 80% CO_x-free hydrogen over the total hydrogen produced during the reaction. Moreover, a study on the influence of hydrogen-rich gas mixtures on the hydrogen permeation through the Pd–Ag membrane is also performed and discussed.

1. Introduction

Nowadays, hydrogen is seen as a future energy carrier, producible from renewable sources, because its energy content is carbon-free. Moreover, hydrogen gives a large amount of energy per unit of weight in combustion and it could be easily converted into electricity by fuel cell technology [1–3]. Currently, the most useful process for producing hydrogen is the steam reforming of methane (1) [4–9]. Because of the endothermic reaction, this process is conventionally performed in fixed bed reactors (FBRs) at high temperatures (above 850 °C) and methane conversion is restricted by the thermodynamic constrains [4–11].

* *Corresponding author*. Tel.: +39 0984 492013; fax: +39 0984 402103.
E-mail address: a.basile@itm.cnr.it (A. Basile).

0360-3199/$ – see front matter © 2010 Professor T. Nejat Veziroglu. Published by Elsevier Ltd. All rights reserved.
doi:10.1016/j.ijhydene.2010.10.101

$$CH_4 + H_2O \leftrightarrow CO + 3H_2 \quad \Delta H^{\circ}_{298\,K} = +206\ kJ/mol \tag{1}$$

$$CO + H_2O \leftrightarrow CO_2 + H_2 \quad \Delta H^{\circ}_{298\,K} = -41 kJ/mol \tag{2}$$

Nevertheless, as reported in the specialized literature [12–22], it is possible to overcome the thermodynamic equilibrium methane conversion of an FBR and to reduce some of the drastic operating conditions such as high pressure (above 20 bar) and temperature (around 850 °C) by using membrane reactors (MRs). Taking into account that dense Pd–Ag membranes are fully hydrogen perm-selective with respect to all other gases, the selective removal of hydrogen from reaction side towards the shell side of a Pd–Ag MR enables MSR reaction to proceed towards completion. As a consequence, it makes it possible to achieve higher conversion than FBR working under the same MR operating conditions or the same conversion of a FBR, but working under milder FBR operating conditions [12].

Moreover, high purity hydrogen could be produced via dense Pd-based MRs, which allows the simultaneous performance of both chemical reaction and mixture gas separation in the same device with respect to a conventional process, consisting of a reactor unit in series with other hydrogen separation/purifying units. As a further benefit, dense Pd-based MRs are able to produce ultra-pure hydrogen for directly supplying PEM fuel cells [23–30].

Generally, MSR reaction is performed by using metals of groups 8–10 as catalysts, which offer very high catalytic activity for this reaction [31]. In particular, Ni-based catalysts represent a valid choice, owing to their excellent C–C bond cleavage ability, low cost and wide availability [31–33]. However, the support can strongly affect the catalytic performances in reforming reactions. Conventionally, methane reforming catalysts are coupled with supports such as alumina and magnesium-aluminate due to their stabilities at high temperature [34]. In fact, being strongly endothermic, MSR reaction is conducted in FBRs at temperatures above 850 °C and with excess of steam to prevent carbon formation [8,35].

Recently, zirconia based supports seem to be very effective for inhibiting nickel sintering at high reaction temperature due to an excellent thermal stability and strong resistance against coke deposition [36–44]. For this reason, in this work the MR is packed with Ni–ZrO catalyst.

However, the present investigation is aimed of studying the hydrogen permeation behaviour of a dense Pd–Ag membrane housed in an MR, paying particular attention to the influence of hydrogen-rich gas mixture supplying on the hydrogen permeation through the membrane. Firstly, at 3.0 bar of reaction pressure and 1.0 bar of permeate pressure, the MSR performances of the Pd–Ag MR packed with a Ni–ZrO are compared to the experimental results of our previous work, in which the MR is packed with a Ni–Al_2O_3 catalyst. Furthermore, the effect of relatively high reaction pressure on methane conversion and CO_x-free hydrogen production is studied for the first time with this kind of membrane by performing MSR at the same total pressure in both retentate and permeate sides (from 3.0 to 9.0 bar) and, afterwards, keeping constant the total retentate pressure at 9.0 bar and varying the total permeate pressure between 5.0 and 9.0 bar.

Fig. 1 – Tubular pine-hole free Pd–Ag membrane.

2. Experimental setup

2.1. Pd–Ag MR description

Fig. 1 illustrates the dense tubular pin-hole free Pd–Ag membrane, produced by cold-rolling and diffusion welding technique [45], reporting its geometric characteristics and material composition in Table 1. The membrane is joined to two stainless steel tubes useful for its housing in the MR module, with one of them completely closed leading to the so-called dead-end configuration.

The MR consists of a tubular stainless steel module (length 280 mm, *i.d.* 20 mm) housing the Pd–Ag membrane. It is subdivided into two zones: a first zone, inside the membrane (reaction side), in which the reaction takes place, and a second zone corresponding to the annulus of the membrane reactor (shell side), in which CO_x-free hydrogen is collected, as shown in Fig. 2. The reactants are fed by means of a stainless steel tube (*o.d.* 1.6 mm, *i.d.* 0.64 mm) placed inside the membrane. The MR is packed with 3.0 g of a Ni–ZrO commercial catalyst (Catal. Intern. Ltd.) inserted into the membrane core. Glass spheres (2 mm diameter) are placed into the two stainless steel extremities of the membrane to avoid catalyst loss. A graphite o-ring (99.5% C and 0.5% S), supplied by Gee Graphite Ltd., is used to avoid the possibility of the permeate and retentate streams mixing with each other.

2.2. Experimental details

In the permeation tests, the gas mixtures are flowed into the MR used as a permeator by means of different mass-flow controllers (Brooks Instruments 5850S), driven by a computer software supplied by Lira (Italy). Owing to the full hydrogen perm-selectivity of the Pd–Ag membrane, in all cases the hydrogen flux permeating through the membrane is measured by means of a bubble flow-meter.

The experimental setup for the reaction tests, illustrated in Fig. 3, consists of a P680 HPLC volumetric pump (Dionex) used for feeding liquid water, which is vaporized before mixing with methane. Afterwards, the mixture of methane and steam is fed to a preheating zone and, then, into the reaction side by means of a tube in the tube solution. The methane feed flow rate is ~0.17 mol/h and the H_2O/methane feed ratio is kept constant at 2/1.

Table 1 – Main characteristics of the dense Pd–Ag membrane used in this work.

Producing technique	Cold-rolling and diffusion welding technique
Membrane (active layer) length	145 mm
Membrane outside diameter	10 mm
Membrane thickness	50 μm
Silver-palladium composition	23 wt.% Ag

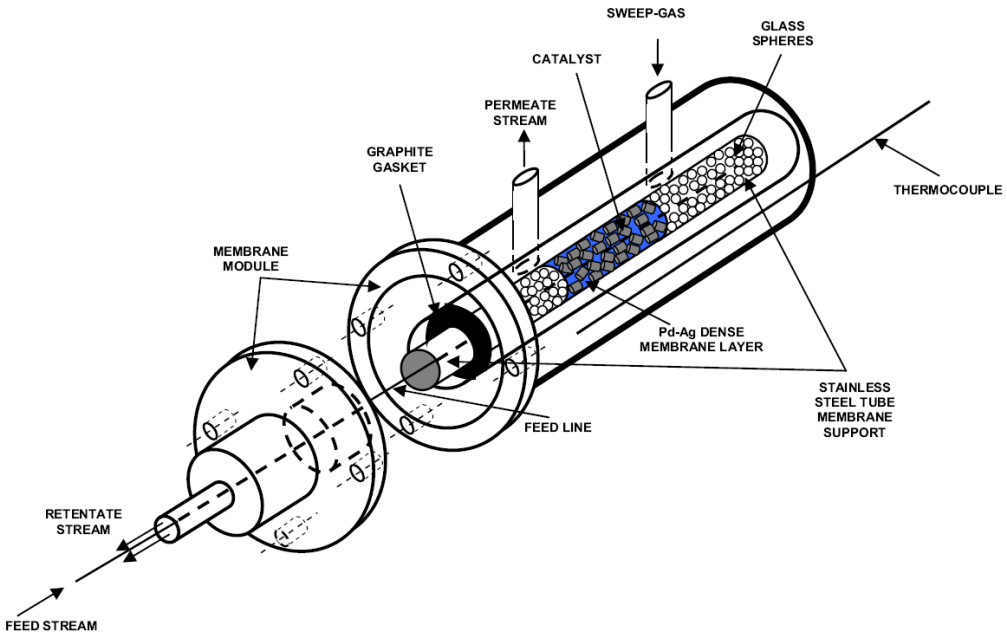

Fig. 2 – Scheme of the dense Pd–Ag membrane reactor.

The Internal Standard Method [46] is used for evaluating the product molar compositions of both retentate and permeate streams. For this reason, a nitrogen stream as internal standard gas (~0.05 mol/h) is fed with the reactants into the reaction side, whereas the nitrogen stream as a sweep gas constitutes even the internal standard gas in the permeate side (~0.27 mol/h).

The sweep gas is supplied only in the reaction tests by means of a mass-flow controller (Brooks Instruments 5850S), driven by a computer software supplied by Lira (Italy), into the permeate side with a ratio sweep gas/methane feed (sweep factor: SF) equal to ~1.6.

The retentate stream, coming out from the MR, is directed to a cold-trap in order to condensate the un-reacted steam. Both permeate and retentate stream compositions are analysed by using a gas chromatography HP 6890, with two thermal conductivity detectors at 250 °C and Ar as a carrier gas. The GC was equipped by three packed columns: Porapack

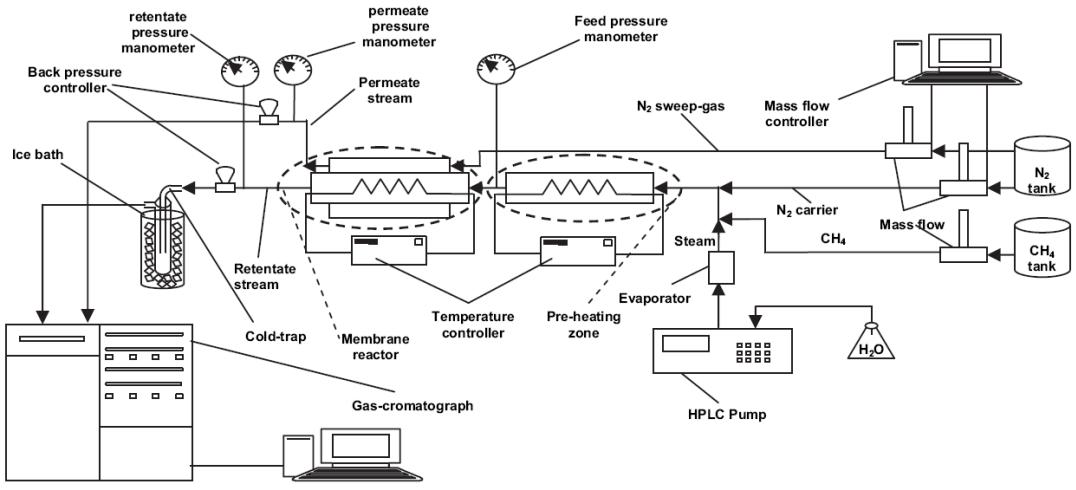

Fig. 3 – Scheme of the plant for the reaction tests.

R 50/80 (8 ft × 1/8 in) and Carboxen™ 1000 (15 ft × 1/8 in) connected in series, and a Molecular Sieve 5Å (6 ft × 1/8 inch).

Before reaction, the catalytic bed was reduced by supplying pure hydrogen (0.07 mol/h) at 450 °C for 2 h.

A flat temperature profile along the reactor was confirmed during the reaction by means of a three points thermocouple placed into the reactor.

The following definitions are used for describing the MR performances:

$$SF(-) = \frac{N_{2,sweep-gas}}{CH_{4-in}}(sweep-factor) \quad (3)$$

$$CH_4\ conversion(\%) = \frac{CH_{4-in} - CH_{4-out}}{CH_{4-in}} \times 100 \quad (4)$$

where $CH_{4\text{-}in}$ is the methane molar flow rate fed to the MR and $CH_{4\text{-}out}$ the methane molar flow rate coming out from the MR,

$$(HR)CO_{x-free}hydrogen\ recovery(\%) = \frac{H_{2-permeate}}{H_{2-TOT}} \times 100 \quad (5)$$

proportional to $H_{2\text{-}permeate}$, which is the hydrogen stream permeated through the membrane and collected in the shell side while $H_{2\text{-}TOT}$ is the total hydrogen produced during the reaction,

$$X\ selectivity(\%) = \frac{X_{out}}{H_{2,out} + CO_{out} + CO_{2,out}} \times 100 \quad (6)$$

where X can be H_2, CO and CO_2, respectively, and the subscript "out" indicates the reformed products coming out from the MR.

3. Results and discussion

3.1. Permeation test

It is well known that dense Pd–Ag membranes offer full hydrogen perm-selectivity with respect to the other gases [47–49] because the palladium metal lattice presents high hydrogen solubility and diffusivity [45]. Therefore, the Pd–Ag membrane of this work was experimentally characterized in terms of permeation with pure gases. The results of these tests showed that the membrane is completely perm-selective towards hydrogen with respect to other gases such as N_2, CO, CO_2 and CH_4. As a matter of fact, at constant temperature the hydrogen molecular transport in these membranes occurs through a solution/diffusion mechanism, where the dissociated molecules on the gas/membrane interface are adsorbed at the atomic level on the membrane surface. The atoms diffuse through the membrane re-combining to form molecules at the gas/membrane interface, afterwards they desorb [50,51]. Therefore, the hydrogen permeating flux can be expressed by means of the following equation:

$$J_{H_2} = Pe_{H_2}\left(p^n_{H_2-retentate} - p^n_{H_2-permeate}\right)\Big/\delta \quad (7)$$

where J_{H_2} is the hydrogen flux permeating through the membrane, Pe_{H_2} the hydrogen permeability, $p_{H_2-retentate}$ and $p_{H_2-permeate}$ the hydrogen partial pressures in the retentate and permeate sides, respectively, n (ranging within 0.5–1) the dependence factor of the hydrogen partial pressure and δ the membrane thickness. The "n" factor is used as an indicator for the rate-controlling step of the permeation. If the diffusion of atomic hydrogen through the dense metal layer is rate-limiting, the equation (7) becomes the Sieverts-Fick's law (8) [52], where the hydrogen permeating flux is directly proportional to the hydrogen partial pressure square root difference between the retentate and permeate sides:

$$J_{H_2,Sieverts-Fick} = Pe_{H_2}\left(p^{0.5}_{H_2-retentate} - p^{0.5}_{H_2-permeate}\right)\Big/\delta \quad (8)$$

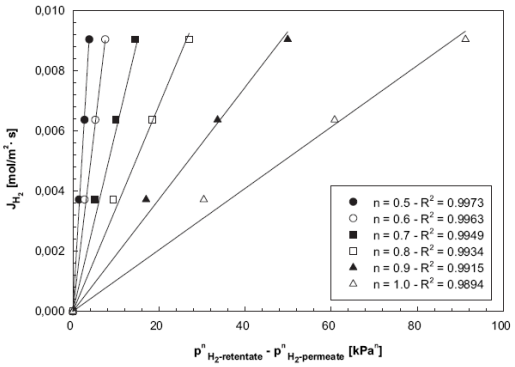

Fig. 4 – Hydrogen flux permeating through the dense Pd–Ag membrane against hydrogen partial pressure difference between retentate and permeate sides at different "n" values, at 450 °C.

Therefore, in Fig. 4 the hydrogen flux permeating through the membrane against hydrogen partial pressure difference between retentate and permeate sides is reported at different "n" values. As shown, the highest linear regression value (R^2) corresponds to $n = 0.5$, confirming that Sieverts-Fick's law is followed.

Furthermore, with the aim of investigating the effect of the co-existing gases partial pressure on the hydrogen permeation through the Pd–Ag membrane, different H_2-rich gas mixtures were supplied to the MR, with molar compositions reported in Table 2. In particular, two binary mixtures (H_2–N_2

Table 2 – Molar feed fraction of mixtures used for the permeation tests using the dense Pd–Ag membrane at 450 °C.

Temperature = 450 °C

Molar fraction	H_2	N_2	CO	CO_2	CH_4	H_2O
H_2–N_2	0.92	0.08	–	–	–	–
	0.80	0.20	–	–	–	–
	0.63	0.37	–	–	–	–
	0.39	0.61	–	–	–	–
	0.22	0.78	–	–	–	–
H_2–CH_4	0.35	–	–	–	0.65	–
	0.57	–	–	–	0.43	–
	0.85	–	–	–	0.15	–
H_2–N2–CO–CO_2–CH_4–H_2O	0.25	0.12	0.01	0.05	0.19	0.38

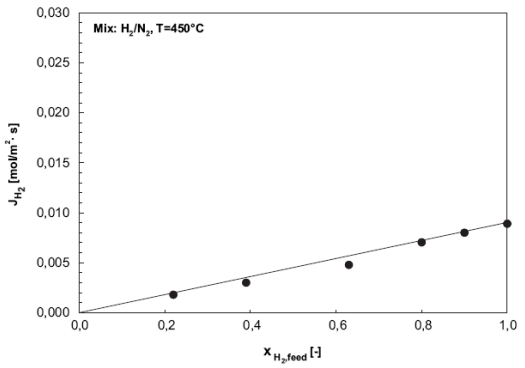

Fig. 5 – Hydrogen permeating flux versus the hydrogen molar fraction in the H_2–N_2 mixture at $T = 450$ °C.

and H_2–CH_4, respectively) were used at different hydrogen molar fractions. Hydrogen permeating flux versus the hydrogen molar fraction is reported in Figs. 5 and 6, keeping at 2.0 bar the total feed pressure and at 1.0 bar the permeate pressure. In these figures, the theoretical hydrogen flux, calculated when pure hydrogen is present in the two sides of the membrane module, is also plotted as a solid line. It represents a kind of reference line for our permeation tests. In fact, if the other gas does not interact with the membrane surface by blocking the permeation, then the higher the partial pressure of the other gas the lower the hydrogen partial pressure in the retentate side. As a consequence, the H_2 permeation driving force becomes lower (Eq. (8)) and the H_2 flux should follow the predicted theoretical trend of the reference line. The experimental data plotted in both Figs. 5 and 6 confirm that the theoretical trend of the reference line is followed and nitrogen and methane do not affect the hydrogen permeation through the membrane.

Another series of tests was carried out to verify the effects of operating with a different hydrogen mixture, containing also carbon monoxide and simulating a mixture with components similar to those generated by a conventional steam reformer [28–30].

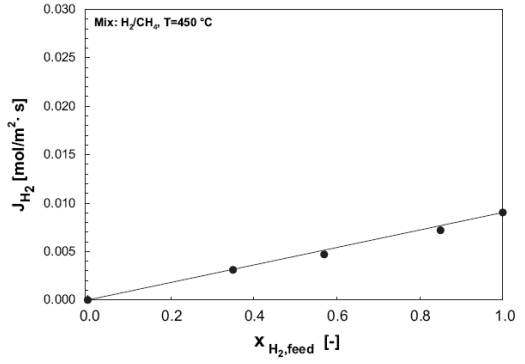

Fig. 6 – Hydrogen permeating flux versus the hydrogen molar fraction in the H_2–CH_4 mixture at $T = 450$ °C.

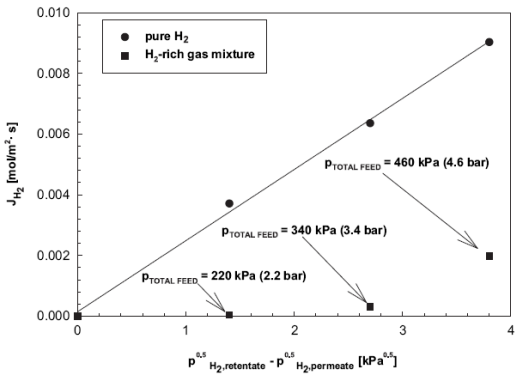

Fig. 7 – Comparison between the hydrogen permeating fluxes through Pd–Ag membrane for hydrogen and hydrogen-rich gas mixture supplied to MR (see Table 2) at 450 °C and 100 kPa (1.0 bar) of total permeate pressure.

As is well known from the specialized literature [53–58], CO presence in a hydrogen-rich gas mixture shows the "surface effect", based on strong interactions between CO and palladium atoms, which reduce the active surface area for hydrogen permeation [58]. This effect determines a rapid decrease of the hydrogen permeating flux just at low CO concentration. However, as confirmed by Amandusson *et al.* [48,53], at temperature above 300 °C, Pd-based membranes are only poorly affected by the CO surface effect. Based on this knowledge, a model mixture (see Table 2) with a molar composition taken from the experimental results of MSR reaction carried out in the Pd–Ag MR at 450 °C and 3.0 bar was reproduced for studying the hydrogen permeation behaviour.

As shown in Fig. 7, a strong decrease of the hydrogen permeating flux when the gaseous mixture is supplied to the membrane module was observed with respect to the case of pure hydrogen supplying. This unexpected reduction probably occurs owing to the concentration polarization effect [59] and, probably, even for a slighter surface effect due to CO. Nevertheless, the most relevant result indicates that, in order to better perform the Pd–Ag MR during MSR reaction, it should be advantageous to operate at reaction pressures higher than 3.0 bar for which a non-negligible hydrogen permeating flux is observed.

Table 3 – Methane conversion, CO_x-free hydrogen recovery and hydrogen selectivity obtained by using two Ni-based catalysts in dense Pd–Ag MR. Operating conditions: $T = 450$ °C, $p_{retentate} = 3.0$ bar, $p_{permeate} = 1.0$ bar, SF = 1.6 and co-current flow configuration of sweep gas.

	Ni–Al_2O_3	Ni–ZrO
Methane conversion	50% ± 0.6	65% ± 1.3
CO_x-free hydrogen recovery	70% ± 1.6	80% ± 1.8
Hydrogen selectivity	42% ± 1.3	77% ± 1.4

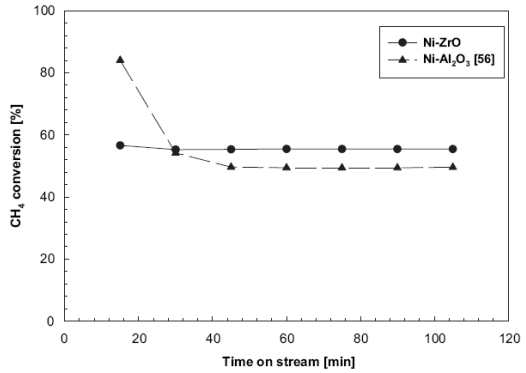

Fig. 8 – Methane conversion against time on stream for MSR reaction over two Ni-based catalysts in the dense Pd–Ag MR. Operating conditions: $T = 450\ ^{\circ}C$, $p_{retentate} = 3.0$ bar, $p_{permeate} = 1.0$ bar, SF = 1.6 and co-current flow configuration of sweep gas.

3.2. *Reaction tests*

As reported above, the MR is packed with an Ni–ZrO catalyst, chosen for its thermal stability and strong resistance against coke formation during MSR reaction. In order to check the performances of the MR in terms of methane conversion, CO_x-free hydrogen recovery and hydrogen selectivity obtained when packed with the Ni–ZrO catalyst, Table 3 summarizes a comparison with the experimental results reached in our previous work [60] (in which MSR reaction was conducted by using Ni–Al_2O_3 catalyst). As shown, Ni–ZrO catalyst allows relatively higher methane conversion, higher CO_x-free hydrogen recovery (by better depleting carbon formation as a main cause of membrane surface coverage) and hydrogen selectivity to be reached. The most significant effect of this catalyst is related to the reduction of carbon deposits on the membrane surface, favouring an improvement of the hydrogen permeation through the membrane than using Ni–Al_2O_3 catalyst.

Moreover, as shown in Fig. 8, where methane conversion is plotted against time on stream, Ni–ZrO catalyst offers an excellent catalytic stability with time. On the contrary, using Ni–Al_2O_3 catalyst, methane conversion presents a progressive decrease up to achieving a constant trend after around 45 min of testing.

Afterwards, based on the results obtained during the aforementioned permeation tests, an experimental campaign on MSR reaction keeping the same total pressure in both retentate and permeate sides at values higher than 3.0 bar was performed. As a general consideration, it should be taken into account that, for the Pd–Ag MR used in this work, a pressure increase makes two competitive effects on methane conversion:

- a negative effect owing to the thermodynamic of the reaction (1), which proceeds with an increase of the moles number and it is not favoured by a pressure increase;

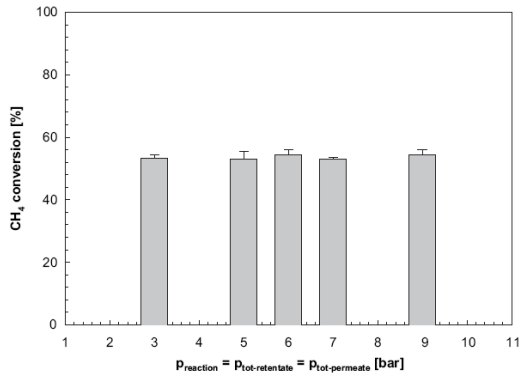

Fig. 9 – Methane conversion against the reaction pressure in dense Pd–Ag MR. Operating conditions: $T = 450\ ^{\circ}C$, SF = 1.6 and co-current flow configuration of sweep gas.

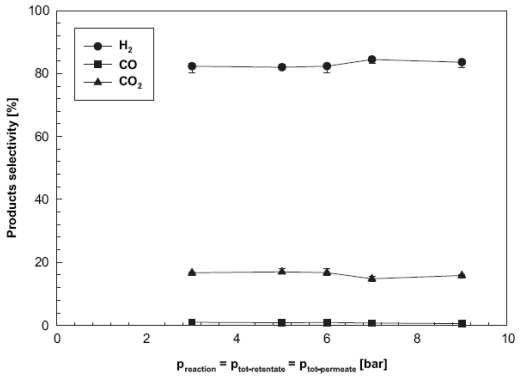

Fig. 10 – Products selectivity against reaction pressure in dense Pd–Ag MR. Operating conditions: $T = 450\ ^{\circ}C$, SF = 1.6 and co-current flow configuration of sweep gas.

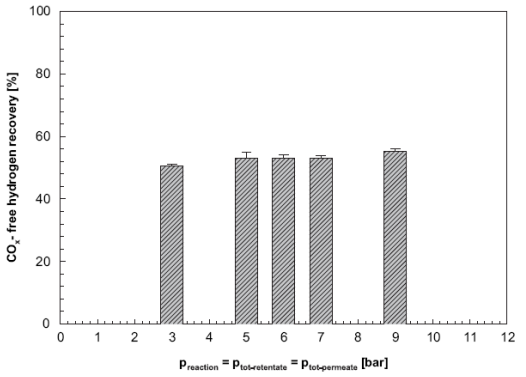

Fig. 11 – CO_x-free hydrogen recovery against the reaction pressure during MSR reaction in the dense Pd–Ag MR. Operating conditions: $T = 450\ ^{\circ}C$, SF = 1.6 and co-current flow configuration of sweep gas.

Table 4 – Hydrogen production at different total pressures in dense Pd–Ag MR. Operating conditions: $T = 450\ ^{\circ}C$, SF = 1.6 and co-current flow configuration of sweep gas.

	$Q_{H2\ retentate}$ [l/h]	$Q_{H2\ permeate}$ [l/h]	$Q_{H2\ tot}$ [l/h]
$p_{tot\text{-}retentate} = p_{tot\text{-}permeate}$ [bar]			
5.0	0,52	0,61	1,13
6.0	0,57	0,63	1,20
7.0	0,58	0,62	1,20
9.0	0,60	0,65	1,25
$p_{tot\text{-}retentate} - p_{tot\text{-}permeate}$ [bar]			
1.0	0,38	0,58	0,96
2.0	0,30	0,66	0,96
3.0	0,30	0,77	1,07
4.0	0,24	0,94	1,18

- a positive effect owing to the increase of the hydrogen permeation driving force. In fact, the higher the pressure the higher the hydrogen partial pressure in the retentate stream, inducing a greater CO_x-free hydrogen recovery in the permeate side. As a consequence, owing to a higher hydrogen removal from the retentate side, MSR reaction is shifted towards further products formation and methane conversion is improved (shift effect).

In our case, as sketched in Fig. 9, since the same total pressure was maintained in both retentate and permeate sides, the aforementioned shift effect only balances the detrimental effect that a pressure increase induces on the thermodynamic of MSR reaction, producing a constant trend of methane conversion (>50%). Accordingly, the product selectivities, reported in Fig. 10, show a constant trend by varying the total pressure. In detail, hydrogen selectivity reaches around 80%, CO_2 around 19% and CO in the range of 0.5–1.0%.

Fig. 11 shows that CO_x-free hydrogen recovery slightly increases from 50% to 58% in the whole range of total pressure

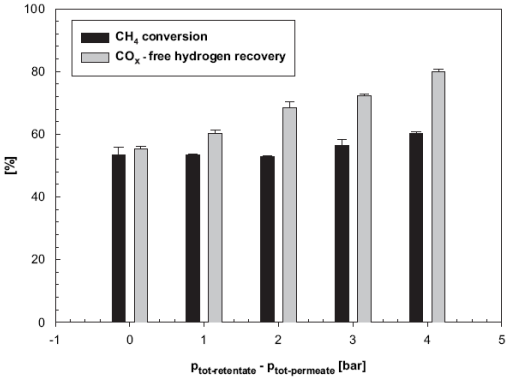

Fig. 12 – Methane conversion and CO_x-free hydrogen recovery against total pressure difference between retentate and permeate sides during MSR reaction in the dense Pd–Ag MR. Operating conditions: $p_{tot\text{-}retentate} = 9.0$ bar (abs.), $T = 450\ ^{\circ}C$, SF = 1.6 and co-current flow configuration of sweep gas.

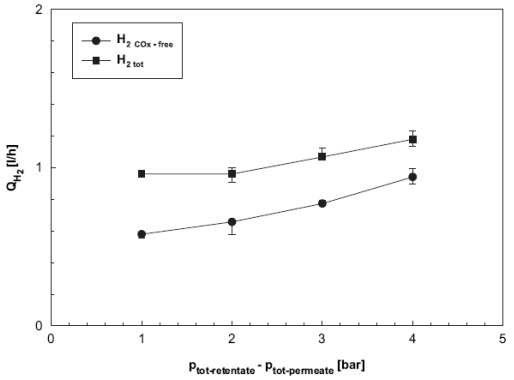

Fig. 13 – Hydrogen production during MSR reaction against total pressure difference between retentate and permeate sides in dense Pd–Ag MR. Operating conditions: $p_{tot\text{-}retentate} = 9.0$ bar (abs.), $T = 450\ ^{\circ}C$, SF = 1.6 and co-current flow configuration of sweep gas.

investigated. Hydrogen production against total pressure is summarized in Table 4. In the case study of reaction pressure equal to both retentate and permeate pressure, total hydrogen production ranged between 1.1 and 1.3 l/h (as a sum within hydrogen from permeate and permeate streams), while as a best result CO_x-free hydrogen production (as the only contribute of the hydrogen stream in the permeate side) was ~0.6 l/h at 9.0 bar.

In a second case study, the total retentate pressure (equal to reaction pressure) was kept constant at 9.0 bar, while the total permeate pressure was varied between 5.0 and 9.0 bar. As illustrated in Fig. 12, ~60% methane conversion and almost 80% CO_x-free hydrogen recovery were reached working at 4.0 bar of retentate/permeate total pressure difference. Furthermore, as reported in Fig. 13, the benefit owing to the retentate/permeate total pressure difference increase is given also in terms of CO_x-free hydrogen production, with around 1.0 l/h of $CO_{x\text{-}free}$ hydrogen produced at 4.0 bar of total pressure difference.

4. Conclusions

Methane steam reforming performed in FBRs is the dominant industrial process for producing hydrogen. Since the reformed stream coming out from the conventional reformers generally contains a hydrogen-rich gas mixture needing several stages of hydrogen separation/purification, palladium-based MRs can be proposed to produce pure, or at least, CO_x-free hydrogen due to their ability to combine two processes (reaction and hydrogen separation) in a single unit.

In this work, MSR reaction was performed at relatively high pressures (3.0–9.0 bar) in a Pd–Ag membrane reactor packed with a Ni–ZrO catalyst, characterized by high thermal stability and strong resistance against coke formation, demonstrating better performances with respect to a previously tested Ni–Al_2O_3 catalyst.

By means of H_2-rich binary gas mixture permeation tests, it was observed that MSR reaction in Pd–Ag MR is better performed at pressure higher than 3.0 bar in order to achieve larger hydrogen permeating flux. Results also indicated the possibility to follow effectively the theoretical reference line for permeability, depending on hydrogen partial pressures, while changing the molar fraction of N_2 and CH_4 in the binary mixture. A different behaviour was observed in a mixture of gases containing also CO, probably due to the concentration polarization effect.

Furthermore, a number of tests were carried out at methane reforming conditions. By studying the reaction pressure influence on the MR performances, it was concluded that the presence of a retentate/permeate total pressure difference in the MR allows the MR performances to be improved with respect to the case study where the pressure at reaction, retentate and permeate side are kept equal. In particular, the best results were achieved at SF equal to 1.6, 450 °C, 4.0 bar of total pressure difference between the retentate and permeate sides, yielding around 65% methane conversion and almost 80% $CO_{x\text{-free}}$ hydrogen recovery.

REFERENCES

[1] Lukyanov BN, Andreev DV, Parmon VN. Catalytic reactors with hydrogen membrane separation. Chem Eng J 2009;154:258–66.

[2] Smith B, Shantha MS. Membrane reactor based hydrogen separation from biomass gas – a review of technical advancements and prospects. Int J Chem Reactor Eng 2007;5:A84.

[3] Crabtree GW, Dresselhaus MS, Buchanan MV. The hydrogen economy. Phys Today 2004;57:39–44.

[4] Yamazaki O, Tomishige K, Fujimoto K. Development of highly stable nickel catalyst for methane steam reaction under low steam to carbon ratio. Appl Catal A Gen 1996;136:49–56.

[5] Hou K, Hughes R. The kinetics of methane steam reforming over a Ni/a-Al_2O catalyst. Chem Eng J 2001;82:311–28.

[6] Choudhary VR, Banerjee S, Rajput AM. Hydrogen from stepwise steam reforming of methane over Ni/ZrO_2: factors affecting catalytic methane decomposition and gasification by steam of carbon formed on the catalyst. Appl Catal A Gen 2002;234:259–70.

[7] Levent M, Gunn DJ, Ali El-Bousiffi M. Production of hydrogen-rich gases from steam reforming of methane in an automatic catalytic micro-reactor. Int J Hydrogen En 2003;28:945–59.

[8] Pistonesi C, Juan A, Irigoyen B, Amadeo N. Theoretical and experimental study of methane steam reforming reactions over nickel catalyst. Appl Surf Sci 2007;253:4427–37.

[9] Castro Luna AE, Becerra AM. Kinetics of methane steam reforming on a Ni on alumina-titania catalyst. React Kinet Catal Lett 1997;61:369–74.

[10] Rostrup-Nielsen JR. In: Anderson JR, Boudart M, editors. Catalytic steam reforming, catalysis: science and technology, vol. 5. Berlin: Springer; 1984 [chap. 1].

[11] Ridler DE, Twigg MV. In: Twigg MV, editor. Steam reforming, catalyst handbook. 2nd ed. England: Wolfe Publishing Ltd., 1989 [chap. 5].

[12] Kikuchi E. Membrane reactor application to hydrogen production. Catal Today 2000;56:97–101.

[13] De Falco M, Di Paola L, Marrelli L. Heat transfer and hydrogen permeability in modeling industrial membrane reactors for methane steam reforming. Int J Hydrogen Energy 2007;32:2902–13.

[14] Shu J, Grandjean BPA, Kaliaguine S. Methane steam reforming in asymmetric Pd- and Pd-Ag/porous SS membrane reactors. Appl Catal A 1994;119:305–25.

[15] Oertel M, Schmitz J, Weirich W, Jendryssek-Neumann D, Schulten R. Steam reforming of natural gas with integrated hydrogen separation for hydrogen production. Chem Eng Tech 1987;10:248–55.

[16] Jørgensen S, Nielsen PEH, Lehrmann P. Steam reforming of methane in membrane reactor. Catal Today 1995;25:303–7.

[17] Petersen KA, Nielsen CS, Jørgensen SL. Membrane reforming for hydrogen. Catal Today 1998;46:193–201.

[18] Kikuchi E, Nemoto Y, Kajiwara M, Uemiya S, Kojima T. Steam reforming of methane in membrane reactors: comparison of electroless-plating and CVD membranes and catalyst packing modes. Catal Today 2000;56:75–81.

[19] Lin YM, Liu SL, Chuang CH, Chu YT. Effect of incipient removal of hydrogen through palladium membrane on the conversion of methane steam reforming. Experimental and modeling. Catal Today 2003;82:127–39.

[20] Tong J, Matsumura Y. Pure hydrogen production by methane steam reforming with hydrogen-permeable membrane reactor. Catal Today 2006;111:147–52.

[21] Chen Y, Wang Y, Xu H, Xiong G. Efficient production of hydrogen from natural gas steam reforming in palladium membrane reactor. Appl Catal B Env 2008;80:283–94.

[22] Matsumura Y, Nakamori T. Steam reforming of methane over nickel catalysts at low reaction temperature. Appl Catal A Gen 2004;258:107–14.

[23] Wee JH. Applications of proton exchange membrane fuel cell systems. Renew Sustain Energy Rev 2007;11:1720–38.

[24] Schaller KV, Gruber C. Fuel cell drive and high dynamic energy storage systems-opportunities for the future city bus. Fuel Cells Bull 2000;3:9–13.

[25] Panik F. Fuel cells for vehicle applications in cars-bringing the future closer. J Power Sources 1998;71:36–8.

[26] Kawatsu S. Advanced PEFC development for fuel cell powered vehicles. J Power Sources 1998;71:150–5.

[27] Weiner SA. Fuel cell stationary power business development. J Power Sources 1998;71:61–4.

[28] Roses L, Bonalumi D, Campanari S, Iora P, Manzolini G. Simulation comparison of PEMFC micro-cogeneration units with conventional and innovative fuel processing. New York: ASME conference proceedings 2010. ASME 2010 eight international fuel cell science, engineering and technology conference.

[29] Campanari S, Macchi E, Manzolini G. Membrane reformer PEMFC cogeneration systems for residential applications - part B: techno-economic analysis and system layout, Asia-Pac. J Chem Eng 2009;4(3):311–21.

[30] Campanari S, Macchi E, Manzolini G. Innovative membrane reformer for hydrogen production applied to PEM micro-cogeneration: simulation model and thermodynamic analysis. Int J Hydrogen Energy 2008;33(4):1361–73.

[31] Kikuchi E, Tanaka S, Yamazaki Y, Morita Y. Steam reforming of hydrocarbons on noble metal catalysts - 1. The catalytic activity in methane-steam reaction. Bull Jpn Pet Inst 1974;16:95–8.

[32] Tong J, Matsumura Y. Effect of catalytic activity on methane steam reforming in hydrogen-permeable membrane reactor. Appl Catal A Gen 2005;286:226–31.

[33] Profeti LPR, Ticianelli EA, Assaf EM. Co/Al_2O_3 catalysts promoted with noble metals for production of hydrogen by methane steam reforming. Fuel 2008;87:2076–81.

[34] Guo J, Lou H, Zhao H, Chai D, Zhen X. Dry reforming of methane over nickel catalysts supported on magnesium aluminate spinels. Appl Catal A Gen 2004;273:75–82.

[35] Shu J, Grandjean BPA, Kaliaguine S. Asymettric Pd-Ag/stainless steel catalytic membranes for methane steam reforming. Catal Today 1995;25:327–32.

[36] Youn MH, Seo JG, Kim P, Kim JJ, Lee HI, Song IK. Hydrogen production by auto-thermal reforming of ethanol over Ni/γ-Al_2O_3 catalysts: effect of second metal addition. J Power Sources 2006;162:1270–4.

[37] Seo JG, Youn MH, Cho KM, Park S, Lee SH, Lee J, et al. Effect of Al_2O_3–ZrO_2 xerogel support on the hydrogen production by steam reforming of LNG over Ni/Al_2O_3–ZrO_2 catalyst. Korean J Chem Eng 2008;25:41–5.

[38] Seo JG, Youn MH, Park S, Lee J, Lee SH, Lee H, et al. Hydrogen production by steam reforming of LNG over Ni/Al_2O_3–ZrO_2 catalysts: effect of ZrO_2 and preparation method of Al_2O_3–ZrO_2. Korean J Chem Eng 2008;25:95–8.

[39] Yamaguchi T. Application of ZrO_2 as a catalyst and a catalyst support. Catal Today 1994;20:199–218.

[40] Pengpanich S, Meeyo V, Rirksomboon T. Methane partial oxidation over Ni/CeO_2-ZrO_2 mixed oxide solid solution catalysts. Catal Today 2004;93–95:95–105.

[41] Roh HS, Jun KW, Dong WS, Chang JS, Park SE, Joe YI. Highly active and stable Ni/Ce-ZrO_2 catalyst for H_2 production from methane. J Mol Catal A Chem 2002;181:137–42.

[42] Montoya JA, Romero-Pascual E, Gimon C, Del Angel P, Monzon A. Methane reforming with CO_2 over Ni/ZrO_2-CeO_2 catalysts prepared by sol–gel. Catal Today 2000;63:71–85.

[43] Li X, Chang JS, Park SE. Carbon as an intermediate during the carbon dioxide reforming of methane over zirconia-supported high nickel loading catalysts. Chem Lett 1999;10:1099–100.

[44] Li X, Chang JS, Tian M, Park SE. Rapid catalytic reforming of methane with CO_2 and its application to other reactions. Appl Organometal Chem 2001;15:87–94.

[45] Tosti S, Bettinali L. Diffusion bonding of Pd-Ag membranes. J Mater Sci 2004;39:3041–6.

[46] Zenkevich IG, Makarov ED. Cromatographic quantitation et losses of analyte during sample preparation. Application of the modified method of double internal standard. J Cromatographia A 2007;1150:117–23.

[47] Shu J, Grandjean BPA, Van Neste A, Kaliaguine S. Catalytic palladium-based membrane reactors: a review. Can J Chem Eng 1991;69:1036–60.

[48] Amandusson H, Ekedahl LG, Dannetun H. Hydrogen permeation through surface modified Pd and PdAg membranes. J Membr Sci 2001;193:35–47.

[49] Li H, Xu H, Li W. Study of n value and α/β palladium hydride phase transition within the ultra-thin palladium composite membrane. J Membr Sci 2008;324:44–9.

[50] Koros WJ, Fleming GK. Membrane-based gas separation. J Membr Sci 1993;83:1–80.

[51] Basile A. Hydrogen production using pd-based membrane reactors for fuel cells. Top Catal 2008;51:107–22.

[52] Dolan MD, Dave NC, Ilyushechkin AY, Morpeth LD, McLennan KG. Composition and operation of hydrogen-selective amorphous alloy membranes. J Membrane Sci 2006; 285:30–55.

[53] Amandusson H, Ekedahl L-G, Dannetun H. The effect of CO and O_2 on hydrogen permeation through a palladium membrane. Appl Surf Sci 2000;153:259–67.

[54] Gallucci F, Chiaravalloti F, Tosti S, Drioli E, Basile A. The effect of mixture gas on hydrogen permeation through a palladium membrane: experimental study and theoretical approach. Int J Hydrogen Energy 2007;32: 1837–45.

[55] Basile A, Gallucci F, Iulianelli A, Tereschenko GF, Ermilova MM, Orekhova NV. Ti-Ni-Pd dense membranes-the effect of the gas mixtures on the hydrogen permeation. J Membr Sci 2008;310:44–50.

[56] Peters TA, Stange M, Klette H, Bredesen R. High pressure performance of thin Pd–23%Ag/stainless steel composite membranes in water gas shift gas mixtures; influence of dilution, mass transfer and surface effects on the hydrogen flux. J Membr Sci 2008;316:119–27.

[57] Unemoto A, Kaimai A, Sato K, Otake T, Yashiro K, Mizusaki J, et al. The effect of co-existing gases from the process of steam reforming reaction on hydrogen permeability of palladium alloy membrane at high temperatures. Int J Hydrogen Energy 2007;32:2881–7.

[58] Li H, Goldbach A, Li W, Xu H. PdC formation in ultra-thin Pd membranes during separation of H_2/CO mixture. J Membr Sci 2007;299:130–7.

[59] Caravella A, Barbieri G, Drioli E. Concentration polarization analysis in self-supported Pd-based membranes. Sep Purif Tech 2009;66:613–24.

[60] Iulianelli A, De Falco M, Longo T, Liguori S, Campanari S, Basile A. H_2 production by low pressure methane steam reforming in a Pd-Ag membrane reactor over a Ni-based catalyst: experimental and modeling. Int J Hydrogen Energy 2010;35:11514–24.

Chapter 2

Methane steam reforming reaction: experimental and simulation analysis

Introduction to paper 2

In the past, much attention has been placed on the preparation of catalysts for the MSR reaction and little work has done on its kinetic and mechanism. As a result, until 1970, kinetic data were lacking and contradictory reaction mechanisms were proposed. Therefore, over the years now, the modeling studies on MSR reaction were focused on the development of reaction kinetic mechanisms and evaluation of its parameters.

Nowadays, almost the totality of academic research use the rate expression and kinetic framework developed by Xu and Froment in 1989 [Xu and Froment (1989a), (1989b)]. Indeed, in their studies, the authors reported a detailed MSR reaction kinetic mechanism considering Ni/$MgAl_2O_4$-spinel catalyst and developed a model intrinsic kinetics. In particular, their proposed reaction scheme consisted of 21 sets of rate equations. Afterwards, the number of possible reaction mechanisms was reduced taking into account a thermodynamic analysis and using Langmuir equilibrium relation.

In particular, the authors identified three reactions (1-3) occurring during SMR reaction and derived rate expressions for these three reactions (4-6). In particular, the rate expressions identify the rate limiting step in the absence of mass-transfer limitations.

$CH_4 + H_2O = CO + 3H_2$	$\Delta H°_{298\ K} = 206$	kJ/mol	(1)
$CO + H_2O = CO_2 + H_2$	$\Delta H°_{298\ K} = -41$	kJ/mol	(2)
$CH_4 + 2H_2O = CO_2 + 4H_2$	$\Delta H°_{298\ K} = 165$	kJ/mol	(3)

$$r_1 = \frac{\frac{k_1}{p_{H_2}^{2.5}} \cdot \left[p_{CH_4} \cdot p_{H_2O} - \frac{p_{H_2}^3 \cdot p_{CO}}{K_{eq1}} \right]}{\left(1 + K_{CO} \cdot p_{CO} + K_{H_2} \cdot p_{H_2} + K_{CH_4} \cdot p_{CH_4} + K_{H_2O} \cdot \frac{p_{H_2O}}{p_{H_2}} \right)^2} \quad (4)$$

$$r_2 = \frac{\frac{k_2}{p_{H_2}} \cdot \left[p_{CO} \cdot p_{H_2O} - \frac{p_{H_2} \cdot p_{CO2}}{K_{eq2}} \right]}{\left(1 + K_{CO} \cdot p_{CO} + K_{H_2} \cdot p_{H_2} + K_{CH_4} \cdot p_{CH_4} + K_{H_2O} \cdot \frac{p_{H_2O}}{p_{H_2}} \right)^2} \quad (5)$$

$$r_3 = \frac{\frac{k_3}{p_{H_2}^{3.5}} \cdot \left[p_{CH_4} \cdot p_{H_2O}^2 - \frac{p_{H_2}^4 \cdot p_{CO2}}{K_{eq3}} \right]}{\left(1 + K_{CO} \cdot p_{CO} + K_{H_2} \cdot p_{H_2} + K_{CH_4} \cdot p_{CH_4} + K_{H_2O} \cdot \frac{p_{H_2O}}{p_{H_2}} \right)^2} \quad (6)$$

where: k_i are the rate coefficient of reactions, K_i adsorption constants and $K_{eq,i}$ equilibrium constant of reactions. These parameters are related to temperature by Arrhenius' expression.

The 20 parameters (10 pre-exponential factors, 3 activation energies, 3 heats of reaction and 4 heats of adsorption) determined by Xu and Froment [(1989a), (1989b)] are given in the following Table 2.1.

Pre-exponential factor	$A(k_1)$	$A(k_2)$	$A(k_3)$	$A(K_1)$	$A(K_2)$	$A(K_3)$	$A(K_{CO})$	$A(K_{H2})$	$A(K_{CH4})$	$A(K_{H2O})$
Value	4.225×10^{15}	1.955×10^{6}	1.020×10^{15}	4.707×10^{12}	1.142×10^{-2}	5.375×10^{10}	8.23×10^{-5}	6.12×10^{-9}	6.64×10^{-4}	1.77×10^{5}
Units	(kgmol $bar^{1/2}$)/(kg catalyst hr)	kgmol /(bar kg catalyst hr)	(kgmol $bar^{1/2}$)/(kg catalyst hr)	bar^2		bar^2	bar^{-1}	bar^{-1}	bar^{-1}	
Energy	$E_a(k_1)$	$E_a(k_2)$	$E_a(k_3)$	$\Delta H(K_1)$	$\Delta H(K_2)$	$\Delta H(K_3)$	$\Delta H(K_{CO})$	$\Delta H(K_{H2})$	$\Delta H(K_{CH4})$	$\Delta H(K_{H2O})$
(kJ/mol)	240.1	67.13	243.9	224.0	-37.3	186.7	-70.65	-82.90	-38.28	88.68

Table 2.1. Model parameters

As aforementioned, nowadays, there are numerous mathematical models in the academic and scientific literature simulating steam methane reformers. These models differ for dimensionality: one-dimension or two-dimensional and complexity: pseudo-homogeneous or heterogeneous.

In a one-dimensional model, gradients are considered only in the axial direction, on the contrary, in a two-dimensional model, gradients are assumed in both the axial and radial directions.

In pseudo-homogeneous models, the process gas and catalyst are assumed to be at the same temperature and to be almost in contact. The pseudo-homogeneous assumption simplifies mass-transfer modeling since external and internal diffusion are not considered explicitly. An effectiveness factor is applied to reaction rates to model the lower concentration of reactants at the catalyst sites. Since the process gas and catalyst are assumed to be at the same temperature, an overall heat-transfer coefficient can be used to describe heat transfer from the inner-tube wall to the catalyst and process gas.

In heterogeneous models, separate material (and energy) balances are performed on the bulk-process gas and on the process gas diffusing through the catalyst particle. Unlike pseudo-homogeneous models, the material balance on the bulk-process gas does not contain a reaction rate expression.

In Table 2.2, an overview of some models based on MSR reaction is reported, pointing out the limits of modeling studies realized in the last twenty years.

Authors	Reactor Model	Reaction kinetic
Singh *et al* (1979)	-1D -pseudo-homogensous -no effectiveness factors used -assumed diffusion limitations accounted for in kinetics -plug flow	-used first order kinetic rate expressions developed by Haldor Topsoe and shown in Singh and Saraf (1979)
Murty *et al* (1988)	-1D -pseuod-homogeneous -diffusion limitations accounted for in kinetics -plug flow	-used first order kinetic rate expressions developed by Haldor Topsoe and shown in Singh and Saraf (1979)
Plehiers *et al* (1989)	-1D -heterogeneous -plug flow	-Xu and Froment (1989a) diffusion limitations
Alhabdan *et al* (1992)	-1D heterogeneous -plug flow (not stated) - derived a material balance on a catalyst pellet using characteristic length	-Xu and Froment (1989a)
Pedernera *et al* (2003)	-2D heterogenous -partial differential equations from momentum balances	-Xu and Froment (1989a)
Yu *et al* (2006)	-1D -pseudo-homogeneous	Yu et al. 2006 -reaction kinetics derived from stoichiometric equations -1D pseudohomogeneous
Wesenberg *et al* (2007)	-2D heterogenous	-Xu and Froment (1989a)
Ebrahimi *et al* (2008)	-1D -pseudo-homogeneous -plug flow	-Xu and Froment (1989a) diffusion limitations

Table 2.2. Several SMR reaction models

Thus, in the Paper 2, a modeling study is carried out on the MSR reaction performed in Pd-Ag MR packed with Ni on alumina catalyst. The mathematical model is based on mass balance in both reaction and permeation zones. In the reaction zone, a two-dimensional and pseudo-homogeneous conditions are considered, whereas, in the permeation zone, a one-dimensional model is developed since radial profiles are considered negligible. Moreover, the kinetic parameters developed by Xu and Froment are used for modeling.

So, the effect of temperature and pressure reaction from 400 °C to 500 °C and from 1.0 bar to 3.0 bar, respectively, on the MR performances is investigated. Moreover, a comparison with a conventional reactor working at same operative conditions is realized.

INTERNATIONAL JOURNAL OF HYDROGEN ENERGY 35 (2010) 11514–11524

Available at www.sciencedirect.com

ScienceDirect

journal homepage: www.elsevier.com/locate/he

H_2 production by low pressure methane steam reforming in a Pd–Ag membrane reactor over a Ni-based catalyst: Experimental and modeling

A. Iulianelli [a], G. Manzolini [b], M. De Falco [c], S. Campanari [b], T. Longo [a], S. Liguori [a,d], A. Basile [a,*]

[a] Institute on Membrane Technology of National Research Council (ITM-CNR), Via P. Bucci Cubo 17/C, c/o University of Calabria, Rende (CS) 87036, Italy

[b] Dept. of Energy, Politecnico di Milano, via Lambruschini 4, Milano (MI) 20156, Italy

[c] Faculty of Engineering, University Campus Bio-Medico of Rome, via Alvaro del Portillo 21, 00128 Rome, Italy

[d] Dept. of Modelling Engineering, via P. Bucci Cubo 39/C, c/o University of Calabria, Rende (CS) 87036, Italy

ARTICLE INFO

Article history:
Received 14 December 2009
Received in revised form
15 June 2010
Accepted 18 June 2010
Available online 27 July 2010

Keywords:
Palladium-based membrane reactor
Methane steam reforming
Hydrogen production

ABSTRACT

Nowadays, there is a growing interest towards pure hydrogen production for proton exchange membrane fuel cell applications. Methane steam reforming reaction is one of the most important industrial chemical processes for hydrogen production. This reaction is usually carried out in fixed bed reactors at 30–40 bar and at temperatures above 850 °C. In this work, a dense Pd–Ag membrane reactor packed with a Ni-based catalyst was used to carry out the methane steam reforming reaction between 400 and 500 °C and at relatively low pressure (1.0–3.0 bar) with the aim of obtaining higher methane conversion and hydrogen yield than a fixed bed reactor, operated at the same conditions. Furthermore, the Pd–Ag membrane reactor is able to produce a pure, or at least, a CO and CO_2 free hydrogen stream. A 50% methane conversion was experimentally achieved in the membrane reactor at 450 °C and 3.0 bar whereas, at the same conditions, the fixed bed reactor reached a 6% methane conversion. Moreover, 70% of high-purity hydrogen on total hydrogen produced was collected with the sweep-gas in the permeate stream of the membrane reactor. From a modeling point of view, the mathematical model realized for the simulation of both the membrane and fixed bed reactors was satisfactorily validated with the experimental results obtained in this work.

1. Introduction

Climate change and air pollution related to the emissions caused by the use of fossil fuels, associated to the depletion of them, drove the scientific efforts towards the use of alternative technologies and renewable energy sources in order to mitigate the effects of the harmful emissions. The proton exchange membrane fuel cells (PEMFCs) are electrochemical devices producing electricity directly from hydrogen and oxygen, without combustion, making the process clean and non-polluting. PEMFCs present several advantages such as low operative temperature (60–100 °C), sustained operation at high current density, compactness, fast start-up and suitability for discontinuous operation [1–5]. These features make

* *Corresponding author*. Tel.: +39 0984 492013; fax: +39 0984 402103.
E-mail address: a.basile@itm.cnr.it (A. Basile).

0360-3199/$ – see front matter © 2010 Professor T. Nejat Veziroglu. Published by Elsevier Ltd. All rights reserved.
doi:10.1016/j.ijhydene.2010.06.049

PEMFCs the most promising and attractive candidate for a wide variety of power applications, ranging from portable/micropower and transportation to larger stationary power systems for buildings and distributed generation [6–12].

The full commercialization of PEMFC systems needs a stable supply of high-purity hydrogen. Traditionally, hydrogen is technologically produced by the steam reforming of natural gas or by coal gasification [13]. In particular, the reformed stream coming out from a fixed bed reactor (FBR) contains a hydrogen-rich gas mixture. Therefore, in the viewpoint of pure hydrogen production, it needs, at least, three successive stages for separating hydrogen from the reformed stream. These stages consist of two different reactors for water gas shift reaction (HTS and LTS) followed by a purification system (PSA or others) [13].

As an alternative to the FBR systems, the Pd-based membrane reactors (MRs) are able to combine two different processes (reaction and hydrogen separation) in the same device. In particular, the use of a dense Pd-based MR allows a CO and CO_2 (CO_x) free hydrogen stream to be collected owing to the infinite hydrogen perm-selectivity of the dense Pd-based membranes with respect to the other gases [14–16]. Nevertheless, it is well known that dense palladium membranes are susceptible to cracking because of the amount of hydrogen absorbed that can cause the phase transition from α to β palladium hydride [16]. This phenomenon is known as hydrogen embrittlement, in which dissolved hydrogen causes the elongation of the metallic film (that produce the α–β hydride transformations), leading to fractures after repeated pressure and thermal cycles. The embrittlement can be avoided alloying the palladium with metals such as silver, gold, etc. [14]. For example, in the case of palladium–silver alloys, the membrane lattice, expanded by the silver atoms, is less influenced by the hydrogen permeation and, thus, less brittle than the pure palladium [14–17].

Industrially, methane steam reforming (MSR) reaction is the most important process to produce hydrogen [18]. Metals of Group 8–10 are used as catalysts, offering very high catalytic activity for this reaction (Ru ≈ Rh > Ni > Ir > Pt ≈ Pd >> Co ≈ Fe) [19]. In particular, Ni-based catalysts represent a valid choice, owing to the low cost and wide availability [20,21].

The MSR reaction is conventionally performed in FBRs at high temperatures (>850 °C) owing to its endothermic character [22–30]. Moreover, thermodynamically it would be preferable to conduct the MSR reaction under moderate pressures. Nevertheless, as reported above the reformed stream coming out from an FBR needs to be purified through the aforementioned successive processes, all of them requiring high operating pressures. Therefore, industrial MSR reaction is generally performed at pressures >10 bar [28–30].

On the contrary, in the last years, many researchers proposed to apply Pd-based MRs for MSR reaction operating at milder operative conditions than the FBRs [19–21,31–38]. To the best of our knowledge, the majority of these papers are realized at relatively high pressure, whereas the novelty of this work is represented by the low operating pressure (1–3 bar) MR with the aim to reach high CO_x-free hydrogen recovery. Operating at low pressure, keeping interesting H_2 conversion rates, allows to project the application of the process to very small scale fuel cell power generation units, using low pressure natural gas as a fuel source, where it would be too demanding to install high pressure fuel compression units [12].

Therefore, the effect of some operating parameters (temperature, pressure and sweep-gas molar flow rate) on the MR performances, in terms of methane conversion, CO_x-free hydrogen recovery and CO_x-free hydrogen yield is investigated from both a modeling and an experimental point of view.

2. Theoretical model

The mathematical model is based on mass balance in both reaction and permeation zones, Fig. 1a, with the following assumptions:

- Only reactions ((1)–(3)) from Xu and Froment [39] are considered (secondary reactions are neglected and between them, Bouduard reaction was not considered due to the S/C used in this work).

$$CH_4 + H_2O \leftrightarrows CO + 3H_2 \quad \Delta H^0_{298K} = 206 \text{ kJ/mol} \tag{1}$$

$$CO + H_2O = CO_2 + H_2 \quad \Delta H^0_{298K} = -41 \text{ kJ/mol} \tag{2}$$

$$CH_4 + 2H_2O \leftrightarrows CO_2 + 4H_2 \quad \Delta DH^0_{298K} = 165 \text{ kJ/mol} \tag{3}$$

- Steady-state conditions.
- Negligible axial dispersion and radial convective terms.
- Ideal gas behaviour.
- Pseudo-homogenous condition inside the reactor (pseudo-homogeneous models make the assumption that the reactor can be described as an entity consisting only of a single phase. In other words, the model assumption is that the catalyst surface and the bulk fluid have the same conditions and, as a consequence, the behaviour of both the phases can be described by the same variables such as concentrations, temperature and pressure).
- 100% hydrogen perm-selectivity of Pd-based membrane to other gases.
- Isothermal and isobaric condition.

In the reaction zone a two-dimensional isothermal model, able to calculate both axial and radial composition profiles, is developed.

In the permeation zone, a one-dimensional model is developed since radial profiles are considered negligible. Equations of the MR model, together with boundary conditions, are:

- Mass balances

Reaction zone: $i = CH_4, H_2O, H_2, CO, CO_2$

$$\frac{\partial(u_z \times c_i)}{\partial \tilde{z}} = \frac{d_P \cdot L}{Pe_{mr} \cdot r_{t,0}^2} \times \left(\frac{\partial^2 (u_z \cdot c_i)}{\partial \tilde{r}^2} + \frac{1}{\tilde{r}} \times \frac{\partial (u_z \cdot c_i)}{\partial \tilde{r}} \right) + \rho_b \cdot L \cdot \sum_{j=1}^{3} \eta_j \cdot R_j \tag{4}$$

where u_z and c_i are gas mixture velocity and mole concentration of component i, $\tilde{z}$ and $\tilde{r}$ are dimensionless axial and radial coordinates reactor length and the catalytic bed tube

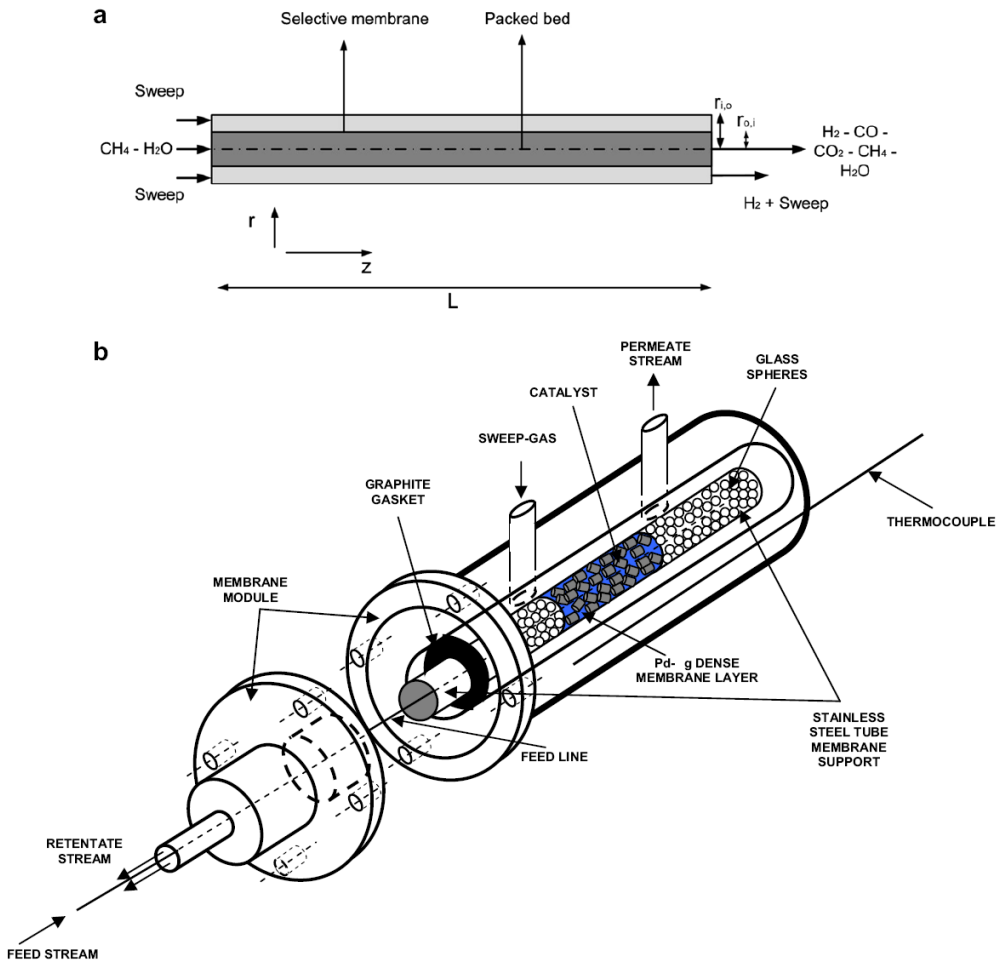

Fig. 1 – (a) Scheme of the Pd–Ag MR for the mathematical modeling. (b) Scheme of the experimental Pd-Ag MR.

radius respectively, p_b is the packed bed density, η and R_j are the effectiveness factor and the intrinsic rate for component i, expressed according to kinetics scheme, and Pe_{mr} is the mass effective radial Peclet number.

Permeation zone:

$$\frac{dY_{H_2}}{d\tilde{z}} = \pm \frac{N^m_{H_2} \cdot 2\pi \cdot r_{0,i}}{F^{in}_{CH_4}} \tag{5}$$

The signs + and − relate to co-current and counter-current configuration of the sweep-gas respectively.

- Boundary conditions

$$z = 0, \ \forall \tilde{r}: \quad u_z \cdot c_i = u_z^{in} \cdot c_i^{in} \tag{6}$$

$$\tilde{z} = 1, \ \forall \tilde{r}: \quad Y_{H_2} = 0 \tag{7}$$

$$r = r_{i,0}, \ \forall \tilde{z}: \quad \frac{\partial (u_z \cdot c_i)}{\partial \tilde{r}} = 0 \tag{8}$$

$$r = r_{0,i}, \ \forall \tilde{z}: \quad \frac{\partial (u_z \cdot c_i)}{\partial \tilde{r}} = 0 \tag{9}$$

$$\frac{d_p}{Pe_{mr}} \cdot \frac{\partial (u_z \cdot c_{H_2})}{\partial \tilde{r}} = N^m_{H_2}.$$

In Eq. (4), the mass effective radial Peclet number (Pe_{mr}) is calculated by the expression reported by Kulkarni and Doraiswamy [40] and it is valid for Re > 1000; η_j and R_j are calculated by Xu–Froment expressions [39].

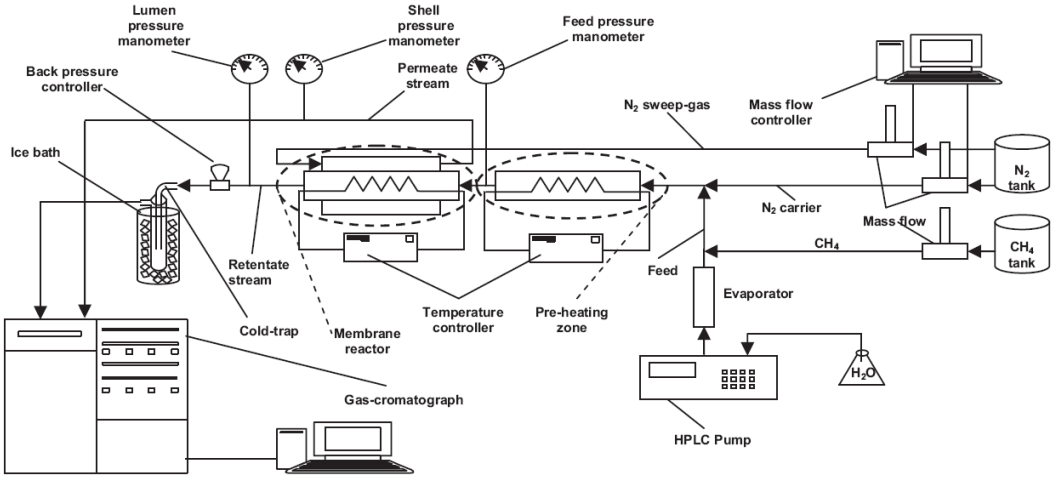

Fig. 2 – Scheme of the plant.

In the Eq. (5), Y_{H2} is the hydrogen recovered per mole of inlet methane and $N_{H_2}^m$ is the hydrogen flux permeating through the membrane.

$$N_{H_2}^m = \frac{B_H}{\delta} \cdot \left(\sqrt{p_{H_2,reac}} - \sqrt{p_{H_2,perm}} \right) \quad (10)$$

Eq. (10) is the Sieverts' law, suitable for thick dense membrane, i.e., in the case of limiting diffusion of atomic hydrogen in the metallic layer; δ is the Pd-based membrane thickness, $p_{H_2,reac}$ and $p_{H_2,perm}$ are hydrogen partial pressures in the reaction and permeation zone, respectively, and B_H is the membrane permeability, which depends on temperature and membrane composition.

In order to simulate the FBR, the Eq. (5) is imposed equal to zero.

To solve the set of partial differential equations, the radial coordinate is discretized by means of central second-order differences. An ODE (Ordinary Differential Equation) set is obtained and solved by a fourth-order Runge–Kutta method.

3. Experimental

3.1. Pd–Ag MR and FBR description

The experimental setup of the MR consists of a tubular stainless steel module (length 280 mm, i.d. 20 mm) housing a tubular pine-hole free Pd–Ag (23 wt% of Ag) membrane, permeable only to hydrogen (thickness 50 μm, o.d. 10 mm, length 145 mm) and produced by cold-rolling and diffusion welding technique [41]. Two zones can be identified inside MR: a first zone, inside the membrane (lumen side), in which the reaction takes place, and a second one, corresponding to the annulus of the membrane reactor (shell side), in which pure or CO_x-free hydrogen is collected, Fig. 1b.

The dense Pd–Ag membrane is joined to two stainless steel tubes for the membrane housing, with one of them closed. The MR is packed with 3.0 g of a Ni–Al_2O_3 commercial catalyst (Catal International Ltd.) inserted into the lumen side and glass spheres (2 mm diameter) are placed into the two stainless steel tubes to avoid loss of catalyst. One graphite o-ring (99.5% C and 0.5% S) by Gee Graphite Ltd. ensures that permeate and retentate streams do not mix with each other in the membrane module.

The tubular membrane is plugged from one side and reactants are fed by means of a stainless steel tube (o.d. 1.6 mm, i.d. 0.64 mm) placed inside the membrane. The experimental tests for the FBR were performed using the MR with the inlet and outlet shell sides completely closed.

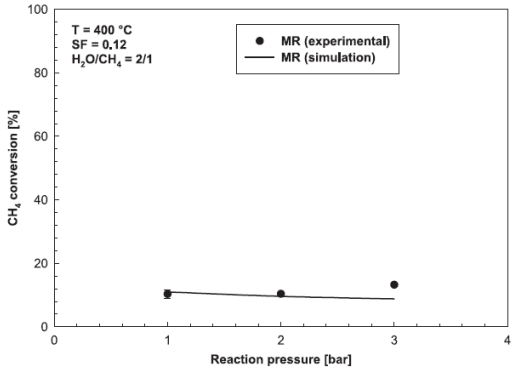

Fig. 3 – Methane conversion against reaction pressure at 400 °C, SF (sweep-factor) = 0.12 and H_2O/CH_4 = 2/1. Comparison between simulation and experimental results in a Pd–Ag MR.

3.2. Experimental details

The scheme of the plant is illustrated in Fig. 2. A P680 HPLC pump (Dionex) was used for feeding liquid water. Afterwards, it is vaporized, mixed with methane and fed into a preheating zone and, thus, to the reaction side of the MR by means of a tube in tube solution. The methane feed molar rate was 2.75×10^{-3} mol/min (GHSV = ~3700 h^{-1}) and H_2O/methane feed molar ratio was kept constant at 2/1. Moreover, a constant nitrogen molar flow rate (7.14×10^{-2} mol/min) as internal standard gas was fed with the reactants into the reaction side. The retentate stream was directed to a cold-trap in order to condensate the excess of water. Both permeate and retentate stream compositions were analysed using a temperature programmed HP 6890 GC with two thermal conductivity detectors at 250 °C and Ar as a carrier gas. The GC was equipped by three packed columns: Porapack R 50/80 (8 ft × 1/8 inch) and Carboxen™ 1000 (15 ft × 1/8 inch) connected in series, and a Molecular Sieve 5 Å (6 ft × 1/8 inch).

The sweep-gas molar flow rate ranged between 0.019 mol/h and 0.261 mol/h, corresponding to the sweep-factor (SF) (11) (defined as the molar ratio between the sweep-gas (N_2) supplied into the shell side and methane as a feed) variation from 0.12 to 1.6.

Being this work realized at lab-scale, nitrogen is used as a sweep-gas for simplicity, while, industrially, steam is preferred, separable readily from the permeate stream by condensation. The sweep-gas is supplied in co-current configuration with respect to the reactants by means of a mass-flow controller (Brooks Instruments 5850S), driven by a computer software furnished by Lira (Italy).

In all the experiments, the absolute MR shell side pressure was kept constant at 1.0 bar.

Each experimental point obtained in this work represents an average value of 6 experimental points taken in 90 min at steady-state conditions. Before reaction, the catalytic bed was reduced by using hydrogen (1.1×10^{-2} mol/min) at 450 °C for 2 h. A flat temperature profile along the reactor was confirmed during the reaction by means of a three points thermocouple placed into the reactor.

The following definitions are used for describing the MR/FBR performances, starting from the sweep-factor (SF):

$$SF = \frac{N_{2,sweep-gas}}{CH_{4-in}} \quad (-) \tag{11}$$

$$CH_4\ conversion = \frac{CH_{4-in} - CH_{4-out}}{CH_{4-in}} \cdot 100 \quad (\%) \tag{12}$$

where $CH_{4\text{-}in}$ is the methane molar flow rate fed to the reactor and $CH_{4\text{-}out}$ the methane molar flow rate going out from the reactor,

$$CO_x - free\ hydrogen\ yield = \frac{H_{2-permeate}}{4 \cdot CH_{4-in}} \cdot 100 \quad (\%) \tag{13}$$

$$CO_x - free\ hydrogen\ recovery = \frac{H_{2-permeate}}{H_{2-TOT}} \cdot 100 \quad (\%) \tag{14}$$

where $H_{2\text{-}permeate}$ is the hydrogen molar flow rate permeating through the membrane and collected in the permeate side, while $H_{2\text{-}TOT}$ is the total hydrogen produced during the reaction. Among the definitions, Eqs. 11, 12 and 14 hold only for the MR. Additionally, the selectivity to a chemical species S_x is defined as:

$$S_x = \frac{X_{OUT}}{H_{2,OUT} + CO_{OUT} + CO_{2,OUT} + CH_{4,OUT}} \cdot 100 \quad (\%) \tag{15}$$

where X can be H_2, CO_2, CH_4 or CO.

The laws regulating the hydrogen flux permeating through the dense Pd–Ag membrane are listed below:

$$J_{H_2} = \frac{Pe}{\delta} \cdot \left(\sqrt{p_{H_2-lumen}} - \sqrt{p_{H_2-shell}}\right) \quad Fick - Sieverts\ law \tag{16}$$

where J_{H_2} is the hydrogen flux permeating through the Pd–Ag membrane, Pe the hydrogen permeability, δ the Pd–Ag membrane thickness (50 μm), $p_{H_2-lumen}$ and $p_{H_2-shell}$ the hydrogen partial pressures in the lumen and shell sides, respectively:

$$Pe = Pe_0 \exp(-Ea/RT) \quad Arrhenius - like\ equation \tag{17}$$

where Pe_0 is the pre-exponential factor, Ea the apparent activation energy, R the universal gas constant and T the absolute temperature. The combination of Eqs. 16 and 17 gives:

$$J_{H_2} = \frac{Pe_0 \cdot \exp\left(-\frac{Ea}{RT}\right) \cdot \left(\sqrt{p_{H_2,lumen}} - \sqrt{p_{H_2,shell}}\right)}{\delta} \quad Richardson\ law \tag{18}$$

expressing the overall hydrogen flux permeating through the Pd–Ag membrane.

4. Results and discussion

4.1. Validation of the model

The simulation tests on MSR in the membrane reactor were realized on the basis of the model above reported and, then, compared with the experimental results obtained in this

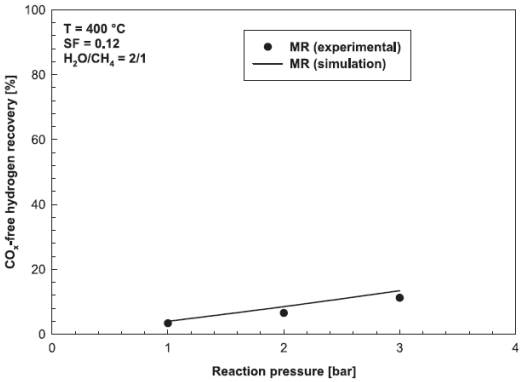

Fig. 4 – CO_x-free hydrogen recovery against reaction pressure at 400 °C, SF (sweep-factor) = 0.12 and H_2O/CH_4 = 2/1. Comparison between simulation and experimental results in a Pd–Ag MR.

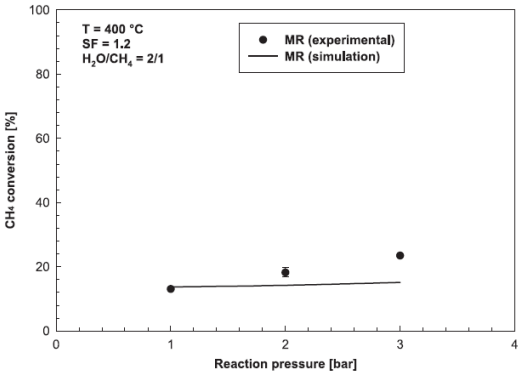

Fig. 5 – Methane conversion against reaction pressure at 400 °C, SF (sweep-factor) = 1.2 and H_2O/CH_4 = 2/1. Comparison between simulation and experimental results in a Pd–Ag MR.

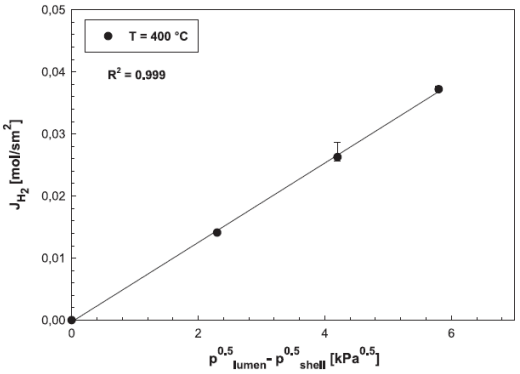

Fig. 7 – Hydrogen flux permeating through the Pd–Ag membrane against hydrogen partial pressure square root difference between lumen and shell sides at 400 °C.

work. Figs. 3 and 4 sketch respectively the methane conversion and CO_x-free hydrogen recovery versus reaction pressure at 400 °C, SF = 0.12 and H_2O/CH_4 = 2/1. It is quite evident that the experimental points match with greatly the theoretical results, validating the model developed in this work. On the contrary, at SF = 1.2 the experimental results mismatch with the theoretical predictions at higher pressures, Fig. 5. In this figure, at 1.0 bar the conversion by simulation totally matches the experimental point, while at 3.0 bar the theoretical model does not estimate exhaustively the methane conversion achievable in the experimental tests. Furthermore, the experimental tests indicate that hydrogen recovery is lower than the one predicted by simulation, Fig. 6. This is probably due to the inevitable differences between the model and the realty of the experimental tests. For example, the theoretical model considers that the permeation of hydrogen as a pure gas follows Sieverts' law, but in the experiments hydrogen is present in the reaction side with other gases and there is no correction in the model for potential interactions with other gases during the permeation phenomena.

4.2. *Permeation test*

The dense Pd–Ag membrane was experimentally characterized to gas permeation tests at different temperature and pressure using pure gases (H_2, N_2, CO, CO_2, CH_4) and steam. It was observed that only hydrogen permeates through the membrane (confirming that it is completely perm-selective to the hydrogen permeation). Thus, the hydrogen permeating flux was measured supplying pure hydrogen into the membrane at 400 °C, by varying the lumen side pressure between 1.5 and 2.5 bar and keeping constant the shell side pressure at 1.0 bar. In Fig. 7, the linear trend of the hydrogen permeating flux against the hydrogen partial pressure square root difference between lumen and shell sides is reported, confirming that Fick–Sieverts' law (16) is followed.

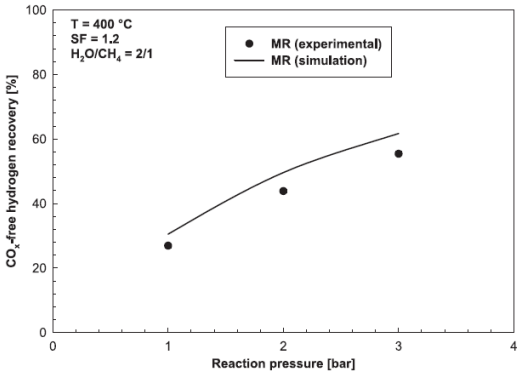

Fig. 6 – CO_x-free hydrogen recovery against reaction pressure at 400 °C, SF (sweep-factor) = 1.2 and H_2O/CH_4 = 2/1. Comparison between simulation and experimental results in a Pd–Ag MR.

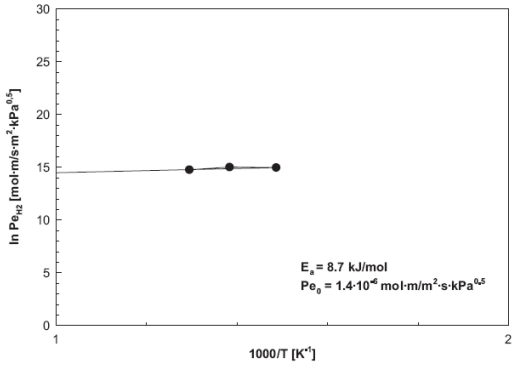

Fig. 8 – Hydrogen permeability dependence on the temperature.

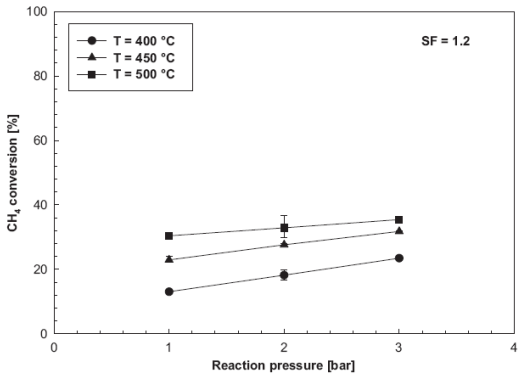

Fig. 9 – Methane conversion against reaction pressure at different temperatures, $H_2O/CH_4 = 2/1$, GHSV = 3710 h^{-1}, $p_{shell} = 1$ bar and co-current flow configuration of sweep-gas.

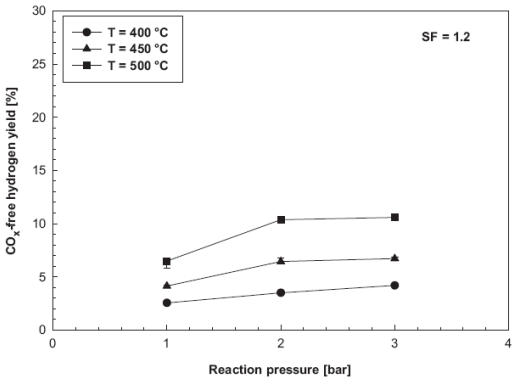

Fig. 11 – CO_x-free hydrogen yield against reaction pressure at different temperatures, $H_2O/CH_4 = 2/1$, GHSV = 3710 h^{-1}, $p_{shell} = 1$ bar and co-current flow configuration of sweep-gas.

Afterwards, at 1.5 bar lumen side pressure, the temperature was varied between 400 and 500 °C, confirming the temperature dependence of the hydrogen permeability (Fig. 8) as an Arrhenius-like Eq. (17).

4.3. Reaction tests

The influence of both temperature and pressure on the MR performances in terms of methane conversion (12), CO_x-free hydrogen yield (13) and CO_x-free hydrogen recovery (14) was evaluated.

The experimental tests were carried out at SF = 1.2 by varying the pressure and the temperature between 1.0 and 3.0 bar and 400 and 500 °C, respectively. According to Richardson law (18), a higher temperature positively affects the methane conversion and involves a higher hydrogen permeating flux and, as a consequence, a higher hydrogen removal through the Pd–Ag membrane, which shifts MSR reaction towards further products formation and induces a higher methane consume. This is confirmed by Fig. 9, where it is possible to observe that at higher temperatures the methane conversion increases (for example, at 3.0 bar, the methane conversion increases from 23% at 400 °C to 35% at 500 °C). On the contrary, a pressure increase makes two competitive effects on methane conversion:

- a negative effect owing to the thermodynamic features of the reaction (3), which proceeds with an increase of the moles number and is not favored by higher pressures;
- a positive effect due to the increase of the hydrogen permeation driving force (Eqs. (16) and (18)). A higher pressure increases the hydrogen partial pressure in the lumen side, inducing a greater CO_x-free hydrogen recovery in the

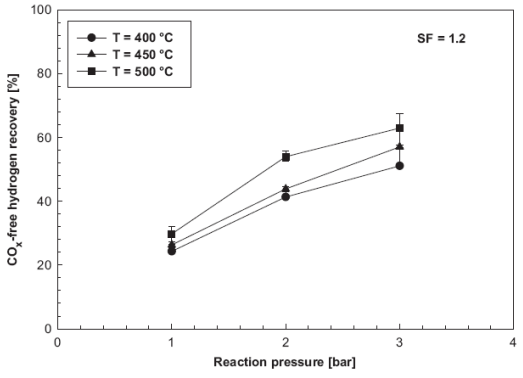

Fig. 10 – CO_x-free hydrogen recovery against reaction pressure at different temperatures, $H_2O/CH_4 = 2/1$, GHSV = 3710 h^{-1}, $p_{shell} = 1$ bar and co-current flow configuration of sweep-gas.

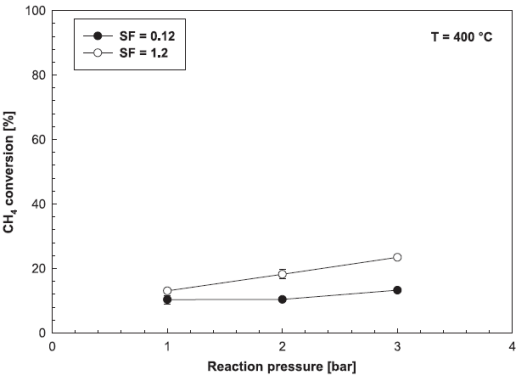

Fig. 12 – Methane conversion against reaction pressure at $T = 400$ °C, $H_2O/CH_4 = 2/1$, GHSV = 3710 h^{-1}, $p_{shell} = 1$ bar and co-current flow configuration of sweep-gas.

INTERNATIONAL JOURNAL OF HYDROGEN ENERGY 35 (2010) 11514–11524

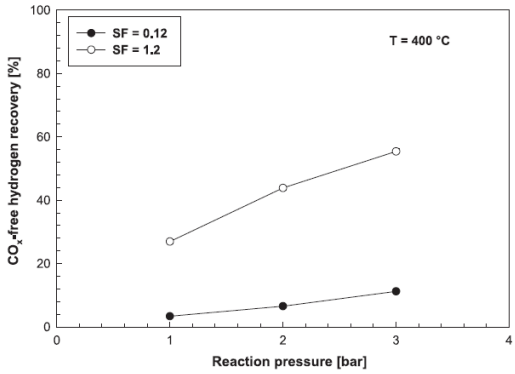

Fig. 13 – CO_x-free hydrogen recovery against reaction pressure at $T = 400$ °C, $H_2O/CH_4 = 2/1$, GHSV = 3710 h^{-1}, $p_{shell} = 1$ bar and co-current flow configuration of sweep-gas.

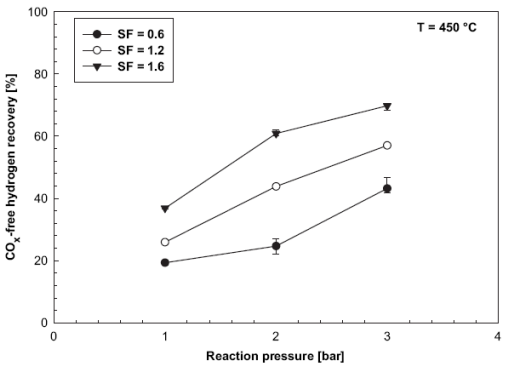

Fig. 15 – CO_x-free hydrogen recovery against reaction pressure at $T = 450$ °C, $H_2O/CH_4 = 2/1$, GHSV = 3710 h^{-1}, $p_{shell} = 1$ bar and co-current flow configuration of sweep-gas.

shell side. Moreover, as a consequence, the MSR reaction is shifted towards further products formation and methane conversion is improved (shift effect).

As shown in Fig. 9, the methane conversion enhancement with the pressure is probably due to the prevalence of the "shift effect" related to the selective removal of hydrogen over the detrimental effect of the pressure increase induced on reaction thermodynamics.

However, the low conversion values shown in Fig. 9 are probably due to the low nickel content as catalyst metal phase used in this work. Even Tong et al. [20,36] observed that, using a Ni-based catalyst for MSR reaction with a relatively low nickel content, the average pressure of hydrogen in the reactor was lower than at the output, probably because of the lower hydrogen production in the central part of the catalyst layer than the amount removed by permeation. Therefore, they concluded that the catalytic activity influences even the hydrogen flow permeating through the membrane and, then, the methane conversion. Probably, this scenario can be proposed for explaining the low conversion achieved in the present study.

Taking into account that the main scope of this work is to produce pure (or at least CO_x-free) hydrogen, particular attention was paid on both CO_x-free hydrogen recovery and CO_x-free hydrogen yield. Fig. 10 sketches that the CO_x-free hydrogen recovery increases as a function of temperature and pressure. In fact, a higher temperature involves a higher hydrogen permeating flux as well as a higher reaction pressure maximizes the hydrogen partial pressure in the lumen side improving the hydrogen permeation driving force. These two effects induce a higher CO_x-free hydrogen recovery in the permeate stream. At 3.0 bar and 500 °C, 63% CO_x-free hydrogen recovery was reached. Similarly, as illustrated in Fig. 11, the CO_x-free hydrogen yields increase with the temperature and pressure. As already stated, the higher the temperature and pressure the higher the hydrogen removal through the membrane that causes an improvement of methane conversion. As a consequence, the hydrogen

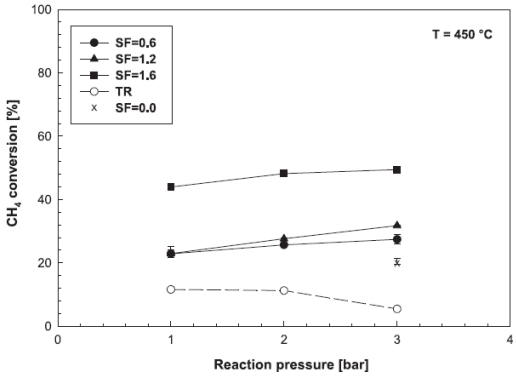

Fig. 14 – Methane conversion against reaction pressure for both MR and FBR at $T = 450$ °C, $H_2O/CH_4 = 2/1$, GHSV = 3710 h^{-1}; MR: $p_{shell} = 1$ bar and co-current flow configuration of sweep-gas.

Table 1 – CO selectivity at different reaction pressures and temperatures for both MR and FBR at $H_2O/CH_4 = 2/1$, GHSV = 3710 h^{-1}; MR: $p_{shell} = 1$ bar, co-current flow configuration of sweep-gas.

	S_{CO} [%]			
	MR at SF = 1.2			FBR
p [bar]	400 °C	450 °C	500 °C	450 °C
1.0	0.1	0.5	1.4	1.1
2.0	0.1	0.4	1.1	1.1
3.0	–	0.2	1.0	1.3

Table 2 – Methane conversion and hydrogen recovery in Pd-based membrane reactors. An experimental comparison between this work and literature data.

Membrane	Thickness [μm]	T [°C]	$P_{reaction}$ [bar]	P_{shell} [bar]	Catalyst	H_2O/CH_4 molar ratio	GHSV [h^{-1}]	Sweep-gas [ml/min]	Conversion [%]	H_2 recovery [%]	Authors
Pd/5.1%Ag	10.3	500	1.4[a]	–	Ni/Al_2O_3	3/1	1067	–	50	–	Shu et al. [22]
Pd-PSS	11	527[a]	3.0[a]	–	47.2wt% Ni/Al_2O_3	3/1	1120	482[a] (N_2)	100	–	Tong et al. [20]
							3360		60		
Pd-PSS	11	527[a]	3.0[a]	–	9.9wt% Ni/Al_2O_3	3/1	1120	482[a] (N_2)	90	–	Tong et al. [20]
							3360		50	–	
Pd-based	8	500[a]	1.0	–	Ni-based	3/1	–	(Ar)	86.4	–	Kikuchi et al. [33]
Pd-SS Tubular	20	500	20.0	1.0	Ni-based	3/1	–	(N_2)	85	90	Lin et al. [35]
Pd-SS Tubular	20	500	9.0	1.0	Ni-based	3/1	–	(N_2)	40	30	Lin et al. [35]
									35	15	
Pd/23% Ag Tubular	100	500	6.1	0.5	Ni e MgO based	2.9/1	–	160[a] (N_2)	50	–	Jorgensen et al. [37]
			10.0						60		
Pd/Al_2O_3	4	550	9.0	–	Ni–La/Mg–Al	3.5/1	–	220	98,8	95	Chen et al. [38]
Pd–Ag Tubular	50	450	3.0	1.0	Ni/Al_2O_3	2/1	3710	98 (N_2)	50	70	This work

a Calculated value.

production as well as the hydrogen stream collected in the shell side is improved. Nevertheless, the low CO_x-free hydrogen yield values of Fig. 11 are probably due to the relatively low methane conversions, as reported in Fig. 9.

Having in mind to maximize the CO_x-free hydrogen stream collected in the shell side, the SF influence on the MR performances was studied. A SF increase reduces the hydrogen partial pressure in the shell side, favoring the hydrogen permeation driving force and, consequently, the methane conversion and CO_x-free hydrogen recovery enhancement, Figs. 12 and 13.

In particular, at 400 °C, SF = 1.2 and 3.0 bar, 23% methane conversion and 55% CO_x-free hydrogen recovery were achieved with respect to SF = 0.12, where 13% methane conversion and 11% CO_x-free hydrogen recovery were reached.

The SF influence on MR performances was even studied at higher temperatures. In particular, Figs. 14 and 15 show the methane conversion and CO_x-free hydrogen recovery at 450 °C and different SF. As best result of this work, 50% methane conversion and 70% hydrogen recovery were obtained at SF = 1.6. Being the experimental campaign carried out at lab-scale, a further increase of SF made an unacceptable increase of the shell side pressure owing to the small volume of the MR. Furthermore, the SF influence at 500 °C was not performed because of the Pd–Ag membrane failure.

Fig. 14 shows a comparison with an FBR exercised at the same MR conditions. The decreasing trend of methane conversion in the FBR against the pressure is due to the negative effect of pressure on the reaction thermodynamics. On the contrary, the MR provides significantly higher methane conversions than the FBR, owing to the selective removal of hydrogen through the membrane. In particular, at 450 °C and 3.0 bar, the methane conversion obtained in the FBR is 6% with respect to 50% obtained with the MR. When no sweep-gas is used on the shell side of the membrane reactor (SF = 0), the conversion decreases, but remaining always higher (around 20% at 3 bar) than that of the FBR.

A further comparison between the MR and FBR is shown in Table 1, where the CO selectivity values are reported as a function of the reaction pressure and temperature. This table shows the lower CO selectivity (corresponding to the outlet retentate CO composition) with respect to the FBR outlet composition at 450 °C. This result can be accounted for the "shift effect", which induces the shift of the WGS reaction (2) towards the products, allowing a greater CO consumption in the MR. Furthermore, the slight CO selectivity increase with the temperature in the MR is probably caused by the WGS reaction, which is exothermic and not favored at high temperature [42].

In conclusion, many investigations were carried out on MSR reaction using both conventional and membrane reactors for different purposes. As a qualitative analysis, Table 2 summarizes some experimental results in terms of methane conversion and hydrogen recovery obtained in this work, compared to other investigations from literature in the field of the Pd-based MRs. As shown in the table, it is evident that the most important result of our work consists of the possibility to reach methane conversion and, primarily, a relevant CO_x-free hydrogen recovery. By this point of view, the MSR performances are comparable with those obtained at more

demanding operating conditions (i.e., the reaction pressure) in literature, making interesting our application for producing hydrogen for PEMFC applications.

5. Conclusions

In this work, the MSR reaction was performed at low pressures (1–3 bar) in a Pd–Ag membrane reactor with the purpose of producing pure, or at least CO_x-free, hydrogen for PEMFCs.

The MR showed better methane conversions compared to a FBR operated at the same conditions with the further advantage of collecting a CO_x-free hydrogen stream in the shell side. In particular, the best results of this work are achieved at 450 °C, 3.0 bar and SF equal to 1.6, consisting of 50% methane conversion and around 70% CO_x-free hydrogen recovery. Instead, at this conditions, 6% methane conversion was reached in the FBR.

However, the limited conversion values obtained can be probably explained by the low nickel content in the catalyst metal phase used in this work. In fact, the catalytic activity greatly affects the performance of the MR. As future developments, the MSR reaction will be studied in Pd–Ag MRs using industrial natural gas as fuel input, rather than pure methane.

Acronyms

FBR	fixed bed reactor
GHSV	gas hourly space velocity
HTS	high temperature shift
LTS	low temperature shift
MR	membrane reactor
MSR	methane steam reforming
PEMFC	proton exchange membrane fuel cell
PSA	pressure swing adsorption
SF	sweep-factor
WGS	water gas shift
ODE	Ordinary Differential equation

Nomenclature

B_H	hydrogen permeability
c_{H_2}	hydrogen concentration
$CH_{4\text{-in}}$	methane molar flow rate fed to the reactor
$CH_{4\text{-out}}$	methane molar flow rate going out from the reactor
c_i	mole concentration of component *i*
c_i^{in}	inlet concentration of component *i*
d_p	catalytic bed tube radius
Ea	apparent activation energy
$F_{CH_4}^{in}$	methane inlet flow rate
$H_{2\text{-permeate}}$	hydrogen molar flow rate permeating through the membrane and collected in the permeate side
$H_{2\text{-TOT}}$	total hydrogen produced during the reaction
i.d.	inside diameter
J_{H_2}	hydrogen flux permeating through the Pd–Ag membrane
L	reactor length
$N_{2,sweep\text{-}gas}$	sweep-gas molar flow rate
$N_{H_2}^m$	hydrogen flux permeating through the membrane.
o.d.	outside diameter
Pe	hydrogen permeability
Pe_0	pre-exponential factor
Pe_{mr}	mass effective radial Peclet number.
$p_{H_2,perm}$	hydrogen partial pressures in the permeation zone
$p_{H_2,reac}$	hydrogen partial pressures in the reaction zone
$p_{H_2-lumen}$	hydrogen partial pressures in the lumen side
$p_{H_2-shell}$	hydrogen partial pressures in the shell side
R	universal gas constant
$\tilde{r}$	dimensionless radial coordinate
$r_{i,0}$	internal radius external tube
R_j	intrinsic rate for component *j*
S_x	selectivity of component *i*
T	absolute temperature
u_z^{in}	inlet gas mixture velocity
u_z	gas mixture velocity
Y_{H_2}	hydrogen recovered per mole of inlet methane
$\Delta H^0_{298\ K}$	heat of reaction in standard conditions
δ Pd–Ag	membrane thickness
η_j	effectiveness factor for component *j*
ρ_b	packed bed density
$\tilde{z}$	dimensionless axial coordinate

REFERENCES

[1] Chalk SG, Miller JF, Wagner FW. Challenges for fuel cells in transport applications. J Power Sources 2000;86:40–51.

[2] Chu D, Jiang R, Gardner K, Jacobs R, Schmidt J, Quakenbush T, et al. Polymer electrolyte membrane fuel cells for communication applications. J Power Sources 2001; 96:174–8.

[3] Costamagna P, Srinivasan S. Quantum jumps in the PEMFC science and technology from the 1960s to the year 2000 Part II. Engineering, technology, development and application aspects. J Power Sources 2001;102:253–69.

[4] Gamburzev S, Appleby AJ. Recent progress in performance improvement of the proton exchange membrane fuel cell (PEMFC). J Power Sources 2002;107:5–12.

[5] Mehta V, Cooper JS. Review and analysis of PEM fuel cell design and manufacturing. J Power Sources 2003;114: 32–53.

[6] Schaller KV, Gruber C. Fuel cell drive and high dynamic energy storage systems – opportunities for the future city bus. Fuel Cells Bull 2000;3:9–13.

[7] Panik F. Fuel cells for vehicle applications in cars – bringing the future closer. J Power Sources 1998;71:36–8.

[8] Kawatsu S. Advanced PEFC development for fuel cell powered vehicles. J Power Sources 1998;71:150–5.

[9] Weiner SA. Fuel cell stationary power business development. J Power Sources 1998;71:61–4.

[10] Campanari S, Macchi E, Manzolini G. Membrane reformer PEMFC cogeneration systems for residential applications – part A: full load and partial load simulation. Asia-Pac J Chem Eng 2009;4(3):301–10.

[11] Campanari S, Macchi E, Manzolini G. Membrane reformer PEMFC cogeneration systems for residential applications – part B: techno-economic analysis and system layout. Asia-Pac J Chem Eng 2009;4(3):311–21.

[12] Campanari S, Macchi E, Manzolini G. Innovative membrane reformer for hydrogen production applied to PEM micro-cogeneration: simulation model and thermodynamic analysis. Int J Hydrogen Energy 2008;33: 1361–73.

[13] Barelli L, Bidini G, Gallorini F, Servili S. Hydrogen production through sorption-enhanced steam methane reforming and membrane technology: a review. Energy 2008;33:554–70.
[14] Shu J, Grandjean BPA, Van Neste A, Kaliaguine S. Catalytic palladium-based membrane reactors: a review. Can J Chem Eng 1991;69:1036–60.
[15] Amandusson H, Ekedahl LG, Dannetun H. Hydrogen permeation through surface modified Pd and PdAg membranes. J Memb Sci 2001;193:35–47.
[16] Li H, Xu H, Li W. Study of n value and α/β palladium hydride phase transition within the ultra-thin palladium composite membrane. J Memb Sci 2008;324:44–9.
[17] Uemiya S, Matsuda T, Kikuchi E. Hydrogen permeable palladium–silver alloy membrane supported on porous ceramics. J Memb Sci 1991;56:315–25.
[18] De Falco M, Di Paola L, Marrelli L. Heat transfer and hydrogen permeability in modeling industrial membrane reactors for methane steam reforming. Int J Hydrogen Energy 2007;32:2902–13.
[19] Kikuchi E, Tanaka S, Yamazaki Y, Morita Y. Steam reforming of hydrocarbons on noble metal catalysts – 1. The catalytic activity in methane-steam reaction. Bull Jpn Pet Inst 1974;16:95–8.
[20] Tong J, Matsumura Y. Effect of catalytic activity on methane steam reforming in hydrogen-permeable membrane reactor. Appl Catal A Gen 2005;286:226–31.
[21] Profeti LPR, Ticianelli EA, Assaf EM. Co/Al_2O_3 catalysts promoted with noble metals for production of hydrogen by methane steam reforming. Fuel 2008;87:2076–81.
[22] Shu J, Grandjean BPA, Kaliaguine S. Asymmetric Pd–Ag/stainless steel catalytic membranes for methane steam reforming. Catal Today 1995;25:327–32.
[23] Pistonesi C, Juan A, Irigoyen B, Amadeo N. Theoretical and experimental study of methane steam reforming reactions over nickel catalyst. Appl Surf Sci 2007;253:4427–37.
[24] Castro Luna AE, Becerra AM. Kinetics of methane steam reforming on a Ni on alumina–titania catalyst. React Kinet Catal Lett 1997;61:369–74.
[25] Matsumura Y, Nakamori T. Steam reforming of methane over nickel catalysts at low reaction temperature. Appl Catal A Gen 2004;258:107–14.
[26] Hou K, Hughes R. The kinetics of methane steam reforming over a $Ni/\alpha-Al_2O_3$ catalyst. Chem Eng J 2001;82:311–28.
[27] Choudhary VR, Banerjee S, Rajput AM. Hydrogen from step-wise steam reforming of methane over Ni/ZrO_2: factors affecting catalytic methane decomposition and gasification by steam of carbon formed on the catalyst. Appl Catal A Gen 2002;234:259–70.
[28] Chen L, Hong Q, Lin J, Dautzenberg FM. Hydrogen production by coupled catalytic partial oxidation and steam methane reforming at elevated pressure and temperature. J Power Sources 2007;164:803–8.
[29] Bharadwaj SS, Schmidt LD. Catalytic partial oxidation of natural gas to syngas. Fuel Proc Technol 1995;42:109–27.
[30] Levent M, Gunn DJ, El-Bousi MA. Production of hydrogen-rich gases from steam reforming of methane in an automatic catalytic microreactor. Int J Hydrogen Energy 2003;28:945–59.
[31] Oertel M, Schmitz J, Weirich W, Jendryssek-Neumann D, Schulten R. Steam reforming of natural gas with integrated hydrogen separation for hydrogen production. Chem Eng Technol 1987;10:248–55.
[32] Kikuchi E, Nemoto Y, Kajiwara M, Uemiya S, Kojima T. Steam reforming of methane in membrane reactors: comparison of electroless-plating and CVD membranes and catalyst packing modes. Catal Today 2000;56:75–81.
[33] Kikuchi E. Membrane reactor application to hydrogen production. Catal Today 2000;56:97–101.
[34] Petersen KA, Nielsen CS, Jørgensen SL. Membrane reforming for hydrogen. Catal Today 1998;46:193–201.
[35] Lin YM, Liu SL, Chuang CH, Chu YT. Effect of incipient removal of hydrogen through palladium membrane on the conversion of methane steam reforming. Experimental and modeling. Catal Today 2003;82:127–39.
[36] Tong J, Matsumura Y. Pure hydrogen production by methane steam reforming with hydrogen-permeable membrane reactor. Catal Today 2006;111:147–52.
[37] Jorgensen S, Nielsen PEH, Lehrmann P. Steam reforming of methane in membrane reactor. Catal Today 1995;25:303–7.
[38] Chen Y, Wang Y, Xu H, Xiong G. Efficient production of hydrogen from natural gas steam reforming in palladium membrane reactor. Appl Catal B Environ 2008;80:283–94.
[39] Xu J, Froment G. Methane steam reforming, methanation and water–gas shift: I. Intrinsic kinetics. AIChE J 1989;35:88–96.
[40] Kulkarni BD, Doraiswamy LK. Estimation of effective transport properties in packed bed reactors. Catal Rev Sci Eng 1980;22:431–83.
[41] Tosti S, Bettinali L. Diffusion bonding of Pd–Ag membranes. J Mater Sci 2004;39:3041–6.
[42] Chen WH, Hsieh TC, Jiang TL. An experimental study on carbon monoxide conversion and hydrogen generation from water gas shift reaction. Energ Convers Manag 2008;49:2801–8.

Conclusion to Part II

The feasibility of Pd-Ag MR for MSR reaction was investigated by experimental and simulation studies, varying some operative conditions as temperature, pressure, catalyst and sweep gas flow rate. It was shown that the use of a dense unsupported hydrogen perm-selective membrane shifts the reaction towards further products formation and enhances hydrogen production and methane conversion. Moreover, using Pd-based MR is possible to carry out the reaction at milder operative conditions with respect to the conventional reactors, realizing also better performances MR in terms of methane conversion and hydrogen yield. Furthermore, a high pure hydrogen stream is obtained, which could be used for supply directly a PEMFC.

Anyhow, each operative variable can play an important role on the MR system. For instance, the catalyst support based on ZrO, used in the Paper 1, showed better MR performances than Al_2O_3 one, used in the Paper 2, owing to its strong resistance against coke deposition and thermal stability.

These two works have been prepared as the starting point for comprehending the reforming reactions of bio-fuels, as ethanol or glycerol, and appreciating the benefits in the use of Pd-based MRs.

References

Alhabdan FM, Abashar MA, Elnashaie SSE, "A flexible computer software package for industrial steam reformers and methanators based on rigorous heterogeneous mathematical models", *Math Comp Modeling,* 16 (1992) 77-86

Barelli L, Bidini G, Gallorini F, Servili S,"Hydrogen production through sorption enhanced steam methane reforming and membrane technology: A review", *Energy,* 33 (2008) 554-570

Chen Y, Wang Y, Xu H, Xiong G, "Efficient production of hydrogen from natural gas steam reforming in palladium membrane reactor", *Appl Catal B: Env,* 80 (2008) 283-294

Ebrahimi H, Mohammadzadeh JSS, Zamaniyan A, Shayegh F, "Effect of design parameters on performance of a top fired natural gas reformer", *Appl Therm Eng,* 28 (2008) 2203-2211

Fernandes FAN, Soares AB, "Modeling of methane steam reforming in a palladium membrane reactor", *Lat Am Appl Res,* 36 (2006) 155-161

Gallucci F, Tosti S, Basile A, "Pd–Ag tubular membrane reactors for methane dry reforming: A reactive method for CO_2 consumption and H_2 production", *J Membrane Sci*, 317 (2008) 96-105

Haag S, Burgard M, Ernst B "Beneficial effects of the use of a nickel membrane reactor for the dry reforming of methane: Comparison with thermodynamic predictions", *J Catal,* 252 (2007) 190-204

Kikuchi E, "Membrane reactor application to hydrogen production", *Catal Today,* 56 (2000a) 97-101

Kikuchi E, Nemoto Y, Kajiwara M, Uemiya S, Kojima T, "Steam reforming of methane in membrane reactors: comparison of electroless-plating and CVD membranes and catalyst packing modes", *Catal Today,* 56 (2000b) 75-81

Lin YM, Liu SL, Chuang CH, Chu YT, "Effect of incipient removal of hydrogen through palladium membrane on the conversion of methane steam reforming. Experimental and modelling", *Catal Today,* 82 (2003) 127-139

Murty CVS, Murthy MV, "Modeling and simulation of a top-fired reformer", *Ind Eng Chem Res,* 27 (1988) 1832-1840

Paturzo L, Gallucci F, Basile A, Vitulli G, Pertici P "An Ru-based catalytic membrane reactor for dry reforming of methane—its catalytic performance compared with tubular packed bed reactors", *Catal Today,* 82 (2003) 57-65

Pedernera MN, Piña J, Borio DO, Bucalá V, "Use of a heterogeneous two-dimensional model to improve the primary steam reformer performance", *Chem Eng J,* 94 (2003) 29-40

Plehiers PM, Froment GF, "Coupled simulation of heat transfer and reaction in a steam reforming furnace", *Chem Eng & Techn,* 12 (1989) 20-26

Rostrup-Nielsen J R, "Catalytic Steam Reforming", in Catalysis Science and Technology, JR Anderson and M Boudard, Ed, Vol. 4, Springer, Berlin (1984), 11-14

Singh CPP, Saraf DN, "Simulation of side fired steam-hydrocarbon reformers", *Ind Eng Chem Proc Des Dev,* 18 (1979) 1-7

Tong J, Matsumura Y, "Effect of catalytic activity on methane steam reforming in hydrogen-permeable membrane reactor", *Appl Catal A: Gen,* 286 (2005b) 226-231

Tong J, Matsumura Y, "Pure hydrogen production by methane steam reforming with hydrogen-permeable membrane reactor", *Catal Today,* 111 (2006) 147-152

Tong J, Matsumura Y, Suda H, Haraya K, "Thin and dense Pd/CeO_2/MPSS composite membrane for hydrogen separation and steam reforming of methane", *Sep Pur Techn,* 46 (2005a) 1-10

Trimm DL, "Coke formation and minimization during steam reforming reactions", *Catal Today,* 37 (1997) 233-238

Tsuru T, Shintani H, Yoshioka T, Asaeda M "A bimodal catalytic membrane having a hydrogen-permselective silica layer on a bimodal catalytic support: Preparation and application to the steam reforming of methane", *Appl Catal A: Gen,* 302 (2006) 78-85

Tsuru T, Yamaguchi K, Yoshioka TI, Asaeda M, "Methane steam reforming by microporous catalytic membrane reactors", *AIChE J,* 50 (2004) 2794-2805

Wagner ES, Froment GF, "Steam reforming analyzed", Hydroc Proc, 71 (1992) 69-77

Wesenberg MH, Svendsen HF, "Mass and heat transfer limitations in a heterogeneous model of a gas-heated steam reformer", *Ind Eng Chem Res,* 46 (2007) 667-676

Xu J, Froment GF, "Methane steam reforming, methanation and water-gas shift: I. Intrinsic kinetics", *AIChE J*, 35 (1989a) 88-96

Xu J, Froment GF, "Methane steam reforming. II. Diffusional limitations and reactor simulation", *AIChE J*, 35 (1989b) 97-103

Yu Z, Cao E, Wang Y, Zhou Z, Dai Z, "Simulation of Natural Gas Steam Reforming Furnace", *Fuel Proc Tech*, 87 (2006) 695-704

Part III

Bio-fuels Reforming Reactions

Introduction to *Part III*

One of the key issues of sustainable development is the transition from fossil feedstocks to renewable sources. The increasing attention towards sustainable use of renewable sources is driven by several factors, mainly: fossil fuels depletion, environmental concerns and stringent norms on pollution emissions.

Nowadays, the bio-fuels (biomass-derived fuels) are recognized as a main renewable energy sources for replacing the derived fossil fuels [Ozcimen et al (2004) Jefferson et al (2006)]. Indeed, they present many advantages such as their easy availability from common biomass sources, considerable environmentally friendly potential and biodegradability [Demirbas (2007)]. The two most common types of bio-sources are ethanol and biodiesel. Ethanol represents an important bio-source and compared to other liquid bio-sources, such as methanol, acetic acid and diethyether, presents both low toxicity and volatility [Ni et al (2007)].

Biodiesel is produced from vegetable oils, is non-toxic, biodegradable and during its production process, glycerol is generated as a byproduct. In particular, this by-product is considered another important bio-sources. Indeed, glycerol is characterized by high energy density, non-toxic, non-volatile, and non-flammable [Xuan et al (2009)].

However, hydrogen, as energy carrier produced exploiting renewable sources, and fuel cells, as efficient energy converters, may play an important role in the sustainable development.

For this reason, the reforming reactions of bio-sources performed in Pd-based MR could be considered for producing high purity hydrogen for feeding a PEMFC.

An outline of hydrogen production via different biosources is shown in Figure 3.1, whereas a list of the main bio-sources is reported below:

- bioethanol: ethanol produced from biomass and/or the biodegradable fraction of waste or agricultures;

- biomethanol: methanol produced from biomass;
- biodiesel: a methyl-ester produced from vegetable or animal oil;
- bioglycerol: glycerol produced as a by-product of biodiesel production;
- biogas: a fuel gas produced from biomass and/or the biodegradable waste that can be treated in a purification plant in order to achieve a quality similar to the natural gas.

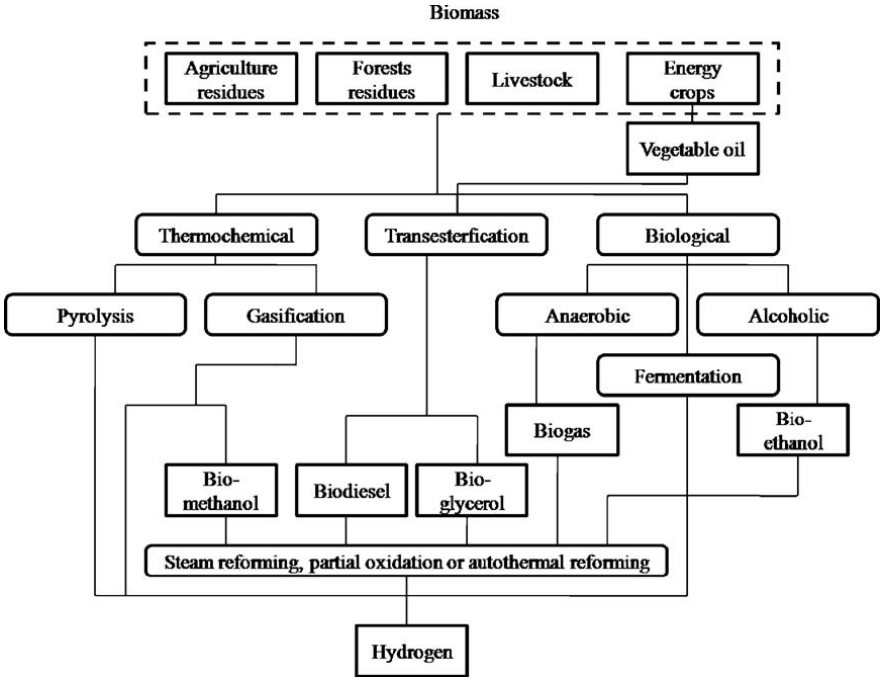

Figure 3.1 Selected hydrogen production technologies from biomass [Xuan et al (2009)]

In the open literature, a consistent number of publications concerning the application of Pd-based MR technology are based on hydrogen production via reforming reaction of biofuels, such as methanol, glycerol, ethanol and biogas. In particular, the main aim of the scientists involved in this field is oriented to emphasize the role of the membrane by analyzing the performances of the reaction system in terms of ethanol conversion, hydrogen yield (defined as the ratio within hydrogen produced during the reaction and that theoretically producible from the stoichiometry of the reaction) and hydrogen recovery (hydrogen collected in the permeate side on the total hydrogen produced during the reaction).

So, the purpose of this Part III is to show the Pd-based MR performances carrying out bio-sources reforming reactions for obtaining a high purity hydrogen stream. In particular, two bio-sources are considered: ethanol and glycerol.

For this reason, the Part III is divided in two Chapters, in the first one a widely study on both unsupported Pd-Ag and Pd/PSS supported MRs performances is carried out, performing ethanol reaction processes, as steam reforming, steam oxidative reforming and partial oxidation. In the second chapter, the potentialities of Pd-Ag MR carrying out glycerol steam reforming (GSR) reaction for producing hydrogen are investigated.

Moreover, in both chapters, a comparative study between the Pd-based MR and a conventional reactor working at the same MR operating conditions is given.

In the Figure 3.2, the scheme followed in research work is shown.

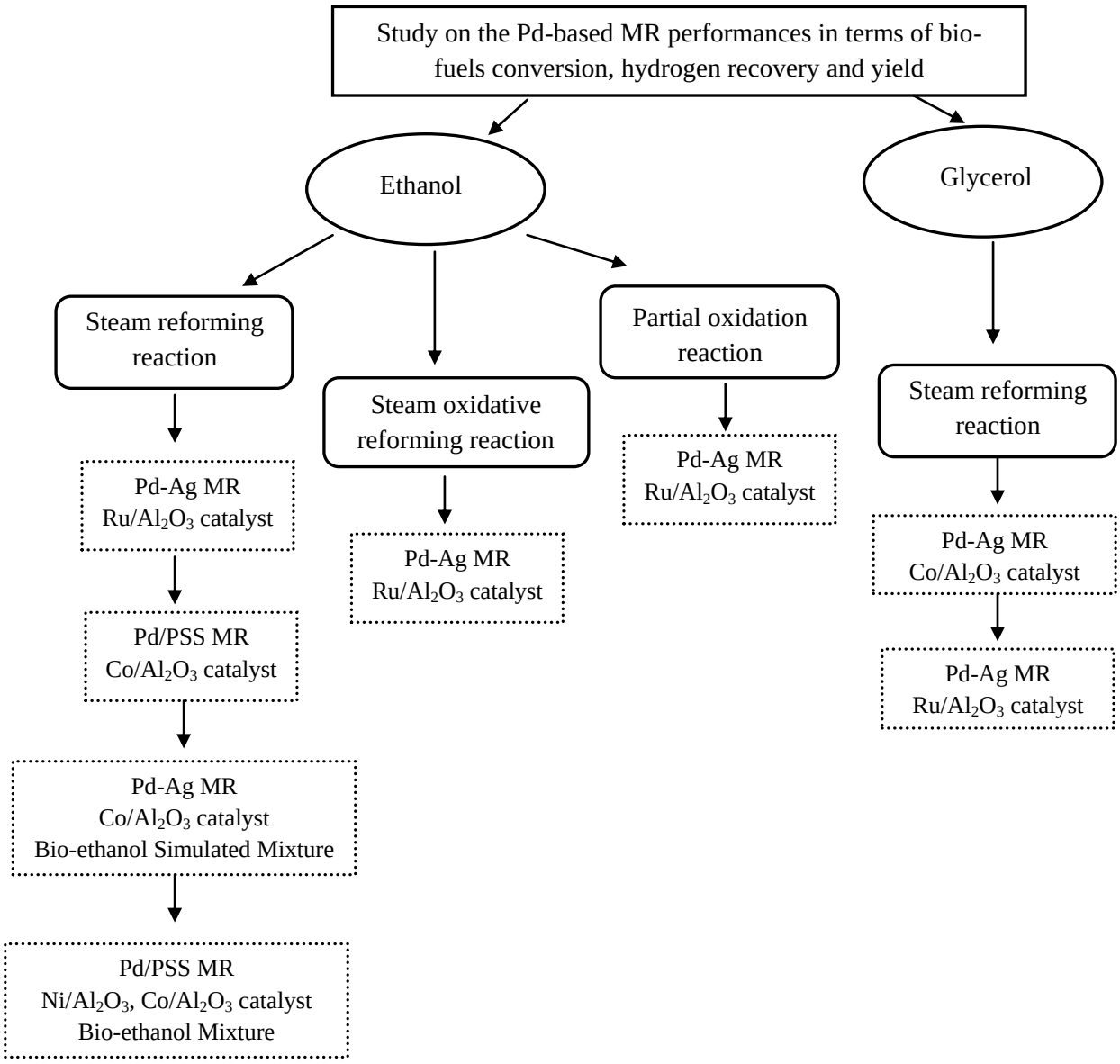

Figure 3.2 Scheme followed during the research work

The research work above summarized is presented hereafter through the papers that have been prepared during the PhD course, according to the following structure:

- A. Basile, F. Gallucci, A. Iulianelli, M. De Falco, **S. Liguori**, "Hydrogen production by ethanol steam reforming: experimental study of Pd-Ag membrane reactor and traditional reactor behaviour, *Int J Chem. React. Eng*, 6 (2008) A30";

- A. Basile, P. Pinacci, M. Broglia, F. Drago, A. Iulianelli, **S. Liguori**, T. Longo, V. Calabrò, "Ethanol steam reforming reaction in a porous stainless steel supported palladium membrane reactor", *Int J Hydr En*, 36 (2011) 2029-2037.

- A. Iulianelli, **S. Liguori**, T. Longo, S. Tosti, P. Pinacci, A. Basile, "An experimental study on bio-ethanol steam reforming in a catalytic membrane reactor. Part II: reaction pressure, sweep factor and WHSV effects", *Int J Hydr En*, 35 (2010) 3159- 3164.

- PK Seelam, **S Liguori**, A Iulianelli, P Pinacci, F Drago, V Calabrò, M Huuhtanen, R Keiski, V Piemonte, S Tosti, M De Falco, A Basile, "Hydrogen production from bio-ethanol steam reforming reaction in a Pd/PSS membrane reactor", *submitted to Catalysis Today*, (2011)

- A. Iulianelli, T. Longo, **S. Liguori**, PK Seelam, R.L. Keiski, A. Basile, "Oxidative steam reforming of ethanol over Ru-Al2O3 catalyst in a dense Pd-Ag membrane reactor to produce hydrogen for PEM fuel cells", *Int J Hydr En*, 34 (2009) 8558-8565

- A. Iulianelli, **S. Liguori**, V. Calabrò, P. Pinacci, A. Basile, "Partial oxidation of ethanol in a membrane reactor for high purity hydrogen production", *Int J Hydr En*, 35 (2010) 12626-12634

- A. Iulianelli, P.K. Seelam, **S. Liguori**, T. Longo, R. Keiski, V. Calabrò, A. Basile, "Hydrogen production for PEM fuel cell by gas phase reforming of glycerol as byproduct of bio-diesel. The use of a Pd-Ag membrane reactor at middle reaction temperature", *Int J Hydr En*, 36 (2011) 3827-3834

- A. Iulianelli, T. Longo, **S. Liguori**, A. Basile, "Production of hydrogen via glycerol steam reforming in a Pd-Ag membrane reactor over Co-Al_2O_3 catalyst", *Asia-Pac J Chem Eng*, 5 (2010), 138-145

Chapter 1

Reforming reactions and partial oxidation of Ethanol

Introduction

Ethanol represents an important bio-source and, compared to other liquid fuels such as methanol, acetic acid, diethyether, etc. seems to be more suitable because of its very low toxicity and volatility [Maggio et al (1998)]. Currently, in the specialized literature there is a misleading approach when describing the use of bio-ethanol as a bio-source. Indeed, many authors indicate bio-ethanol as pure ethanol derived from biomass after the distillation and the extraction procedures, whereas bio-ethanol is an aqueous solution containing between 8 and 12wt% of ethanol and other by-products [Song et al (2007), Ni et al (2007), Pfeffer et al (2007)].

In the open literature, the majority of scientific publications deals with performing ethanol steam reforming (ESR) reaction in conventional reactors.

In two interesting studies [Haryanto e al (2005), Breen et al (2009)], the state of the art for ESR reaction in conventional reactors was reviewed, making a comparative analysis on the performances using different catalysts such as: Rh-, Ru-, Pd-, Pt-, Ni-, Co- and Cu-based catalysts. The authors pointed out that conventional reactors performances can vary greatly depending on the catalyst choice and reaction conditions. Nevertheless, Haga et al. [Haga et al. (1998)] affirm that Co/Al_2O_3 catalyst seems to be the most selective towards ESR reaction. Furthermore, other authors support the role of cobalt as the most effective catalyst for ESR reaction owing to its high catalytic activity and because it is more cost effective than noble metal-based catalysts like Rh, Pt and Pd [Llorca et al (2002), Kaddouri et al (2004), Batista et al (2003)].

However, taking into account as previously mentioned on a bio-ethanol mixture, it is well known that a water excess during the ESR reaction reduces the formation of carbon monoxide in the reformed stream. Therefore, it could be advantageous to supply directly into reactor a real bio-ethanol mixture (corresponding to a water/ethanol feed molar ratio between 29.0/1 – 18.7/1), without making any distillation of further ethanol separation/purification process. This approach could be economically relevant, considering that in the purification of ethanol, extracting 99% water presents a high cost owing to the ethanol/water azeotrope.

Over the years now, MR technology has been applied with the intent to produce hydrogen based on the exploitation of ethanol as a renewable source. Figure 3.3 illustrates the number of scientific studies per year dealing with hydrogen production via ESR reaction combined to MR technology with respect to the total number of publications in this field, considering both conventional reactor and MR applications.

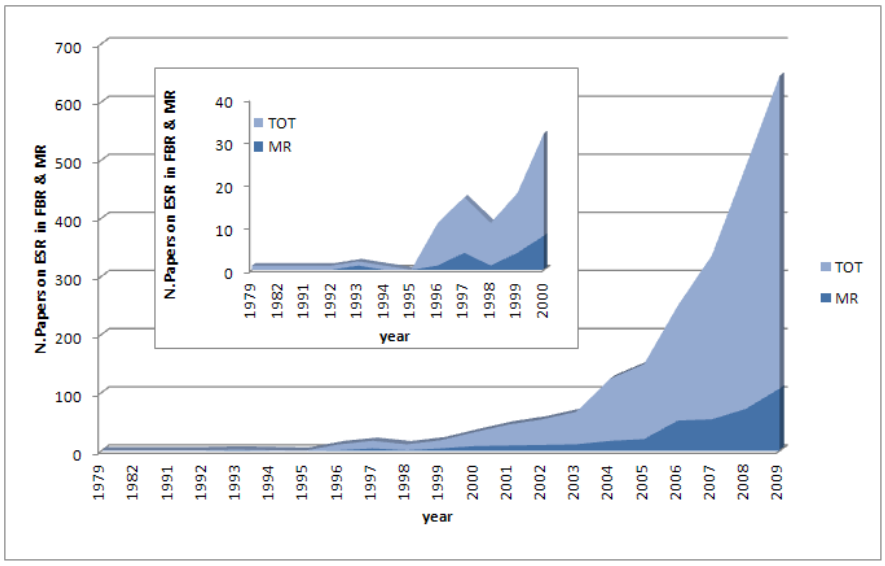

Figure 3.3 Number of scientific publications vs year on ESR reaction in both FBR and MR.

Furthermore, Figure 3.4 highlights the percentage distribution of the most used catalysts for ethanol reforming reactions in MRs. Ni-, Co- and Ru-based catalysts are preferentially used, probably because they are less expensive than other catalysts.

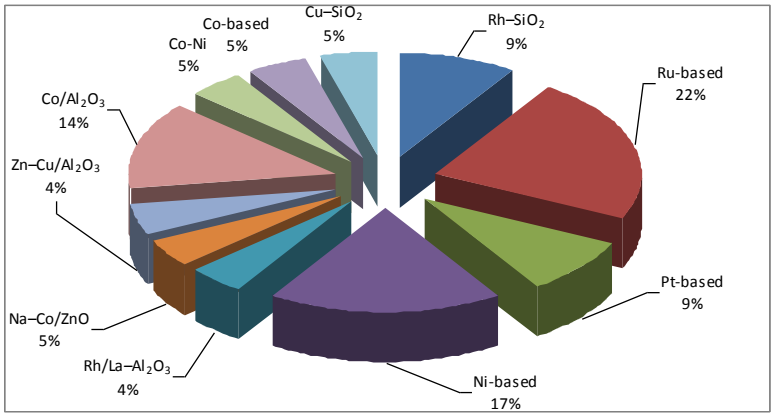

Figure 3.4. Percentage distribution of the most used catalysts in ethanol reforming reactions performed in MRs.

However, as aforementioned, the main aim of the scientists involved in this field is oriented to emphasizing the role of the membrane by analyzing the performances of the reaction system.

For this reason, the research work of this chapter I is focused on the Pd-based MR performances carrying out ethanol reforming reactions and partial oxidation. Therefore, as a first step the unsupported Pd-Ag MR performances, packed with Ru/Al_2O_3, are studied analyzing the influence of temperature and pressure reaction. In this study a feed molar ratio of H_2O/C_2H_5OH = 11/1 is used for avoiding coke formation and to reduce CO production.

Successively, the Pd-Ag membrane is replaced by Pd/PSS supported membrane owing to its low mechanical resistance to high pressure.

Firstly, the Pd/PSS supported membrane is characterized in terms of permeation with pure gases and afterwards the MR performances is analyzed at high reaction pressure and using Co/Al_2O_3 catalyst and a stoichiometric feed molar ratio.

After this first research work, for simplicity and as a first approach, a simulated bioethanol mixture (without presenting the other typical contaminants such as methanol, acetic acid, glycerol, etc.) is used to carry out the ESR reaction in dense Pd-Ag MR packed with a Co/Al_2O_3 catalyst analyzing the influence of reaction pressure and sweep-gas on MR system.

Consecutively, a simulated bio-ethanol mixture taking into account also the minor impurities as acetic acid and glycerol is used investigating the performances of Pd/PSS supported MR at high reaction pressure.

It is well known, that an addition of oxygen during the ESR reaction can affects positively the performances of overall system preventing the ethylene and ethane formation and avoid carbon deposition. For this reason, the performances of Pd-Ag MR are analyzed conducting the oxidative ethanol steam reforming (OESR) at different feed molar ratio ($C_2H_5OH/O_2/H_2O$) and reaction pressure.

Moreover, the ethanol partial oxidation (POE) performed in Pd-Ag MR is also investigated in order to produce a high purity hydrogen stream.

INTERNATIONAL JOURNAL OF CHEMICAL REACTOR ENGINEERING

Volume 6 2008 *Article* A30

Hydrogen Production by Ethanol Steam Reforming: Experimental Study of a Pd-Ag Membrane Reactor and Traditional Reactor Behaviour

Angelo Basile* Fausto Gallucci† Adolfo Iulianelli‡
Marcello De Falco** Simona Liguori††

*Italian National Research Council, a.basile@itm.cnr.it
†Italian National Research Council, f.gallucci@itm.cnr.it
‡Italian National Research Council, a.iulianelli@itm.cnr.it
**University of Rome, marcello.defalco@uniroma1.it
††University of Calabria, liguori.simona@libero.it

ISSN 1542-6580

Hydrogen Production by Ethanol Steam Reforming: Experimental Study of a Pd-Ag Membrane Reactor and Traditional Reactor Behaviour

Angelo Basile, Fausto Gallucci, Adolfo Iulianelli, Marcello De Falco, and Simona Liguori

Abstract

In this experimental work, the ethanol steam reforming reaction for producing hydrogen was studied in both a traditional reactor (TR) and a Pd-Ag dense membrane reactor (MR). Both reactors have been packed with a commercial Ru-based catalyst. The experimental tests have been performed in the temperature range 400-500 °C and in the pressure range 2.0-3.6 bar.

The results are reported in terms of ethanol conversion, hydrogen production, product selectivities and hydrogen recovery (for the MR only). It has been found that the MR is able to increase the ethanol conversion as well as increase the hydrogen production with respect to a traditional reactor. Moreover, part of the hydrogen produced in the MR is recovered as a CO-free hydrogen stream and is suitable for feeding a PEM fuel cell system.

KEYWORDS: ethanol steam reforming, hydrogen production, membrane reactor, Pd-based membranes, Ru catalyst

1. Introduction

As it is well known, hydrogen is commercially produced by gasification, partial oxidation reactions of heavy oil and steam reforming reactions: the current worldwide production is around $5 \cdot 10^{11}$ Nm^3 per year, as reported by Vaidya *et al.* (2006). Hydrogen is used as a feedstock in the chemical industry as well as in the manufacture of ammonia and methanol, in refinery reprocessing and conversion processes [Vaidya *et al.* (2006) and Sun *et al.* (2004)]. The increased hydrogen demand for fuel cell applications in combination with the global request to reduce the atmospheric pollution and greenhouse gas emission impose the development of new methods for hydrogen production, especially from renewable sources such as biomass. Hydrogen production from biomass transformation is a very promising way, which attracted increasing attention. Particularly interesting are methods in which the biomass is converted into intermediate liquid bio-fuels such as pyrolysis oil or ethanol, as reported by Vaidya *et al.* (2006).

Bio-derived ethanol is usually produced as an aqueous solution containing ethanol within the range 8-12 %wt [Vaidya *et al.* (2006)]. It can be used as an alternative fuel, feedstock for producing chemicals (e.g. ethylene, acetaldehyde, acetone, etc.) or it can be converted into hydrogen for feeding fuel cells for clean electricity production. In particular, ethanol presents high energy density, ease of handling and storage safety. With respect to other liquid fuels such as methanol, ethanol seems to be more suitable because it is less toxic, as reported by Maggio *et al.* (1998).

Many authors studied different catalysts for the ethanol steam reforming (ESR) in traditional reactors. In particular, the catalyst mainly affects the reaction conversion and the products selectivity: Rh, Ru, Pd, Pt, Ni, Co and Cu are used as catalyst materials.

The most part of the literature on the hydrogen production by ESR reaction is focused on the traditional reactors (TRs). However, few papers dealing with the use of membrane reactors (MRs) recently appear in Keuler *et al.* (2002), Fayyaz *et al.* (2005) and Gallucci *et al.* (2007).

Typically, the ESR reaction system is represented by the following reactions:

$$C_2H_5OH + H_2O = CH_4 + CO_2 + 2H_2 \qquad \Delta H^\circ_{298K} = -8.0 \text{ kJ/mol} \qquad (1)$$

$$CO + H_2O = CO_2 + H_2 \qquad \Delta H^\circ_{298\,K} = -41.2 \text{ kJ/mol} \qquad (2)$$

$$CH_4 + H_2O = CO + 3H_2 \qquad \Delta H^\circ_{298\,K} = 206.2 \text{ kJ/mol} \qquad (3)$$

However, other reactions can occur in the process depending on the catalyst used, as noted by Haryanto *et al.* (2005). In fact, the research in this field is manly

Published by The Berkeley Electronic Press, 2008

focused on the catalyst development. Generally, the hydrogen rich-gas going out from the TR contains secondary products such as CO_2, CO, CH_4, C_2H_4, acetaldehyde, ethylene, and ethane. Therefore, with the aim to produce a CO-free hydrogen stream, the hydrogen rich-gas stream needs purification. For this purpose, the ESR process involves a traditional reformer followed by water gas shift (WGS) reactors, devoted to remove the carbon monoxide, and a purification device [Haryanto *et al.* (2005)].

In a previous work, a Pd-Ag MR was used to carry out the ESR reaction with particular attention to the influence on the reaction system of parameters such as the sweep-gas flow rate and the flow configuration, as reported by Gallucci *et al*. (2007). It was pointed out that the advantages of the Pd-Ag MR are:

- Possibility to perform both the ESR reaction and the CO-free hydrogen separation in the same device.
- Possibility to produce a CO-free hydrogen stream available for feeding a polymeric electrolyte membrane (PEM) fuel cell.

The aim of this experimental work is to investigate the ESR in both a TR and a dense Pd-Ag MR with particular interest on the effect of both the temperature and the pressure on the reactors performances. The results in terms of ethanol conversion, hydrogen production, and CO-free hydrogen recovery are presented and discussed.

2. Experimental

Traditional and membrane reactors description

The TR consists of a stainless steel tube, length 250 mm, *i.d.* 10 mm with the reaction zone 150 mm. The MR consists of a tubular stainless steel module, length 280 mm, *i.d.* 20 mm, containing a pine-hole free Pd-Ag thin wall membrane tube permeable only to hydrogen, having thickness 50 μm, *o.d.* 10 mm, length 145 mm. In particular, the dense membrane is joined to two stainless steel tube ends useful for the membrane housing. A finger like configuration [Gallucci *et al*. (2007)] has been used in order to assure a long lifetime for the membrane. In the MR, catalyst pellets are packed in the membrane zone (145 mm length) while glass spheres (2 mm diameter) are placed into the supports on both extremities of the membrane.

The preparation method of the Pd-Ag membrane was already discussed elsewhere in Tosti and Bettinali (2004) and Tosti *et al.* (2001). The membrane presents an infinite perm-selectivity H_2/other gases and the hydrogen flux follows the well-known Richardson equation:

4

$$J_{H2} = \frac{Pe_0 \cdot \exp\left(-\frac{Ea}{RT}\right) \cdot \left(\sqrt{p_{H2,lumen}} - \sqrt{p_{H2,shell}}\right)}{\delta}$$

where δ is the membrane thickness (50 μm), Pe_0, $E_{a,}$ R and T are the pre-exponential factor, the apparent activation energy, the universal gas constant, and the absolute temperature, respectively.

Experimental details

The reactor (TR or MR) is placed in a temperature-controlled P.I.D. (Proportional + Integral + Derivative Control) oven. Reaction and permeation temperatures are in the range between 400 and 500 °C. The sweep gas (N_2) is fed (only for MR) by means of a mass-flow controller (Brooks Instruments 5850S) driven by a computer software furnished by Lira (Italy) and used for all of the experiments. H_2O and ethanol are fed by means of a HPLC pump furnished by Dionex.

The reaction pressure is in the range 2.0-3.6 bar regulated by means of a back pressure controller. Considering the MR, permeate pressure is always 1.0 bar, and N_2 is used as the sweep gas with the flow rate of $1.422 \cdot 10^{-4}$ mol/s.

The ethanol feed flow rate is $1.948 \cdot 10^{-5}$ mol/s while the H_2O/ethanol feed ratio is 11. The same equipment has been used for permeation tests. The liquid reactants are mixed and vaporised, and then are fed into the reactor (both TR and MR). The outlet streams are completely condensed in order to remove the un-reacted H_2O and the alcohol, and then the liquid phase is analysed by means of a Perkin Helmer Gas Chromatograph (GC). The dry gaseous stream flow rate is measured by means of bubble flow-meters; its composition is detected by using a temperature programmed HP 6890 GC with two TCDs (Thermal Conductivity Detector) at 250 °C and Ar as carrier gas. The GC is equipped by three packed columns: Porapack R 50/80 (8 ft x 1/8 in) and Carboxen™ 1000 (15 ft x 1/8 in) connected in series, Molecular Sieve 5Å (6 ft x 1/8 inch). The internal standard method has been used. Each experimental point obtained in this work is an average value of 7 experimental points taken in 90 min with a maximum error lower than 5%.

All the TR and the MR were packed with 3 g of a 5%wt Ru-Al_2O_3 commercial catalyst furnished by Johnson Matthey. Before reaction, the catalyst has been pre-heated using N_2 at 400 °C under atmospheric pressure for 3 hours and, afterwards, reduced by using H_2 ($1.5 \cdot 10^{-3}$ mol/min) at the same temperature for 2 hours.

Published by The Berkeley Electronic Press, 2008

A flat temperature profile along the reactor during the reaction has been observed by using a three points thermocouple inserted into the lumen of both the reactors TR and MR.

The following definitions are used for describing the TR and the MRs performances:

5

$$C_2H_5OH \text{ conversion}, (X_{C_2H_5OH}, \%) = \frac{C_2H_5OH_{IN} - C_2H_5OH_{OUT}}{C_2H_5OH_{IN}} \cdot 100$$

6

$$H_2 \text{ selectivity}, (S_{H_2}, \%) = \frac{H_{2,OUT}}{H_{2,OUT} + CO_{OUT} + CO_{2,OUT} + CH_{4,OUT}} \cdot 100$$

7

$$CH_4 \text{ selectivity}, (S_{CH4}, \%) = \frac{CH_{4,OUT}}{H_{2,OUT} + CO_{OUT} + CO_{2,OUT} + CH_{4,OUT}} \cdot 100$$

8

$$H_2 \text{ recovery}, (\%) = \frac{H_{2,OUT\text{-}SHELL}}{H_{2,OUT\text{-}SHELL} + H_{2,OUT\text{-}LUMEN}} \cdot 100$$

The subscript "OUT" indicates the total outlet flow rate of each species. In particular, for the TR only one outlet stream is present for each species, while for the MR there are two outlet streams (retentate + permeate). All the experimental results have been obtained at steady-state condition.

3. Results and discussion

Figs. 1 and 2 show the Sievert plot and the Arrhenius plot for the Pd-Ag dense membrane, respectively. The data are referred to the membrane before the reaction. It can easily seen that both Sievert and Arrhenius laws are followed.

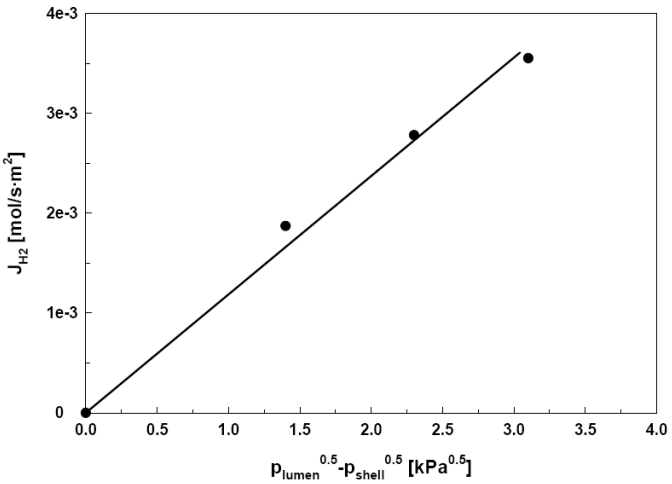

Fig. 1. Sievert plot for the Pd-Ag dense membrane. T = 400 °C

Moreover, the membrane presents an infinite perm-selectivity H_2/other gases. The membrane has an apparent activation energy =32.36 kJ/mol and a pre exponential factor of $2.032 \cdot 10^{-5}$ mol m/(s m^2 kPa^{05}). These values are in good agreement with Gallucci *et al.* (2004).

A high value (11/1) of the H_2O/ethanol feed molar ratio has been chosen having in mind an ethanol concentration near to that of the bio-ethanol solutions. As also suggested by Mas *et al.* (2006), working in the TRs, at high H_2O/ethanol feed molar ratio, it is avoided the carbon coke formation. Moreover, in our previous work [Basile *et al.* (2008)] in a Pd-Ag MR, no coke formation was detected operating at a H_2O/ethanol feed molar ratio equal to 9/1.

Published by The Berkeley Electronic Press, 2008

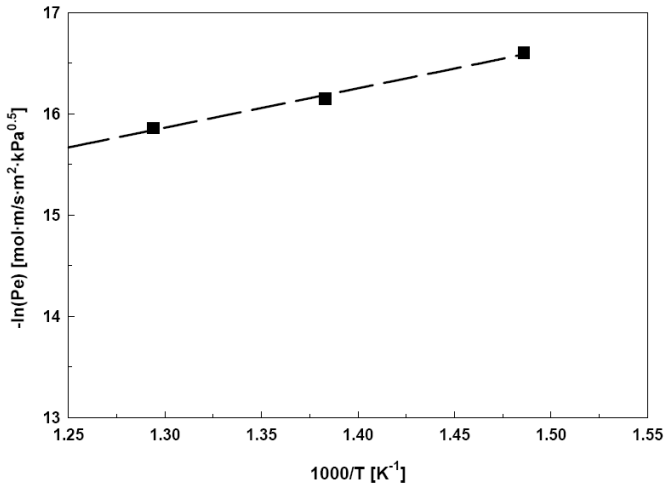

Fig. 2. Arrhenius plot for the Pd-Ag dense membrane, $p_{lumen}^{0.5}$-$p_{shell}^{0.5}$ = 2.3 $kPa^{0.5}$

Fig. 3 reports the ethanol conversion versus the reaction pressure for both TR and MR at 400 °C. The MR presents a higher conversion than the TR for the whole range of pressure investigated. In particular, it can be noted that the pressure has a negative effect on the conversion in the TR.

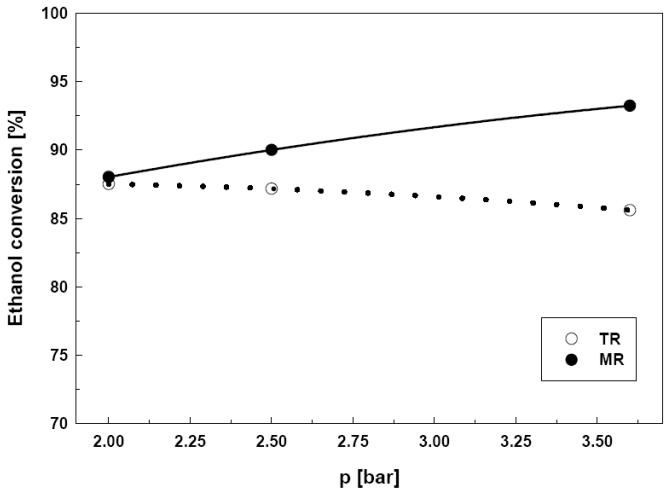

Fig. 3 Ethanol conversion versus reaction pressure for both TR and MR. T = 400 °C

It is possible to explain this fact by considering that the ethanol steam reforming reaction system presents an increase of the mole number. Being the conversion of the TR close to the equilibrium one, the reaction system is negatively influenced by the pressure due to the increase of the mole number. On the other hand, the ethanol conversion in the MR increases with the pressure. In order to explain this behaviour, it has to be taken into account that, the reaction pressure has two effects on the performances of the MR.

From one hand, the pressure negatively affects the ethanol conversion due to the increase of the mole number (as already seen for the TR). From the other side, the increase of the reaction pressure results on an increase of the hydrogen partial pressure in the lumen side of the membrane. Thus, the driving force for the hydrogen permeation increases by increasing the pressure, bringing about an increase of the hydrogen flux through the membrane, as indicated by the Richardson equation. The higher the hydrogen removal from the reaction side, the greater the ethanol conversion due to the Le Chatelier principle. In particular, at 2.0 bar the MR gives an ethanol conversion only a little bit (1%) higher than the TR; at 3.6 bar the ethanol conversion in the TR is around 85% while it is around 93% in the MR.

Therefore, the positive effect of the pressure on the MR performance is stronger than the negative one.

Published by The Berkeley Electronic Press, 2008

Fig. 4 sketches the ethanol conversion in the TR and the MR versus the reaction pressure at 450 °C. Also at this temperature, the trend of Fig. 3 is repeated.

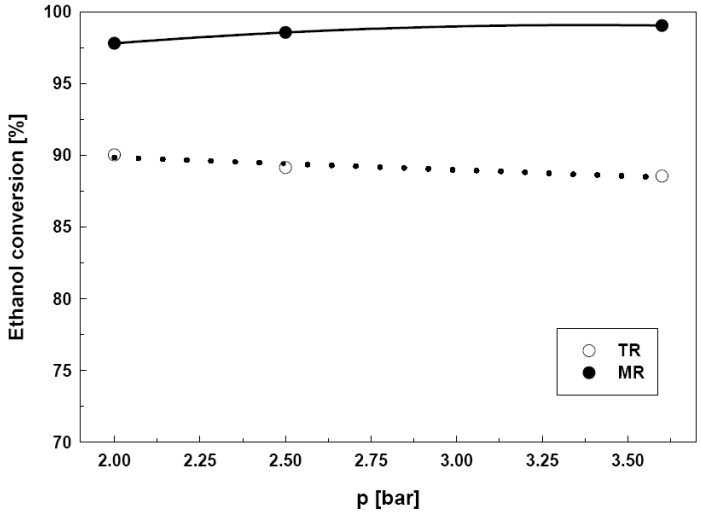

Fig. 4 Ethanol conversion versus reaction pressure for both TR and MR. T = 450 °C

The conversion in the TR slightly decreases by increasing the pressure, while the MR presents an ethanol conversion increasing with the pressure and always higher than the TR. By comparing Figs. 3 and 4, it can be stated that the temperature has a positive effect on both the TR and the MR. In fact, the ethanol steam reforming reaction is an endothermic reaction system and so it is favoured by high temperatures. However, the effect of the temperature is higher in the MR with respect to the TR. Also this fact can be explained by considering the Richardson equation which indicates that the hydrogen flux through the membrane increases with the temperature. Thus, the higher the temperature the higher the positive effect of the membrane on the reaction system. It can be also seen that the MR gives an ethanol conversion higher than 95% for the whole range of pressure investigated while the TR gives a conversion not higher than 90%. Finally, Fig. 5 shows the effect of the reaction pressure on the ethanol steam reforming at 500 °C. In this case, the MR is able to give an ethanol conversion always higher than 98% and always higher than the TR which still gives a conversion decreasing with increasing the reaction pressure. It is to point out that, in both the reactors and in all the experimental texts, no ethylene and acetaldehyde formation was detected.

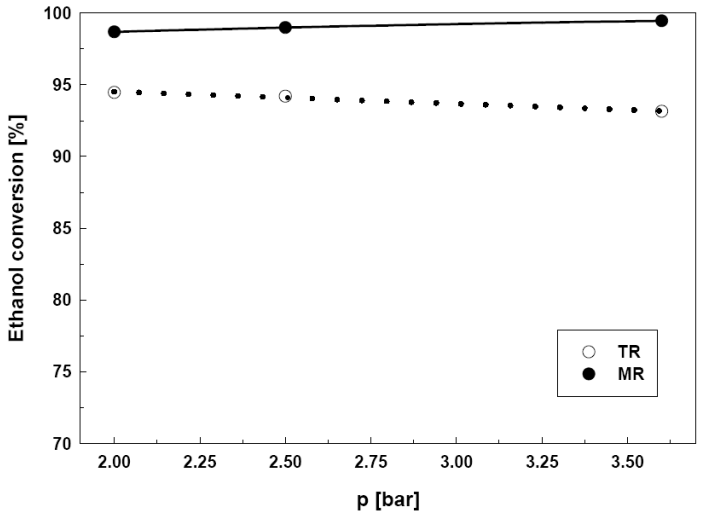

Fig. 5 Ethanol conversion versus reaction pressure for both TR and MR. T = 500 °C

The effect of the pressure on the total hydrogen produced at 400 °C is shown in Fig. 6. It can be noted that, for the whole range of pressure investigated the hydrogen produced in the MR is higher than the hydrogen produced in the TR. In particular, the MR is able to give at least 30% more hydrogen than the TR does. This can be explained by considering that, by removing hydrogen through the membrane, the reactions which produce hydrogen are shifted towards the products. Let us consider again the total hydrogen produced ($Q_{H2\text{-}TOT}$) versus the reaction pressure (Figs. 6-8). $Q_{H2\text{-}TOT}$ is a combination of the pressure effect on both the ethanol conversion and the hydrogen selectivity. In fact, as shown by the reactions (1)-(3), the ethanol is converted in both hydrogen and methane.

Published by The Berkeley Electronic Press, 2008

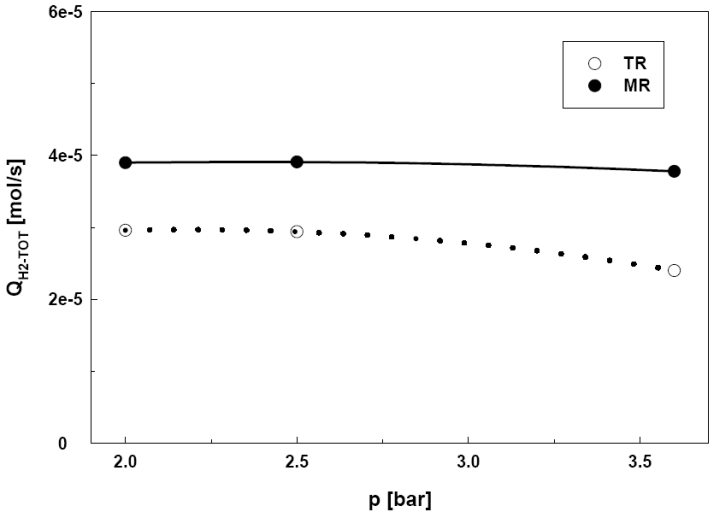

Fig. 6 Total hydrogen produced versus reaction pressure for both TR and MR. T = 400 °C

As indicated in Table 1, the hydrogen selectivity decreases with increasing the pressure in the whole range of temperature investigated for both the reactors.

T [°C]	p [bar]	H_2 Selectivity [%]		CH_4 Selectivity [%]	
		MR	TR	MR	TR
400	2.0	53.89	47.40	19.27	28.37
	2.5	52.95	46.67	20.45	30.35
	3.6	50.57	41.12	23.07	35.22
450	2.0	61.58	56.23	11.94	18.26
	2.5	60.70	56.08	13.20	19.76
	3.6	58.64	53.21	15.40	23.70
500	2.0	65.01	62.70	8.60	12.15
	2.5	64.54	62.00	9.24	13.11
	3.6	64.24	59.55	10.54	16.31

Table 1. Hydrogen and methane selectivity for both TR and MR at different pressures and temperatures.

In the meanwhile, the methane selectivity increases with increasing the pressure but decreases with increasing the temperature (Table 1).

Moreover, in both the TR and the MR the CO selectivity was lower than 1%. However, the MR always gives a higher hydrogen selectivity than the TR. Taking into account that the ethanol conversion as well as the hydrogen selectivity increase with the temperature, the hydrogen produced increases with the temperature too, for both the reactors, as indicated in Figs. 7-8.

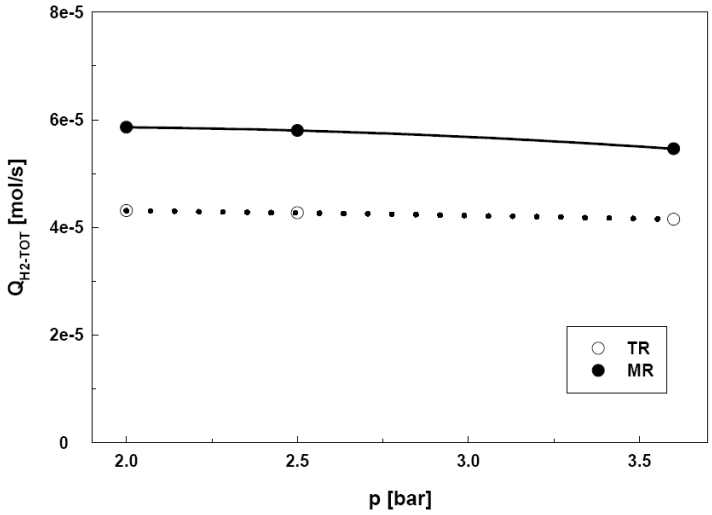

Fig. 7 Total hydrogen produced versus reaction pressure for both TR and MR. T = 450 °C

In particular, the higher hydrogen production is obtained in the MR at 500 °C and 3.6 bar.

All the experimental results show that, owing to the hydrogen permeation through the membrane, the MR is able to give better results in terms of ethanol conversion, hydrogen selectivity and hydrogen production than the TR. However, a very important parameter to be taken into account when using the MR is the amount of hydrogen that permeates through the membrane and then recovered as CO-free hydrogen stream.

Fig. 9 shows the hydrogen recovery versus the reaction pressure and the temperature for the MR: the hydrogen recovery increases by increasing both the temperature and the pressure. This is easily explained by considering the already discussed Richardson equation.

Published by The Berkeley Electronic Press, 2008

It can be noted that, in our experimental conditions, up to 25% of the hydrogen produced is recovered as CO-free steam and so it is directly suitable for feeding a PEM fuel cell.

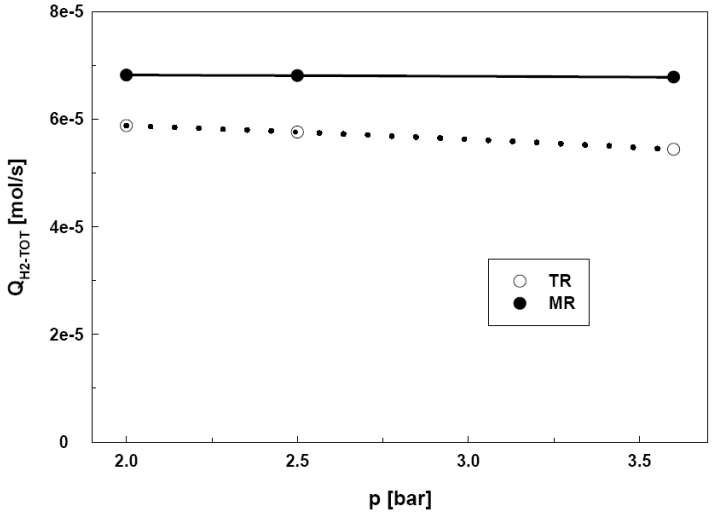

Fig. 8 Total hydrogen produced versus reaction pressure for both TR and MR. T = 500 °C

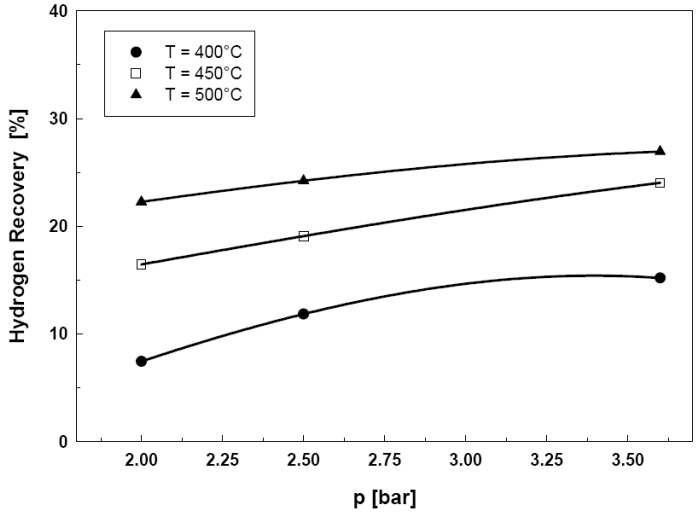

Fig. 9 Hydrogen recovery versus reaction pressure for MR at different temperatures.

Another important parameter to be considered when using a dense Pd-Ag MR is the effect of the by-products (CO, CH_4 and CO_2) and of the thermal cycles on the performances of the membrane. During our experiments the Pd-Ag dense membrane always showed an infinite perm-selectivity H_2/other gases, so that only hydrogen was permeating through the membrane.

Moreover, as shown in Table 2, also the values of permeability were constant before and after the reaction tests, indicating a high resistance of the dense Pd-Ag membrane to the temperature and hydrogen cycles.

T [°C]	Permeability (Pe) before reaction [mol·m/s·m^2·kPa$^{0.5}$]	Permeability (Pe) after reaction [mol·m/s·m^2·kPa$^{0.5}$]	-ln(Pe) before reaction [mol·m/s·m^2·kPa$^{0.5}$]	-ln(Pe) after reaction [mol·m/s·m^2·kPa$^{0.5}$]
400	6.15E-08	5.89E-08	16.60	16.65
450	9.70E-08	9.33E-08	16.15	16.19
500	1.30E-07	1.25E-07	15.86	15.90

Table 2. Membrane hydrogen permeability before and after the reaction tests. Δp = 0.5 bar

4. Conclusions

In this experimental work the ethanol steam reforming reaction for producing hydrogen was studied in both the TR and a dense Pd-Ag MR, demonstrating the possibility to reach a higher ethanol conversion in the MR. In particular, at 500 °C more than 98% of ethanol conversion is achieved in the MR.

Moreover, due to the hydrogen permeation through the dense membrane, the hydrogen selectivity increases and the methane selectivity decreases. In the meanwhile, up to 25% of hydrogen is recovered as CO-free stream in the shell side of the MR. The performances of the MR increase with increasing the reaction pressure while the TR is negatively affected by the pressure.

5. References

Basile A., Gallucci F., Iulianelli A. and Tosti S., CO-free hydrogen production by ethanol steam reforming in a Pd-Ag membrane reactor, Fuel Cells, 1 (2008) 62-68

Benito M., Sanz J.L., Isabel R., Padilla R., Arjona R. and Daza L., Bio-ethanol steam reforming: Insights on the mechanism for hydrogen production, *J. Power Sou.*, 2005,151,11-17

Breen J.P., Burch R. and Coleman H.M., Metal-catalysed steam-reforming of ethanol in the production of hydrogen for fuel cell applications, *Appl. Catal.,* 2002,39,65-74

Domok M., Toth M., Rasko J. and Erdohelyi A., Adsorption and reactions of ethanol and ethanol–water mixture on alumina-supported Pt catalysts, *Appl. Catal. B: Env.*, 2007,69,262-272

Erdohelyi A., Rasko J., Kecske's T., Toth M., Domok M. and Baan K., Hydrogen formation in ethanol reforming on supported noble metal catalysts, *Catal. Tod.*, 2006,116,367-376

Fayyaz B., Harale A., Park B.G., Liu P.K.T., Sahimi M. and Tsotsis T., Design aspects of hydrogen adsorbent – membrane reactors for hydrogen production, *Ind. Eng, Chem. Res*, 2005,44,9398-9408.

Freni S., Cavallaro S., Mondello N., Spadaro L. and Frusteri F., Steam reforming of ethanol on Ni/MgO catalysts: H_2 production for MCFC, *J. Power Sou.*, 2002,108(1-2),53-57

Freni S., Mondello N., Cavallaro S. and Cacciola G., V.N. Pardon and V.A. Sobyanin, Hydrogen production by steam reforming of ethanol: a two step process, *React. Kinet Catal. Lett.,* 2000,71,143-152

Frusteri F., Freni S., Spadaro L., Chiodo V., Bonura G., Donato S. and Cavallaro S., H_2 production for MC fuel cell by steam reforming of ethanol over MgO supported Pd, Rh, Ni and Co catalysts, *Catal. Comm.*, 2004,5(10),611-615

Frusteri F., Freni S., Chiodo V., Spadaro L., Di Blasi O., Bonura G. and Cavallaro S., Steam reforming of bio-ethanol on alkali-doped Ni/MgO catalysts: hydrogen production for MC fuel cell, *Appl. Catal. A: Gen*., 2004,270(1-2),1-7

Frusteri F., Freni S., Chiodo V., Donato S., Bonura G. and S. Cavallaro, Steam and auto-thermal reforming of bio-ethanol over MgO and CeO_2 Ni supported catalysts, *Int. J. Hydrogen En*., 2006,31(15),2193-2199

Gallucci F., Basile A., Tosti S., Iulianelli A. and Drioli E., Methanol and ethanol steam reforming in membrane reactors: an experimental study, *Int. J. Hydrogen. En.*, 2007,32,1201-1210

Gallucci F., Paturzo L., Famà A. and Basile A., "An experimental study of the Methane Steam Reforming Reaction in a dense Pd/Ag Membrane Reactor", *Ind. & Eng. Chem. Res.,* 2004,43,928-933

Haga F., Nakajima T., Yamashita K. and Mishima S., Effect of Cristallite Size on the Catalysis of alumina-supported cobalt catalyst for steam reforming of ethanol, *React. Kinet. Catal. Lett.*, 1998,63,253-259

Haryanto A., Fernando S., Murali N. and Adhikari S., Current status of hydrogen production techniques by steam reforming of ethanol: a review, *En. Fuels*, 2005,19,2098-2106

Kaddouri A. and Mazzocchia C., A study of the influence of the synthesis conditions upon the catalytic properties of Co/SiO_2 or Co/Al_2O_3 catalysts used for ethanol steam reforming, *Catal. Comm.,* 2004,5,339-345

Keuler J.N. and Lorenzen L, Comparing and modeling the dehydrogenation of ethanol in a plug-flow reactor and a Pd-Ag membrane reactor, *Ind. Eng. Chem. Res.,* 2002,41,1960-1966

Published by The Berkeley Electronic Press, 2008

Liguras D.K, Kondarides D.I. and Verykios X.E., Production of hydrogen for fuel cells by steam reforming of ethanol over supported noble metal catalysts, *Appl. Catal.,* 2003,43,345-354

Llorca J., Homs N., Sales J. and de la Piscina P.R., Efficient Production of Hydrogen over Supported Cobalt Catalysts from Ethanol Steam reforming, *J. Catal.,* 2002,209,306-317

Maggio G., Freni S. and Cavallaro S., Light alcohols/methane fuelled molten carbonate fuel cells: a comparative study", *J. Power Sou.,* 1998,74,17-23

Mas V., Kipreos R., Amadeo N. and Laborde M., Thermodynamic analysis of ethanol/water system with the stoichiometric method, *Int. J. Hydrogen En.*, 2006,31,21-28.

Roh H.S., Wang Y., King D.L., Platon A. and Chin Y.H., Low temperature and H_2 selective catalysts for ethanol steam reforming, *Catal. Lett.*, 2006,108,1-2

Srinivas D., Satyanarayana C.V.V., Potdar H.S. and Ratnasamy P., Structural studies on NiO-CeO_2-ZrO_2 catalysts for steam reforming of ethanol, *Appl. Catal. A: Gen.,* 2003,246,323-334

Sun J., Qiu X., Wu F., Wang W. and Hao S., Hydrogen from steam reforming of ethanol in low and middle temperature range for fuel cell application, *Int. J. Hydrogen En.*, 2004,29,1075-1081

Tosti S. and Bettinali L., Diffusion Bonding of Pd-Ag Membranes, *J. Materials Sci.*, 2004,39,3041-3046

Tosti S., Bettinali L., Lecci D., Marini F. and Violante V., Method of bonding thin foils made of metal alloys selectively permeable to hydrogen, particularly providing membrane devices, and apparatus for carrying out the same, European Patent EP 1184125, 2001

Vaidya P.D. and Rodrigues A.E., Insight into steam reforming of ethanol to produce hydrogen for fuel cells, *Chem. Eng. J.*, 2006,117,39-49

Wieland S., Melin T. and Lamm A., Membrane reactors for hydrogen production, *Chem. Eng. Sci.*, 2002,57,1571-1576

Yang Y., Ma J. and Wu F., Production of hydrogen by steam reforming of ethanol over a Ni/ZnO catalyst, *Int. J. Hydrogen En.*, 2006,31,877-882

Interconnection between Paper 1 & Paper 2

In this work, the ESR reaction for producing hydrogen was studied in both a conventional reactor and a Pd-Ag dense MR. Both reactors have been packed with a commercial Ru-based catalyst. The experimental tests have been performed in the temperature and pressure range of 400-500 °C and 2.0-3.6 bar respectively and the feed molar ratio is kept constant at H_2O/C_2H_5OH=11/1 in order to avoid coke formation and reduce the CO production.

As a main result, the Pd-Ag based MR is able to realize higher ethanol conversion (achieving 98%) and hydrogen production with respect to conventional one. No coke formation was detected.

Moreover, the increasing of both reaction temperature and pressure affect positively the MR performances recovering up to 25% hydrogen as CO_x-free stream in the permeate side.

Nevertheless, although the Pd-Ag unsupported membrane offers a full H_2 perm-selectivity to permeation with respect to other gases, it presents low mechanical resistance as main drawbacks. Indeed, it is not possible to overcome 5.0 bar as pressure difference between retentate and permeate side.

Therefore, in the next paper, this kind of membrane is replaced by composite one as Pd/PSS supported membrane.

So, the aim of successive work was to explore the potentiality of a PSS-supported Pd-layer membrane reactor for H_2 production via ESR reaction, determining the main parameters controlling the overall performance of the MR.

INTERNATIONAL JOURNAL OF HYDROGEN ENERGY 36 (2011) 2029–2037

Available at www.sciencedirect.com

ScienceDirect

journal homepage: www.elsevier.com/locate/he

Ethanol steam reforming reaction in a porous stainless steel supported palladium membrane reactor

A. Basile [a,*], P. Pinacci [b], A. Iulianelli [a], M. Broglia [b], F. Drago [b], S. Liguori [a,c], T. Longo [a], V. Calabrò [c]

[a] CNR-ITM, c/o University of Calabria, Via Pietro Bucci, Cubo 17/C, 87030 Rende (CS), Italy
[b] ERSE S.p.A., Via Rubattino 54, 20134 Milano, Italy
[c] University of Calabria, Department of Engineering Modeling, University of Calabria, Via Pietro Bucci, Cubo 39/C, 87030 Rende (CS), Italy

ARTICLE INFO

Article history:
Received 17 July 2010
Received in revised form
29 October 2010
Accepted 9 November 2010
Available online 21 December 2010

Keywords:
Hydrogen production
Porous stainless steel supported palladium membrane reactor
Ethanol steam reforming

ABSTRACT

In this experimental work, the ethanol steam reforming reaction is performed in a porous stainless steel supported palladium membrane reactor with the aim of investigating the influence of the membrane characteristics as well as of the reaction pressure. The membrane is prepared by electroless plating technique with the palladium layer around 25 μm deposited onto a stainless steel tubular macroporous support. The experimental campaign is directed both towards permeation and reaction tests. Firstly, pure He and H_2 are supplied separately between 350 and 400 °C in the MR in permeator modality for calculating the ideal selectivity $\alpha_{H_2/He}$. Thus, the MR is packed with 3 g of a commercial Co/Al_2O_3 catalyst and reaction tests are performed at 400 °C, by varying the reaction pressure from 3.0 to 8.0 bar. Experimental results in terms of ethanol conversions as well as recovery and purity of hydrogen are given and compared with some results in the same research field from the open literature.

As best result of this work, 100% ethanol conversion is reached at 400 °C and 8 bar, recovering a hydrogen-rich stream consisting of more than 50% over the total hydrogen produced from reaction, having a purity around 65%.

1. Introduction

Hydrogen is recognized as one of the most promising energy carriers in the future and it could have an important role to reduce the environmental pollution whether combined to proton exchange membrane fuel cells (PEMFCs).

Today, hydrogen is mainly produced from natural gas as a derived fossil source via steam reforming, autothermal reforming and partial oxidation reactions [1,2]. Nevertheless, recently in the viewpoint of reducing the environmental pollution, much attention was paid for producing hydrogen from reforming reactions of non derived fossil fuels. In particular, among different renewable sources, ethanol produced by fermentation of biomasses seems to represent an excellent candidate owing to low toxicity, high safety and high hydrogen content [3–7].

One of the most used processes to produce a H_2-rich stream from ethanol is the steam reforming reaction (ESR) (1), [8,9]:

$$C_2H_5OH + 3H_2O = 2CO_2 + 6H_2 \quad \Delta H_{298K}^{\circ} = 157.0 \text{ kJ/mol} \qquad (1)$$

Ethanol steam reforming, carried out in fixed bed reactors (FBRs), has been widely studied as confirmed by the open literature on this field [10–25].

* *Corresponding author*. Tel.: +39 0984 492013; fax: +39 0984 402103.
E-mail address: a.basile@itm.cnr.it (A. Basile).
0360-3199/$ – see front matter © 2010 Professor T. Nejat Veziroglu. Published by Elsevier Ltd. All rights reserved.
doi:10.1016/j.ijhydene.2010.11.020

Generally, the H_2-rich gas coming out from a FBR contains secondary products such as CO_2, CO, CH_4, C_2H_4, acetaldehyde, ethylene and ethane. The research on this field is still concentrated on the catalyst development by using FBRs. Otherwise, the membrane reactor (MR) technology was already studied with particular reference to dense self-supported Pd–Ag membrane [5–7,10] as well as to Pd layers deposited onto different supports [3,4,14,15]. The membrane plays an important role in the reaction/separation system and its typology is chosen depending on several parameters such as: productivity, separation selectivity, membrane life time, mechanical and chemical integrity at the operating conditions and, particularly, the cost [26].

Dense metallic Pd-based membranes offer an infinite H_2 perm-selectivity with respect to other gases, but owing to the low availability of Pd in the nature, it results to be very expensive [27]. Furthermore, the membrane surface poisoning in the presence of CO, H_2S, SO_2, sulphur, arsenic, chlorine and unsaturated hydrocarbons represents the most relevant drawback [28].

Porous membranes, such as aluminium, titanium or silica oxides, are chemically inert, stable at high temperatures and exhibit relatively high H_2 permeability, resulting available at moderate cost [29]. On the contrary, as a main drawback, they show a poor H_2 perm-selectivity and a significant amount of reactants lost for permeation through the membrane [29]. Composite membranes combine the benefits of the two aforementioned typologies. On this route, the behaviour of a composite membrane is not only determined by the properties of the selective Pd-based barrier layer, but it is also affected by the properties of the microporous support film. Thus, a Pd layer over a porous support can be used for obtaining high H_2 perm-selectivity and high permeability. Concerning the support, mechanical stability and simplicity of assembling in a module are the main benefits of using porous stainless steel (PSS) rather than porous ceramic and Vycor glass supports [30]. Additionally, the thermal expansion coefficient of stainless steel is similar to Pd, ensuring good mechanical properties during temperature cycling [30]. Therefore, a PSS-supported Pd-based membrane could offer an interesting compromise among moderate cost, high H_2 permeability and selectivity and good mechanical resistance.

The aim of the present work is to explore the potentiality of a PSS-supported Pd-layer membrane reactor for H_2 production via ESR reaction, determining the main parameters controlling the overall performance of the membrane reactor.

2. Experimental

2.1. Membrane preparation

A 25 μm thick composite Pd membrane has been prepared by electroless plating onto a stainless steel tubular macroporous support.

The support is a 10 mm O.D. AISI 316 L porous tube, with a nominal pore size of 0.1 μm, supplied by Mott Metallurgical Corporation. Nominal pore size is determined by the manufacturer based on a 95% rejection of particles with size greater than 0.1 μm. The actual pore size is however much larger: a mean and maximum value of about 2 and 5 μm, respectively, have been determined by mercury intrusion measurements [31].

The porous support was welded to two non porous AISI 316 L tubes, one of them closed in order to allow a proper housing in the reactor (see Fig. 1). The total length of the support is 20 cm and the active length of the porous support is 7.7 cm. The active area of the membrane is 24.2 cm^2. The membrane preparation has been performed according to the procedure described elsewhere [32] and consists of the following steps:

- Cleaning up of the support in an ultrasonic bath with acetone, followed by successive rinsing in water, diluted hydrochloric acid, de-ionized water up to a neutral pH and acetone.
- Oxidation of the support in oven with static air at the temperature of 500 °C for two successive cycles of 10 h.
- Activation of the oxidised support by dipping into a stannous chloride solution and a Pd chloride solution, alternately, for many times.
- Deposition of Pd by electroless plating performed in a solution of Pd chloride, ammonia (to control pH), $EDTANa_2$ (complexing agent) and hydrazine (reducing agent). Pd plating is obtained by circulating the solution in a reactor where the membrane is immersed and kept in rotation in order to obtain a homogeneous deposit onto the outer surface and to facilitate nitrogen evacuation from the reaction zone; the temperature is kept constant at 45–50 °C by a thermostatic bath.

At the end of each bath, the membrane thickness has been estimated by gravimetric measurements and, thereafter, at room temperature He permeance through the membrane was measured. The membrane was considered as dense and, consequently, palladium deposition stopped, when helium permeance was reduced below 10^{-9} mol/(s m^2 Pa) at trans-membrane pressure difference higher than 5 bar.

2.2. Membrane reactor setup

The MR consists of a tubular stainless steel module (length 280 mm, i.d. 20 mm) containing the membrane as a tubular Pd layer deposited onto a PSS support, Fig. 1. The Pd layer of the membrane is deposited via electroless plating technique onto an AISI 316 L porous tube, having nominal particle retention size of 0.1 μm. The membrane tube is closed at one end. The working temperature range for this membrane varies from 300 °C to 420 °C.

A commercial Co/Al_2O_3 catalyst in pellet form was packed in the annulus of the MR within glass spheres (2 mm diameter) to avoid catalyst dispersion, Fig. 1.

2.3. Experimental details

The experimental setup, illustrated in Fig. 2, includes a P680 HPLC pump (Dionex) used for feeding both liquid H_2O and C_2H_5OH, which are vaporized before entering into the pre-heating zone. Afterwards, the vapour mixture is flowed into the annulus of the MR as a reaction side. The total feed flow

INTERNATIONAL JOURNAL OF HYDROGEN ENERGY 36 (2011) 2029–2037

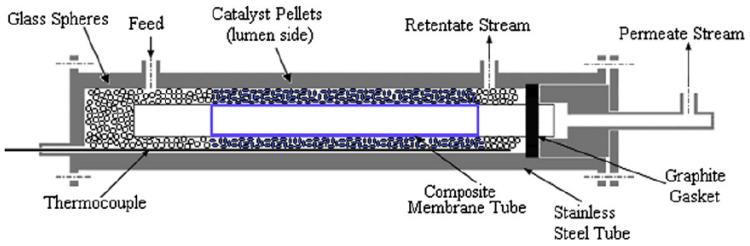

Fig. 1 – Membrane reactor configuration.

rate is equal to 0.1 mL/min and the H_2O/C_2H_5OH feed ratio is kept constant at 3/1.

Both retentate and permeate streams are analyzed using a temperature programmed HP 6890 GC with two thermal conductivity detectors at 250 °C and Ar as carrier gas. The GC is equipped by three packed columns: Porapack R 50/80 (8 ft × 1/8 in) and Carboxen™ 1000 (15 ft × 1/8 in) connected in series, and a Molecular Sieve 5 Å (6 ft × 1/8 in). The retentate and permeate flow rates are measured by means of a bubble flow meter and the Absolute Calibration Curve Method was used for calculating their molar compositions. It consists of a preparation of standard solutions containing graded amount of the standard object component and the injection of a constant volume of each standard solution, exactly measured. With the obtained chromatograms, a calibration curve is done by plotting the peak heights or peak areas of the standard object component on the ordinate and the amounts of the standard object component on the abscissa. The calibration curve is usually a straight line through the origin. Then, the solution test, as carried out in the individual monograph, is realized recording a chromatogram under the same conditions as for the preparation of the calibration curve. Afterwards, the peak height or peak area of the object component is measured using the calibration curve.

The vapour fraction of both retentate and permeate streams is condensed through cold traps and the liquid fractions are analyzed by means of a Perkin Elmer GC.

Before reaction, the membrane is activated using He at 400 °C under atmospheric pressure for 48 h and, then, H_2 for 24 h. Thus, permeation tests using separately pure He and H_2 were performed between 350 and 400 °C in the MR used as a permeator. Then, it was cooled down at room temperature and packed with 3 g of Co/Al_2O_3 catalyst. Finally, the MR was heated up again to 400 °C for realizing the reaction tests in the reaction pressure ranges between 3.0 and 8.0 bar, regulated by means of a back pressure controller. In all the experiments,

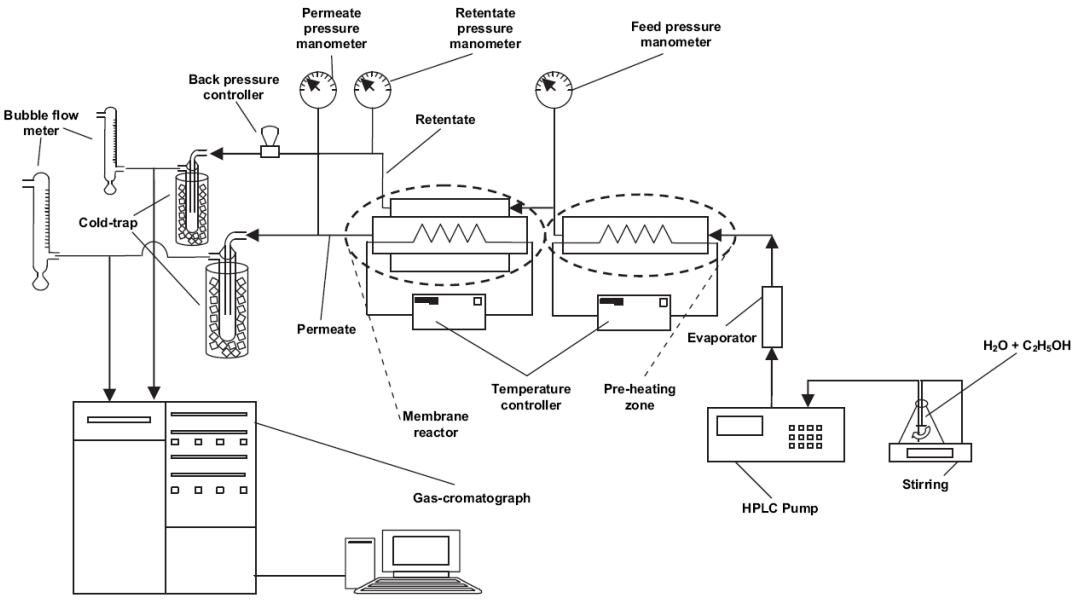

Fig. 2 – Scheme of the experimental plant.

Table 1 – Linear regression value (R^2) related to hydrogen permeation at 350 °C, calculated at different dependence factor "*n*".

Dependence factor "*n*"	Linear regression value (R^2)
0.5	0.9998
0.6	0.9999
0.7	0.9992
0.8	0.9978
0.9	0.9956
1.0	0.9926

the absolute permeate pressure of the MR was kept constant at 1.0 bar without using any sweep gas into the permeate side.

A flat temperature profile along the reactor was confirmed during the reaction by means of a three points thermocouple placed inside the MR annulus.

Each experimental point obtained in this work is an average value of 6 experimental reaction tests taken in 90 min. After each experimental cycle (90 min), the catalyst is regenerated using H_2 (1.8×10^{-3} mol/min) for 2 h. Moreover, the C balance between inlet and outlet carbon-based gaseous streams was closed in all the reaction tests with ±2.0% as maximum error by also considering the unreacted ethanol condensed in the cold traps.

2.4. *Reactions and equations*

Despite the apparent simplicity of the stoichiometric reaction for maximum H_2 production via gas phase ethanol steam reforming (1), this reaction involves a complex reaction system that produces undesirable by-products besides H_2, depending on the catalyst used [33].

According to Sahoo et al. [34], the main secondary reactions occurring during ESR performed in a FBR packed with a Co/Al_2O_3 catalyst are the water gas shift (2) and ethanol decomposition (3):

$$CO + H_2O = CO_2 + H_2 \quad \Delta H_{298K}^{\circ} = -41.2 \text{ kJ/mol} \tag{2}$$

Table 2 – Ideal selectivity ($\alpha_{H_2/He}$) at different pressure and at 350 °C.

Retentate side pressure [kPa]	Permeate side pressure [kPa]	$\alpha_{H_2/He}$ [–]
150	100	886.75
200	100	792.54
250	100	698.75

$$C_2H_5OH = CH_4 + CO + H_2 \quad \Delta H_{298K}^{\circ} = 33.16 \text{ kJ/mol} \tag{3}$$

Moreover, at temperatures higher than 200 °C, Co-based catalysts are able to produce methane from methanation reaction (4) as well as from ethanol decomposition reaction (3) [22].

$$CO + 3H_2 = CH_4 + H_2O \quad \Delta H_{298K}^{\circ} = -206.2 \text{ kJ/mol} \tag{4}$$

Concerning the description of the MR performances, some equations are defined as reported below:

$$C_2H_5OH \text{ Conversion } (\%) = \frac{(CO + CO_2 + CH_4)_{out}}{2C_2H_5OH_{in}} \cdot 100 \tag{5}$$

$$H_2 - \text{Permeate purity}(\%) = \frac{H_{2,permeate}}{(H_2 + CO + CO_2 + CH_4)_{permeate}} \cdot 100 \tag{6}$$

$$\text{yield}_{H_2-TOT}\ (\%) = \frac{H_{2,out}}{6C_2H_5OH_{in}} \cdot 100 \tag{7}$$

$$\text{Hydrogen Recovery Factor (HRF) } (\%) = \frac{H_{2,permeate}}{H_{2,permeate} + H_{2,retentate}} \cdot 100 \tag{8}$$

$$(\text{Ideal selectivity})\alpha_{H_2/He} = \frac{\text{Permeance}_{H_2}}{\text{Permeance}_{He}} \tag{9}$$

where the subscript "OUT" indicates the total (retentate and permeate sides) outlet flow rate of each species, while "IN" refers to the feed stream.

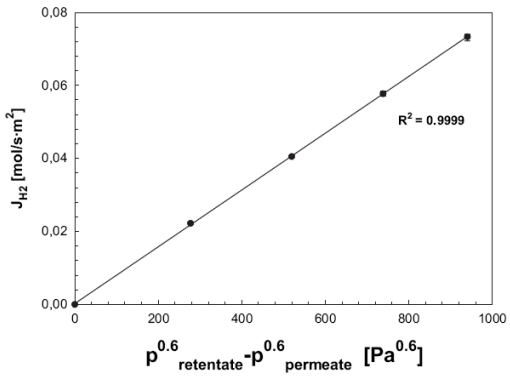

Fig. 3 – H_2 permeation flux versus H_2 partial pressure drops across membrane at "*n*" = 0.6 value at 350 °C.

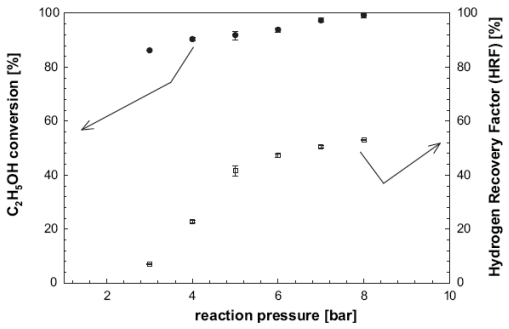

Fig. 4 – C_2H_5OH conversion and Hydrogen Recovery Factor (HRF) versus reaction pressure at 400 °C, permeate pressure = 1.0 bar, H_2O/C_2H_5OH feed molar ratio = 3/1, Co/Al_2O_3 catalyst in pellet form.

INTERNATIONAL JOURNAL OF HYDROGEN ENERGY 36 (2011) 2029–2037

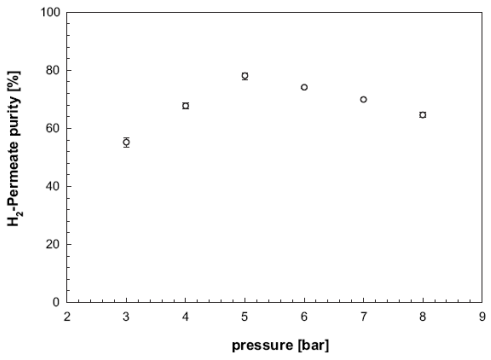

Fig. 5 – H_2-permeate purity versus reaction pressure at 400 °C, permeate pressure = 1.0 bar, H_2O/C_2H_5OH feed molar ratio = 3/1, Co/Al_2O_3 catalyst in pellet form.

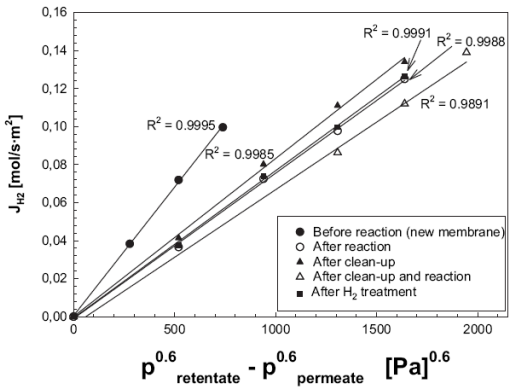

Fig. 7 – H_2 permeation flux through the Pd-supported membrane during different steps of experimental analysis carried out at 400 °C.

3. Results and discussion

3.1. *Membrane permeation tests*

Firstly, permeation tests with pure gases such as He and H_2 were made at 350 °C from 1.5 bar to 2.5 bar as a retentate pressure and keeping constant at 1.0 bar the permeate pressure. Therefore, the permeation behaviours of the system under different H_2 or He partial pressure drops across the membrane were estimated. Generally, at constant temperature, the H_2 permeation through dense Pd-based membranes occurs via solution/diffusion mechanism. This transport can be described by the following general expression (10) [35]:

$$J_{H_2} = \frac{Pe}{\delta}\left(p^n_{H_2-retentate} - p^n_{H_2-permeate}\right) \quad (10)$$

where: J_{H_2} is the H_2 flux permeating through the Pd-based membrane, Pe the H_2 permeability, δ the membrane thickness, $p_{H_2-retentate}$ and $p_{H_2-permeate}$ the H_2 partial pressure in the retentate and permeate sides, respectively, and "n" the dependence factor of H_2 partial pressure, in the range 0.5–1.0, used as an indicator for the rate-controlling step of the permeation [35]. Therefore, by considering the H_2 flux permeating through the membrane against H_2 permeation driving force, the linear regression factor (R^2 – square of correlation coefficient) was calculated at different "n" values, Table 1. Fig. 3 shows the H_2 permeation flux versus H_2 partial pressure drops across the membrane at the highest R^2 corresponding to "n" = 0.6. Thus, in this case the H_2 permeating flux is described by the following expression (11):

$$J_{H_2} = \frac{Pe}{\delta}\left(p^{0.6}_{H_2-retentate} - p^{0.6}_{H_2-permeate}\right) \quad (11)$$

Furthermore, He permeation tests were performed in order to check the presence of any defect in the palladium layer and, accordingly, the H_2/He ideal selectivity ($\alpha_{H_2/He}$) was calculated. As shown in Table 2, ideal selectivity decreases while increasing pressure drop across the membrane. Such a trend

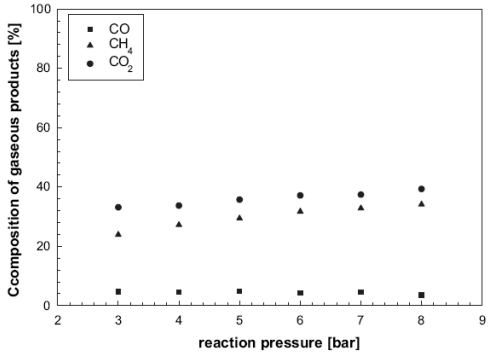

Fig. 6 – The gaseous products composition in the retentate side versus reaction pressure at 400 °C, permeate pressure = 1.0 bar, H_2O/C_2H_5OH feed molar ratio = 3/1, Co/Al_2O_3 catalyst in pellet form.

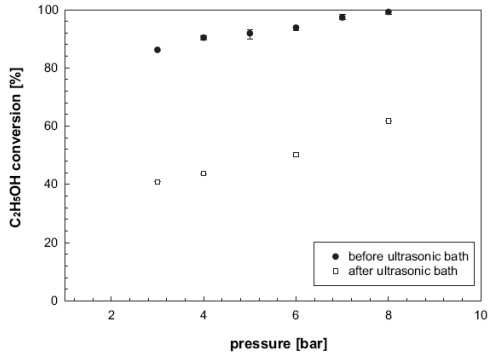

Fig. 8 – C_2H_5OH conversion versus reaction pressure at 400 °C, permeate pressure = 1.0 bar, H_2O/C_2H_5OH feed molar ratio = 3/1, Co/Al_2O_3 catalyst in pellet form before and after ultrasonic bath.

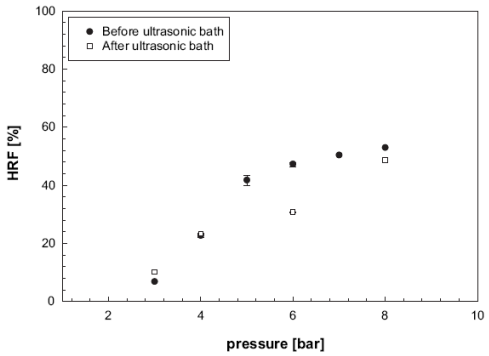

Fig. 9 – Hydrogen Recovery Factor (HRF) versus reaction pressure at 400 °C, permeate pressure = 1.0 bar, H_2O/C_2H_5OH feed molar ratio = 3/1, Co/Al_2O_3 catalyst in pellet form before and after ultrasonic bath.

has also been reported by Rothenberger et al. [36] for two composite Pd–porous stainless steel membranes, 22 μm thick, similar to the one tested in this work, and can be attributed to the viscous flow component through the defects (pinholes) in the Pd layer, as discussed in reference [37].

3.2. ESR reaction in composite membrane reactor tests

Fig. 4 shows both C_2H_5OH conversion and HRF versus reaction pressure. The conversion increases as much as reaction pressure is higher, reaching almost 100% at 8.0 bar. The increasing pressure gives two conflicting effects on the MR reaction system: the first, as a drawback, on the thermodynamic of the overall ESR reaction (1) (it proceeds with an increase of the moles number) and the second, as a benefit, on the H_2 permeation through the membrane (the higher the H_2 permeation driving force the higher the H_2 stream removed from the reaction to the permeate side, favouring the shift of the ESR reaction towards the products as well as higher

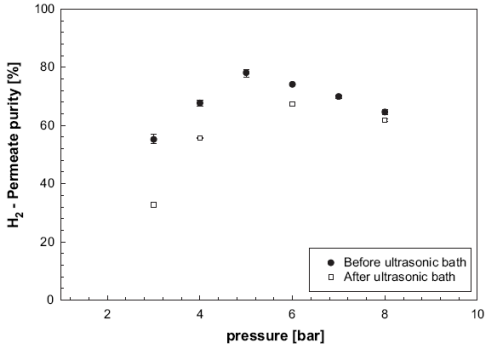

Fig. 10 – H_2-permeate purity versus reaction pressure at 400 °C, permeate pressure = 1.0 bar, H_2O/C_2H_5OH feed molar ratio = 3/1, Co/Al_2O_3 catalyst in pellet form before and after ultrasonic bath.

Table 3 – Ideal selectivity $\alpha_{H_2/He}$ after ultrasonic bath in particular before and after reaction tests.

	After ultrasonic bath		
	Retentate side pressure [kPa]	Permeate side pressure [kPa]	$\alpha_{H_2/He}$ [–]
Before reaction tests	200	100	109.79
	300	100	112.37
	400	100	105.98
	500	100	96.29
After reaction tests	300	100	86.34
	400	100	65.25
	500	100	52.68
	600	100	37.43

C_2H_5OH consume). Therefore, the increasing trend of C_2H_5OH conversion probably takes place since the membrane effect is prevalent on the thermodynamic one. As a consequence, more consistent amount of H_2 is removed from the reaction side and collected in the permeate side, globally improving the HRF. As a result, at 8.0 bar the HFR is more than 50.0%.

The H_2-permeate purity is illustrated in Fig. 5. In the pressure range from 3.0 bar to 5.0 bar, it increases owing to the membrane effect, which probably overcomes the unfavourable effect due to the thermodynamic. Otherwise, at a pressure higher than 5.0 bar H_2-permeate purity decreases, probably because of the catalyst deactivation due to carbon coke deposition. In details, as indicated by Zhang et al. [38], using Co-based catalysts a rapid deactivation is noticeable owing to coke formation during ESR reaction. This fact induces higher CH_4 and CO_2 formation in the annulus of reactor, as shown in Fig. 6. Therefore, higher permeation of these compounds through the defects of the membrane occurs.

Moreover, the carbon coke, deposited on the membrane surface, probably does not allow an efficient H_2 permeation. This is stated because the H_2 permeating flux was tested after the reaction experimental tests and compared to the permeation before the reaction. Fig. 7 clearly illustrates that it is lower than before reaction cycles. Taking into account what reported in the open literature [39], the deactivation of Co-

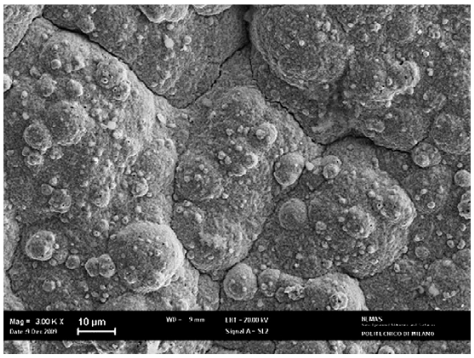

Fig. 11 – SEM image of the membrane surface at the end of the tests.

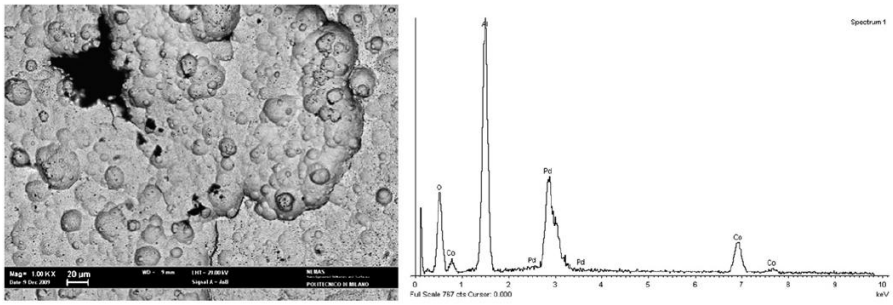

Fig. 12 – SEM image, in back scattering modality of the membrane surface contaminated by catalyst fragments (a) and related EDS spectra (b).

based catalysts due to the carbon coke built up on its surface can be recovered under H_2 treatment, which proceeds with methane formation. Therefore, H_2 was flowed into the catalytic bed for 2 h, then removing the carbon coke deposited on the membrane surface with methane formation noticed during the H_2 treatment. Nevertheless, after the H_2 treatment useful for the carbon coke deposition on the membrane surface, H_2 permeation tests were repeated and, as shown in Fig. 7, its permeating flux through the membrane was not improved. Therefore, the membrane was cleaned up in demineralised water in an ultrasonic bath at 40 °C, for 2–3 min. This procedure has been repeated several times until the water appeared as clean.

Afterwards, fresh catalyst was placed inside the annulus and the MR was heated up again to 400 °C. The permeation and some reaction tests (at 3.0, 4.0, 6.0 and 8.0 bar) were repeated to confirm the repeatability of the permeation/reaction results after the membrane clean-up.

The H_2 permeating flux was enhanced after the membrane clean-up. In fact, as illustrated in Fig. 7, it is higher than H_2 permeating flux through the membrane after reaction tests as well as after the H_2 treatment. However, the trend achieved before reaction tests is not observed, confirming the loss of membrane permeating performance even after the clean-up procedure.

Concerning the reaction tests on ESR, a comparison within the MR performances in terms of C_2H_5OH conversion, HRF and H_2-permeate purity before and after the membrane clean-up procedure was done. Fig. 8 depicts the drastic decrease of around 40.0% within C_2H_5OH conversion before and after the membrane treatment. In details, at 8.0 bar the C_2H_5OH conversion reduces from 100% to 62.0%. As a consequence, low H_2 production is realized and, as reported in Figs. 9 and 10, both HFR and H_2-permeate purity are decreased too.

At the end of the experimental reaction cycles, a further decrease of both H_2 permeating flux, as shown in Fig. 7 ("after clean-up and reaction"), and $\alpha_{H_2/He}$, as summarized in Table 3, was observed.

Therefore, to investigate the causes of the membrane degradation as well as the loss of its performances, the membrane was analyzed by Scanning Electron Microscope (SEM). SEM images of pieces of the membrane surface are shown in Fig. 11, which highlights the characteristic cauliflower morphology of Pd clusters and the presence of other deposits on the Pd layer. EDS micro-analysis, performed at several locations in correspondence of deposits, evidenced the

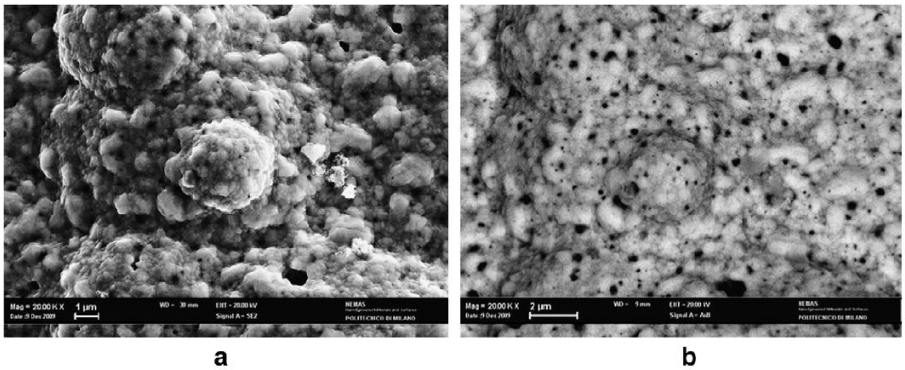

Fig. 13 – SEM image with secondary electrons (a) and in back scattering modality (b) of the membrane surface.

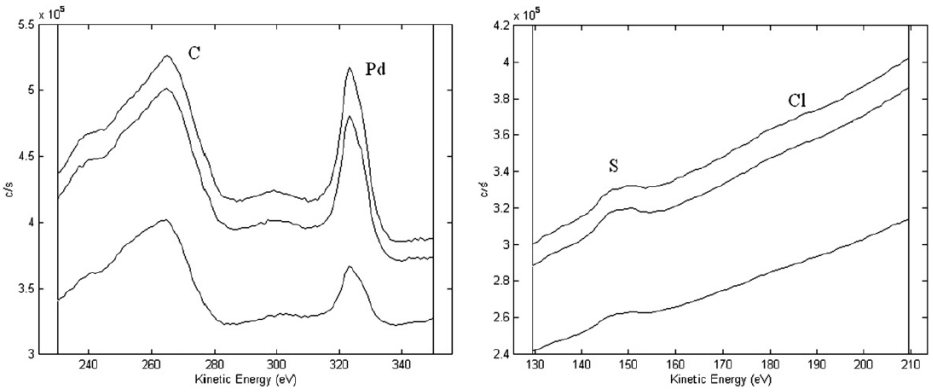

Fig. 14 – Auger spectra measured on the membrane surface at three different locations.

presence either of iron (concentration ranging between 0.5 and 2% by weight) or alumina and cobalt, e.g. catalyst fragments (see Fig. 12). By increasing magnification, SEM images evidenced the presence of small holes from ten to hundred of nanometers in size (see Fig. 13).

Membrane samples were further analyzed in correspondence of the areas where defects were detected by an Auger spectroscopy (SAM), coupled with sputtering, by using a beam of argon ions with a kinetic energy of 4 kev and a current of 1 μA.

SAM analysis of the membrane surfaces was carried out at three different locations; as shown in Fig. 14, all measurements evidenced relevant carbon contamination as well as low concentration of sulphur and chlorides was detected (about the 2% and 1%, respectively).

The sample surface was subsequently eroded for a total of 20 min, corresponding to an equivalent thickness of SiO_2 of about 600 nm; after each sputtering cycle, Auger spectra were determined. Carbon was removed after a brief sputtering time (10 nm of equivalent thickness), thus suggesting that its presence on membrane surface is determined by the sample manipulation. Besides, sulphur concentration remained constant up to 300 nm and it was completely removed only at 600 nm. Finally, chloride concentration remained constant until the end of the sputtering cycle.

Both chloride and sulphur can be detrimental to Pd [40]. Sulphur has been accidentally introduced in the gas feed, e.g. could be leached from seals used in the pilot loop; in particular sulphur, even in small concentration, poisons Pd surfaces and converts Pd into bulk sulphides such as Pd S_4. Besides chloride can be present as $PdCl_2$ which has been used in the electroless bath for deposition, and has not been completely removed by the subsequent rinsing. The observed decrease of H_2 permeance and formation of defects on the Pd layer, therefore, can be primarily attributed to the presence of sulphur.

4. Conclusion

In this experimental work, the ethanol steam reforming reaction was carried out in a porous stainless steel supported palladium membrane reactor packed with a Co/Al_2O_3 catalyst and operated at 400 °C from 3.0 to 8.0 bar. Ethanol conversion varied from 85.0 to 100% in the reaction pressure range of 3.0–8.0 bar. At 8.0 bar, the hydrogen recovery was more than 50% with a purity of around 65%.

However, by comparing the MR performances in terms of C_2H_5OH conversion, HRF and H_2-permeate purity before and after the reaction tests, an evident decrease of the permeation capacity as well as of the overall efficiency of the MR was observed. SEM images and EDS micro-analysis showed the presence of iron, alumina and cobalt in correspondence of some deposits on the palladium layer of the membrane. In particular, SEM images evidenced the presence of small holes from ten to hundred of nanometers in size. Furthermore, SAM analyses highlighted a consistent carbon contamination and a low concentration of sulphur and chlorides. All these aspects negatively affected the permeation capacity of the supported palladium membrane, globally decreasing the performances of the membrane reactor during ethanol steam reforming reaction.

Therefore, in a near future a new study will be devoted to minimize the effects of the contaminants on the membrane, further improving the performances of the membrane reactor in terms of higher hydrogen recovery and, mostly, of hydrogen purity.

REFERENCES

[1] Vizcaino AJ, Carrero A, Calles JA. Hydrogen production by ethanol steam reforming over Cu–Ni supported catalysts. Int J Hydrogen Energy 2007;32:1450–61.
[2] Heinzel A, Vogel B, Hübner P. Reforming of natural gas-hydrogen generation for small scale stationary fuel cell systems. J Power Sources 2002;105:202–7.
[3] Yu CY, Lee DW, Park SJ, Lee KY, Lee KH. Study on a catalytic membrane reactor for hydrogen production from ethanol steam reforming. Int J Hydrogen Energy 2009;34:2947–54.
[4] Yu CY, Lee DW, Park SJ, Lee KY, Lee KH. Ethanol steam reforming in a membrane reactor with Pt-impregnated Knudsen membranes. Appl Catal B Environ 2009;86:121–6.

[5] Basile A, Gallucci F, Iulianelli A, Tosti S. CO-free hydrogen production by ethanol steam reforming in a Pd–Ag membrane reactor. Fuel Cell 2008;8:62–8.

[6] Iulianelli A, Basile A. An experimental study on bio-ethanol steam reforming in a catalytic membrane reactor. Part I: temperature and sweep-gas flow configuration effects. Int J Hydrogen Energy 2010;35:3170–7.

[7] Iulianelli A, Liguori S, Longo T, Tosti S, Pinacci P, Basile A. An experimental study on bio-ethanol steam reforming in a catalytic membrane reactor. Part II: reaction pressure, sweep factor and WHSV effects. Int J Hydrogen Energy 2010; 35:3159–64.

[8] Vasudeva K, Mitra N, Umasankar P, Dhingra SC. Steam reforming of ethanol for hydrogen production: thermodynamic analysis. Int J Hydrogen Energy 1996;21: 13–8.

[9] Fishtik I, Alexander A, Datta R, Geana D. A thermodynamic analysis of hydrogen production by steam reforming of ethanol via response reactions. Int J Hydrogen Energy 2000; 25:31–45.

[10] Santucci A, Borgognoni F, Cordiner S, Traversa E, Tosti S. Low temperature ethanol steam reforming in a Pd–Ag membrane reformer. ECS Trans 2008;6:29–35.

[11] Barroso MN, Gomez MF, Arrua LA, Abello MC. Hydrogen production by ethanol reforming over NiZnAl. Appl Catal A Gen 2006;304:116–23.

[12] Biswas P, Kunzru D. Steam reforming of ethanol for production of hydrogen over $Ni/CeO_2–ZrO_2$ catalyst: effect of support and metal loading. Int J Hydrogen Energy 2007;32: 969–80.

[13] Carrero A, Calles JA, Vizcaino AJ. Hydrogen production by ethanol steam reforming over Cu–Ni/SBA-15 supported catalysts prepared by direct synthesis and impregnation. Appl Catal A Gen 2007;327:82–94.

[14] Mendes D, Tosti S, Borgognoni F, Mendes A, Madeira LM. Integrated analysis of a membrane-based process for hydrogen production from ethanol steam reforming. Catal Today 2010;156:107–17.

[15] Lin WH, Liu YC, Chang HF. Hydrogen production from oxidative steam reforming of ethanol in a palladium–silver alloy composite membrane reactor. J Chin Inst Chem Eng 2008;39:435–40.

[16] Fajardo HV, Probst LFD. Production of hydrogen by steam reforming of ethanol over Ni/Al_2O_3 spherical catalysts. Appl Catal A Gen 2006;306:134–41.

[17] Erdohelyi A, Rasko J, Kecskes T, Toth M, Domok M, Baan K. Hydrogen formation in ethanol reforming on supported noble metal catalysts. Catal Today 2006;116:367–76.

[18] Liguras DK, Kondarides DI, Verykios XE. Production of hydrogen for fuel cells by steam reforming of ethanol over supported noble metal catalysts. Appl Catal B Environ 2003; 43:345–54.

[19] Orucu E, Gokaliler F, Aksoylu AE, Onsan ZI. Ethanol steam reforming for hydrogen production over bimetallic $Pt–Ni/Al_2O_3$. Catal Lett 2008;120:198–202.

[20] Haryanto A, Fernando S, Murali N, Adhikari S. Current status of hydrogen production techniques by steam reforming of ethanol: a review. Energy Fuels 2005;19:2098–106.

[21] Breen JP, Burch R, Coleman HM. Metal-catalyzed steam-reforming of ethanol in the production of hydrogen for fuel cell applications. Appl Catal 2002;39:65–74.

[22] Haga F, Nakajima T, Yamashita K, Mishima S. Effect of crystallite size on the catalysis of alumina-supported cobalt catalyst for steam reforming of ethanol. React Kinet Catal Lett 1998;63:253–9.

[23] Llorca J, Homs N, Sales J, de la Piscina PR. Efficient production of hydrogen over supported cobalt catalysts from ethanol steam reforming. J Catal 2002;209:306–17.

[24] Kaddouri A, Mazzocchia C. A study of the influence of the synthesis conditions upon the catalytic properties of Co/SiO_2 or Co/Al_2O_3 catalysts used for ethanol steam reforming. Catal Commun 2004;5:339–45.

[25] Batista MS, Santos RKS, Assaf EM, Assaf JM, Ticianelli EA. Characterization of the activity and stability of supported cobalt catalysts for the steam reforming of ethanol. J Power Sources 2003;124:99–103.

[26] Julbe A, Farrusseng D, Guizard C. Porous ceramic membranes for catalytic reactors – overview and new ideas. J Memb Sci 2001;181:3–20.

[27] Lin YS. Microporous and dense inorganic membranes: current status and prospective. Sep Purif Tech 2001;25:39–55.

[28] Amandusson H, Ekedahl LG, Dannetun H. The effect of CO and O_2 on hydrogen permeation through a palladium membrane. Appl Surf Sci 2000;153:259–67.

[29] Lu GQ, Diniz da Costa JC, Dukec M, Giessler S, Socolow R, Williams RH, et al. Inorganic membranes for hydrogen production and purification: a critical review and perspective. J Colloid Interface Sci 2007;314:589–603.

[30] Shu J, Grandjean BPA, Kaliaguine S. Asymmetric Pd–Ag/stainless steel catalytic membranes for methane steam reforming. Catal Today 1995;25:327–32.

[31] Mardilovich IP, Engwall E, Ma YH. Dependence of hydrogen flux on the pore size and plating surface topology of asymmetric Pd–porous stainless steel membranes. Desalination 2002;144:85–9.

[32] Pinacci P, Broglia M, Valli C, Capannelli G, Comite A. Evaluation of the water gas shift reaction in a palladium membrane reactor. Catal Today 2010;156:165–72.

[33] Mas V, Kipreos R, Amadeo N, Laborde M. Thermodynamic analysis of ethanol/water system with the stoichiometric method. Int J Hydrogen Energy 2006;31:21–8.

[34] Sahoo DR, Vajpai S, Patel S, Pant KK. Kinetic modeling of steam reforming of ethanol for the production of hydrogen over Co/Al_2O_3 catalyst. Chem Eng J 2007;125:139–47.

[35] Dittmeyer R, Höllein V, Daub K. Membrane reactors for hydrogenation and dehydrogenation processes based on supported palladium. J Mol Catal A Chem 2001;173:135–84.

[36] Rothenberger KS, Cugini AV, Howard BH, Killemeyer RP, Ciocco MV, Morreale BD, et al. High pressure hydrogen permeance of porous stainless steel coated with a thin palladium film via electroless plating. J Memb Sci 2004;244: 55–68.

[37] Mardilovich IP, She Y, Ma YH, Rei MH. Defect-free palladium membranes on porous stainless-steel support. AIChE J 1998; 44:310–22.

[38] Zhang B, Tang X, Li Y, Xu Y, Shen W. Hydrogen production from steam reforming of ethanol and glycerol over ceria-supported metal catalysts. Int J Hydrogen Energy 2007;32: 2367–73.

[39] Lin SSY, Kim DH, Ha SY. Hydrogen production from ethanol steam reforming over supported cobalt catalysts. Catal Lett 2008;122:295–301.

[40] Munschau MV, Xie X, Everson IV CR, Sammells AF. Dense inorganic membranes for production of hydrogen from methane and coal with carbon dioxide sequestration. Catal Today 2006;118:12–23.

Interconnection between Paper 2 & Paper 3

In this work, ESR reaction was performed in a Pd/PSS supported MR packed with Co/Al_2O_3, at 400 °C, high reaction pressure (3.0 – 8.0 bar) and stoichiometric feed molar ratio.

As best result, 100% ethanol conversion is realized at 400 °C and 8.0 bar, recovering a hydrogen-rich stream consisting of more than 50% over the total hydrogen produced from reaction, having a purity around 65%. A relevant carbon contamination was detected by SAM analysis of the membrane surface.

Making a qualitative comparison with a previous work is that:

- Using a Pd-Ag based MR is possible to obtain a pure hydrogen stream to supply directly to PEMFC;
- On the contrary, employing a Pd/PSS MR, the hydrogen permeate stream is contaminated by other by-products of reaction, nevertheless a higher hydrogen recovery is realized.

It is well known that a water excess during the ESR reaction reduces the CO content of the reformed stream and avoids carbon formation. Therefore, it could be advantageous to feed into the reactor a bio-ethanol mixture (corresponding to a water/ethanol feed molar ratio of 29.0/1–18.7/1), allowing utilization of bio-derived ethanol without effecting any distillation process.

So the purpose of next experimental work has been to investigate the BESR in both a dense Pd–Ag MR and a conventional reactor working at the same operating conditions, particularly focusing on the effect of the reaction temperature and sweep-gas flow configurations on the reaction system.

For simplicity and as a first approach, a simulated bioethanol mixture (without presenting the other typical contaminants such as methanol, diethyl ether, acetone, etc.) was used.

INTERNATIONAL JOURNAL OF HYDROGEN ENERGY 35 (2010) 3159–3164

Available at www.sciencedirect.com

ScienceDirect

journal homepage: www.elsevier.com/locate/he

An experimental study on bio-ethanol steam reforming in a catalytic membrane reactor. Part II: Reaction pressure, sweep factor and WHSV effects

A. Iulianelli [a], S. Liguori [a], T. Longo [a], S. Tosti [b], P. Pinacci [c], A. Basile [a,*]

[a] CNR-ITM, c/o University of Calabria, Via Pietro Bucci, Cubo 17/C, 87030 Rende (CS), Italy
[b] ENEA, Dipartimento FPN, C.R. ENEA Frascati, Via E. Fermi 45, Frascati, Roma I-00044, Italy
[c] CESI RICERCA, Via Rubattino 54, 20134 Milano (MI), Italy

ARTICLE INFO

Article history:
Received 3 October 2009
Accepted 7 November 2009
Available online 24 November 2009

Keywords:
Bio-ethanol mixture
Ethanol steam reforming
CO-free hydrogen production
Pd–Ag membrane reactor

ABSTRACT

A catalytic Pd–Ag membrane reactor has been packed with a Co–Al_2O_3 catalyst to perform the ethanol steam reforming reaction using a simulated bio-ethanol mixture (H_2O/C_2H_5OH feed molar ratio = 18.7/1). In Part I of this work, low hydrogen recovery (≤30%) and CO-free hydrogen yield (≤20%) were obtained. In this second study the influence of higher pressure and sweep-gas flow rate was studied in order to improve the membrane reactor performances in terms of higher ethanol conversion, CO-free hydrogen yield and hydrogen recovery.

The counter-current sweep-gas flow configuration was used for studying the effect of the reaction pressure and the sweep factor on the reaction system, while the co-current flow configuration was also considered for analysing the weight hourly space velocity effect. Moreover, a comparison with a traditional reactor working at the same MR operating conditions was also realized.

As best results, the membrane reactor showed 100% ethanol conversion, 95.0% CO-free hydrogen recovery and ~60.0% CO-free hydrogen yield, operating at 400 °C and 3.0 (abs) bar.

1. Introduction

In this experimental work, the second part of our recent study is illustrated. Previously (Part I of this work), pure (or at least CO-free) hydrogen production produced by steam reforming reaction of renewable sources through membrane reactors (MRs) for potential applications in PEM fuel cells was the topic of Part I.

$$C_2H_5OH + 3H_2O = 2CO_2 + 6H_2 \quad \Delta H^\circ_{298\ K} = 157.0\ kJ/mol \qquad (1)$$

In particular, a simulated bio-ethanol mixture (water/ethanol feed molar ratio = 18.7/1) as renewable source was used for carrying out the ethanol steam reforming (ESR) (1) reaction in a Pd–Ag tubular membrane reactor: the influence of parameters such as temperature and sweep-gas flow configuration on the MR performances in terms of ethanol conversion, CO-free hydrogen recovery (HR), hydrogen yield and gas selectivity was studied. Furthermore, in order to emphasize the advantages of using a Pd–Ag MR, a comparison with a traditional reactor (TR) working at the same MR operating conditions was realized [1]. In particular, as best

* *Corresponding author*. Tel.: +39 0984 492013; fax: +39 0984 402103.
E-mail address: a.basile@itm.cnr.it (A. Basile).
0360-3199/$ – see front matter © 2009 Professor T. Nejat Veziroglu. Published by Elsevier Ltd. All rights reserved.
doi:10.1016/j.ijhydene.2009.11.034

result in Part I, an ethanol conversion close to 95.0%, almost 20.0% of CO-free hydrogen yield and 30.0% of CO-free hydrogen recovery were obtained at 400 °C, 1.5 (abs) bar of reaction pressure, 1.0 (abs) bar of permeate pressure and a sweep factor (SF) of 5.5.

As mentioned in Part I, different authors studied the ESR performances in traditional reactors, in terms of ethanol conversion, hydrogen yield and hydrogen selectivity by using various catalysts [2–7]. In particular, it was pointed out that the Co–Al_2O_3 catalyst is the most selective towards ESR reaction due to the high catalytic activity [4]. Moreover, it is well known that Co-based catalysts are cheaper than other noble metal-based catalysts such as: Rh, Pt and Pd [4–7].

Only a few papers deal with the use of membrane reactors for carrying out the ESR reaction in order to produce hydrogen [8–12].

Concerning the bio-ethanol mixture used in the steam reforming reaction, to the best of our knowledge only a few studies have been realized on TRs [13–16] and only one on MRs [17].

It is to be pointed out that a bio-ethanol solution is a mixture containing an ethanol concentration of 8.0–12.0 wt.%, corresponding to a water/ethanol molar ratio of 29.0/1–18.7/1. Moreover, contaminants are present in the bio-ethanol mixture. In Part I, as well as in this work, as first approach the contaminants effect on the performances of both the reactors (MR and TR) was not considered, even though in the near future it will be carefully taken into account.

In this second part, special attention is paid to the effect of a higher reaction pressure and the sweep factor variation at the operating conditions giving the best results ($T = 400\,^{\circ}C$ and counter-current flow configuration) in Part I.

In fact, in the previous work no more than 30% CO-free hydrogen recovery was reached probably due to a relatively low operating reaction pressure (max: 1.5 bar) and sweep-gas flow rate (~143 ml/min). Therefore, in this second part a higher reaction pressure and SF were utilized in order to improve the MR hydrogen permeation driving force, allowing better performances in terms of CO-free hydrogen recovery and CO-free hydrogen yield to be achieved.

Moreover, at the operating conditions involving the best MR performances obtained in this work (reaction pressure of 3.0 (abs) bar and SF = 25.2), a study on the weight hourly space velocity (WHSV) influence on the reaction system is presented.

A comparison with a conventional reactor working at the same MR operating conditions is also proposed and discussed.

2. Experimental

2.1. Operating conditions

The description of the plant and both the reactors is reported elsewhere [1]. The reaction temperature is kept constant at 400 °C, while the reaction pressure ranges between 1.5 and 3.0 (abs) bar and the sweep factor (SF) (defined as the molar ratio between the sweep-gas (N_2) flow rate and the ethanol feed molar rate) between 2.5 and 25.2. Below, in the second sub-section of Results and discussion (''Sweep-factor and reaction pressure effects''), the ethanol molar flow rate fed to the reactor is kept constant at $2.53 \cdot 10^{-4}$ mol/min, with a water/ethanol feed molar ratio of 18.7/1. Moreover, 3 g of Co–Al_2O_3 catalyst was packed into both the reactors involving, consequently, a constant WHSV of 5.5 h^{-1}.

In the third sub-section of Results and discussion (''The WHSV effect''), the ethanol feed molar rate was varied between $2.53 \cdot 10^{-4}$ mol/min and $7.60 \cdot 10^{-4}$ mol/min, corresponding to WHSVs ranging within 0.2 h^{-1} and 0.7 h^{-1}.

However, $1.34 \cdot 10^{-3}$ mol/min of nitrogen (N_2) was fed into both the reactors as internal standard gas.

The ethanol conversion was calculated as follows:

$$C_2H_5OH\ \text{conversion},(\%) = \frac{CO_{OUT} + CO_{2,OUT} + CH_{4,OUT}}{C_2H_5OH_{in}} \times 100 \quad (2)$$

where the subscript ''OUT'' means the total outlet flow rate of each species, while ''IN'' is referred to the inlet flow rate of each species fed to the reactors.

The Richardson equation is reported below:

$$J_{H2} = \frac{Pe_0 \cdot \exp\left(-\frac{Ea}{RT}\right) \cdot \left(\sqrt{p_{H2,retentate}} - \sqrt{p_{H2,permeate}}\right)}{\delta} \quad (3)$$

(Pe_0 is the pre-exponential factor, Ea the apparent activation energy, R the universal gas constant, T the absolute temperature, δ the Pd–Ag membrane thickness (50 μm), $p_{H2\text{-}retentate}$ the hydrogen partial pressure in the retentate side and $p_{H2\text{-}permeate}$ the hydrogen partial pressure in the permeate side).

CO-free hydrogen yield is defined as the molar ratio between the hydrogen stream in the permeate side and the total hydrogen theoretically producible from the stoichiometry of reaction (1) (equal to 6 times the ethanol molar flow rate fed to the MR):

$$\text{CO-free}\ H_2\ \text{yield}(\%) = \frac{H_{2,permeate}}{6C_2H_5OH_{IN}} \times 100 \quad (4)$$

CO-free hydrogen recovery is defined as the molar ratio between the CO-free hydrogen permeated stream and the total hydrogen really produced:

$$\text{CO-free}\ H_2\ \text{recovery},(\%) = \frac{H_{2,permeate}}{H_{2,permeate} + H_{2,retentate}} \times 100 \quad (5)$$

2.2. Pd–Ag MR and TR description

The Pd–Ag MR consists of a tubular stainless steel module (length 280 mm, *i.d.* 20 mm) containing a tubular pin-hole free Pd–Ag membrane permeable only to hydrogen (thickness 50 μm, *o.d.* 10 mm, length 145 mm) and joined to two stainless steel tube ends useful for the membrane housing, whose one of them is closed (illustrations are present in [1]). The membrane is produced by cold rolling and diffusion welding technique and details on the synthesis procedure can be found in [18]. The Co–Al_2O_3 catalyst is given by Johnson Matthey in pellet form and is packed into lumen of the MR with glass spheres (2 mm diameter) placed at both the stainless steel tube ends of the membrane. Before reaction, the catalytic bed was pre-heated using nitrogen up to 400 °C under atmospheric pressure and, afterwards, reduced by

using hydrogen ($1.8 \cdot 10^{-3}$ mol/min) at the same temperature for 2 h. Hydrogen permeation tests were realized before and after each reaction cycle measurement (80 min) in order to check whether any changes happened on the hydrogen permeation behaviour of the Pd–Ag membrane during the reaction.

The experimental tests for the TR were performed using the MR with the inlet and outlet permeate sides completely closed.

3. Results and discussion section

3.1. Permeation tests

Permeation tests on the Pd–Ag membrane using such pure gases as H_2 and N_2 were realized in order to validate the permeation parameters reported in [1]. The hydrogen permeation parameters calculated in this work showed a maximum standard deviation of ±2.0% with respect to those of Part I.

3.2. Sweep-factor and reaction pressure effects

First of all, each experimental point reported in this work is an average value of 6 experimental points taken in 80 min and the maximum standard deviation was lower than 1.0%. Moreover, the C balance was closed with ± 1.0% as maximum error. As evidenced in Part I, in this case it was also confirmed that such by-products as ethane, ethylene and acetaldehyde were not detected by the GC.

Fig. 1 shows the MR ethanol conversion (2) versus the reaction pressure at different SFs. Moreover, for comparison, the conversion of a TR working at the same MR operating conditions is reported. As shown, the MR ethanol conversion decreases by increasing the reaction pressure, but it increases overcoming 2.0 bar at SFs higher than 15.2 and 2.5 bar at SF = 5.5, reaching almost 100% at 3.0 bar in all cases. Keeping in mind that the pressure increase produces two conflicting effects, the first one (negative) on the thermodynamic of the reaction (the complete ESR reaction (1) proceeds with an increase of the moles number) and the second one (positive) on the Pd–Ag membrane (a higher hydrogen permeating flux), the decreasing trend of the MR ethanol conversion occurs probably since the thermodynamic effect overcomes the membrane one.

Depending on the SF, at a pressure higher than 2.0–2.5 bar, the membrane effect overcomes the thermodynamic one, inducing an increase of ethanol conversion. In fact, a higher reaction pressure maximizes the hydrogen partial pressure square root difference between the retentate and the permeate sides, inducing an increase of the hydrogen permeation driving force. According to Richardson equation (3), this effect results in a higher hydrogen flux permeating through the membrane, which affects (owing to the Le Chatelier principle) the ESR reaction equilibrium, shifting the reaction (1) towards further products formation, overcoming the negative effect due to the thermodynamics.

Moreover, the higher the SF the lower the reaction pressure where the membrane effect overcomes the thermodynamic one. This occurs since a higher SF corresponds to a higher sweep-gas flow rate that reduces the hydrogen partial pressure in the permeate side, inducing a higher hydrogen permeation driving force and, then, the positive effects above mentioned. In potential industrial applications, steam instead of nitrogen could be adopted as a sweep-gas avoiding further hydrogen separations and without needing relatively high operating pressures.

For the TR, only the thermodynamic effect is present by increasing the pressure; therefore, TR ethanol conversion decreases from around 85.0% at 1.5 bar to 67.0% at 3.0 bar.

In Part I, around 18.0% CO-free hydrogen yield (4) was achieved at 400 °C, 1.5 bar of reaction pressure, SF = 5.5 and counter-current flow configuration.

As illustrated in Fig. 2, by increasing both the reaction pressure and the SF, the CO-free hydrogen yield is enhanced.

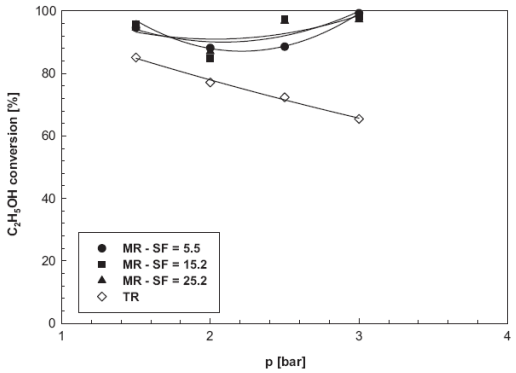

Fig. 1 – Ethanol conversion against reaction pressure at T = 400 °C, H_2O/C_2H_5OH = 18.7/1 (mol/mol) and WHSV = 0.2 h^{-1} for the MR (at different separation factor - SF) and TR; MR conditions: counter-current flow configuration, permeate pressure = 1.0 (abs) bar.

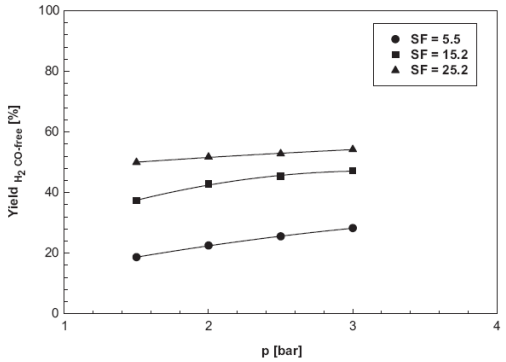

Fig. 2 – CO-free hydrogen yield against reaction pressure at different SF for the Pd–Ag MR in counter-current flow configuration, T = 400 °C, WHSV = 0.2 h^{-1}, permeate pressure = 1.0 (abs) bar and H_2O/C_2H_5OH = 18.7/1 (mol/mol).

This is due to the positive effect that both a higher pressure and a higher SF induce on the hydrogen permeation driving force. In detail, the CO-free hydrogen yield ranges from 18.0% to 54.0% by varying the reaction pressure and SF.

Also for the CO-free hydrogen recovery (5) higher reaction pressures and SFs act positively.

In fact, a higher reaction pressure maximizes the hydrogen partial pressure in the retentate side and a higher SF minimizes the hydrogen partial pressure in the permeate side, globally improving the hydrogen permeation driving force and inducing, for the Richardson equation, a higher hydrogen stream recovered in the permeate side. In the previous paper, at 400 °C, SF = 5.5, p = 1.5 bar and counter-current flow configuration, around 28.0% of HR was achieved. Fig. 3 shows that, by increasing the reaction pressure up to 3.0 bar, the HR reaches almost 50.0%, while, at 1.0 bar by increasing the SF up to 25.2, the HR achieves around 72.0%. As best result, n HR of around 90.0% was obtained at the maximum SF and pressure used in this work.

In conclusion, an increase of both the reaction pressure and the SF induces an improving of the MR performances in terms of higher ethanol conversions, CO-free hydrogen yields and HRs. Furthermore, as another positive result, the retentate stream coming out from the MR constitutes an enriched "high-pressure" CO_2 stream that could possibly be separated and sequestered.

3.3. *The WHSV effect*

The experimental tests proposed in this section were realized at the experimental conditions giving the best MR performances reported in Section 3.2 that are: 3.0 bar of reaction pressure, 1.0 bar of permeate pressure and SF = 25.2. Fig. 4 shows the ethanol conversion versus WHSV for both the MR and the TR. In particular, the co-current flow configuration of the MR was also analysed. In both co-current and counter-current flow configurations, the MR ethanol conversion is higher than the TR one due to the hydrogen removal through the Pd–Ag membrane. Moreover, this advantage is also present when the MR works at a higher WHSV than the TR. Therefore, it is possible to say that, for achieving the same TR ethanol conversion, the Pd–Ag MR needs a lower mass of catalyst, with a consequent advantage in terms of a lower unit operating volume and cost benefits.

However, in both the reactors the conversion decreases by increasing the WHSV. More in detail, the MR ethanol conversion ranges from 93.1 to 72% in co-current mode and from 97.0 to 87.3% in counter-current one, while the TR ethanol conversion varied from 63.0 to 58.0%. This occurs since the higher the WHSV the lower the residence time of the reactants in the catalyst bed.

Fig. 5 shows that, in both co-current and counter-current mode, respectively, the HR also decreases by increasing the WHSV. In fact, a lower WHSV results in a higher residence

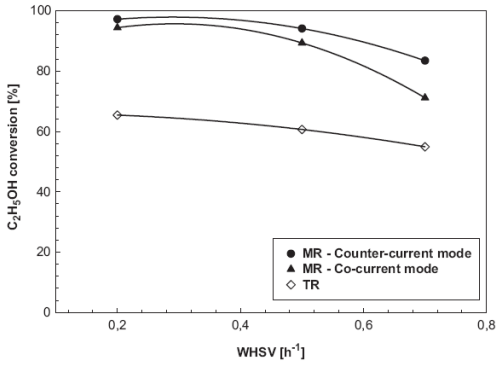

Fig. 4 – Ethanol conversion against WHSV for both the MR and TR at T = 400 °C and H_2O/C_2H_5OH = 18.7/1 (mol/mol); MR conditions: SF = 25.2, reaction pressure = 3.0 (abs) bar and permeate pressure = 1.0 (abs) bar.

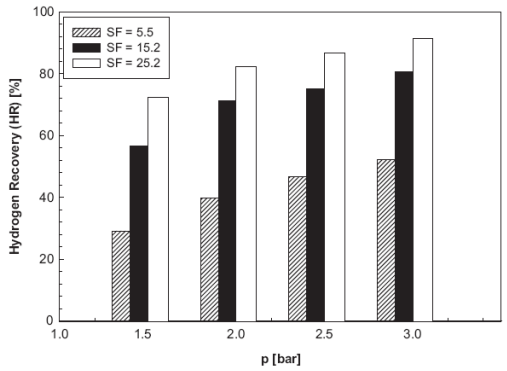

Fig. 3 – CO-free hydrogen recovery against reaction pressure at different SF for the Pd–Ag MR in counter-current flow configuration, T = 400 °C, WHSV = 0.2 h^{-1}, permeate pressure = 1.0 (abs) bar and H_2O/C_2H_5OH = 18.7/1 (mol/mol).

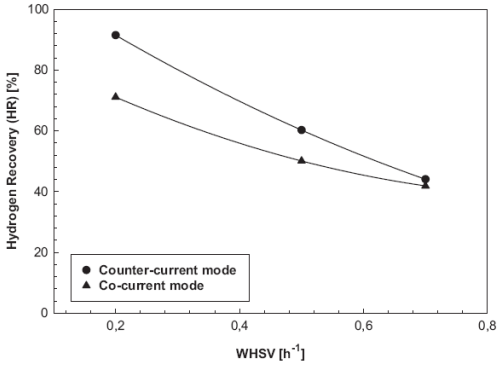

Fig. 5 – CO-free hydrogen recovery against WHSV for the Pd–Ag MR in both co-current and counter-current flow configurations, T = 400 °C, SF = 25.2, reaction pressure = 3.0 (abs) bar, permeate pressure = 1.0 (abs) bar and H_2O/C_2H_5OH = 18.7/1 (mol/mol).

time, which is advantageous for generating more hydrogen, resulting in a higher hydrogen retentate partial pressure and, then, in an enhancement of the hydrogen permeation driving force. Moreover, at lower WHSV, the counter-current flow configuration seems to be a better choice for recovering a CO-free hydrogen stream. In fact, as recently reported by Gallucci et al. [20] in a modelling study on ESR reaction carried out in a Pd–Ag MR, the performances of the MR depend on the hydrogen partial pressure distribution in the retentate and permeate sides along the reactor, concluding that counter-current flow configuration is more effective than co-current one.

During the experimental tests, by varying the WHSV in counter-current mode the HR ranged from 93.0 to 48.0%, while in co-current mode from 72.0 to 45.0%. Therefore, by increasing the WHSV, the advantage of the counter-current mode decreases, probably because at low residence times the HR is not influenced by the sweep-gas flow configuration. In order to study this aspect more deeply, in the near future a simulation study will be carried out.

In Fig. 6, the CO-free hydrogen yield versus WHSV is illustrated. At higher WHSVs, the decreasing trend of the yield at both the flow configurations is due to the hydrogen recovery decrease. In fact, a higher residence time (corresponding to a lower WHSV) involves a higher HR that results in a more effective shifting of the ESR reaction (1) towards the products. This gives a further ethanol consumption and a greater hydrogen production as well as a higher hydrogen stream permeated through the membrane. Therefore, the lower the WHSV the higher the HR and the CO-free hydrogen yield.

3.4. *Carbon deposition*

Also in this work, carbon deposition was not detected. In fact, as already reported in Part I [1], working at a very high H_2O/C_2H_5OH feed molar ratio (18.7/1) and at 400 °C, the ESR reaction is carried out in no carbon region and coke formation is thermodynamically not feasible [19].

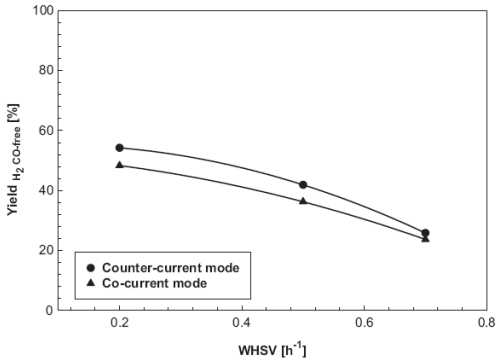

Fig. 6 – CO-free hydrogen yield against WHSV for the Pd–Ag MR in both co-current and counter-current flow configurations, T = 400 °C, SF = 25.2, reaction pressure = 3.0 (abs) bar, permeate pressure = 1.0 (abs) bar and H_2O/C_2H_5OH = 18.7/1 (mol/mol).

4. Conclusions

The experimental campaign of this second part of the work focused on using a simulated bio-ethanol mixture for carrying out ethanol steam reforming reaction in a Pd–Ag membrane reactor packed with a $Co–Al_2O_3$ catalyst. In particular, owing to both the low hydrogen recovery (≤30%) and CO-free hydrogen yield (≤20%) obtained at the operating conditions used in the experimental tests of Part I, in this second study the influence of higher pressure and sweep-gas flow rate was studied in order to improve the above cited parameters. As best result of Part II, the MR working at 400 °C, 3.0 (abs) bar of reaction pressure, SF = 25.2, WHSV = 0.2 h^{-1} and counter-current flow configuration was able to give: 100% ethanol conversion (~85.0% for the TR), around 95.0% hydrogen recovery and ~60.0% CO-free hydrogen yield. Moreover, by studying the WHSV effect on the MR performances, the counter-current mode proved to be a better solution in the experimental conditions used in this work for carrying out the ESR reaction in the MR.

Moreover, it was highlighted that in all the experimental tests of Part II, no carbon deposition was detected.

However, as general conclusion, this work was realized experimentally at lab scale and in the viewpoint of a potential real application, it should be considered that steam instead of nitrogen could be advantageously adopted as a sweep-gas avoiding further hydrogen separation of the permeate stream (steam could be separated by condensation), giving the possibility of avoiding high operating pressures.

In the near future, a real bio-ethanol mixture will be used in order to point out the influence of such contaminant on the performances of the Pd–Ag MR.

REFERENCES

[1] Iulianelli A, Basile A. An experimental study on bio-ethanol steam reforming in a catalytic membrane reactor. Part I: temperature and sweep-gas flow configuration effects, in press.
[2] Haryanto A, Fernando S, Murali N, Adhikari S. Current status of hydrogen production techniques by steam reforming of ethanol: a review. Energ Fuel 2005;19:2098–106.
[3] Breen JP, Burch R, Coleman HM. Metal-catalysed steam reforming of ethanol in the production of hydrogen for fuel cell applications. Appl Catal B Environ 2002;39:65–74.
[4] Haga F, Nakajima T, Yamashita K, Mishima S. Effect of cristallite size on the catalysis of alumina-supported cobalt catalyst for steam reforming of ethanol. React Kinet Catal Lett 1998;63:253–9.
[5] Llorca J, Homs N, Sales J, de la Piscina PR. Efficient production of hydrogen over supported cobalt catalysts from ethanol steam reforming. J Catal 2002;209:306–17.
[6] Kaddouri A, Mazzocchia C. A study of the influence of the synthesis conditions upon the catalytic properties of Co/SiO_2 or Co/Al_2O_3 catalysts used for ethanol steam reforming. Catal Comm 2004;5:339–45.

[7] Batista MS, Santos RKS, Assaf EM, Assaf JM, Ticianelli EA. Characterization of the activity and stability of supported cobalt catalysts for the steam reforming of ethanol. J Power Sourc 2003;124:99–103.
[8] Gallucci F, Basile A, Tosti S, Iulianelli A, Drioli E. Methanol and ethanol steam reforming in membrane reactors: an experimental study. Int J Hydrogen Energy 2007;32:1201–10.
[9] Keuler JN, Lorenzen L. Comparing and modeling the dehydrogenation of ethanol in a plug-flow reactor and a Pd-Ag membrane reactor. Ind Eng Chem Res 2002;41:1960–6.
[10] Basile A, Gallucci F, Iulianelli A, Tosti S. CO-free hydrogen production by ethanol steam reforming in a Pd-Ag membrane reactor. Fuel Cell 2008;1:62–8.
[11] Basile A, Gallucci F, Iulianelli A, De Falco M, Liguori S. Hydrogen production by ethanol steam reforming: experimental study of a Pd-Ag membrane reactor and traditional reactor behaviour. Int J Chem Reactor Eng 2008;6:A30.
[12] Lin WH, Chang HF. A study of ethanol dehydrogenation reaction in a palladium membrane reactor. Catal Today 2004; 97:181–8.
[13] Ni M, Leung DYC, Leung MKH. A review on reforming bio-ethanol for hydrogen production. Int J Hydrogen Energy 2007;32:3238–47.
[14] Dolgykh L, Stolyarchuk I, Denyega I, Strizhak P. The use of industrial dehydrogenation catalyst for hydrogen production from bioethanol. Int J Hydrogen Energy 2006;31:1607–10.
[15] Frusteri F, Freni S, Chiodo V, Donato S, Bonura G, Cavallaro S. Steam and auto-thermal reforming of bio-ethanol over MgO and CeO_2 Ni supported catalysts. Int J Hydrogen Energy 2006; 31(15):2193–9.
[16] Benito M, Sanz JL, Isabel R, Padilla R, Arjona R, Daza L. Bio-ethanol steam reforming: insights on the mechanism for hydrogen production. J Power Sourc 2005;151:11–7.
[17] E. Gernot, F. Aupretre, A Deschamps, F. Epron, P. Merecot, D. Duprez, et-al. Production of hydrogen from bioethanol in catalytic membrane reactor, 16th Confèrence Mondiale de l'Hydrogène Energie (WHEC16), 13–16 June 2006-Lyon (France). http://www.ceth.fr/download/presse/art_ceth_3.pdf.
[18] Tosti S, Bettinali L. Diffusion bonding of Pd-Ag membranes. J Mater Sci 2004;39:3041–6.
[19] Mas V, Kipreos R, Amadeo N, Laborde M. Thermodynamic analysis of ethanol/water system with the stoichiometric method. Int J Hydrogen Energy 2006;31:21–8.
[20] Gallucci F, De Falco M, Tosti S, Marrelli L, Basile A. Co-current and counter-current configurations for ethanol steam reforming in a dense Pd-Ag membrane reactor. Int J Hydrogen Energy 2008;33:6165–71.

Interconnection between Paper 3 & Paper 4

In this paper a simulated bio-ethanol mixture (water/ethanol feed molar ratio = 18.7/1 mol/mol) was used to carry out the BESR reaction in both conventional reactor and Pd-Ag based MR, packed with a Co/Al_2O_3 catalyst for producing a high purity hydrogen stream. The influence of reaction pressure and sweep-gas flow rate was varied in order to investigated the MR performances in terms of ethanol conversion, hydrogen yield and hydrogen recovery.

As best results, the MR showed 100% ethanol conversion, 95.0% CO-free hydrogen recovery and ~ 60.0% hydrogen yield, operating at 400 °C and 3.0 (abs) bar and high sweep gas flow rate.

As a consequence, in the next paper, a simulated bio-ethanol mixture containing also acetic acid and glycerol as by-products was utilized for investigating the effect of the by-products on the Pd/PSS MR performance packed with two different commercial reforming catalysts, i.e. $Ni\text{-}ZrO_2$ and $Co\text{-}Al_2O_3$

The following paper is *submitted to Catalysis Today*

Hydrogen Production from Bio-ethanol Steam Reforming Reaction in a Pd/PSS Membrane Reactor

Prem K. Seelam[1], Simona Liguori[2,3], Adolfo Iulianelli[2], Pietro Pinacci[4], Francesca Drago[4], Vincenza Calabrò[2], Mika Huuhtanen[1], Riitta Keiski[1], Vincenzo Piemonte[5], Silvano Tosti[6], Marcello De Falco[5], Angelo Basile[3*]

[1]*Department of Process and Environmental Engineering, Mass and Heat Transfer Process Laboratory, University of Oulu, P.O. Box 4300, FI-90014 Oulu, Finland*
[2]*Dept. of Modeling Engineering, University of Calabria, via P. Bucci Cubo 39/C, Rende (Cs) – 87036 – Italy*
[3]*Institute on Membrane Technology of Italian National Research Council (ITM-CNR), c/o University of Calabria, via P. Bucci Cubo 17/C, Rende (Cs) – 87036, Italy*
[4]*RSE S.p.A., Via Rubattino 54, Milano (Mi) – 20134, Italy*
[5]*University Campus Biomedico of Rome, via Alvaro del Portillo 21, Rome – 00148 – Italy*
[6] *ENEA, Unita` Tecnica Fusione, C.R. ENEA Frascati, Via E. Fermi 45, Frascati (RM) – 00044 – Italy*

Abstract

The aim of this work is to explore the potentiality of a porous stainless steel (PSS) supported Pd-based membrane reactor (MR) for hydrogen production via bio-ethanol steam reforming reaction (BESR). Bio-ethanol may be produced from fermentation of cheese by-product waste, which contains major impurities like acetic acid and glycerol. In this work, a simulated bio-ethanol mixture is utilized and contains besides ethanol and water also acetic acid and glycerol with 1:13:0.18:0.04 molar ratio, directly supplied to the MR. In the overall experimental campaign, BESR reaction is performed at 400 °C and in a reaction pressure range of 8 – 12 bar (abs.) using both Ni/ZrO_2 and Co/Al_2O_3 commercial catalysts, packed in the annulus of the MR. The present study illustrates the influence of the reaction pressure and gas-hourly-space-velocity on the MR performance in terms of bio-ethanol conversion, hydrogen recovery factor (HRF), hydrogen permeate purity (HPP) and yield of hydrogen. Furthermore, the effect of the by-products on the MR performance is investigated. The best Pd/PSS MR performance is obtained at 12 bar and 800 h^{-1}, using the Co-based catalyst. In these conditions, about 94% of bio-ethanol conversion, 40% of hydrogen yield and HRF ~40% with a HPP of 95% have been obtained.

Keywords: bio-ethanol steam reforming, Pd/PSS membrane reactor, hydrogen production

* Corresponding author: Angelo Basile; e-mail: *a.basile@itm.cnr.it*

1. Introduction

Most of the hydrogen produced today comes from catalytic steam reforming (SR) of natural gas [1]. Indeed, SR is a mature technology for hydrogen production, which is not only used in chemicals, fertilizers production and petroleum refineries but also, in high purity concentration, as a clean fuel to supply PEM fuel cells. However, owing to the environmental pollution caused by using derived of fossil fuels, the scientific community is involved on studying the use of alternative and renewable materials having minimal or no impact on the environment [2]. In particular, biomass-derived feedstocks, especially 2nd generation bio-fuels from agro, industrial and food wastes (potato, cheese waste by-product, etc.), may represent alternative raw materials for hydrogen production [3]. For example, bio-fuels like ethanol, glycerol and buthanol can be easily reformed to hydrogen and carbon dioxide [3,4].

However, reformed gases with high hydrogen concentration and a CO content lower than 10 ppm are needed for supplying PEM fuel cells used in both transport and stationary applications [5]. Therefore, BESR reaction (1) (main reaction) for hydrogen production is widely studied due to its availability, low feed toxicity and high H/C ratio [5].

$$C_2H_5OH + 3H_2O \longleftrightarrow 6H_2 + 2CO_2 \qquad \Delta H° = 157.0 \text{ kJ/mol} \qquad (1)$$

Using hydrogen from bio-ethanol is much more efficient than bio-ethanol used directly in internal combustion engine (ICE) and/or blended with gasoline. In fact, the fuel up-grade of ethanol requires various purification steps prior to be blended with gasoline or supplied to an ICE. In details, the expensive distillation as a crucial step of ethanol purification makes high capital and operating costs for water free ethanol production. On the contrary, the unpurified or crude ethanol from fermentation broth could be used directly in steam reforming reaction to produce hydrogen rich-stream, which can be more energy efficient and cost effective for commercial applications [5-7].

The crude or raw bio-ethanol contains various impurities, mainly higher alcohols, with minor acids, aldehydes, ethers, esters, etc. These impurities and ethanol concentration may vary based on the type of biomass raw materials exploited. The concentration of ethanol from fiber beer is around 5-6% with water and other residues [6-8] as well as the raw bio-ethanol obtained from sugar beet contains 87% impurities and also higher alcohols like methyl-3-butan-1-ol etc. [8-10]. In the present study, a simulated bio-ethanol mixture coming from waste by-product of cheese industry was considered, taking into account that the most common impurities from the fermentation broth of cheese by-products are acetic acid, glycerol and other minor impurities [6].

1.1. Catalytic membrane reactor

Applying process intensification strategy to hydrogen production via BESR reaction can be a huge advantage both from an environmental and economical point of view. In this contest, membrane reactor technology could represent the tool to achieve this intent. Indeed, the MR makes possible the integration of two unit operations, i.e. reaction and hydrogen separation process, in only one unit, representing an economical benefit with respect to the conventional systems as well as avoiding the utilization of further hydrogen separation devices [11]. In the meanwhile, MR could be used for CO_2 sequestration during BESR process [12]. However, the synergic effect of catalyst and membrane has been poorly investigated in SR of ethanol carried out in MRs. As well known in literature, both catalyst and membrane play an important role to achieve high MR performance in terms of ethanol conversion and hydrogen yield and their joint effect should be deeply studied in order to achieve maximum MR efficiency and performance.

The MR technology applied to SR of ethanol is reported in several scientific articles and literatures [13-19] and, in the majority of them, the benefits due to the MRs use for producing high purity hydrogen over the conventional systems is descript and emphasized.

As recently reported by Iulianelli and Basile [16], when a dense self-supported Pd-Ag membrane is used in a MR, exhibiting full hydrogen perm-selectivity with respect to the other gases, poor hydrogen permeability is observed, making the process less economical viable for industrial applications. In other aspects, composite porous supported membranes like ceramic or alumina based Pd-MRs provide not full hydrogen perm-selectivity, but higher hydrogen fluxes compared to dense. Furthermore, to limit the cost of Pd-based membranes, Pd thickness is reduced, proportionally increasing the hydrogen flux permeating through the membrane. Composite Pd-based membranes have been already explored in many applications and, as a particular case, also in SR reactions to produce hydrogen via ethanol steam reforming reaction, showing relatively high hydrogen perm-selectivity compared to other gases [17,19-22,28]. Composite Pd on porous stainless steel (Pd/PSS) MRs provide both factors, i.e. reasonable perm-selectivity with high hydrogen permeability and also economical benefits. Moreover, porous substrate provides good mechanical stability, resistance to cracking and simplicity in module construction [20]. Therefore, the aim of this work is to explore both the potentiality of a composite Pd supported porous stainless steel MR in BESR and the effects of crude bio-ethanol impurities like acetic acid and glycerol on MR performances in terms of bio-ethanol conversion, hydrogen recovery factor (HRF), hydrogen permeate purity (HPP), hydrogen yield and selectivity of product gases. Moreover, comparison of two commercial catalysts and their behavior in MR is also reported.

2. Methods and materials

2.1. Experimental set-up

The MR experimental set-up is shown in Figure 1. It consists of mass flow controllers (Brooks Instruments 5850S), temperature controllers and a membrane reactor module housing a composite porous stainless steel supported Pd membrane. The catalyst is packed inside the MR annulus. The

reaction pressure is controlled by means of a back pressure controller at the retentate side. Two different mixtures (ranging from 0.05 to 0.2 mL/min as a mass flow rate) are supplied by using a HPLC pump (furnished by Dionex) to a pre-heating zone and, then, to the MR. The first one is a simulated bio-ethanol mixture containing some typical by-products as impurities, Table 1, while the second one is the first mixture without the impurities, useful for analyzing the effects of the presence of the by-products. Both mixtures are pre-heated before entering in the MR, where the reaction temperature is kept constant at 400 °C. No sweep gas is used in the MR permeate side, which is maintained constant at 1.0 bar (absolute) in the whole experimental campaign.

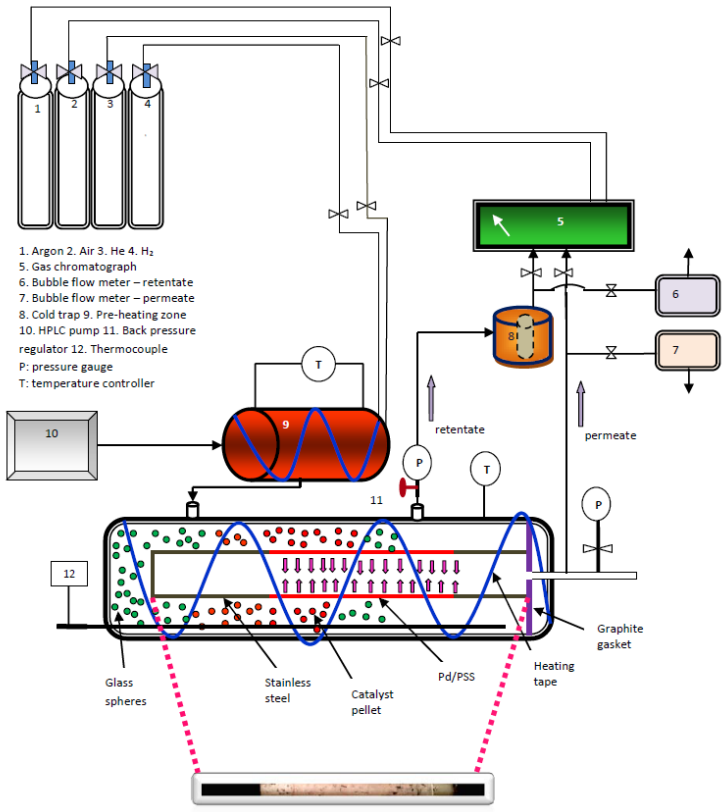

Figure 1. Membrane reactor experimental set-up.

The products from retentate side are passed over a cold trap in order to condense the unreacted (condensable) products. Both permeate and retentate dry stream compositions are analyzed by a temperature programmed HP 6890 gas chromatograph (GC) with two thermal conductivity

detectors at 250 °C and Argon used as a carrier gas. GC is equipped with three packed columns: Porapack R 50/80 (8 ft × 1/8 inch) and Carboxen™ 1000 (15 ft × 1/8 inch) connected in series, and a Molecular Sieve 5 Å (6 ft × 1/8 inch).

Components of Bio-ethanol mixture	**Composition vol %**
H_2O	76
C_2H_5OH	19
$C_3H_8O_3$	4
C_2H_3OOH	1

Table 1. Composition of the simulated mixture in steam reforming of bio-ethanol.

2.2. Composite Pd/ PSS membrane reactor

The MR consists of a tubular stainless steel module with length 280 mm, internal diameter of 20 mm, housing a PSS supported Pd tubular membrane having 20 µm thickness of Pd layer, 7 cm of active layer length on the porous support and an outer diameter around 1 cm, Figure 1. The Pd-based membrane was produced at RSE laboratories by electroless plating using a stainless steel tubular macroporous support as reported in [22]. The porous support was welded to two non-porous AISI 316L tubes, one of them closed in order to provide proper housing inside the reactor.

2.3. Reaction test procedure

In this study, two commercial non-noble catalysts Ni/ZrO_2 (CATACOL) and Co/Al_2O_3 (Johnson Matthey) were used, respectively, in BESR. In both cases, 3.0 g of catalyst in pellet shape were packed with glass spheres (2 mm diameter) in the MR annulus. The tubular reactor module with catalyst bed was heated up to 400 °C under N_2 flow with slow heating rate. Before reaction test, the catalyst was subjected to reduction for 2 h under H_2 flow at 400 °C (under atmospheric pressure). After reduction step, reaction tests were conducted in the MR shell side and each experimental

result represents an average value taken, at least, within three experimental reaction cycles realized during 90-120 min of testing at steady state conditions. The thermocouple was inserted in the shell side, separated from the reaction side. The experimental tests were performed in a MR configuration, where one side is closed and the reformed gases in permeate and retentate sides were analyzed by GC. Membrane reactor performance was evaluated in terms of the following equations (2), (3), (4) and (5):

$$\text{Conversion (into gas)} = \frac{CO_{2_{p,r}} + CH_{4_{p,r}} + CO_{p,r}}{2EtOH_{in} + 3GlyOH_{in} + 2AcAc_{in}} \quad (2)$$

where $CO_{p,r}$, $CO_{2\text{-}p,r}$, $CH_{4\text{-}p,r}$ represent the sum of the molar flow rates in both permeate and retentate sides of carbon monoxide, carbon dioxide and methane produced during the reaction, respectively; $EtOH_{in}$, $GlyOH_{in}$ and $AcAc_{in}$ represent the inlet molar flow rate of ethanol, glycerol and acetic acid (the two last ones, if any).

$$\text{Hydrogen recovery factor (HRF)} = \frac{H_{2_p}}{H_{2-TOT}} \cdot 100 \quad (3)$$

where H_{2p} is the hydrogen molar flow rate collected in the permeate side and $H_{2\text{-}TOT}$ is the total hydrogen molar flow rate produced during the reaction.

$$\text{Hydrogen permeate purity (HPP)} = \frac{H_{2_p}}{H_{2_p} + CO_p + CO_{2_p} + CH_{4_p}} \cdot 100 \quad (4)$$

where H_{2p}, CO_p, CO_{2p}, CH_{4p} are, respectively, the hydrogen, carbon monoxide, carbon dioxide and methane molar flow rates collected in the permeate side.

$$\text{Hydrogen yield } (Y_{H2}) = \frac{H_{2\text{-produced}}}{6EtOH_{in} + 7GlyOH + 4AcAc_{in}} 100 \quad (5)$$

where $H_{2,produced}$ represents the total hydrogen molar flow rate produced during BESR. In this equation, $6EtOH_{in}$, $7GlyOH_{in}$ and $4AcAc_{in}$ corresponds to the maximum H_2 theoretically producible when the simulated bio-ethanol mixture EtOH:H_2O:GlyOH:AcAc = 1:13:0.18:0.04 molar ratio (denoted as EWAG mixture) is supplied to the MR. In case of the ethanol/water mixture with EtOH:H_2O = 1:13 (denoted as EW), the contribute related to GlyOH and AcAc is not considered.

$$\text{Selectivity}_i\ (S_i) = \frac{Q_{i-TOT}}{Q_{H2-TOT} + Q_{CO2-TOT} + Q_{CO-TOT} + Q_{CH4-TOT}} 100 \qquad (6)$$

Selectivity of the gases coming out from the MR, where i = H_2, CO, CO_2, CH_4 and $Q_{i\text{-}TOT}$ represents the total molar flow rate of the i-compound; $Q_{H2\text{-}TOT}$, $Q_{CO\text{-}TOT}$, $Q_{CH4\text{-}TOT}$, $Q_{CO2\text{-}TOT}$ represent the total molar flow rate of hydrogen, carbon monoxide, methane and carbon dioxide, respectively, coming out from the MR.

3. Results and discussions

3.1. H_2 Permeation test

Permeation tests are an important step to verify the H_2 flux permeating through the membrane-and its selectivity towards the other gases of interest as well as to evaluate the membrane permeation characteristics after reaction tests. Firstly, permeation tests were performed flowing pure hydrogen through the Pd/PSS membrane at 400 °C with a transmembrane pressure difference depending on the variation of the retentate pressure in the range of 2 - 4 bar and keeping constant permeate pressure at 1.0 bar.

Generally, the hydrogen permeation through a Pd-based membrane is described by the following equation (7):

$$J_{H2} = Pe(p^n_{H_2,r} - p^n_{H_2,p}) \qquad (7)$$

where, J_{H2} is the hydrogen flux permeating through Pd/PSS membrane; Pe the H_2 permeance; and $p^n_{H2,}$ and $p^n_{H2,p}$ the hydrogen partial pressures in the retentate and permeate sides, respectively.

The dependence factor "n" for the hydrogen partial pressure ranges between 0.5 - 1.0 and is used as an indicator for the rate-controlling step of hydrogen permeation. As shown in Figure 2, in the present study, the factor n = 0.7 is evaluated to be the most accurate compared to the other ones owing to the highest linear regression correlation coefficient equal to $R^2 = 0.9997$.

Furthermore, after each reaction test, a hydrogen permeation test was performed to verify the eventual variation of the membrane permeation characteristics. In particular, Figure 3 shows the hydrogen flux before and after a reaction test as well as after a regeneration step performed as a pure hydrogen stream (around 18 mL/min) flowed in the reaction side for one h at 400 °C. In particular, Figure 3 shows that after 1 hour of regeneration procedure, the hydrogen permeation characteristics are not completely recovered. Then, each regeneration step was performed for, at least, 2 hours up to recover completely the hydrogen permeation behavior of the Pd composite membrane.

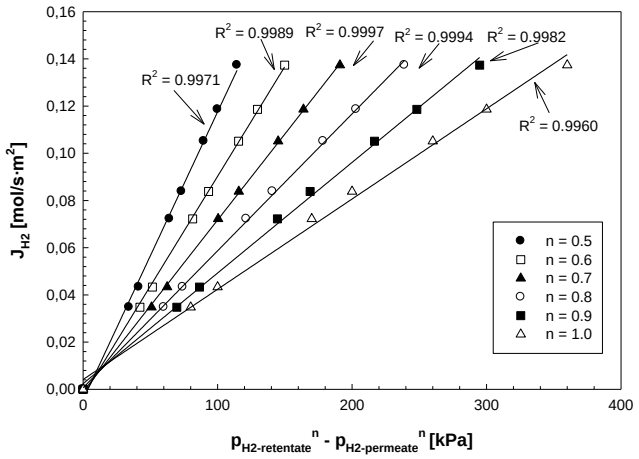

Figure 2. H_2 permeating flux through the Pd/PSS membrane at 400 ^oC vs. H_2 permeation driving force at different "n" factor.

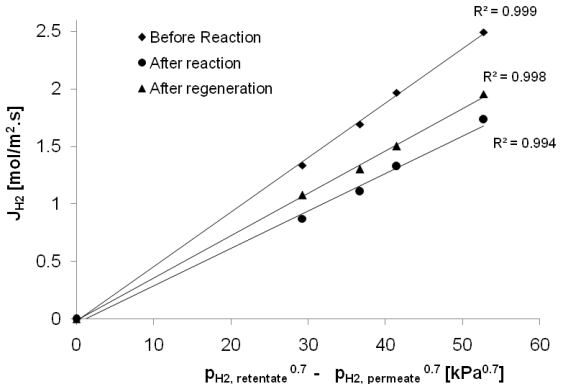

Figure 3. Hydrogen flux vs. driving force – hydrogen partial pressure difference at retentate and permeate to the power of 0.7.

3.2. Effect of reaction pressure

As above mentioned, the steam reforming of EW and EWAG were tested to study the effect of bio-ethanol impurities in BESR performed in a Pd/PSS MR. Firstly, the mixtures (0.2 mL/min feed flow rate) were tested over Ni/ZrO_2 catalyst at 400 °C, GHSV equal to 3200 h^{-1} (STP) and in a reaction pressure range of 8 - 12 bar. From Figure 4, both bio-ethanol conversion and HRF increase as the reaction pressure increases.

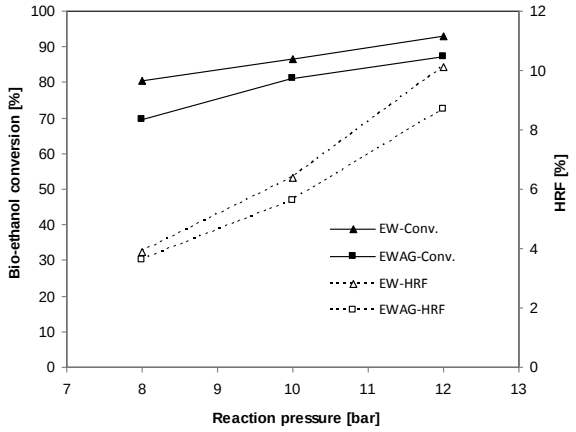

Figure 4. Bio-ethanol conversion and HRF against the reaction pressure in Pd/PSS MR over Ni/ZrO_2 catalyst at 400 °C, SR of EW and EWAG mixtures (bio-ethanol conversion as solid lines and HRF as dotted lines).

As a general consideration, a reaction pressure increase has two main effects on the MR system. Indeed, from a thermodynamic point of view at higher pressures bio-ethanol conversion is lowered since BESR proceeds towards the products with an increase of the moles number. The same scenario takes place also in the presence of impurities such as glycerol and acetic acid, because steam reforming of glycerol (8) and acetic acid (9) both proceed with an increase of moles number towards the products.

$$C_3H_8O_3 + 3H_2O = 3CO_2 + 7H_2 \qquad \Delta H° = 128.0 \text{ kJ/mol} \qquad (8)$$

$$CH_3COOH + 2H_2O = 2CO_2 + 4H_2 \qquad \Delta H° = 134.8 \text{ kJ/mol} \qquad (9)$$

Otherwise, the higher the reaction pressure the higher the hydrogen permeation driving force, which allows a higher hydrogen stream to be removed from the reaction side and collected in the permeate side, causing a shift effect of the BESR reaction (and, in case, also of both glycerol and acetic acid steam reforming) towards the products. As illustrated in Figure 4, it is evident that the benefit due to the pressure increase (the shift effect) is more pronounced and prevalent than the detrimental effect caused by the thermodynamic, globally determining an increasing trend of conversion with the pressure.

As previously mentioned, higher reaction pressures involve higher hydrogen permeation driving force, which determines higher hydrogen flux permeating through the membrane. Then, HRF increases with reaction pressure. However, HRF values are quite low owing to carbon deposition on the membrane surface, which affects negatively the hydrogen permeation through the Pd/PSS membrane. Indeed, as an indirect proof of coke presence on the membrane surface, during the regeneration step in which pure hydrogen is flowed in the MR, methane formation was detected as the reaction (10) reported below:

$$C + H_2 \rightarrow CH_4 \qquad \Delta H° = -75.0 \text{ kJ/mol} \qquad (10)$$

No oxygen was used to regenerate the catalyst and eliminate the coke deposits on the membrane surface because, firstly, higher temperature are required (~ 600 °C) and, secondly, to avoid the formation of palladium oxides, which could damage dramatically the Pd-layer and its performance. However, when nickel catalyst is used, carbon formation during reaction is high, causing catalyst deactivation and, also, inhibition of hydrogen permeation through membrane surface. Furthermore, by performing BESR with the EW mixture, higher HRF and conversion are obtained compared to the EWAG mixture, Figure 4. This is due to the fact that the presence of glycerol and acetic acid affect negatively the reaction system because more coke is produced, further depressing the MR performance. This is also confirmed by Le Valant et al. [8,9], who reported that, by adding acid or

alcohol impurities to a pure ethanol-water mixture, bio-ethanol conversion, hydrogen selectivity and catalyst stability are lowered [10].

3. *Comparison of two catalysts in MR: Ni/ZrO_2 vs. Co/Al_2O_3*

BESR using only the EWAG mixture with the composition of Table 1 was also performed in the Pd/PSS MR packed with Co-Al_2O_3 catalyst. Figure 5 shows that, as previously explained, also for Co-based catalyst both bio-ethanol conversion and HRF increase with reaction pressure. The conversion values achieved in the MR over Co-based catalyst range between 42% and 82%, respectively at 8.0 and 12.0 bar, while over Ni-based catalyst they vary from 70% at 8.0 bar to 87% at 12.0 bar.

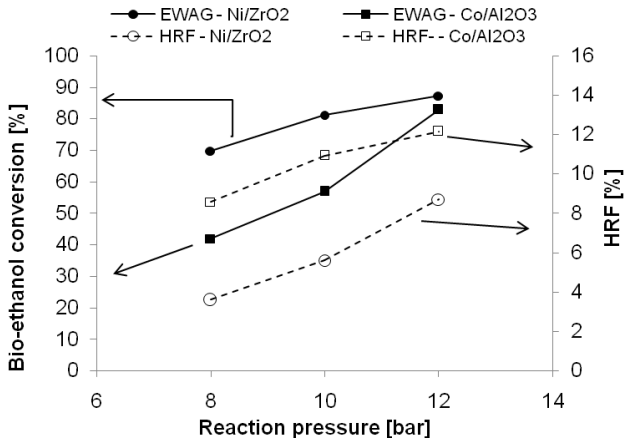

Figure 5. Bio-ethanol conversion and HRF against the reaction pressure in PSS/Pd MR over Ni and Co catalysts at 400 °C.

Therefore, it can be concluded that nickel is more active in bio-ethanol conversion compared to cobalt. Nevertheless, even though nickel better performs in terms of conversion than cobalt, when it is used during BESR reaction, lower HRFs are reached. This depends on the characteristics of the Co-based catalyst, which is more selective than Ni-based catalyst in the production of hydrogen, as reported in Table 2.

a. Ni/ZrO2

P (bar)	S_{H2}	S_{CO}	S_{CH4}	S_{CO2}
8	36.0	3.2	23.2	37.6
10	33.1	2.3	27.1	37.4
12	31.2	1.2	28.4	39.2

b. Co/Al_2O_3

P (bar)	S_{H2}	S_{CO}	S_{CH4}	S_{CO2}
8	53.7	3.5	8.0	34.8
10	49.6	2.7	11.1	36.6
12	48.5	3.1	11.9	36.5

Table 2. Selectivity of product gases at different reaction pressures during BESR reaction performed in a Pd/PSS MR at 400 °C over Ni/ZrO_2 and Co/Al_2O_3 catalysts.

Indeed, hydrogen selectivity (6) over cobalt ranges from ~54% at 8.0 bar to ~49% at 12.0 bar, while over nickel it ranges from ~36% at 8.0 bar to 31% at ~12.0 bar and methane production instead of hydrogen is favored. As a consequence, also the hydrogen yield results to be higher when using the Co-based catalyst than the Ni-based one, Figure 6.

During the regeneration step, carbon deposition was confirmed by GC analysis using both the catalysts. In the case of Ni, carbon deposition is more pronounced, probably because carbon coke is less reactive [26]. Moreover, ZrO_2 as a support is not particularly active in steam reforming reaction compared to alumina. As a consequence, the coke formation takes place with higher deposition rates, showing low reactive coke during regeneration compared to the other catalyst support materials like alumina [26].

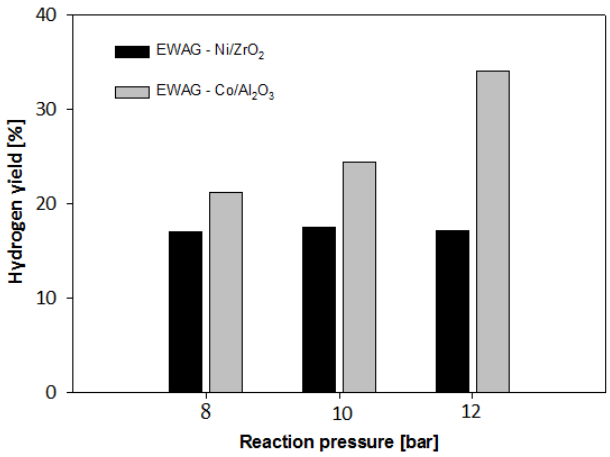

Figure 6. Hydrogen yield against reaction pressure at 400 °C over Ni/ZrO_2 and Co/Al_2O_3 catalysts in Pd/PSS MR.

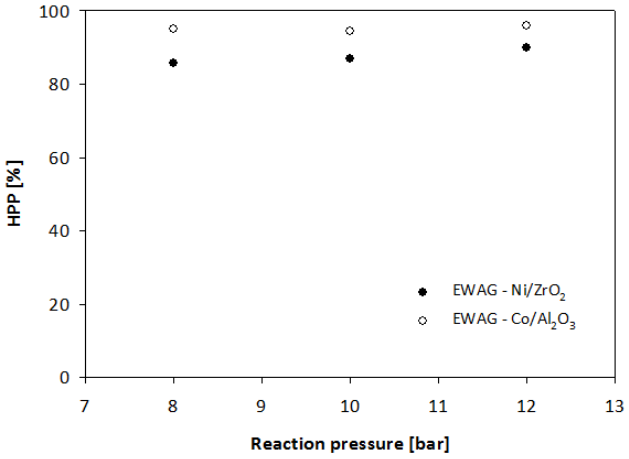

Figure 7. Hydrogen permeate purity against reaction pressure at 400 °C over $Ni\text{-}ZrO_2$ and $Co\text{-}Al_2O_3$ catalysts in Pd/PSS MR.

Concerning the hydrogen permeate purity, Figure 7 illustrates that HPP does not vary with pressure in both catalysts used. In detail, depending on the greater hydrogen production when Co-based catalyst is packed in the Pd/PSS MR, HPP is higher compared to the Ni-based one. Indeed, in the case of Co catalyst, both hydrogen yield, Figure 6, and hydrogen selectivity, Table 2, are higher, globally favoring a higher hydrogen content to be collected in the permeate side. Therefore, in this case, HPP is around 95%, while in the case of Ni catalyst it is around 85%, Figure 7.

Table 2 summarizes the product gases selectivity at different reaction pressures obtained during BESR in the Pd/PSS MR using the simulated EWAG mixture and over both Ni and Co-based catalysts, respectively. The hydrogen selectivity over cobalt is higher compared to nickel in the pressure range of 8.0-12.0 bar, pointing out that $Co\text{-}Al_2O_3$ catalyst is more appropriate to be used in BESR reaction. Furthermore, CO selectivity decreases by increasing the reaction pressure, confirming the membrane effect, which gives a positive influence on CO reduction by shifting the water gas shift reaction (11) to consume more CO.

$$CO+H_2O = H_2+CO_2 \qquad \Delta H° = -41.1 \text{ kJ/mol} \qquad (11)$$

This trend can be justified by considering the correspondent increasing trend of CO_2 selectivity with reaction pressure, Table 2. However, in the case of Ni-ZrO_2 catalyst, hydrogen is consumed in methanation reaction and, as a consequence, the hydrogen selectivity is lower. This is also confirmed by Seelam et al. [27], who demonstrated in a conventional system that Ni-based catalyst is more prone to methane formation by methanation reaction at low temperatures (i.e. < 400 °C).

3.3. Effect of GHSV over cobalt catalyst in MR

As a further investigation of this work, the influence of GHSV variation on BESR reaction (using only the simulated EWAG mixture) performed in the Pd/PSS MR packed with only Co-Al_2O_3 catalyst was studied. As expected, a rapid increase of bio-ethanol conversion and HRF with a decrease of the GHSV from 3200 to 800 h^{-1} was found at 12 bar, Figure 8. By decreasing the space velocity, a higher residence or contact time between the catalyst and reactants is favored. Thus, this is more effective for higher hydrogen production and, then, for higher hydrogen yield, Figure 8.

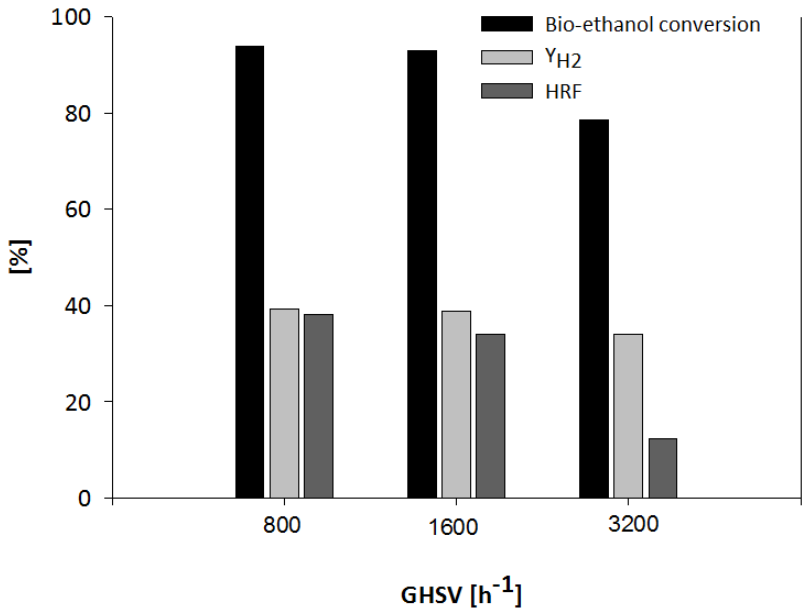

Figure 8. Bio-ethanol conversion, hydrogen yield (Y_{H2}) and HRF against reaction pressure at 400 ^{o}C over Co/Al_2O_3 catalysts for SR of EWAG mix in Pd/PSS MR.

At GHSV = 800 h^{-1}, the HRF is enhanced up to 40% with respect to 12% at GHSV = 3200 h^{-1}. In the meanwhile, also the bio-ethanol conversion increases from 83% (at 3200 h^{-1}) to 94% (at 800 h^{-1}). From Figure 8, it can be concluded that the hydrogen yield increases by decreasing the GHSV. In fact, lowering the GHSV is advantageous for generating more hydrogen in the reaction side, resulting in a higher retentate hydrogen partial pressure that enhances the hydrogen permeation driving force with a consequent more effective shifting of BESR reaction towards the products. Therefore, this gives more bio-ethanol consumption and a greater hydrogen production as well as a higher hydrogen stream permeating through the membrane. However, in all the experimental values reported in Figure 8, the HPP was almost constant around 95%.

4. Conclusions

Bio-ethanol steam reforming reaction was carried out in a Pd/PSS MR packed, respectively, with two different commercial reforming catalysts, i.e. Ni-ZrO_2 and Co-Al_2O_3. The reaction was performed at 400 °C from 8.0 to 12.0 bar as a reaction pressure keeping constant the permeate pressure at 1.0 bar. Two simulated bio-ethanol mixtures were when supplied to the MR, by comparing the effect of the presence of such impurities as glycerol and acetic acid over a simple ethanol/water mixture. The simulated bio-ethanol mixture containing impurities was related to a typical bio-ethanol mixture produced from fermentation of cheese. The effect of reaction pressure and GHSV on the MR performance was evaluated in terms of bio-ethanol conversion, HRF, HPP and hydrogen yield and product gases selectivity. The permeating flux of H_2 through the membrane was declining after each reaction test, thus resulting in decreasing in the overall efficiency of MR due to coke deposition on the membrane surface, causing a decrease of the MR performance, particularly the HRF. The impurities are, also, major precursors for the carbon coke formation, which was confirmed during the GC analysis of regeneration process performed by flowing pure hydrogen in the reaction side.

Concerning BESR performed in the Pd/PSS MR by supplying the EWAG mixture, the use of the Co-based catalyst at 12.0 bar of reaction pressure performs better in terms of HRF (nearly 40%), HPP (95%) and hydrogen yield of 40% than Ni-based one, probably because Ni is more prone to produce methane than hydrogen, globally lowering the hydrogen produced in the reaction side. On the contrary, using the latter, higher conversions than the Co-based one are achieved. However, with the aim of producing as much high purity hydrogen as possible, the best results of this work can be identified with the Pd/PSS MR packed with the Co-Al_2O_3 catalyst and working at 12.0 bar of reaction pressure, where 94% of bio-ethanol conversion, HRF around 40% with a HPP of 95% and a hydrogen yield of around 40% were reached. In the future, as a next step of investigation, a real bio-ethanol mixture (containing also other minor by-products) will be supplied to the Pd/PSS MR in a steam reforming process to compare the experimental performances achieved using the simulated EWAG mixture.

Acknowledgements

The financial support from the Graduate School of Energy Science and Technology (EST), Finlandis acknowledged.

The present study is also inserted in the research activities of COST Action 543.

This work has been realized under a contract ITM-RSE, 2010.

References

[1] J.D. Holladay, J. Hu, D.L. King, Y. Wang, An overview of hydrogen production technologies, Catal. Today, **139** (**2009**) 244-260.

[2] R. Kleijn, E. van der Voet, Resource constraints in a hydrogen economy based on renewable energy sources: An exploration, Renew. Sust. Energ. Rev., 14 (**2010**) 2784-2795.

[3] A. Tanksale, J. Norberto Beltramini, G. Max Lu, A review of catalytic hydrogen production processes from biomass, Renew. Sust. En. Rev., 14 (**2010**) 166-182.

[4] G. Marbán, T. Valdés-Solís, Towards the hydrogen economy?, Int. J. Hydrogen En., 32 (**2007**) 1625-1637.

[5] P.D. Vaidya, A.E. Rodrigues, Insight into steam reforming of ethanol to produce hydrogen for fuel cells , Chem. Eng. J., 117 (**2006**) 39-49.

[6] M. Ni, D.Y.C. Leung, M.K.H. Leung, A review on reforming bio-ethanol for hydrogen production, Int. J. Hydrogen En., 32 (**2007**) 3238-3247.

[7] J.R. Hansen, R. Johansson, M. Møller, C. Hviid Christensen, Steam reforming of technical bioethanol for hydrogen production, Int. J. Hydrogen En., 33 (**2008**) 4547-4554.

[8] A. Le Valant, A. Garron, N. Bion, F. Epron, D. Duprez, Hydrogen production from raw bioethanol over $Rh/MgAl_2O_4$ catalyst: impact of impurities: heavy alcohol, aldehyde, ester, acid and amine, Catal. Today, 138 (**2008**) 169-174.

[9] A. Le Valant, F. Can, N. Bion, D. Duprez, F. Epron, Hydrogen production from raw bioethanol steam reforming: Optimization of catalyst composition with improved stability against various impurities, Int. J. Hydrogen En., 35 (**2010**) 5015-5020.

[10] A. Le Valant, N. Bion, F. Can, D. Duprez, F. Epron, Preparation and characterization of bimetallic $Rh\text{-}Ni/Y_2O_3\text{-}Al_2O_3$ for hydrogen production by raw bioethanol steam reforming: influence of the addition of nickel on the catalyst performances and stability, Appl. Catal. B: Env., 97 (**2010**) 72-81.

[11] E. Drioli, A. Criscuoli, E. Curcio, Membrane contactors and catalytic membrane reactors in process intensification, Chem. Eng. Techn., 26 (**2003**) 957-981.

[12] D. Jansen, J.W. Dijkstra, R.W. van den Brink, T.A. Peters, M. Stange, R. Bredesen, A. Goldbach, H.Y. Xu, A. Gottschalk, A. Doukelis, Hydrogen membrane reactors for CO_2 capture, Energy Procedia, 1 (**2009**) 253-260.

[13] D.D. Papadias, S.H.D. Lee, M. Ferrandon, S. Ahmed, An analytical and experimental investigation of high-pressure catalytic steam reforming of ethanol in a hydrogen selective membrane reactor, Int. J. Hydrogen En., 35 (**2010**) 2004-2017.

[14] A. Iulianelli, A. Basile, An experimental study on bio-ethanol steam reforming in a catalytic membrane reactor. Part I: Temperature and sweep-gas flow configuration, Int. J. Hydrogen En., 35 (**2010**) 3170-3177.

[15] A. Iulianelli, S. Liguori, T. Longo, S. Tosti, P. Pinacci, A. Basile, An experimental study on bio-ethanol steam reforming in a catalytic membrane reactor. Part II: Reaction pressure, sweep factor and WHSV effects, Int. J. Hydrogen En., 35 (**2010**) 3159-3164.

[16] A. Iulianelli, A. Basile, Hydrogen production from ethanol via inorganic membrane reactors technology: a review, Catal. Sci. Technol., 1 (**2011**) 366-379.

[17] H. Lim, Y. Gu, S.T. Oyama, Reaction of primary and secondary products in a membrane reactor: Studies of ethanol steam reforming with a silica-alumina composite membrane, J. Membrane Sci., 351 (**2010**) 149-159.

[18] W.H. Lin, H-F. Chang, A study of ethanol dehydrogenation reaction in a palladium membrane reactor, Cat. Today, 97 (**2004**) 181-188.

[19] C.Y. Yu, D.W. Lee, S.J. Park, K.Y Lee, K.H. Lee, Study on catalytic membrane reactor for hydrogen production from ethanol steam reforming, Int. J. Hydrogen En., 34 (**2009**) 2947-2954.

[20] Y. Hua Ma, E.E. Engwall, I.P. Mardilovich, Composite palladium and palladium-alloy membranes for high temperature hydrogen separations, Fuel Chem. Div. Preprints, 48 (**2003**) 333-334.

[21] I.P. Mardilovich, Y. She, Y.H. Ma, M.H. Rei, Defect-free palladium membranes on porous stainless-steel support, AIChE J., 44 (**1998**) 310-322.

[22] A. Basile, P. Pinacci, A. Iulianelli, M. Broglia, F. Drago, S. Liguori, T. Longo, V. Calabrò, Ethanol steam reforming reaction in a porous stainless steel supported palladium membrane reactor, Int. J. Hydrogen Energy, 36 (**2011**) 2029-2037.

[23] S. Miachon, J.A. Dalmon, Catalysis in membrane reactors: what about the catalyst?, Top. Catal., 29 (**2004**) 59-65.

[24] A. Iulianelli, P.K. Seelam, S. Liguori, T. Longo, R. Keiski, V. Calabrò, A. Basile, Hydrogen production for PEM fuel cell by gas phase reforming of glycerol as byproduct of bio-diesel. The use of a Pd–Ag membrane reactor at middle reaction temperature, Int. J. Hydrogen En., 36 (**2011**) 3827-3834.

[25] J. Shu, B. P. A. Grandjean, A. Van Neste, S. Kaliaguine, Catalytic Palladium-based Membrane reactors: A Review, Can. J. Chem. Eng. 69 (**1991**) 1036-1060.

[26] P. Ferreira-Aparicio, M. Benito, K. Kouachi, S. Menad, Catalysis in membrane reformers: a high-performance catalytic system for hydrogen production from methane, J. Catal. 231 (**2005**) 331–343.

[27] P.K. Seelam, M. Huuhtanen, A. Sápi, K. Kordás, M. Szabó, E. Turpeinen, R. L. Keiski, CNT-based catalysts for H_2 production by ethanol reforming, Int. J. Hydrogen En., 35 (**2010**) 12588-12595.

[28] J.A. Calles, R. Sanz, D. Alique, Comparison of composite Pd-Ag and Pd-Cu membranes over PSS supports for hydrogen separation,18th WHEC 2010, Energy & Environment, 78-3 (**2010**) 459-466.

Interconnection between Paper 4 & Paper 5

Actually, steam reforming process is usually claimed as the most useful reaction to convert ethanol into hydrogen.

Nevertheless, in the open literature other processes as oxidative steam reforming and partial oxidation are taken into account. In particular, by supplying oxygen, ESR energy consumption due to the endothermic nature of reaction is counterbalanced by exothermic nature of the partial oxidation. Moreover, the addition of oxygen can prevent ethylene and ethane formation (due to the dehydration reaction of ethanol) and avoid carbon deposition.

For this reason in the next paper, the performances of Pd-Ag MR carrying out the ethanol oxidative steam reforming were analyzed changing the oxygen supplying and reaction pressure.

INTERNATIONAL JOURNAL OF HYDROGEN ENERGY 34 (2009) 8558–8565

Available at www.sciencedirect.com

ScienceDirect

journal homepage: www.elsevier.com/locate/he

Oxidative steam reforming of ethanol over Ru–Al_2O_3 catalyst in a dense Pd–Ag membrane reactor to produce hydrogen for PEM fuel cells

A. Iulianelli[a], T. Longo[a], S. Liguori[a], P.K. Seelam[b], R.L. Keiski[b], A. Basile[a,*]

[a]Institute on Membrane Technology of National Research Council (ITM-CNR), Via P. Bucci Cubo 17/C, c/o University of Calabria, Rende (CS) 87036, Italy

[b]Department of Process and Environmental Engineering Mass and Heat Transfer Process Laboratory, P.O. Box 4300, FI90014 University of Oulu, Finland

ARTICLE INFO

Article history:
Received 3 June 2009
Received in revised form
21 July 2009
Accepted 21 July 2009
Available online 28 August 2009

Keywords:
Oxidative ethanol steam reforming
Pd–Ag membrane reactor
Pure hydrogen production

ABSTRACT

This study focuses on the influence of oxygen addition on ethanol steam reforming (ESR) reaction performed in a dense Pd–Ag membrane reactor (MR) for producing hydrogen directly available for feeding a polymer electrolyte membrane fuel cell (PEMFC). In particular, oxygen addition can prevent ethylene and ethane formation caused by dehydration of ethanol as well as carbon deposition. The MR is operated at 400 °C, H_2O:C_2H_5OH = 11:1 as feed molar ratio and space velocity (GHSV) ~2000 h^{-1}. A commercial Ru-based catalyst was packed into the MR and a nitrogen stream of 8.4×10^{-2} mol/h as sweep gas was flowed into the permeate side of the reactor. Both oxidative ethanol steam reforming (OESR) and ESR performances of the Pd–Ag MR were analyzed in terms of ethanol conversion to gas, hydrogen yield, gas selectivity and CO-free hydrogen recovery by varying O_2:C_2H_5OH feed molar ratio and reaction pressure. Moreover, the experimental results of the OESR and ESR reactions carried out in the same Pd–Ag MR are compared in order to point out the benefits due to the oxygen addition. Experimentally, this work points out that, overcoming O_2:C_2H_5OH = 1.3:1, ethanol conversion is lowered with a consequent drops of both hydrogen yield and hydrogen recovery. Vice versa, a complete ethanol conversion is achieved at 2.5 bar and O_2:C_2H_5OH = 1.3:1, whereas the maximum CO-free hydrogen recovery (~30%) is obtained at O_2:C_2H_5OH = 0.6:1.

1. Introduction

In the last years, the growing attention on the fossil fuel crisis and environmental pollution imposed to consider new and clean processes and renewable materials for power generation. Polymer electrolyte membrane fuel cells are considered one of the most efficient and convenient technology. In fact, PEMFCs are zero emission power generation systems, available for both mobile and stationary applications. PEMFCs are fed by pure hydrogen and suffer CO concentrations >10 ppm, which can cause serious poisoning of the anode electrocatalysts [1]. Usually, hydrogen production from liquid and gaseous fuels can be realized by means of the following processes:

* *Corresponding author*. Tel.: +39 0984 492013; fax: +39 0984 402103.
E-mail address: a.basile@itm.cnr.it (A. Basile).
0360-3199/$ – see front matter © 2009 Published by Elsevier Ltd on behalf of Professor T. Nejat Veziroglu.
doi:10.1016/j.ijhydene.2009.07.063

- Steam reforming.
- Partial oxidation.
- Autothermal reforming.

Actually, steam reforming of natural gas is the most used technology for producing hydrogen from derived fossil fuels. It is an endothermic process, needing heat to be supplied, and more suitable for stationary applications owing to a slow start-up [2]. Recently, in the viewpoint of reducing the environmental pollution, much attention was paid for producing hydrogen from reforming reactions of not derived fossil fuels. In particular, among different renewable sources, bio-ethanol produced by fermentation of biomasses seems to represent an excellent candidate owing to its high hydrogen content and low toxicity.

In literature, different papers focus on hydrogen production via ESR and bio-ethanol steam reforming reactions in both conventional and membrane reactors [3–13]. In this field, one of the most important aspects of research in conventional reactors focuses on investigating the performances of different reforming catalysts at several operating conditions [3–7]. Vice versa, the growing interest towards MRs (in particular, dense Pd-based MRs) is aimed by the important issue of the Process Intensification Strategy. In fact, using dense Pd–Ag MRs, the main benefit consists of the possibility to carry out both reaction and separation processes (in this contest: pure (or CO-free) hydrogen production via steam reforming reaction of alcohols) in only one device, without requiring any further separation/purification unit [8–13].

Taking into account the endothermic nature of ESR reaction (1), a significant energy consumption is required for performing this process.

$$C_2H_5OH + 3H_2O \rightarrow 2CO_2 + 6H_2 \quad \Delta H^0_{298} = 173.1\ \text{kJ/mol} \tag{1}$$

By supplying oxygen, ESR energy consumption can be decreased due to the exothermic nature of the partial oxidation of ethanol (2):

$$C_2H_5OH + 1.5O_2 \rightarrow 2CO_2 + 3H_2 \quad \Delta H^0_{298} = -552.21\ \text{kJ/mol} \tag{2}$$

Globally, reactions (1) and (2) involve in the oxidative ethanol steam reforming (OESR) reaction (3).

$$C_2H_5OH + 2H_2O + 0.5O_2 \rightarrow 2CO_2 + 5H_2 \quad \Delta H^0_{298} = -84.8\ \text{kJ/mol} \tag{3}$$

Moreover, the addition of oxygen can prevent ethylene and ethane formation (due to the dehydration reaction of ethanol) and avoid carbon deposition. In fact, different authors studied the OESR reaction in conventional reactors, paying particular attention to the properties of different catalysts. In particular, de Lima et al. [14] investigated the reaction mechanism of steam reforming, partial oxidation and oxidative steam reforming of ethanol, studying the effect of oxygen addition on the catalyst stability, hydrogen selectivity and ethanol conversion. Liu et al. [15] proposed a thermodynamic analysis of OESR reaction using a Gibbs free energy minimization method, pointing out that hydrogen production is favoured at low O_2:C_2H_5OH and high H_2O:C_2H_5OH molar ratio, respectively, and that carbon monoxide selectivity increases with the temperature. However, the majority of the papers focusing on OESR reaction in conventional reactors is particularly devoted to study the influence of different catalysts on parameters such as production of undesirable by-products, hydrogen selectivity and ethanol conversion as well as the choice of the most adequate operating conditions [16–22].

To our knowledge, only in few cases OESR reaction was studied in MRs [23,24]. In these works, the reaction was performed using a MR allocating an inorganic composite membrane realized by electroless plating deposition of Pd–Ag thin layers on a porous stainless steel tube. The authors found that the Pd–Ag/PSS MR is able to better perform OESR reaction than a TR working at the same MR operating conditions as well as to give a hydrogen reach stream going out from the MR [23,24]. Moreover, it was highlighted that, at relatively high pressure, ethanol conversion is not favoured whereas, owing to the hydrogen permeation through the membrane, hydrogen flux proportionally increases with increasing pressure. In the meanwhile, CO_2 concentration increases at higher oxygen flow rate, while the CO remains almost constant.

The scope of this experimental work is to perform OESR reaction in a dense Pd–Ag MR in order to produce pure or, at least, CO-free hydrogen to be directly fed to a PEMFC (as well known, a CO content >10 ppm is able to poison the PEMFC electrocatalyst), working at relatively low reaction temperature (400 °C). The influence of oxygen supplying (estimated in terms of O_2:C_2H_5OH feed molar ratio) and reaction pressure on the MR performances was analyzed in terms of ethanol conversion to gas, hydrogen yield, CO-free hydrogen recovery and product selectivity. A comparison within the results of both ESR and OESR reactions, when carried out in the same Pd–Ag MR, is also given.

2. Experimental section

2.1. Experimental details

The experimental setup for OESR reaction consists of a tubular stainless steel module, length 280 mm, internal diameter 20 mm, allocating a pin-hole free dense Pd–Ag membrane having wall thickness of 50 μm, outer diameter 10 mm, length 150 mm. The membrane is produced by cold-rolling and diffusion welding technique [25] and it has an upper temperature limit around 450 °C. It is joined to two stainless steel tube ends for the membrane housing, whose one of them is closed.

Fig. 1 sketches the scheme of Pd–Ag MR, packed with 3.0 g of a 0.5% $Ru–Al_2O_3$ commercial catalyst (in pellet form) placed between glass spheres (<2 mm diameter) in the membrane core. The MR is operated at 400 °C during all the experimental tests. Before reaction, it is conducted for permeation tests using hydrogen and other pure gases in order to verify the complete permselectivity of hydrogen and also if any cracks or holes are present in the membrane.

In Fig. 2, the scheme of the experimental plant used for performing both ESR and OESR reactions is represented. In detail, the MR is heated by means of heating filaments connected to a temperature-controller. The operating temperature is measured by a three-point thermocouple inserted into the MR module. The reaction pressure is controlled by means

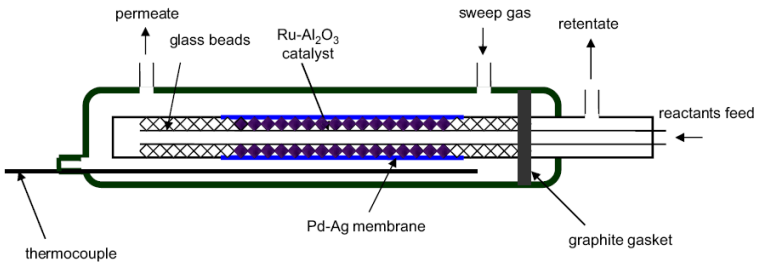

Fig. 1 – Pd–Ag membrane reactor packed with a commercial 0.5 wt% Ru–Al_2O_3 catalyst and operated in counter-current flow configuration.

of a regulating-valve system placed at the retentate stream, while the permeate pressure is kept constant at 1.0 bar.

By means of a mass-flow controller (Brooks Instruments 5850S), a nitrogen stream (8.4×10^{-2} mol/h) as sweep gas is fed into the permeate side in counter-current flow configuration with respect to the feed. Vice versa, oxygen is flowed with the reactants in the range of 2.45×10^{-4}–1.23×10^{-3} mol/min, correspondent to O_2:C_2H_5OH feed molar ratio ranging between 0.6:1 and 3.1:1.

By means of an HPLC pump (Dionex), the reactants (ethanol and water) are mixed (molar flow rate = 1.95×10^{-5} mol/s and H_2O:C_2H_5OH feed molar ratio = 11:1) and pumped into a pre-heating zone, where the water:ethanol mixture is vaporized before entering the MR reaction side. After reaction, the liquid fraction in the retentate side, obtained by passing the retentate stream in a cold trap immersed in an ice bath, is analyzed using a Perkin Elmer Gas Chromatograph. In the meanwhile, the retentate gaseous products are analyzed by an HP 6890 gas chromatograph (GC). The GC is equipped with two thermal conductivity detectors (TCD) at 250 °C and three packed columns: a Porapack R 50/80 (8ft × 1/8 in), Carboxen™ 1000 (15ft × 1/8 in), connected in series, and a Molecular sieve 5 Å (6ft × 1/8 in). Argon is used as carrier gas and a 10-way valve is used to optimize the analysis total time. Both permeate and retentate flow rates are measured by means of bubble flow meters. The GHSV was chosen equal to ~2000 h^{-1}.

Before reaction, the catalytic bed is pre-heated using nitrogen up to 400 °C under atmospheric pressure and, afterwards, reduced by using hydrogen (1.8×10^{-3} mol/min) at the same temperature for 2 h. After each experimental cycle (around ~240 min), the catalyst is regenerated for 2 h by using hydrogen (1.8×10^{-3} mol/min).

Concerning the description of the membrane reactor performances, some equations are defined as reported below.

Conversion of ethanol (to gas):

$$X_{\text{ethanol}}(\%) = \frac{CO_{\text{out}} + CH_{4,\text{out}} + CO_{2,\text{out}}}{2C_2H_5OH_{\text{in}}} \times 100 \quad (4)$$

where suffixes "in" and "out" denote the MR inlet and outlet molar flow rate of the products, respectively.

Selectivity of product gases:

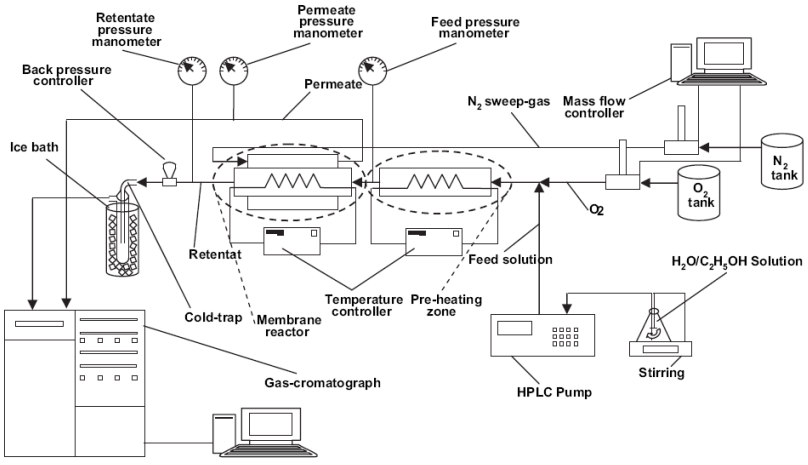

Fig. 2 – Scheme of the experimental plant.

INTERNATIONAL JOURNAL OF HYDROGEN ENERGY 34 (2009) 8558–8565

$$S_i(\%) = \frac{i_{out}}{H_{2,out} + CO_{out} + CH_{4,out} + CO_{2,out}} \times 100 \quad (5)$$

where $i = H_2$, CO, CH_4, and CO_2, respectively. Moreover, $H_{2,out}$ indicates the total hydrogen produced during reaction, calculated by adding the hydrogen flow rate of both retentate and permeate sides.

CO-free hydrogen recovery is defined as:

$$HR(\%) = \frac{H_{2,permeate}}{H_{2,out}} \times 100 \quad (6)$$

where $H_{2,permeate}$ represents hydrogen molar flow rate in the permeate side.

Yield of hydrogen for ESR reaction is represented as follows:

$$Y_{H_2} = \frac{H_{2,out}}{6C_2H_5OH_{in}} \times 100 \quad (7)$$

Yield of hydrogen for OESR reaction:

$$Y_{H_2} = \frac{H_{2,out}}{5C_2H_5OH_{in}} \times 100 \quad (8)$$

Eqs. (7) and (8) indicate the ratio between the hydrogen really produced and that theoretically producible from the stoichiometry of ESR (1) and OESR (3) reactions.

3. Results and discussion

3.1. Gas permeation tests on the dense Pd–Ag membrane

Permeation tests with pure gases such as H_2 and N_2 were performed on the dense Pd–Ag membrane, following the procedure described elsewhere [9]. However, the experimental results confirmed that the membrane is permeable only to hydrogen and, as summarized in Fig. 3, the linear trend of hydrogen permeating flux indicates that Sieverts' law (9) is followed:

$$J_{H_2} = \frac{Pe}{\delta} \cdot \left(p^{0.5}_{H_2\text{-retentate}} - p^{0.5}_{H_2\text{-permeate}} \right) \quad (9)$$

where J_{H_2} is the hydrogen flux permeating through Pd–Ag membrane, Pe the hydrogen permeability, δ the Pd–Ag membrane thickness, $p_{H_2\text{-retentate}}$ and $p_{H_2\text{-permeate}}$ the hydrogen partial pressure in the retentate and permeate sides, respectively.

The hydrogen flux permeating through Pd–Ag membrane was measured before and after each reaction test cycle (represented by 12 consecutive measurements whose each of them realized in 15 min) in order to check the presence of some changes on the Pd–Ag membrane permeation behaviours.

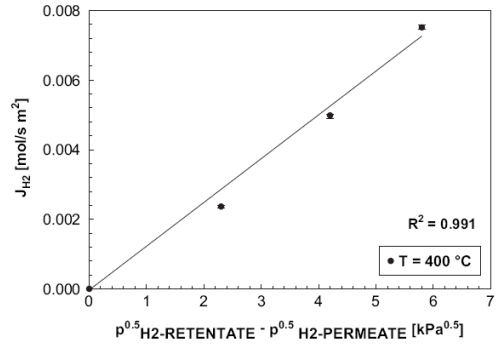

Fig. 3 – Sieverts' plot for the H_2 permeating flux through the Pd–Ag membrane at 400 °C.

3.2. OESR and ESR in the dense Pd–Ag membrane reactor

First of all, each experimental point obtained during the reaction tests represents an average value of at least five points, taken in 75 min at steady state conditions. Moreover, the carbon balance was closed in all the experimental tests with a ±2% of maximum error.

The ESR reaction is a complex reaction and by adding oxygen it becomes more complicated. In fact, at relatively low feed oxygen content, the ESR reaction could prevail, whereas a high oxygen addition could favour a scenario in which the partial oxidation of ethanol (2) is prevalent [23,24].

As shown in Fig. 4, without oxygen supply, ESR conversion is around 50.0% at 400 °C, ambient reaction pressure, GHSV = 2000 h^{-1} and H_2O:C_2H_5OH = 11:1. At the same operating conditions, more than 80.0% of ethanol conversion is reached when oxygen is fed with O_2:C_2H_5OH molar ratio = 1.3:1. Oxygen addition prevents by-products' formation such as ethylene and ethane (caused by ethanol dehydration reaction) as well as carbon deposition, reducing the risk of catalyst deactivation. Vice versa, a further increase of O_2:C_2H_5OH molar ratio involves in a decreasing trend of ethanol conversion, which reaches around 64.0% at O_2:C_2H_5OH = 3.1:1. In fact, once Ru–Al_2O_3 catalyst is exposed to a larger amount of oxygen at relatively low temperatures, it oxidizes to RuO_4 that, being volatile, induces an activity loss.

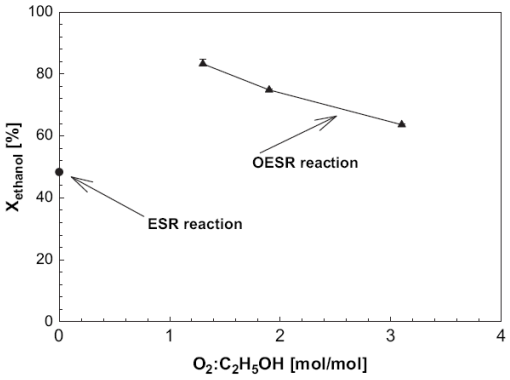

Fig. 4 – Ethanol conversion versus O_2:C_2H_5OH for both OESR and ESR reactions in a Pd–Ag MR at T = 400 °C, $p_{retentate} = p_{permeate}$ = 1.0 bar, GHSV = 2000 h^{-1}, $Q_{sweep\ gas} = 8.4 \times 10^{-2}$ mol/h, H_2O:C_2H_5OH = 11:1 and counter-current flow configuration of sweep gas.

This aspect can explain why ethanol conversion is lowered when a considerable amount of oxygen is used in the feed [26].

Fig. 5 depicts gas selectivities against O_2:C_2H_5OH molar ratio. As reported in literature [14,23,24], oxygen supply should favour CO_2 and acetaldehyde formation. In fact, the higher the amount of oxygen, the higher CO_2 selectivity. Vice versa, at higher O_2:C_2H_5OH ratio CO and CH_4 selectivities show a slightly decreasing trend and hydrogen selectivity drops from 52.2% at O_2:$C_2H_5OH = 1.3:1$ to 7.0% at O_2:$C_2H_5OH = 3.1:1$, because as even conformed by literature [27] it is oxidized to water. No acetaldehyde formation was detected owing to the high H_2O:C_2H_5OH feed molar ratio used in this work.

As summarized in Table 1, at the same OESR operating conditions hydrogen and CO selectivities during ESR reaction were 46.4% and ~ 9.0%, respectively. Thus, by supplying oxygen in the feed with O_2:$C_2H_5OH = 1.3:1$, hydrogen and CO_2 selectivities are slightly improved as well as CO selectivity is favourably lowered (~2.5%).

Fig. 6 points out that, at 400 °C, ambient reaction pressure, GHSV = 2000 h^{-1} and H_2O:$C_2H_5OH = 11:1$, hydrogen yield for OESR is around 37.0% at O_2:$C_2H_5OH = 1.3:1$ versus 14.0% for ESR. This is due to a higher ethanol conversion when oxygen is supplied in the feed, which involves in a higher hydrogen production and, then, in a higher hydrogen yield. Vice versa, at O_2:$C_2H_5OH > 1.3:1$ hydrogen selectivity drops and, as a consequence, hydrogen yield decreases dramatically up to ~2.0% at O_2:$C_2H_5OH = 3.1:1$.

CO-free hydrogen recovery for both OESR and ESR reactions is resumed in Table 2. In both cases, a great hydrogen stream is not collected in the permeate side owing to a low reaction pressure (1.0 bar) that involves a low hydrogen permeation driving force. However, hydrogen recovery for OESR is around 8.0% at O_2:$C_2H_5OH = 1.3:1$ versus 2.0% for ESR because of the higher hydrogen production in the reaction side during OESR (at O_2:$C_2H_5OH = 1.3:1$) with respect to ESR, which involves in a higher hydrogen partial pressure in the retentate side that favours a slight increase of hydrogen permeation driving force and, then, a higher HR.

Table 1 – Gas selectivity of the ESR reaction in the Pd–Ag MR. Operating conditions: T = 400 °C, H_2O:C_2H_5OH = 11:1, $p_{reaction} = p_{permeation}$ = 1.0 bar, GHSV = 2000 h^{-1}, counter-current flow configuration of sweep gas.

	ESR reaction
S_{H2} [%]	46.4
S_{CO} [%]	8.9
S_{CO2} [%]	37.7
S_{CH4} [%]	7.0

Therefore, taking into account the experimental results in terms of HR obtained at ambient reaction pressure and with the aim to produce as much as possible CO-free hydrogen, we paid attention to the influence of a higher reaction pressure on the performances of OESR reaction in the Pd–Ag MR. In particular, the reaction pressure influence for OESR reaction was only investigated at O_2:$C_2H_5OH = 0.6:1$ and 1.3:1 since higher ratios affect negatively the reaction, causing the oxidation of hydrogen to water and, then, lowering the MR performances in terms of HR, hydrogen yield and hydrogen selectivity.

Despite the ethanol conversion trend shown in Fig. 4 and as demonstrated by other authors [16,23,24] for O_2:$C_2H_5OH \leq 1:1$, ethanol conversion increases with increasing oxygen addition. Even in our case, ethanol conversion was always higher at O_2:$C_2H_5OH = 1.3:1$ than at O_2:$C_2H_5OH = 0.6:1$, Fig. 7. In detail, at O_2:$C_2H_5OH = 0.6:1$ the conversion increases with the reaction pressure, favouring the hydrogen permeation driving force with a consequent increase of CO-free hydrogen collected in the permeate side. In fact, the higher the hydrogen flux the higher the shift effect on the reaction system, which results in a higher ethanol conversion. Vice versa, at O_2:$C_2H_5OH = 1.3:1$, a minimum of ethanol conversion is

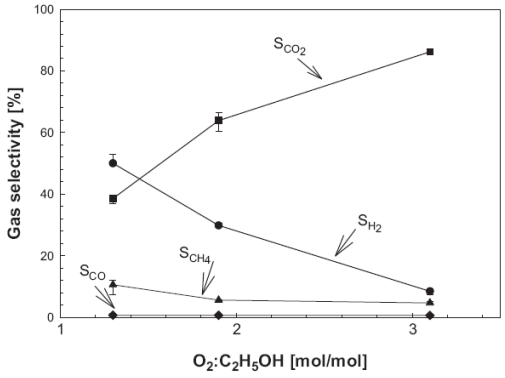

Fig. 5 – Gas selectivity versus O_2:C_2H_5OH molar ratio for both OESR and ESR in the Pd–Ag MR, at T = 400 °C, H_2O:C_2H_5OH = 11:1, $p_{reaction} = p_{permeation}$ = 1.0 bar, GHSV = 2000 h^{-1}, counter-current flow configuration of sweep gas.

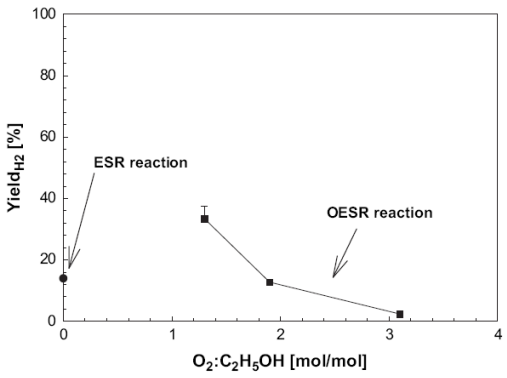

Fig. 6 – Hydrogen yield against O_2:C_2H_5OH for both ESR and OESR reactions in a Pd–Ag MR at T = 400 °C, H_2O:C_2H_5OH = 11:1, $p_{reaction} = p_{permeation}$ = 1.0 bar, GHSV = 2000 h^{-1}, $Q_{sweep\ gas} = 8.4 \times 10^{-2}$ mol/h and counter-current flow configuration of sweep gas.

INTERNATIONAL JOURNAL OF HYDROGEN ENERGY 34 (2009) 8558–8565

Table 2 – CO-free hydrogen recovery versus O_2:C_2H_5OH molar ratio for both OESR and ESR reactions in the Pd–Ag MR, at $T = 400$ °C, H_2O:$C_2H_5OH = 11:1$, $p_{reaction} = p_{permeation} = 1.0$ bar, GHSV = 2000 h^{-1}, counter-current flow configuration of sweep gas.

	OESR	ESR
O_2/C_2H_5OH	1.3	–
CO-free H_2 recovery [%]	7.6	2.2

Table 3 – Gas product selectivity against reaction pressure in the OESR reaction carried out in a Pd–Ag MR at different O_2:C_2H_5OH molar ratio, $T = 400$ °C, GHSV = 2000 h^{-1}, $p_{permeate} = 1.0$ (abs) bar, H_2O:$C_2H_5OH = 11:1$ and counter-current flow configuration of sweep gas.

p [bar]	O_2:$C_2H_5OH = 0.6:1$				O_2:$C_2H_5OH = 1.3:1$			
	S_{H2} [%]	S_{CO} [%]	S_{CO2} [%]	S_{CH4} [%]	S_{H2} [%]	S_{CO} [%]	S_{CO2} [%]	S_{CH4} [%]
1.0	52.6	14.7	27.7	4.9	50.1	0.7	38.6	10.6
2.0	47.1	16.7	30.7	5.5	38.5	12.2	44.7	4.3
2.5	44.6	15.3	35.0	5.1	36.2	12.4	45.6	5.8

reached at 2.0 bar. Taking into account that OESR reaction proceeds with an increase of the mole number, probably the thermodynamic effect due to a reaction pressure increase is prevalent on the shift effect, causing an ethanol conversion decrease. However, a further increase of reaction pressure probably determines a new scenario in which the shift effect overcomes the negative one caused by thermodynamics. In fact, at 2.5 bar ethanol conversion is improved, reaching 100%.

Table 3 reports the gaseous product selectivities at different reaction pressure and O_2:C_2H_5OH molar ratio. As shown, at O_2:$C_2H_5OH = 0.6:1$ hydrogen selectivity decreases at higher reaction pressures, ranging from around 53% at 1.0 bar to 45% at 2.5 bar. The same trend is observed at O_2:$C_2H_5OH = 1.3:1$, although in this case hydrogen selectivity is 50% at 1.0 bar and around 36% at 2.5 bar. Therefore, the higher the oxygen supply the higher hydrogen oxidized to water, lowering as a consequence the hydrogen content in the reaction side and, then, hydrogen selectivity. Moreover, at higher oxygen amount in the reaction side corresponds an increase of CO and CO_2 selectivities.

Fig. 8 sketches hydrogen yield versus reaction pressure at different O_2:C_2H_5OH feed molar ratio. Both the hydrogen yield trends reported in the graph are coherent with the trends of ethanol conversion. As a consequence, at O_2:$C_2H_5OH = 1.3:1$ hydrogen yield presents a minimum corresponding to a minimum value of ethanol conversion (Fig. 7). In particular, although at 2.5 bar ethanol conversion is complete, around 25% of hydrogen yield is reached versus 37% at 1.0 bar owing to a lower hydrogen selectivity at 2.5 bar than at 1.0 bar. In fact, by increasing O_2:C_2H_5OH molar ratio and reaction pressure, OESR reaction proceeds favourably towards CO and CO_2 than H_2 formation. Vice versa, at O_2:$C_2H_5OH = 0.6:1$ hydrogen yield follows a slightly increasing trend passing from 13.4% at 1.0 bar to 14.5% at 2.5 bar.

Fig. 9 depicts HR at different reaction pressure and O_2:C_2H_5OH feed molar ratio. At both O_2:C_2H_5OH ratio, HR improves by increasing reaction pressure. In fact, a higher pressure affects favourably hydrogen permeation driving force, inducing a higher hydrogen stream collected in the permeate side. In the whole reaction pressure range investigated in this work, both ethanol conversion and hydrogen yield at O_2:$C_2H_5OH = 1.3:1$ are higher than those at O_2:$C_2H_5OH = 0.6:1$, whereas HR resulted lower. This can be due to the influence of a higher oxygen content in the feed stream during OESR reaction, which allows that more hydrogen can be oxidized to water, lowering the hydrogen partial pressure in the reaction side and, then, the hydrogen permeation driving force. The higher the reaction pressure the higher this effect is considerable. Table 3 confirms what reported above, highlighting that hydrogen selectivity is lower at higher O_2:C_2H_5OH and reaction pressure. However, as maximum value a HR of

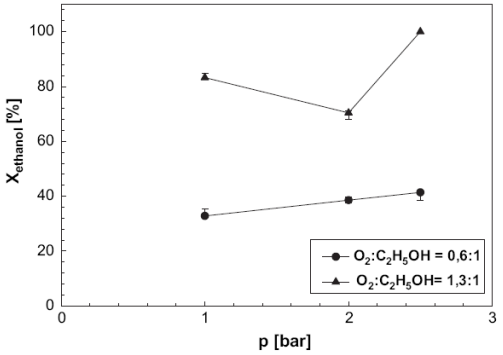

Fig. 7 – Ethanol conversion versus reaction pressure during OESR reaction in a Pd–Ag MR at O_2:$C_2H_5OH = 0.6:1$ and 1.3:1, $T = 400$ °C, $p_{permeate} = 1.0$ bar, GHSV = 2000 h^{-1}, $Q_{sweep\ gas} = 8.4 \times 10^{-2}$ mol/h, H_2O:$C_2H_5OH = 11:1$ and counter-current flow configuration of sweep gas.

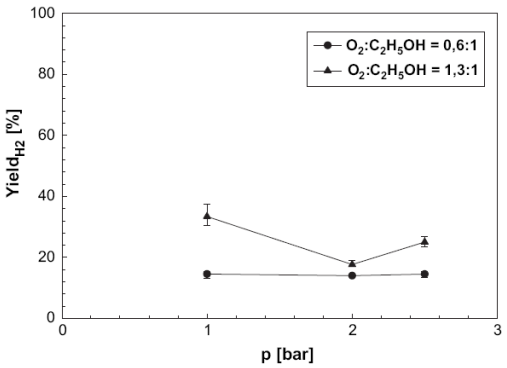

Fig. 8 – Hydrogen yield against reaction pressure at different O_2:C_2H_5OH feed molar ratio in OESR reaction carried out in a Pd–Ag MR at $T = 400$ °C, GHSV = 2000 h^{-1}, $p_{permeate} = 1.0$ (abs) bar, H_2O:$C_2H_5OH = 11:1$ (mol/mol).

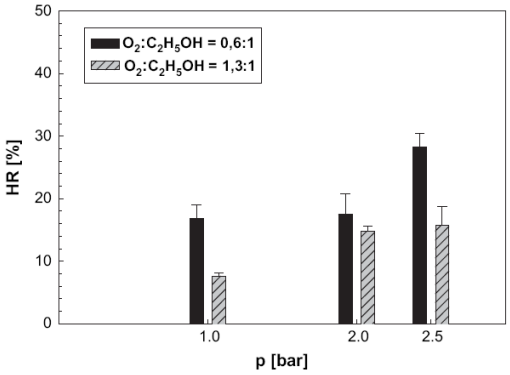

Fig. 9 – CO-free hydrogen recovery against reaction pressure at different O_2:C_2H_5OH molar ratio, $T = 400$ °C, GHSV = 2000 h^{-1}, permeate pressure = 1.0 (abs) bar, H_2O:C_2H_5OH = 11:1 (mol/mol) and counter-current flow configuration of sweep gas.

around 30% was reached at O_2:$C_2H_5OH = 0.6$:1 and 2.5 bar versus 16% at O_2:$C_2H_5OH = 1.3$:1 and same reaction pressure.

Concerning the important issue of carbon deposition, as confirmed by the closure of carbon balance, no coke formation was observed during the reaction tests. In fact, working at H_2O:C_2H_5OH = 11:1 and $T = 400$ °C, OESR reaction is in no carbon region [15].

4. Conclusions

The potential use of hydrogen as an energy carrier will be certainly exploited in future energy systems. Therefore, the scientific community, industrial companies and academic institutions are paying attention to develop attractive systems to produce hydrogen environmentally and economically, based on the idea of using renewable sources (for example bio-ethanol). Conventionally, hydrogen upgrading in refinery applications is realized by means of PSA systems, hydrogen selective membranes or cryogenic separation processes. In particular, dense Pd-based membranes are excellent candidates for hydrogen purification, particularly when incorporated into membrane reactors, able to combine the reaction and separation process in a single device. In this experimental work, hydrogen was produced by performing OESR reaction in a dense Pd–Ag MR operated at 400 °C in counter-current flow configuration of sweep gas in order to produce pure or, at least CO-free, hydrogen to be directly fed to a PEMFC. The influence of O_2:C_2H_5OH feed molar ratio and reaction pressure on the MR performances was analyzed in terms of ethanol conversion, hydrogen yield, CO-free hydrogen recovery and gas selectivity, highlighting the benefits and the drawbacks of supplying oxygen during ESR reaction. When oxygen supplying overcomes O_2:$C_2H_5OH = 1.3$:1, ethanol conversion is not favoured and both hydrogen yield and hydrogen recovery drop dramatically. As best result, an ethanol conversion of ~100% was achieved at 2.5 bar and O_2:$C_2H_5OH = 1.3$:1, although the maximum CO-free hydrogen stream collected in the permeate side was reached at O_2:$C_2H_5OH = 0.6$:1 (HR = ~30%) owing to a better hydrogen permeation driving force.

In a next future, the important aspect of pure or, at least, CO-free hydrogen production will be particularly stressed in order to improve the results obtained in this work, paying much attention on the effect of a higher reaction temperature as well as sweep gas stream on the MR performances.

REFERENCES

[1] Wee JH. Applications of proton exchange membrane fuel cell systems. Renewable Sustainable Energy Rev 2007;11:1720–38.
[2] Perna A. Hydrogen from ethanol: theoretical optimization of a PEMFC system integrated with a steam reforming processor. Int J Hydrogen Energy 2007;32:1811–9.
[3] Vaidya PD, Rodrigues AE. Insight into steam reforming of ethanol to produce hydrogen for fuel cells. Chem Eng J 2006; 117:39–49.
[4] Sun J, Qiu X, Wu F, Wang W, Hao S. Hydrogen from steam reforming of ethanol in low and middle temperature range for fuel cell application. Int J Hydrogen Energy 2004;29:1075–81.
[5] Haryanto A, Fernando S, Murali N, Adhikari S. Current status of hydrogen production techniques by steam reforming of ethanol: a review. Energy Fuels 2005;19:2098–106.
[6] Song H, Zhang L, Watson RB, Braden D, Ozkan US. Investigation of bio-ethanol steam reforming over cobalt-based catalysts. Catal Today 2007;129:346–54.
[7] Ni M, Leung DYC, Leung MKH. A review on reforming bio-ethanol for hydrogen production. Int J Hydrogen Energy 2007; 32:3238–47.
[8] Gallucci F, Basile A, Tosti S, Iulianelli A, Drioli E. Methanol and ethanol steam reforming in membrane reactors: an experimental study. Int J Hydrogen Energy 2007;32:1201–10.
[9] Basile A, Gallucci F, Iulianelli A, Tosti S. CO-free hydrogen production by ethanol steam reforming in a Pd–Ag membrane reactor. Fuel Cells 2008;1:62–8.
[10] Basile A, Gallucci F, Iulianelli A, De Falco M, Liguori S. Hydrogen production by ethanol steam reforming: experimental study of a Pd–Ag membrane reactor and traditional reactor behaviour. Int J Chem Reactor Eng 2008;6:A30.
[11] Lin WH, Chang HF. A study of ethanol dehydrogenation reaction in a palladium membrane reactor. Catal Today 2004; 97:181–8.
[12] Iulianelli A, Longo T, Basile A. An experimental study on bio-ethanol steam reforming in a catalytic membrane reactor. Part I: temperature and sweep-gas flow configuration effects. Fuel Cells, submitted for publication.
[13] Iulianelli A, Longo T, Basile A. An experimental study on bio-ethanol steam reforming in a catalytic membrane reactor. Part II: reaction pressure, sweep-factor and WHSV effects. Fuel Cells, submitted for publication.
[14] de Lima S, da Cruz IO, Jacobs G, Davis BH, Mattos LV, Noronha FB. Steam reforming, partial oxidation and oxidative steam reforming of ethanol over Pt/CeZrO2 catalyst. J Catal 2008;257:356–68.
[15] Liu S, Zhang K, Fang L, Li Y. Thermodynamic analysis of hydrogen production from oxidative steam reforming of ethanol. Energy Fuels 2008;22:1365–70.
[16] Velu S, Satoh N, Gopinath CS, Suzuki K. Oxidative reforming of bioethanol over CuNiZnAl mixed oxide catalysts for hydrogen production. Catal Lett 2002;82:145–52.
[17] Laosiripojana N, Assabumrungrat S, Charojrochkul S. Steam reforming of ethanol with co-fed oxygen and hydrogen over

Ni on high surface area ceria support. Appl Catal A Gen 2007; 327:180–8.
[18] Pereira EB, Homs N, Martì S, Fierro JLG, De la Piscina PR. Oxidative steam-reforming of ethanol over Co/SiO_2, $Co–Rh/SiO_2$ and $Co–Ru/SiO_2$ catalysts: catalytic behaviour and deactivation/regeneration processes. J Catal 2008;257:206–14.
[19] Kugai J, Velu S, Song C. Low-temperature reforming of ethanol over CeO_2-supported Ni–Rh bimetallic catalysts for hydrogen production. Catal Lett 2005;101:255–64.
[20] Frusteri F, Freni S, Chiodo V, Donato S, Bonura G, Cavallaro S. Steam and auto-thermal reforming of bioethanol over MgO and CeO_2 Ni supported catalysts. Int J Hydrogen Energy 2006; 31:2193–9.
[21] Fierro V, Klouz V, Akdim O, Mirodatos C. Oxidative reforming of biomass derived ethanol for hydrogen production in fuel cell applications. Catal Today 2002;75:141–4.
[22] Navarro RM, Alvarez-Galvan MC, Sanchez MCS, Rosa F, Fierro JLG. Production of hydrogen by oxidative reforming of ethanol over Pt catalyst supported on Al_2O_3 modified with Ce and La. Appl Catal B Environ 2005;55:229–41.
[23] Lin WH, Hsiao CS, Chang HF. Effect of oxygen addition on the hydrogen production from ethanol steam reforming in a Pd–Ag membrane reactor. J Membr Sci 2008;322:360–7.
[24] Lin WH, Liu YC, Chang HF. Hydrogen production from oxidative ethanol steam reforming in a palladium–silver alloy composite membrane reactor. J Chin Inst Chem Eng 2008;39:435–40.
[25] Tosti S, Bettinali L. Diffusion bonding of Pd–Ag membranes. J Mater Sci 2004;39:3041–6.
[26] Lanza R, Jära's SG, Canu P. Partial oxidation of methane over supported ruthenium catalysts. Appl Catal A Gen 2007;325: 57–67.
[27] Vesselli E, Comelli G, Rosei R, Freni S, Frusteri F, Cavallaro S. Ethanol auto-thermal reforming on rhodium catalysts and initial steps simulation on single crystals under UHV conditions. Appl Catal A Gen 2005;281:139–47.

Interconnection between Paper 5 & Paper 6

The influence of O_2:C_2H_5OH feed molar ratio and reaction pressure on the Pd-Ag MR performances was analyzed highlighting the benefits and the drawbacks of supplying oxygen during ESR reaction. When oxygen supplying overcomes O_2:C_2H_5OH = 1.3:1, ethanol conversion is not favoured and both hydrogen yield and hydrogen recovery drop dramatically.

As best result of this work, a complete ethanol conversion is achieved at 2.5 bar and O_2:C_2H_5OH = 1.3:1, whereas the maximum hydrogen recovery (~30%) is obtained at O_2:C_2H_5OH = 0.6:1.

So, in the next work the novelty is to perform the partial oxidation of ethanol (POE) in a Pd-Ag MR packed with Rh-based catalyst. To the best of my knowledge, this work can be considered as the first study. The POE was realized in the MR at 450 °C by varying the feed molar ratio (O_2:C_2H_5OH) between 0.33:1 and 0.62:1 and in a reaction pressure range from 1.0 to 3.0 bar, achieving as best result of this work 100% ethanol conversion and around 40% hydrogen recovery.

INTERNATIONAL JOURNAL OF HYDROGEN ENERGY 35 (2010) 12626–12634

Available at www.sciencedirect.com

ScienceDirect

journal homepage: www.elsevier.com/locate/he

Partial oxidation of ethanol in a membrane reactor for high purity hydrogen production

A. Iulianelli [a,*], S. Liguori [a,b], V. Calabrò [b], P. Pinacci [c], A. Basile [a]

[a] Institute on Membrane Technology of Italian National Research Council (ITM-CNR), Via P. Bucci Cubo 17/C, c/o University of Calabria, Rende (CS) 87036, Italy

[b] Modeling Engineering Department, Via P. Bucci Cubo 39/C, University of Calabria, Rende (CS) 87036, Italy

[c] Pietro Minacci, ERSE S.p.A., Via Rubattino 54, 20134 Milano, Italy

ARTICLE INFO

Article history:
Received 15 March 2010
Received in revised form
28 May 2010
Accepted 22 July 2010

Keywords:
Hydrogen production
Pd-based membrane reactor
PEM fuel cell
Partial oxidation of ethanol

ABSTRACT

Partial oxidation of ethanol was performed in a dense Pd–Ag membrane reactor over Rh/Al_2O_3 catalyst in order to produce a pure or, at least, CO_x-free hydrogen stream for supplying a PEM fuel cell. The membrane reactor performances have been evaluated in terms of ethanol conversion, hydrogen yield, CO_x-free hydrogen recovery and gas selectivity working at 450 °C, GHSV ~ 1300 h^{-1}, O_2:C_2H_5OH feed molar ratio varying between 0.33:1 and 0.62:1 and in a reaction pressure range from 1.0 to 3.0 bar. As a result, complete ethanol conversion was achieved in all the experimental tests. A small amount of C_2H_4 and C_2H_4O formation was observed during reaction. At low pressure and feed molar ratio, H_2 and CO are mainly produced, while at stronger operating conditions CH_4, CO_2 and H_2O are prevalent compounds. However, in all the experimental tests no carbon formation was detected. As best results of this work, complete ethanol conversion and more than 40.0% CO_x-free hydrogen recovery were achieved.

Furthermore, at 450 °C, ambient pressure and stoichiometric feed molar ratio, partial oxidation of ethanol was performed in the Pd–Ag membrane reactor as a case study without using any catalyst. In this case, Pd–Ag membrane acts as a catalyst on the reaction. As a result, an ethanol conversion around 85% was reached, while low CO_x-free hydrogen recovery and carbon formation was the main drawback.

1. Introduction

Growing attention on environmental problems such as the emissions of green-house gases is giving rise to consistent efforts for developing new and sustainable technologies. Proton exchange membrane (PEM) fuel cells are a promising candidate for clean power generation since they have zero pollutant emission. It is well known that PEMFCs are fuelled by high purity hydrogen because they suffer catalyst poisoning in the presence of a few ppm of CO (PEMFCs need CO concentration <10 ppm) [1]. The possibility of producing hydrogen from renewable feedstock is interesting and, among the latter, ethanol is the most suitable because of its low cost and toxicity and its easy storage and transportation [2]. Furthermore, ethanol is producible from biomass and, coupled to different reaction processes such as steam reforming, partial oxidation and autothermal reforming, it can be converted into hydrogen. In the specialized literature,

* Corresponding author. Tel.: +39 0984 492011; fax: +39 0984 402103.
E-mail address: a.iulianelli@itm.cnr.it (A. Iulianelli).

0360-3199/$ – see front matter © 2010 Professor T. Nejat Veziroglu. Published by Elsevier Ltd. All rights reserved.
doi:10.1016/j.ijhydene.2010.07.120

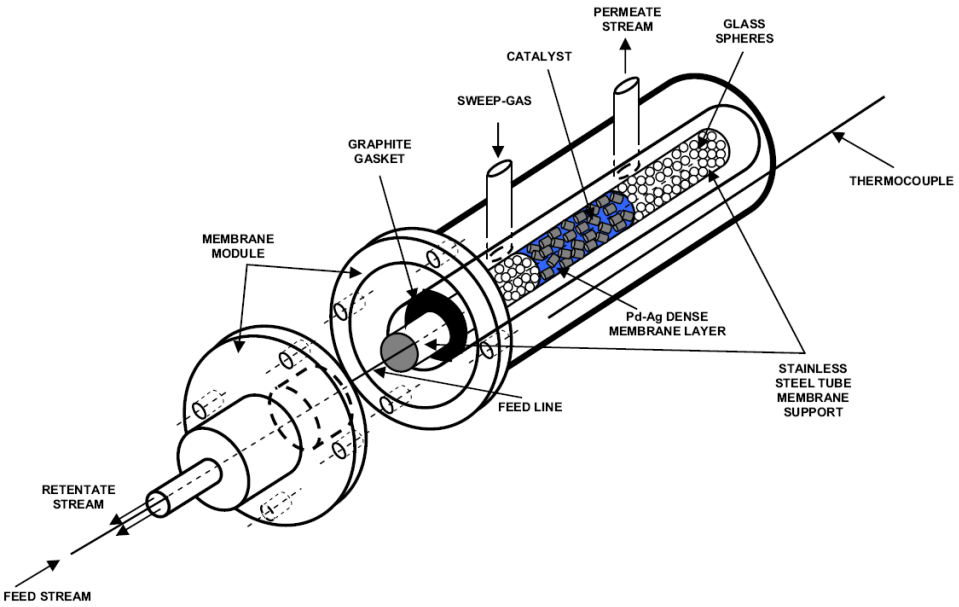

Fig. 1 – Scheme of the Pd–Ag membrane reactor.

different studies have been realized on steam and auto-thermal reforming of ethanol in both fixed bed (FBR) and membrane reactors (MRs) [3–13], but only few papers focus on the partial oxidation of ethanol (POE) in FBRs [1,2,14–18]. In particular, they point out that POE reaction can be proposed as an alternative approach to steam reforming of ethanol (ESR), usually claimed as the most useful reaction to convert ethanol into hydrogen. ESR reaction presents different drawbacks such as pronounced catalyst deactivation and an elevated thermal demand due to its high endothermic character [19]. On the contrary, POE shows a fast start-up without needing any indirect heat addition [18].

From the viewpoint of high purity hydrogen production for supplying PEM fuel cells, as proposed for example by Silva et al. [18], an integrated fuel processing system based on POE performed in an FBR is followed by a water gas shift (WGS) reactor and a pressure swing adsorption (PSA) system in order to produce and purify the hydrogen rich-stream going out from the conventional reformer.

Nevertheless, it should be taken into account that the growing interest in MRs (in particular, dense Pd-based MRs) is due mainly to their possibility of performing both the reaction and hydrogen separation/purification processes in only one device, without requiring any further separation/purification unit. Therefore, with respect to the aforementioned conventional system, a Pd–Ag MR can convert ethanol directly into pure hydrogen to be supplied directly to a PEMFC system via partial oxidation reaction, with the benefit of avoiding other hydrogen purification steps.

As stated above, the novelty of the present work is to perform the POE reaction in a dense, tubular, pin-hole free Pd–Ag membrane reactor over a Rh-based catalyst to produce pure or, at least, CO_x-free hydrogen for directly supplying a PEMFC. Furthermore, the Pd–Ag MR was operated as a catalytic membrane reactor (CMR) as a case study without packing the catalyst inside the MR and a comparison between the experimental results of the CMR and the MR was proposed and discussed.

2. Experimental section

2.1. *Experimental details*

The experimental setup for POE reaction consists of a tubular stainless steel module, length 280 mm, internal diameter 20 mm, allocating a dense pin-hole free self-supported Pd–Ag membrane having thickness of 50 μm, outer diameter 10 mm and length 150 mm, Fig. 1. The membrane is produced by cold-rolling and diffusion welding technique [20] and is joined to two stainless steel tube ends for the membrane housing, where one of them is closed. Fig. 1 shows the Pd–Ag membrane packed with 2.5 g of 5% Rh/Al_2O_3 commercial catalyst (in pellet form), given by Catal International Ltd, placed between glass spheres in the membrane core. When the POE is performed in the CMR, the Pd-based membrane acts as a catalyst on the reaction. Both the MR and CMR are operated at 450 °C and in the pressure range from 1.0 to 3.0 bar for the MR case and at 1.0 bar for the CMR case. The GHSV was kept constant at around 1300 h^{-1} (calculated as the ratio between the volume of the total feed stream at standard conditions and the catalyst volume).

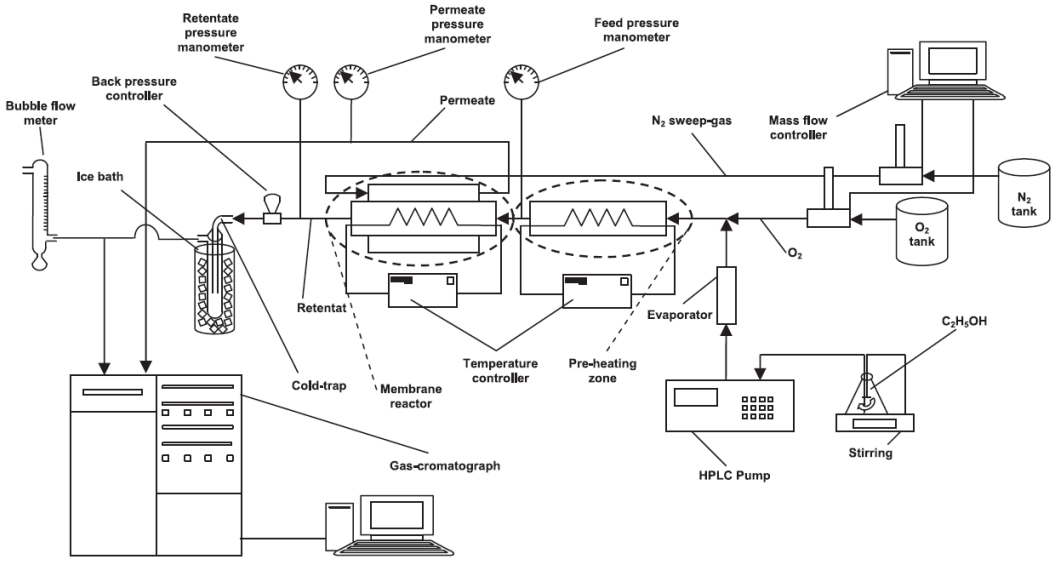

Fig. 2 – Scheme of the experimental plant.

Before reaction, permeation tests are conducted on the MR by supplying hydrogen and other pure gases in order to confirm the complete hydrogen perm-selectivity of the Pd–Ag membrane and to check whether any cracks or holes are present on its surface.

Fig. 2 sketches the scheme of the experimental setup used for performing the POE. The MR is heated through heating filaments connected to a temperature-controller. The operating temperature is measured by a three-points thermocouple inserted into the MR module (Fig. 1). The reaction pressure is varied by means of a regulating-valve system placed at the retentate stream, while the permeate pressure is kept constant at 1.0 bar.

Using a mass-flow controller (Brooks Instruments 5850S), a nitrogen stream is flowed as a sweep gas (8.97×10^{-2} mol/h) into the permeate side. Furthermore, oxygen is supplied with ethanol in the range of 6.29×10^{-4}– 9.61×10^{-4} mol/min, corresponding to a O_2:C_2H_5OH feed molar ratio ranging between 0.33:1 and 0.62:1. Liquid ethanol (molar feed flow rate = 1.89×10^{-3} mol/min) is pumped into a pre-heating zone by means of a HPLC pump (Dionex), where it is mixed to oxygen before entering in the MR reaction side.

After reaction, a liquid fraction is obtained from the retentate side by condensing the condensable fraction of the retentate stream through a cold trap immersed in an ice bath. Thus, the liquid fraction is analyzed using a Perkin Helmer Gas Chromatograph. Meanwhile, the gaseous products are analysed by an HP 6890 gas chromatograph (GC). The GC is equipped with two thermal conductivity detectors (TCD) at 250 °C and three packed columns: a Porapack R 50/80 (8ft × 1/8 in), Carboxen™ 1000 (15ft × 1/8 in), connected in series, and a Molecular sieve 5 Å (6ft × 1/8 in). Argon is used as carrier gas and a 10-way valve is used to optimize the analysis total time. The Internal Standard Method is used for evaluating the permeate molar flow rate, whereas the Absolute Calibration Curve Method is used for calculating the retentate products molar composition and the retentate molar flow rate is measured by means of a bubble flow meter.

Before reaction tests, the catalytic bed is pre-heated using nitrogen up to 450 °C under atmospheric pressure and, afterwards, reduced by using hydrogen (8.71×10^{-4} mol/min) at the same temperature for 2 h.

Each experimental point obtained in this work is an average value of 6 experimental reaction tests with a maximum error lower than 2%. Moreover, C balance between inlet and outlet carbon-based gaseous streams was closed with ±2.0% as

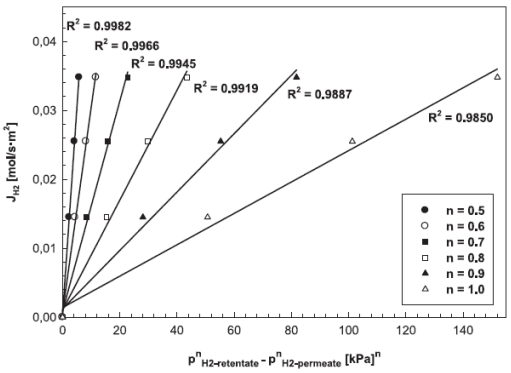

Fig. 3 – Hydrogen flux permeating through the membrane by varying "*n*" values, at 450 °C.

INTERNATIONAL JOURNAL OF HYDROGEN ENERGY 35 (2010) 12626–12634

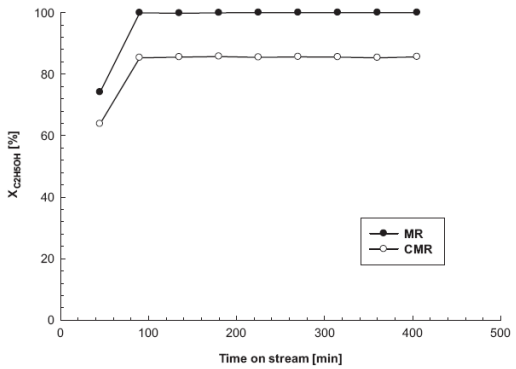

Fig. 4 – Ethanol conversion vs time on stream for the POE reaction carried out in Pd–Ag MR and CMR, at $T = 450\ ^{\circ}C$, $p_{reaction} = 1.0$ bar, $p_{permeate} = 1.0$ bar, O_2:C_2H_5OH = 0.5:1 mol/mol, sweep gas = 8.97×10^{-2} mol/h and GHSV ~ 1300 h^{-1}.

maximum error by also considering the unreacted ethanol and acetaldehyde condensed in the cold trap.

The POE reaction can be indicated as reported in [21,22]

$$C_2H_5OH + 0.5O_2 = 2CO + 3H_2 \quad \Delta H^{\circ}_{298\ K} = 17.0\ kJ/mol \tag{1}$$

As general information, Wang and Wang [23] proposed the possible reaction pathways of POE as summarized below:

$$C_2H_5OH + 1.5O_2 = 2CO_2 + 3H_2 \quad \Delta H^{\circ}_{298\ K} = -549.0\ kJ/mol \tag{2}$$

$$C_2H_5OH = C_2H_4O + H_2 \ \text{(dehydrogenation)} \quad \Delta H^{\circ}_{298\ K} = 71.6\ kJ/mol \tag{3}$$

$$C_2H_4O = CH_4 + CO \ \text{(acetaldehyde decomposition)} \quad \Delta H^{\circ}_{298\ K} = -19.0\ kJ/mol \tag{4}$$

$$C_2H_4O + 0.5O_2 = 2H_2 + 2CO \ \text{(acetaldehyde POX)} \quad \Delta H^{\circ}_{298\ K} = -54.6\ kJ/mol \tag{5}$$

$$C_2H_5OH = C_2H_4 + H_2O \ \text{(dehydration)} \quad \Delta H^{\circ}_{298\ K} = 48.7\ kJ/mol \tag{6}$$

$$CO + 3H_2 = CH_4 + H_2O \ \text{(methanation)} \quad \Delta H^{\circ}_{298\ K} = -206.2\ kJ/mol \tag{7}$$

$$CO_2 + 4H_2 = CH_4 + 2H_2O \quad \Delta H^{\circ}_{298\ K} = -165.0\ kJ/mol \tag{8}$$

$$2CO = CO_2 + C \ \text{(Boudouard reaction)} \quad \Delta H^{\circ}_{298\ K} = -172.5\ kJ/mol \tag{9}$$

$$CO + 0.5O_2 = CO_2 \ \text{(CO oxidation)} \quad \Delta H^{\circ}_{298\ K} = -283.0\ kJ/mol \tag{10}$$

$$CO + H_2O = CO_2 + H_2 \ \text{(water gas shift)} \quad \Delta H^{\circ}_{298\ K} = -41.2\ kJ/mol \tag{11}$$

$$CH_4 + 0.5O_2 = CO + 2H_2 \ \text{(methane POX)} \quad \Delta H^{\circ}_{298\ K} = 35.6\ kJ/mol \tag{12}$$

$$CH_4 + 2O_2 = CO_2 + 2H_2O \quad \Delta H^{\circ}_{298\ K} = -802.2\ kJ/mol \tag{13}$$

$$H_2 + O_2 = H_2O \ \text{(hydrogen oxidation)} \quad \Delta H^{\circ}_{298\ K} = -241.8\ kJ/mol \tag{14}$$

Concerning the description of the MR performances, some equations are defined as reported below:

Conversion of ethanol:

$$X_{C_2H_5OH}(\%) = \frac{C_2H_5OH_{in} - C_2H_5OH_{out}}{C_2H_5OH_{in}} \times 100 \tag{15}$$

where suffixes "in" and "out" indicate the MR inlet and outlet molar flow rates of ethanol. Selectivity of the products:

$$S_i(\%) = \frac{i_{out}}{H_{2,out} + CO_{out} + CH_{4,out} + CO_{2,out} + C_2H_{4,out} + C_2H_4O_{out} + H_2O_{out}} \times 100 \tag{16}$$

where i = H_2, CO, CH_4, CO_2, C_2H_4, C_2H_4O and H_2O, respectively. Moreover, $H_{2,out}$ indicates the total hydrogen produced during reaction, calculated as the total amount of hydrogen both from retentate and permeate sides.

The hydrogen recovery (HR) is defined as the CO_x-free hydrogen collected in the permeate side ($H_{2,permeate}$) with respect to the total hydrogen produced from reaction ($H_{2,out}$):

$$HR(\%) = \frac{H_{2,permeate}}{H_{2,out}} \times 100 \tag{17}$$

The yield of hydrogen for POE reaction is represented as reported below:

$$Y_{H_2}(\%) = \frac{H_{2,out}}{3C_2H_5OH_{in}} \times 100 \tag{18}$$

Eq. (18) indicates the ratio between the hydrogen really produced and that theoretically producible from the stoichiometry of the POE reaction (1).

3. Results and discussion

3.1. Catalyst deactivation and membrane permeation tests

First of all, the Pd–Ag membrane was characterized in terms of permeation with pure gases. The results of these tests showed that the Pd–Ag membrane is completely perm-selective towards H_2 with respect to other gases, such as N_2, CO, CO_2 and CH_4. Generally, at constant temperature the hydrogen permeation through a dense Pd-based membrane occurs via solution/diffusion mechanism. This transport is described by the following general expression:

$$J_{H_2} = \frac{Pe}{\delta}\left(p^n_{H_2-retentate} - p^n_{H_2-permeate}\right) \quad (19)$$

where: J_{H_2} is the hydrogen flux permeating through Pd-based membrane, Pe the hydrogen permeability, δ the Pd-based membrane thickness, $p_{H_2-retentate}$ and $p_{H_2-permaeate}$ the hydrogen partial pressure in the retentate and permeate sides, respectively, and "n" the dependence factor of hydrogen partial pressure, in the range 0.5–1.0. [24]. The "n" value is used as an indicator for the rate-controlling step of the permeation. If the diffusion of atomic hydrogen through the dense metal layer is rate-limiting, then the hydrogen flow is directly proportional to the hydrogen partial pressure square root difference between the retentate and permeate sides (Sieverts–Fick's law).

Therefore, in Fig. 3 the hydrogen flux permeating through the membrane against hydrogen partial pressure difference between retentate and permeate sides is reported at different "n" values. As shown, the highest linear regression value (R^2) corresponded to $n = 0.5$, confirming that Sieverts–Fick's law (Eq. (20)) is followed:

$$J_{H_2} = \frac{Pe}{\delta}\left(p^{0.5}_{H_2-retentate} - p^{0.5}_{H_2-permeate}\right) \quad (20)$$

Afterwards, reaction tests were carried out paying close attention to the POE performed in both CMR and MR packed with Rh/Al_2O_3 catalyst and, as a result, Fig. 4 shows the ethanol conversion against time on stream at 450 °C, $p = 1$ bar and stoichiometric O_2:C_2H_5OH feed ratio. After transient phenomena, ethanol conversion (100%) in the MR shows a constant trend in the range time of each reaction cycle up to 6 h of operation at steady state conditions, reached after around 90 min of testing. Moreover, the trend illustrated in Fig. 4 was reproduced in the overall MR experimental campaign. When POE is performed in the CMR, although the ethanol conversion trend is comparable to the MR one, the absence of catalyst lowers the conversion from 100% to around 85%, Table 1.

However, during the reaction tests carbon deposition was detected only in the CMR case. Therefore, after each reaction cycle, the hydrogen permeating flux was measured in order to confirm that no changes happened in the permeation behaviour of the Pd–Ag membrane. Unfortunately, as sketched in Fig. 5, the hydrogen flux permeating through the membrane decreases after reaction in CMR modality. Different effects could be claimed for justifying what occurred in CMR: a high amount of CO and CO_2 formed during the POE [25,26] as well as carbon coke deposits. In particular, as reported by Zhang et al. [25], CO_2 could retard the absorption and dissociation of hydrogen on the surface of the dense membrane. They suggested that the CO_2 gas influence occurs only during reaction and this poisoning effect is not permanent. Taking further into account the study of Gao et al. [26], under high CO concentration, CO coverage (in the adsorbed molecular form) on the surface of Pd-based membranes increases. Hence, the number of available hydrogen dissociation sites is significantly reduced. As a consequence, the influence of competitive adsorption of CO on hydrogen permeation could be increased causing the decrease of the hydrogen permeating flux through the membrane. Nevertheless, as confirmed in the specialized literature, the inhibitive effects of CO on hydrogen permeation through Pd-based membranes are reversible [26]. However, in both aforementioned cases, owing to the operating temperature (450 °C) of the experimental tests, the detrimental effect due to CO and CO_2 influence cannot be accounted for justifying the hydrogen permeation decrease. Therefore, it is probably due to the unfavourable aspect of coke formation, which, covering the Pd–Ag membrane surface, lowers the hydrogen permeating flux through the membrane. In fact, Salge et al. [28] studied the POE in FBR over different catalysts and pointed out that, at similar operating

Table 1 – Comparison between the performance in terms of products selectivities, ethanol conversion and hydrogen yield of the MR and CMR performing POE reaction at T = 450 °C, stoichiometric feed molar ratio (O_2:C_2H_5OH = 0.5:1), $p_{retentate}$ = 1 bar, $p_{permeate}$ = 1.0 bar, GHSV ~ 1300 h^{-1} and N_2 sweep gas molar flow rate = 8.97 × 10^{-2} mol/h.

	[%]								
	$X_{C_2H_5OH}$	Y_{H_2}	S_{H_2}	S_{CO}	S_{CH_4}	S_{CO_2}	S_{H_2O}	$S_{C_2H_4O}$	$S_{C_2H_4}$
MR	100.0	33.0	33.6	18.9	15.0	11.8	20.7	Trace	Trace
CMR	85.3	8.0	10.6	15.4	8.0	5.0	42.0	14.8	4.1

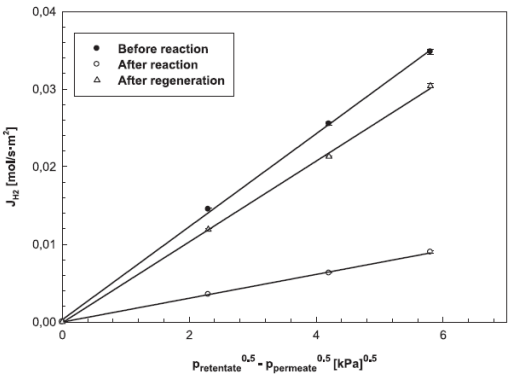

Fig. 5 – Sieverts' plot for the hydrogen permeating flux through the Pd–Ag membrane, before and after reaction in the CMR case and after regeneration at 450 °C.

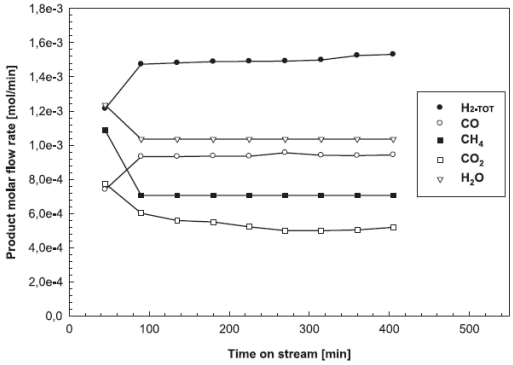

Fig. 6 – Product molar flow rate vs time on stream for the POE reaction in the Pd–Ag MR at $T = 450\ ^{\circ}C$, $p_{reaction} = 1.0$ bar, $p_{permeate} = 1.0$ bar, O_2:C_2H_5OH = 0.50:1 mol/mol, sweep gas = 8.97×10^{-2} mol/h and GHSV ~ 1300 h^{-1}.

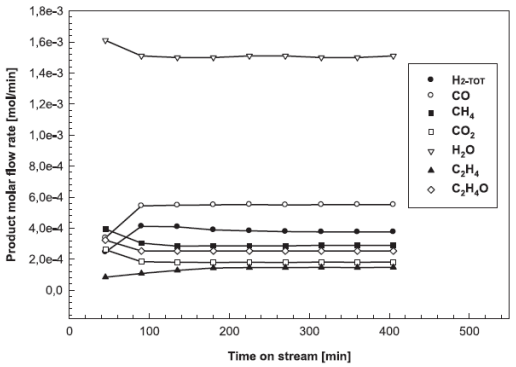

Fig. 7 – Product molar flow rate vs time on stream for the POE reaction in the CMR at $T = 450\ ^{\circ}C$, $p_{reaction} = 1.0$ bar, $p_{permeate} = 1.0$ bar, O_2:C_2H_5OH = 0.5:1 mol/mol, sweep gas = 8.97×10^{-2} mol/h and GHSV ~ 1300 h^{-1}.

conditions to the present work, Pd immediately shows coke formation rather than Rh and other catalysts. On the contrary, using Rh-based catalyst in the MR case, coke formation was avoided instead of CMR case, operated at favourable conditions to coke formation [23,24] with the Pd of the membrane acting as a catalyst on the POE. Therefore, in order to recover the hydrogen permeation characteristics shown before reaction, a "membrane regeneration" procedure was carried out by means of pure hydrogen (8.71×10^{-4} mol/min) flowed in the retentate side at 450 °C and for around 2 h. As matter of fact, methane formation was detected by GC, confirming that the carbon coke on the palladium-based membrane was removed until methane formation was no longer observed. Afterwards, as illustrated in Fig. 5, the hydrogen permeability through the membrane was almost completely recovered.

3.2. *POE reaction in CMR and Pd–Ag dense MR*

Table 1 reports the gas selectivity at 450 °C, ambient pressure and stoichiometric feed ratio (O_2:C_2H_5OH = 0.5:1 mol/mol), pointing out that the main products formed during the POE in the MR were H_2, CO, CO_2, CH_4, H_2O and traces of C_2H_4O and C_2H_4. Nevertheless, Table 1 shows that, at the same MR operating conditions, in the CMR a consistent amount of C_2H_4O and C_2H_4 was formed. However, in both cases expected by-products such as C_2H_6, CH_3COCH_3 and $C_2H_5OC_2H_5$ were not detected.

At the above mentioned operating conditions, the main MR product molar flow rates as a function of time on stream are shown in Fig. 6. Depending on the constant trend of the conversion (Fig. 4), after transient phenomena the products flow rates of Fig. 6 are quite constant. This trend was confirmed in all the MR experimental tests. Moreover, Table 2 shows that the hydrogen production increases at lower O_2:C_2H_5OH feed ratio. In detail, around 2.1×10^{-3} mol/min was the maximum hydrogen stream produced under defect of oxygen (O_2:C_2H_5OH = 0.33:1 mol/mol). Unfortunately, exercising the MR at lower feed ratio than stoichiometric, CO formation is more pronounced (~1.2×10^{-3} mol/min). On the contrary, at higher feed ratio hydrogen production is lowered but CO formation is greatly depressed (6.3×10^{-4} mol/min at O_2:C_2H_5OH = 0.62:1 mol/mol).

Fig. 7 depicts the product molar flow rate distribution when POE is carried out in the CMR at stoichiometric feed ratio. In this case, water and CO rather than hydrogen are the main

Table 2 – Products molar flow rate versus O_2:C_2H_5OH feed molar ratio for POE reaction carried out in both MR and CMR at reaction pressure = 1.0 bar, $p_{permeate} = 1.0$ bar, $T = 450\ ^{\circ}C$, GHSV ~ 1300 h^{-1} and N_2 sweep gas molar flow rate = 8.97×10^{-2} mol/h.

Product molar flow rate [mol/min]	MR			CMR
	O_2:C_2H_5OH = 0.33:1	O_2:C_2H_5OH = 0.5:1	O_2:C_2H_5OH = 0.62:1	O_2:C_2H_5OH = 0.5:1
H_2	2.116E–03	1.742E–03	1.62E–03	3.871E–04
CO	1.198E–03	9.395E–04	6.30E–04	5.497E–04
CH_4	8.207E–04	7.052E–04	9.30E–04	2.892E–04
CO_2	5.190E–04	5.317E–04	8.68E–04	1.807E–04
H_2O	7.769E–04	1.035E–03	7.44E–04	1.505E–03
C_2H_4	Trace	Trace	Trace	1.389E–04
C_2H_4O	Trace	Trace	Trace	2.529E–04

Fig. 8 – Dense Pd–Ag membrane used in POE reaction without catalyst: before and after reaction test.

products. Water is produced from the dehydration reaction of ethanol (Eq. (6)) and its stoichiometry indicates that the same amount of ethylene should be produced with respect to water. As indicated by both Cavallaro [33,36] and Rostrup-Nielsen [37], carbon is formed from ethylene as a precursor. Thus, the amount of ethylene in the products is lower than water because it is partially converted into coke.

As a consequence, lower hydrogen yield is achieved in the CMR ($Y_{H_2} = \sim 8\%$) than in the MR ($Y_{H_2} = 33\%$), Table 1.

Fig. 8 shows the effect of carbon coverage on Pd–Ag membrane surface. Nevertheless, the experimental campaign was firstly realized on the MR and, successively, on the CMR as a case study. Therefore, owing to the damage to the membrane surface probably due to local temperature increase related to exothermal reactions such as methane oxidation (Eq. (13)), methanation reaction (Eq. (7)) and so on, the tests on the CMR were performed only at stoichiometric feed ratio and ambient pressure.

However, over the whole range of O_2:C_2H_5OH feed ratio and reaction pressure investigated in this work, ethanol conversion obtained in the Pd–Ag MR was always 100%. To the best of our knowledge the present work is the first study (or, at least, one of the first ones) on the POE in MRs, while in addition, only few papers deal with the POE reaction performed in FBRs. Therefore, in order to emphasize the benefits of using MRs, in Table 3 a comparison between the performances of the MR in terms of ethanol conversion and hydrogen selectivity with respect to those of FBRs from the specialized literature [2,14,27–31] is shown qualitatively. On the one hand, the MR gives the highest conversion (100%), even when the FBR is packed with the same catalyst used in this work and operated at stronger operating conditions ($X_{C_2H_5OH} = 85\%$), on the other hand, at comparable conditions, ethanol conversion of the FBRs is much lower than that of the MR.

Table 3 – Qualitative comparison between the POE experimental results of FBRs from literature and both the MR and CMR of this work.

Reactor type	Catalyst	$X_{C_2H_5OH}$ [%]	S_{H_2} [%]	O_2: C_2H_5OH	T [°C]	Reference
FBR	Pt/Al_2O_3	~80.0	–	0.5:1	300	[27]
FBR	$Ni_{60}–Fe_{40}$	~45.0	–	0.5:1	300	[2]
FBR	Rh/Al_2O_3	~85.0	60[a]	0.5:1	700	[28]
FBR	Rh/Y_2O_3	~65.0	10	0.5:1	400	[29]
FBR	$Pt/CeZrO_2$	~60.0	0[b]	0.5:1	500	[30]
FBR	Pd/CeO_2	~60.0	13[b]	0.5:1	400	[31]
FBR	$CuO/\gamma Al_2O_3$	~52.0	2.2	0.5:1	400	[14]
MR	Rh/Al_2O_3	100.0	34	0.5:1	450	This work
CMR	–	85.3	11	0.5:1	450	This work

a Product selectivities were calculated on an atomic basis.
b This value represents H_2 composition.

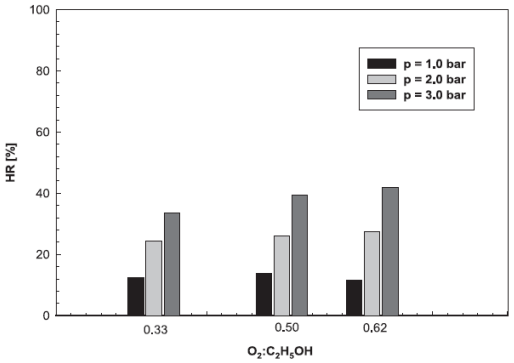

Fig. 9 – Hydrogen recovery against O_2:C_2H_5OH feed molar ratio for POE reaction in the Pd–Ag MR, at different reaction pressure, $p_{permeate}$ = 1.0 bar, T = 450 °C, N_2 sweep gas molar flow rate = 8.97×10^{-2} mol/h and GHSV ~ 1300 h^{-1}.

The benefit owing to the MR is given by the hydrogen removal through the Pd–Ag membrane, which shifts the reaction system towards further products formation, favouring higher ethanol conversion. In the membranologist's area, this is the well known "shift effect" [32], in which the hydrogen removed from the reaction side and collected into the permeate side (shell side) through a selective permeation affects the POE reaction equilibrium that, owing to the Le Chatelier principle, is shifted towards the products.

However, the most important aspect of this work was the ability of the MR to collect a CO_x-free hydrogen stream in the permeate side. Therefore, a key parameter for evaluating this ability is the hydrogen recovery (HR) (Eq. (17)), indicating the fraction of CO_x-free hydrogen recovered in the permeate side with respect to the total hydrogen produced. Specifically, Fig. 9 depicts HR versus O_2:C_2H_5OH feed ratio at different pressure. At each feed ratio, the higher the pressure the higher HR. This effect is due to the pressure dependence of the hydrogen flux permeating through the membrane when Sieverts–Fick's law (Eq. (20)) is followed. In this case, the hydrogen permeation driving force is improved by a retentate pressure (reaction pressure) increase. Furthermore, Fig. 9 shows that around 40% HR is achieved as maximum value at 450 °C, 3 bar and O_2:C_2H_5OH = 0.62:1.

In Table 4, the gas selectivities at 450 °C, different reaction pressure and O_2:C_2H_5OH feed ratio are shown. The hydrogen selectivity decreases by increasing the pressure. For instance, at O_2:C_2H_5OH = 0.33:1, it drops from around 39.0% at 1.0 bar to 23% at 3.0 bar, while the methane selectivity shows a great increase from 15% at 1.0 bar to 33% at 3.0 bar and O_2:C_2H_5OH = 0.33:1. This result can be explained taking into account that, from a thermodynamic point of view, an increase of reaction pressure favours the methanation

Table 4 – Product selectivities versus O_2:C_2H_5OH feed molar ratio for POE reaction carried out in a Pd–Ag MR at different reaction pressures, $p_{permeate}$ = 1.0 bar, T = 450 °C, GHSV ~ 1300 h^{-1} and N_2 sweep gas molar flow rate = 8.97 × 10^{-2} mol/h.

	O_2:C_2H_5OH	S_{H_2}	S_{CO}	S_{CH_4}	S_{CO_2}	S_{H_2O}	$S_{C_2H_4O}$	$S_{C_2H_4}$
		[%]						
p = 1.0 bar	0.33:1	38.6	22.3	15.1	9.6	14.4	Trace	Trace
	0.50:1	33.6	19.0	15.0	11.8	20.7	Trace	Trace
	0.62:1	31.7	18.5	18.2	17.0	14.6	Trace	Trace
p = 2.0 bar	0.33:1	25.3	13.8	31.3	17.5	12.1	Negligible	Negligible
	0.50:1	23.9	12.2	31.1	20.5	12.3	Negligible	Negligible
	0.62:1	26.3	12.8	28.0	23.2	9.7	Negligible	Negligible
p = 3.0 bar	0.33:1	23.3	12.4	32.6	17.5	14.2	Negligible	Negligible
	0.50:1	22.8	10.8	32.3	20.9	13.2	Negligible	Negligible
	0.62:1	20.2	6.7	35.4	27.4	10.3	Negligible	Negligible

reactions (13) and (14), whereas hydrogen production is reduced [23,34]. Relating to CO_2 and CO selectivities, a higher pressure acts positively on the hydrogen permeation driving force, inducing an increase of the hydrogen stream collected in the permeate side, shifting the WGS reaction (18) towards the products, then giving higher CO consumption [35]. Moreover, a higher O_2:C_2H_5OH feed ratio favours the hydrogen oxidation reaction (14) [23]. As a consequence, a higher H_2O production is obtained, which further favours WGS reaction [35]. Therefore, as shown in Table 3, by increasing both pressure and feed molar ratio, a drastic CO selectivity decrease, a CO_2 selectivity increase and a constant H_2O selectivity are reached.

Another important parameter to take also into account is the hydrogen yield. In particular, Fig. 10 shows that at each O_2:C_2H_5OH feed ratio investigated, the hydrogen yield decreases by increasing reaction pressure. In detail, at O_2:C_2H_5OH = 0.33:1, the hydrogen yield decreases from 35% at 1.0 bar to 20% at 3.0 bar. This occurs since the higher the pressure the lower the hydrogen selectivity (Table 4), causing a detrimental effect on hydrogen yield. However, the hydrogen yield shows a constant trend by increasing the feed ratio, although the hydrogen selectivity decreases at higher feed ratio (Table 4). In fact, keeping constant the total molar feed flow rate, a higher O_2:C_2H_5OH involves a lower ethanol stream fed to the MR.

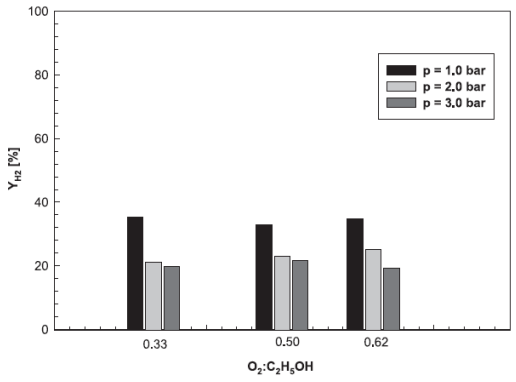

Fig. 10 – Hydrogen yield vs O_2:C_2H_5OH feed molar ratio for POE reaction in the Pd–Ag MR, at different reaction pressure, $p_{permeate}$ = 1.0 bar, T = 450 °C, GHSV ~ 1300 h^{-1} and N_2 sweep gas molar flow rate = 8.97 × 10^{-2} mol/h.

It should be taken into account that, as shown in Table 4, performing the POE reaction in Pd–Ag MR, high hydrogen selectivity was achieved at lower O_2:C_2H_5OH feed molar ratio (below stoichiometric value). Moreover, as illustrated in Figs. 9 and 10, at each pressure hydrogen recovery and hydrogen production are constant with increasing the feed ratio. Therefore, it would be advantageous to carry out the POE reaction below stoichiometric feed ratio (O_2:C_2H_5OH < 0.5:1) in order to also maximize hydrogen production.

4. Conclusion

The POE reaction was studied from an experimental point of view in a dense Pd–Ag MR using a commercial Rh-based catalyst. To the best of our knowledge, this work can be considered as the first study in which the POE reaction is carried out in the MR. The advantage of the MR consists of the ability to recover a CO_x-free hydrogen stream for supplying a PEMFC. The POE was realized in the MR at 450 °C, GHSV ~ 1300 h^{-1}, by varying the feed molar ratio (O_2:C_2H_5OH) between 0.33:1 and 0.62:1 and in a reaction pressure range from 1.0 to 3.0 bar, achieving as best result of this work 100% ethanol conversion and around 40% CO_x-free hydrogen recovery. Furthermore, the POE was carried out in the MR without catalyst as a case study, thus acting as a catalytic membrane reactor (CMR). At stoichiometric feed ratio, the CMR presented ~85.0% ethanol conversion and around 13% hydrogen recovery. Furthermore, in the CMR carbon deposition was the main drawback of the case study, which affected the membrane reactor performances negatively, covering the Pd–Ag membrane surface and lowering its hydrogen permeation capacity.

In the near future, the important aspect of pure or, at least, CO_x-free hydrogen production will be particularly stressed in order to improve the results obtained in this work, paying particular attention to the effect of a higher sweep gas stream on the MR performances.

REFERENCES

[1] Mattos LV, Noronha FB. Hydrogen production for fuel cell applications by ethanol partial oxidation on Pt/CeO_2 catalysts: the effect of the reaction conditions and reaction mechanism. J Catal 2005;233:453–63.

[2] Wang W, Wang Z, Ding Y, Xi J, Lu G. Partial oxidation of ethanol to hydrogen over Ni–Fe catalysts. Catal Lett 2002;81 (1–2):63–8.

[3] Vaidya PD, Rodrigues AE. Insight into steam reforming of ethanol to produce hydrogen for fuel cells. Chem Eng J 2006; 117:39–49.

[4] Sun J, Qiu X, Wu F, Wang W, Hao S. Hydrogen from steam reforming of ethanol in low and middle temperature range for fuel cell application. Int J Hydrogen Energy 2004;29:1075–81.

[5] Haryanto A, Fernando S, Murali N, Adhikari S. Current status of hydrogen production techniques by steam reforming of ethanol: a review. Energy Fuels 2005;19:2098–106.

[6] Frusteri F, Freni S, Chiodo V, Donato S, Bonura G, Cavallaro S. Steam and auto-thermal reforming of bioethanol over MgO and CeO_2 Ni supported catalysts. Int J Hydrogen Energy 2006; 31:2193–9.

[7] Gallucci F, Basile A, Tosti S, Iulianelli A, Drioli E. Methanol and ethanol steam reforming in membrane reactors: an experimental study. Int J Hydrogen Energy 2007;32:1201–10.

[8] Basile A, Gallucci F, Iulianelli A, Tosti S. CO-free hydrogen production by ethanol steam reforming in a Pd–Ag membrane reactor. Fuel Cells 2008;1:62–8.

[9] Basile A, Gallucci F, Iulianelli A, De Falco M, Liguori S. Hydrogen production by ethanol steam reforming: experimental study of a Pd–Ag membrane reactor and traditional reactor behaviour. Int J Chem Reactor Eng 2008;6:A30.

[10] Iulianelli A, Longo T, Pinacci P, Basile A. An experimental study on bio-ethanol steam reforming in a catalytic membrane reactor. Part I: temperature and sweep-gas flow configuration effects. Int J Hydrogen Energy 2010;35:3170–7.

[11] Iulianelli A, Longo T, Basile A. An experimental study on bio-ethanol steam reforming in a catalytic membrane reactor. Part II: reaction pressure, sweep-factor and WHSV effects. Int J Hydrogen Energy 2010;35:3159–64.

[12] Lin WH, Hsiao CS, Chang HF. Effect of oxygen addition on the hydrogen production from ethanol steam reforming in a Pd–Ag membrane reactor. J Membr Sci 2008;322:360–7.

[13] Lin WH, Liu YC, Chang HF. Hydrogen production from oxidative ethanol steam reforming in a palladium–silver alloy composite membrane reactor. J Chin Inst Chem Eng 2008;39:435–40.

[14] Rodrigues CP, da Silva VT, Schmal M. Partial oxidation of ethanol on Cu/Alumina/cordierite monolith. Catal Commun 2009;10:1697–701.

[15] Liguras DK, Goundani K, Verykios XE. Production of hydrogen for fuel cells by catalytic partial oxidation of ethanol over structured Ru catalysts. Int J Hydrogen Energy 2004;29:419–27.

[16] Hsu SN, Bi J-L, Wang W-F, Yeh C-T, Wang C-B. Low-temperature partial oxidation of ethanol over supported platinum catalysts for hydrogen production. Int J Hydrogen Energy 2008;33:693–9.

[17] Liguras DK, Goundani K, Verykios XE. Production of hydrogen for fuel cells by catalytic partial oxidation of ethanol over structured Ni catalysts. J Power Sources 2004;130:30–7.

[18] Silva AM, Duarte de Farias AM, Costa LOO, Barandas APMG, Mattos LV, Fraga MA, et al. Partial oxidation and water–gas shift reaction in an integrated system for hydrogen production from ethanol. Appl Catal A Gen 2008;334: 179–86.

[19] Mas V, Kipreos R, Amadeo N, Laborde M. Thermodynamic analysis of ethanol/water system with the stoichiometric method. Int J Hydrogen Energy 2006;31:21–8.

[20] Tosti S, Bettinali L. Diffusion bonding of Pd–Ag membranes. J Mater Sci 2004;39:3041–6.

[21] Ni M, Leung DYC, Leung MKH. A review on reforming bio-ethanol for hydrogen production. Int J Hydrogen Energy 2007; 32:3238–47.

[22] Cheekatamarla PK, Finnerty CM. Synthesis gas production via catalytic partial oxidation reforming of liquid fuels. Int J Hydrogen Energy 2008;33:5012–9.

[23] Wang W, Wang Y. Thermodynamic analysis of hydrogen production via partial oxidation of ethanol. Int J Hydrogen Energy 2008;33:5035–44.

[24] Dittmeyer R, Höllein V, Daub K. Membrane reactors for hydrogenation and dehydrogenation processes based on supported palladium. J Mol Catal A Chem 2001;173:135–84.

[25] Zhang Y, Gwak J, Murakoshi Y, Ikehara T, Maeda R, Nishimura C. Hydrogen permeation characteristics of thin Pd membrane prepared by microfabrication technology. J Membr Sci 2006;277:203–9.

[26] Gao H, Lin YS, Li Y, Zhang B. Chemical stability and its improvement of palladium-based metallic membranes. Ind Eng Chem Res 2004;43:6920–30.

[27] Mattos LV, Noronha FB. Partial oxidation of ethanol on supported Pt catalysts. J Power Sources 2005;145:10–5.

[28] Salge JR, Deluga GA, Schmidt LD. Catalytic partial oxidation of ethanol over noble metal catalysts. J Catal 2005;235: 69–78.

[29] Silva AM, Barandas APMG, Costa LOO, Borges LEP, Mattos LV, Noronha FB. Partial oxidation of ethanol on Ru/Y_2O_3 and Pd/Y_2O_3 catalysts for hydrogen production. Catal Today 2007; 129:297–304.

[30] de Lima SM, da Cruz IO, Jacobs G, Davis BH, Mattos LV, Noronha FB. Steam reforming, partial oxidation, and oxidative steam reforming of ethanol over $Pt/CeZrO_2$ catalyst. J Catal 2008;257:356–68.

[31] Costa LOO, Silva AM, Borges LEP, Mattos LV, Noronha FB. Partial oxidation of ethanol over Pd/CeO_2 and Pd/Y_2O_3 catalysts. Catal Today 2008;138:147–51.

[32] Zaman J, Chakma A. Inorganic membrane reactors. J Membr Sci 1994;92:1–28.

[33] Cavallaro S, Chiodo V, Vita A, Freni S. Hydrogen production by auto-thermal reforming of ethanol on Rh/Al_2O_3 catalyst. J Power Sources 2003;123:10–6.

[34] Rabenstein G, Hacker V. Hydrogen for fuel cells from ethanol by steam-reforming, partial-oxidation and combined auto-thermal reforming: a thermodynamic analysis. J Power Sources 2008;185:1293–304.

[35] Uemiya S, Sato N, Ando H, Kikuchi E. The water gas shift reaction assisted by a palladium membrane reactor. Ind Eng Chem Res 1991;30:585–9.

[36] Cavallaro S. Ethanol steam reforming on $Rh–Al_2O_3$ catalysts. Energy Fuels 2000;14:1195–9.

[37] Rostrup-Nielsen JR. In: Boudart Anderson, editor. Catalytic steam reforming in catalysis science and technology, vol. 5. Springer Verlag; 1984 [chapter 1].

Conclusion to Chapter 1

As extensively discussed in this Part, the MR technology has been applied with the intent to produce hydrogen based on the exploitation of ethanol as a renewable source.

As a general consideration of these works is that the experimental results may vary greatly depending on the operating conditions adopted as well as the typology of inorganic membrane utilized. Therefore, a direct quantitative comparison among them is not possible, but only from a qualitative point of view.

Table 3.1 summarizes the most significant performances of these studies; moreover, it shows the operating conditions of the MRs exercised as well as the type of inorganic membranes housed inside.

Concerning the membrane, a self supported Pd-Ag and Pd/PSS supported ones are used, produced by cold-rolling and welding technique, respectively. They are both tubular and joined to two stainless steel ends useful for the membrane housing inside the MR, whose one of them is closed. In all cases, the Pd-Ag membranes are full perm-selective to hydrogen permeation, whereas the Pd/PSS presented an ideal selectivities hydrogen/helium of ~ 900 at 400 °C.

H_2O/C_2H_5OH	O_2/ C_2H_5OH	T [°C]	p [bar]	Catalyst	H_2 recovery	H_2 yield	Membrane type	Paper
11/1	-	500	3.6	Ru/Al_2O_3	25 %	-	Pd/Ag	1
3/1	-	400	8.0	Co/Al_2O_3	50 %	-	Pd/PSS	2
18.7/1	-	400	3.0	Co/Al_2O_3	98 %	53 %	Pd/Ag	3
13/1 + impurities	-	400	12.0	Co/Al_2O_3	40 %	40 %	Pd/PSS	4
11/1	0.6/1	400	2.5	Ru/Al_2O_3	30 %	18 %	Pd/Ag	5
-	0.62/1	450	3.0	Rh/Al_2O_3	40 %	22 %	Pd/Ag	6

Table 3.1 Performances and operating conditions of MRs for ethanol reforming processes in these studies

With the aim of improving both conversion and hydrogen yield, the author of this thesis analyzed the ethanol reforming reactions paying particular attention to the influence of high steam to ethanol feed molar ratio and working at relatively low reaction temperature (400 - 500 °C) using a self supported Pd-Ag and Pd/PSS supported MRs.

At 11/1 of steam to ethanol feed ratio, at 500 °C and at 3.6 bar, hydrogen recovery ~ 25% is realized using a Ru/Al_2O_3 catalyst (paper 1). Nevertheless, by means of oxygen addition it is possible to obtain higher hydrogen recovery (30%) at lower operative conditions (paper 5). In particular, by supplying oxygen ESR energy consumption can be decreased due to the exothermic nature of the partial oxidation of ethanol. Moreover, the addition of oxygen can prevent coke precursor such as ethylene and ethane formation (due to the dehydration reaction of ethanol) and, then, avoid carbon deposition. However, the oxygen content in the feed stream could not overcome the molar ratio O_2:C_2H_5OH = 1.3:1 because, in this condition, ethanol conversion is not favoured and both hydrogen yield and hydrogen recovery drop dramatically.

The benefits of adding oxygen are demonstrated also in paper 6, in which ethanol partial oxidation is performed in Pd-Ag MR. In this case, better MR performances with respect of previous studies are realized. In particular, at feed molar ratio O_2:C_2H_5OH = 0.62 the hydrogen recovery is almost 40% higher than the one obtained performing ESR in paper 1. Nevertheless, to the best of my knowledge, this work can be considered as the first study in which the POE reaction is carried out in MR. Therefore, further studies has to be carried out in order to analyze deeply benefits and drawbacks of POE reaction.

In the meanwhile, in the paper 3 has been confirmed that higher steam to ethanol feed ratios give better performance. Indeed, ESR reaction is carried out at high steam to ethanol feed ratio (18.7/1), 400 °C, catalyzed by Co/Al_2O_3 and the effect of an increase of reaction pressure is analyzed. A hydrogen yield ranging from ~ 20% to more than 50% as well as a hydrogen recovery (defined as the CO_x-free hydrogen collected in the permeate side on the total hydrogen produced during the reaction) from 30% to around 90%, by varying the reaction pressure between 1.5 – 3.0 bar and keeping constant the permeate pressure at 1.0 bar, were realized. These results are due to the effect of higher reaction pressures, which favour the “shift effect” owing to an increase of the hydrogen permeation driving force (see Sieverts equation, ch 1, Part I). This involves a greater removal of

hydrogen from the reaction side to the permeate side as a CO_x-free hydrogen stream, improving both conversion and hydrogen yield as well as the CO_x-free hydrogen recovery.

In this study, for simplicity and as a first approach, a simulated mixture of bio-ethanol (without presenting the other typical contaminants such as glycerol, diethyl ether, acetic acid, etc) has been considered. Therefore, in paper 4, the influence of some impurities on MR performances is analyzed. In particular, the ESR reaction is performed at 400 °C and in a reaction pressure range of 8 – 12 bar (abs.) using both Ni/ZrO and Co/Al_2O_3 commercial catalysts and adding glycerol and acetic acid as impurities. The Pd/PSS supported MR showed lower performances in terms of hydrogen recovery (40%) and yield (40%) with respect to the Pd-Ag MR performances obtained by using a simulated mixture (paper 3). This negative effect is probably due to the impurities addition.

This is also confirmed comparing the hydrogen recovery obtained in the paper 4, with the one realized in paper 2. In particular, it is evident that by using a mixture steam/ethanol, the MR shows better hydrogen recovery with respect to the one obtained by supplying the mixture with the impurities.

As a consequence, on the one hand, it could be advantageous to supply directly into MR a real bio-ethanol mixture without making any distillation of further ethanol separation/purification process, but on the other hand further studies are necessary in order to understand how to minimize or avoid the detrimental effects of the impurities on the MR performances and, at the same time, to try the optimization of them.

As a further benefit of MR, in the majority of studies a comparison with a conventional reactor, working at the same operating conditions of Pd-based MR, has been realized confirming that the MR shows better performances in terms of ethanol conversion and hydrogen yield with respect the conventional one.

Chapter 2

Steam reforming reaction of Glycerol

Introduction

Glycerol can be considered as an important bio-source for producing hydrogen. Nowadays, glycerol is produced in large quantities as by-products of bio-diesel production. It is characterized by high energy density, it is non toxic and inflammable [Xuan et al (2009)].

Currently, glycerol is used in many applications as personal care, polymer and pharmaceutical applications. However, growth of bio-diesel industry has created a huge amount of glycerol which led, as a consequence, a reduction in glycerol market price [(Adhikari et al (2007)]. Therefore, an alternative use for glycerol is important and one possibility is to use it as renewable feedstock for producing hydrogen and syngas by steam reforming reaction.

To the best of my knowledge, few studies are focused on glycerol steam reforming (GSR) for hydrogen production using only conventional reactor. In particular, the GSR reaction can be carried out in either the aqueous or the gas phase. When operated in the aqueous phase, its low catalyst deactivation is an advantage, but it has to be operated at high pressures. On the contrary, in the gas phase, it can be carried out at atmospheric pressure presenting a great catalyst deactivation as a drawback [Hirai et al (2005)].

It could be useful to give an overview of the studies present in the open literature. At the moment, the researches are focused on the effects of catalysts on GSR reaction for hydrogen production, by performing the reaction in conventional reactor.

For instance, Adhikari et al. [Adhikari et al. (2008)] studied nickel-based catalysts with MgO, CeO_2, and TiO_2 supports. They found maximum hydrogen yield could be obtained at 650 ºC with

MgO supported catalysts. Iriondo et al. [Iriondo et al. (2008)] modified alumina-supported nickel catalysts with Ce, Mg, Zr and La to produce hydrogen from glycerol. They found that the use of Ce, La, Mg and Zr as promoters of Ni based catalysts increases the hydrogen selectivity. Furthermore, the authors deduced that Ce and La can increase stability of nickel; Mg can enhance surface nickel concentration; Zr can improve the capacity to activate steam.

Besides nickel based catalysts, other types of catalysts were also evaluated for GSR reaction. Ceria supported Ir, Co and Ni catalysts have been studied by Zhang et al. [Zhang et al. (2007)]. All the catalysts investigated exhibited significant activity and selectivity since the dehydration of glycerol to ethylene or propylene didn't occur, which can cause coke formation and deactivate the catalysts.. As comparison, Hirai et al. [Hirai et al (2005)] developed a novel efficient catalyst for GSR. Ruthenium catalysts were preferred and high performance was observed for the Ru/Y_2O_3 catalysts.

So, the research work of this chapter II is focused on the Pd-Ag MR performances carrying out GSR reaction for producing a high purity hydrogen stream, taking into account also the catalyst choice. This latter is due to the fact that the main purpose of each process is to obtain a total conversion of the reactants limiting by-products production. Therefore, in the first paper, the (0.5 wt%) Ru/Al_2O_3 catalyst was chosen according to the activity scale towards GSR reaction: Ru ~ Rh > Ni > Ir > Co> Pt > Pd > Fe given by Hirai et al. [Hirai et al (2005)].

In the second paper, the Co-based catalyst was chosen owing to the presence of ethanol as by-products during the GSR reaction. Indeed, it has chosen a selective catalyst that is able to convert such a by-product as ethanol and catalyze the GSR reaction.

The purpose of these two papers is to study the influence of some operative conditions on Pd-Ag MR performances in terms of glycerol conversion, hydrogen recovery and products selectivities carrying out the GSR reaction.

INTERNATIONAL JOURNAL OF HYDROGEN ENERGY 36 (2011) 3827–3834

Available at www.sciencedirect.com

ScienceDirect

journal homepage: www.elsevier.com/locate/he

Hydrogen production for PEM fuel cell by gas phase reforming of glycerol as byproduct of bio-diesel. The use of a Pd–Ag membrane reactor at middle reaction temperature

A. Iulianelli [a,*], P.K. Seelam [b], S. Liguori [a,c], T. Longo [a], R. Keiski [b], V. Calabrò [c], A. Basile [a]

[a] Institute on Membrane Technology of Italian National Research Council (ITM-CNR), Via P. Bucci, c/o University of Calabria – Cubo 17/C, 87036 Rende (CS), Italy

[b] Department of Process and Environmental Engineering mass and heat transfer process Laboratory, P.O. Box 4300, FI-90014, University of Oulu, Finland

[c] Department of Engineering Modeling, Via P. Bucci, c/o University of Calabria, Cubo 39/C, 87036 Rende (CS), Italy

ARTICLE INFO

Article history:
Received 15 January 2010
Received in revised form
15 February 2010
Accepted 16 February 2010
Available online 16 March 2010

Keywords:
Glycerol steam reforming
Pd–Ag membrane
CO-free hydrogen
PEM fuel cell

ABSTRACT

Glycerol as a byproduct of biodiesel production represents a renewable energy source. In particular, glycerol can be used in the field of hydrogen production via gas phase reforming for proton exchange membrane fuel cell (PEMFC) applications. In this work, glycerol steam reforming (GSR) reaction was investigated using a dense palladium–silver membrane reactor (MR) in order to produce pure (or at least CO-free) hydrogen, using 0.5 wt% Ru/Al_2O_3 as reforming catalyst. The experiments are performed at 400 °C, water to glycerol molar feed ratio 6:1, reaction pressure ranging from 1 to 5 bar and weight hourly space velocity (WHSV) from 0.1 to 1.0 h^{-1}. Moreover, a comparative study is given between the Pd–Ag MR and a traditional reactor (TR) working at the same MR operating conditions. The effect of the WHSV and reaction pressure on the performances of both the reactors in terms of glycerol conversion and hydrogen yield is also analyzed. The MR exhibits higher conversion than the TR (~60% as best value for the MR against ~40% for the TR, at WHSV = 0.1 h^{-1} and 5 bar), and high CO-free hydrogen recovery (around 60% at WHSV = 0.1 h^{-1} and 5 bar). During reaction, carbon coke is formed limiting the performances of the reactors and inhibiting, in particular, the hydrogen permeation through the membrane with a consequent reduction of hydrogen recovery in the permeate side.

1. Introduction

Sustainability in energy production is the key factor in the contemporary world. In the last decades, the consumption of fuel and energy sources is raised due to population growth. Moreover, depletion of fossil fuels, environmental pollution and climate change represent serious problems. According to EU energy and climate policy, 20% as a reduction of greenhouse gas emissions and 10% as an increase of the biofuels in the transports represent the targets for 2020 [1]. Today, many initiatives have been taken to implement alternative technologies and use renewable sources such as bioethanol, biodiesel and biogas [2]. In particular, EU is the largest producer of biodiesel, targeting its use at 5.75% by the end of 2010 [1]. Generally, biodiesel is obtained via trans-esterification of vegetable (edible) or non-edible oils using

* *Corresponding author*. Tel.: +39 0984 492011; fax: +39 0984 402103.
E-mail address: a.iulianelli@itm.cnr.it (A. Iulianelli).

0360-3199/$ – see front matter
doi:10.1016/j.ijhydene.2010.02.079

methanol as solvent, where glycerol is the main byproduct. Moreover, the use of biodiesel as a direct replacement for traditional diesel is increasing every year [3]. Nevertheless, it presents a negative aspect: the cost of biodiesel production is expensive and makes it uncompetitive in the market. Therefore, taking into account that the production of glycerol is rapidly growing, biodiesel production could be more economical viable using glycerol as value added product. Glycerol is a natural organic building block [3] and it can be used in many applications: production of pharmaceutical, polymer products and also in the synthesis of 1, 2-propanediol and 1, 3-propanediol. The crude glycerol consists of many impurities and its purification is an expensive distillation process [4]. Thus, it could be directly utilized in aqueous or gas phase reforming reactions for producing hydrogen [5–7]. At the moment, to the best of our knowledge, glycerol steam reforming (GSR) reaction is carried out conventionally in fixed bed reactors and hydrogen is produced with other byproduct gases like CO, CH_4 and CO_2 [8–12]. With the aim of producing hydrogen for feeding a PEMFC system, the GSR reformed stream going out from a TR needs to be purified. In fact, a concentration of CO >10 ppm is able to poison the anodic catalyst of a PEM fuel cell device. Using a dense palladium-based MR, pure or at least CO-free hydrogen can be obtained without requiring any further separation/purification process. Furthermore, the benefits of using a dense palladium-based MR consist of the possibility of simultaneously coupling the reaction process with the hydrogen separation/purification step in only one device.

Palladium-based membrane reactors are widely studied for carrying out several kind of reforming reactions such as methane, ethanol, methanol and acetic acid steam reforming, oxidative steam reforming and/or partial oxidation and so on in order to produce pure or at least CO-free hydrogen [13–19].

The aim of the present study is to investigate the GSR reaction performed at middle temperature (400 °C) in a dense Pd–Ag MR packed with a Ru-based catalyst in order to produce pure (or at least CO-free) hydrogen. The influence of parameters like WHSV and reaction pressure on the performances in terms of glycerol conversion, hydrogen yield and gas selectivity (as well as CO-free hydrogen recovery for only the MR) of both the MR and a TR (exercised at the same MR operating conditions) is presented.

2. Experimental section

2.1. Experimental setup

Fig. 1 illustrates the MR consisting of a dense, tubular pin-hole free Pd–Ag membrane, having wall thickness of 50 μm, outer diameter 10 mm, length 150 mm. It is inserted in a tubular stainless steel (SS) module, length 280 mm and internal diameter of 20 mm. The dense Pd–Ag membrane is produced by cold-rolling and diffusion welding technique [20] and presents an upper working temperature limit around 450 °C. It is joined to two stainless steel tube ends for the membrane housing, whose one of them is closed. In order to avoid the mixing of retentate and permeate streams, a graphite gasket is used. The MR is heated by means of heating filaments connected to a temperature-controller with a three points thermocouple placed inside MR. The sweep gas (31.3 ml/min) is fed into the permeate side in counter current flow configuration with respect to the reactants by means of mass-flow controller (Brooks Instruments 5850S). Liquid water and glycerol are mixed in a solution with a feed molar ratio $H_2O/C_3H_8O_3 = 6/1$ and it is pumped ($Q_{TOT\text{-}reactants} = 3.9 \cdot 10^{-3}$ mol/min) into reaction side by means of a HPLC pump (Dionex). The MR is operated at 400 °C and the absolute reaction pressure ranges between 1.0 and 5.0 bar, regulated by means of a back pressure controller placed at the retentate outlet stream pipeline. WHSV is varied from 0.1 h^{-1} to 1.0 h^{-1}.

A constant nitrogen molar rate (28.5 ml/min) as internal standard gas is fed with the reactants into MR reaction side. The retentate stream is passed over a cold-trap in order to condensate unreacted products (glycerol, water, etc.). Thus, dry outlet streams from permeate and retentate sides are analyzed using a temperature programmed HP 6890 GC with two thermal conductivity detectors at 250 °C and Ar as carrier gas. The GC is equipped by three packed columns: Porapack R 50/80 (8 ft × 1/8 in) and Carboxen™ 1000 (15 ft × 1/8 inch) connected in series, and a Molecular Sieve 5 Å (6 ft × 1/8 inch).

The MR is packed in the membrane lumen with 3 g of a commercial 0.5 wt% Ru–Al_2O_3 reforming catalyst, furnished by Johnson Matthey. The catalyst is placed between glass spheres (<2 mm diameter) layers. Before reaction, the catalytic bed was pre-heated using nitrogen up to 400 °C under

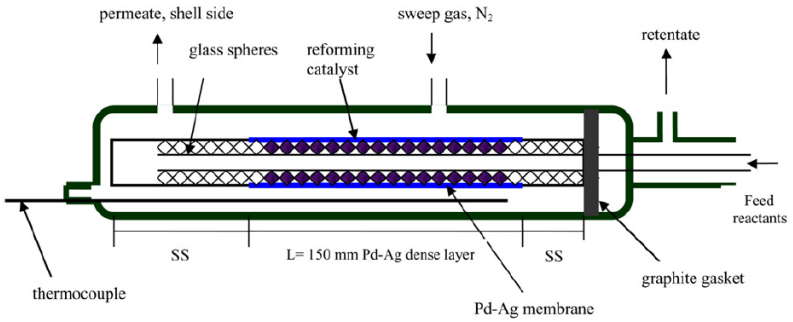

Fig. 1 – MR scheme.

atmospheric pressure and, afterwards, reduced by using hydrogen (1.8×10^{-3} mol/min) at the same temperature for 2 h.

The experimental tests for the TR were performed using the MR with the inlet and outlet permeate side completely closed. Therefore, in this case only the reformed stream was analyzed by GC.

Each experimental point obtained in this work is an average value of 10 experimental measurements, whose one of them takes place during 15 min. After each experimental cycle, (around ~150 min), the catalyst is subjected to regeneration process using pure hydrogen (1.8×10^{-3} mol/min) for 2–3 hr.

For each experimental measurement, carbon balance was closed with a maximum error lower than 3%.

2.2. Definitions for MR and TR performances

Glycerol steam reforming reaction is a process involving a complex mechanism of reactions as confirmed by Valliyappan et al. [12]. As a general information, Valliyappan proposed a scheme of reactions taking place during GSR process at T <700 °C as summarized below:

Steam reforming of pure glycerol:

$$C_3H_8O_3 \xrightarrow{H_2O} 3CO + 4H_2 \quad (1)$$

Water gas shift reaction:

$$CO + H_2O \rightleftarrows CO_2 + H_2 \quad (2)$$

Overall glycerol steam reforming reaction:

$$C_3H_8O_3 + 3H_2O \rightleftarrows 3CO_2 + 7H_2 \quad (3)$$

Steam reforming of methane:

$$CH_4 + H_2O \rightleftarrows CO + 3H_2 \quad (4)$$

Steam reforming of ethanol:

$$C_2H_5OH + H_2O \rightleftarrows CO_2 + CH_4 + 2H_2 \quad (5)$$

Steam reforming of aldehyde:

$$CH_3CHO + H_2O \rightleftarrows CO_2 + CH_4 + 2H_2 \quad (6)$$

The following definitions are used for describing both TR and MR performances:

$$C_3H_8O_3 \text{ conversion (into gas)}, (\%) = \frac{CO_{OUT} + CO_{2,OUT} + CH_{4,OUT}}{C_3H_8O_{3,IN}} \times 100 \quad (7)$$

$$\text{Selectivity}, (S_x, \%) = \frac{i_{OUT}}{CO_{OUT} + CO_{2,OUT} + CH_{4,OUT}} \times 100 \quad (8)$$

where "i" can represent CO_2, CH_4 and CO products, respectively, whereas suffix "OUT" refers to the outlet stream of each species going out from the reactor (retentate stream for the MR).

$$\text{CO-free } H_2 \text{ recovery}, (\%) = \frac{H_{2,\,permeate}}{H_{2,permeate} + H_{2,\,retentate}} \times 100 \quad (9)$$

(only for the MR)

$$H_2 \text{ yield } (\%) = \frac{H_{2,\,OUT}}{7C_3H_8O_{3,IN}} \times 100 \quad (10)$$

The hydrogen yield is calculated referring to the overall GSR reaction stoichiometry (3). Therefore, it represents the ratio between the hydrogen totally produced from the reaction and that theoretically producible from overall GSR reaction. Suffix "IN" refers to the feed stream.

3. Results and discussion

3.1. Permeation tests

Pd–Ag membrane was characterized in terms of permeation with pure gases, resulting that it is completely perm-selective towards H_2 with respect to other gases, such as N_2, CO, CO_2 and CH_4. Generally, keeping constant the temperature the hydrogen permeation through a dense palladium-based membrane occurs via solution/diffusion mechanism. This transport is described by the following general expression (11-a):

$$J_{H_2} = \frac{Pe}{\delta}\left(p^n_{H_2-retentate} - p^n_{H_2-permeate}\right) \quad (11\text{-a})$$

where: J_{H2} is the hydrogen flux permeating through Pd–Ag membrane, Pe the hydrogen permeability, δ the Pd–Ag membrane thickness, $p_{H_2-retentate}$ and $p_{H_2-permeate}$ the hydrogen partial pressure in the retentate and permeate sides, respectively, and "n" the dependence factor of hydrogen partial pressure (in the range 0.5–1.0 [21]). Factor "n" is an indicator of the rate-controlling step of the permeation. If the diffusion of atomic hydrogen through the dense metal layer is rate-limiting, then the hydrogen flow is directly proportional to the hydrogen partial pressure square root difference between the retentate and permeate sides (Sievets' law).

In Fig. 2(a), the hydrogen flux permeating through the membrane is illustrated by varying "n", with the highest linear regression value (R^2) corresponding to $n = 0.5$. Therefore, this result confirms that Sieverts' law is followed (11-b):

$$J_{H_2} = \frac{Pe}{\delta}\left(p^{0.5}_{H_2-retentate} - p^{0.5}_{H_2-permeate}\right) \quad (11\text{-b})$$

Previous permeation experimental tests on this membrane were carried out at different temperatures [22]. They depicted that temperature dependence of the hydrogen permeability can be expressed by means of an Arrhenius-like Eq. (12):

$$Pe = Pe_0 \exp(-E_a/RT) \quad (12)$$

where Pe_0 is the pre-exponential factor, E_a the apparent activation energy, R the universal gas constant, T the absolute temperature. The calculated E_a, 8.58 kJ/mol, and Pe_0, 1.14×10^{-6} mol m/(m^2 s kPa$^{0.5}$) are in good agreement with other experimental data found in literature for the same kind of Pd-based membranes [23].

Furthermore, in Fig. 2b the reduction of permeating capacity of the membrane in terms of hydrogen permeating flux after the first reaction cycle (corresponding to 10 consecutive measurements) is reported. This phenomenon occurred after all reaction cycles and, as even reported by

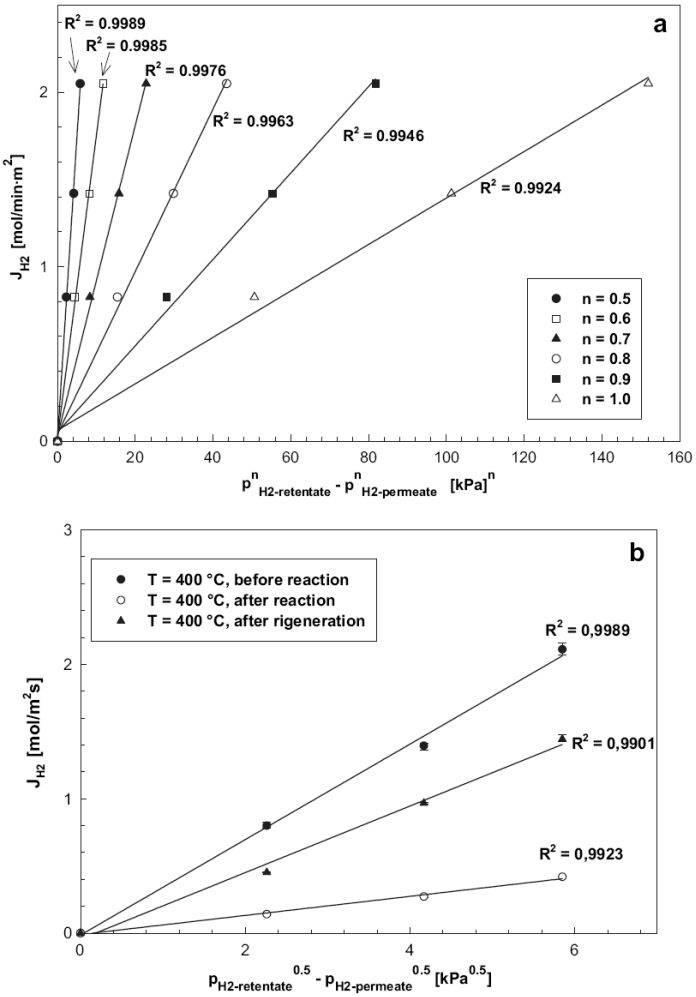

Fig. 2 – (a). Hydrogen flux permeating through Pd–Ag membrane at 400 °C vs hydrogen permeation driving force at different "*n*" factor. (b). Hydrogen flux permeating through Pd–Ag membrane at 400 °C vs hydrogen partial pressure square root difference between retentate and permeate sides: before and after a reaction cycle, and after regeneration procedure.

Slinn et al. [7], it is probably due to carbon deposition on the membrane surface taking place during the reaction. In particular, Slinn reported a carbon–hydrogen–oxygen equilibrium phase diagram, where carbon deposition boundary is present. The carbon boundary is the line below carbon is present as by-product. The authors highlighted that fossil fuels show a relatively low oxygen content within their molecular structure and are placed above the carbon boundary, in equilibrium with solid carbon. On the contrary, glycerol shows a higher oxygen content with an oxygen/carbon ratio equal to 1/1 and, then, exactly at the carbon boundary [7].

Moreover, in a thermodynamic study, Adhikari et al. [6] showed the possible reactions that can cause carbon formation during GSR reaction. In particular, no carbon is formed at temperature higher than ~730 °C and water to glycerol feed ratio higher than 6/1. In this study, after each reaction cycle, a hydrogen stream is flowed for 2 h into the reaction side in order to convert the carbon deposited on the membrane surface into methane (as verified analyzing the retentate stream by GC), according to the following reaction (13):

$$C + 2H_2 = CH_4 \qquad \Delta H = -75\ \text{kJ/mol} \tag{13}$$

As confirmed by Lin et al. [24], this reaction is favoured at relatively low temperature despite of using oxygen, more favorable at higher temperature. However, Fig. 2(b) illustrates that, after the catalyst regeneration procedure, a complete

recovery of permeating capacity of the membrane was not achieved. Therefore, it was necessary to supply a hydrogen stream in a time range of 4 h in order to completely recover the permeating capacity.

The catalyst used in this work (0.5% Ru/Al_2O_3) was chosen according to the activity scale towards GSR reaction [9]: Ru ≈ Rh > Ni > Ir > Co > Pt > Pd > Fe. Moreover, since the decomposition of glycerol to methane is highly favorable during the reforming process [11], the catalyst has to show a sufficient capacity of reforming the produced methane into hydrogen and carbon monoxide (4), favouring the water gas shift reaction (2) in order to convert CO into CO_2 and H_2.

Taking also into account the catalyst activity scale for methane steam reforming reaction [9] (Ru ≈ Rh > Ni > Ir > Pt ≈ Pd > Co ≈ Fe), it appears quite evident that ruthenium should be highly favorable for GSR reaction.

Concerning the operative temperature (400 °C), it is well known that steam reforming of oxygenated hydrocarbons is thermodynamically favorable at lower temperatures than non-oxygenated hydrocarbon [7,25]. Moreover, the Pd–Ag membrane used in this work cannot operate at temperature higher than 450 °C (maximum Pd–Ag membrane temperature limit).

3.2. *Reaction pressure effect*

Fig. 3 shows glycerol conversion versus reaction pressure for both MR and TR. MR glycerol conversion slightly increases by increasing the reaction pressure, reaching almost 15.0% at 5.0 bar. Keeping in mind that the pressure increase produces two conflicting effects: the first one (negative) on the thermodynamic of the overall GSR reaction (3) (it proceeds with an increase of the moles number) and the second one (positive) on hydrogen permeation through the membrane (a higher hydrogen permeation driving force causes a higher hydrogen stream removed from the reaction to the permeate side, favouring the shift of the GSR reaction towards the products and a higher glycerol consume), the increasing trend of MR glycerol conversion probably occurs since the shift effect is prevalent on the thermodynamic one.

Concerning the TR, by increasing the pressure only the detrimental effect on glycerol conversion due to the Thermodynamics is observed. In fact, TR glycerol conversion decreases from around 9.0% at 1.0 bar to 5.0% at 5.0 bar.

However, the low conversions of both MR and TR are probably due to the catalyst's support (Al_2O_3). Although Al_2O_3 is used as a favorable support in catalysts useful for steam reforming of hydrocarbons and ruthenium is one of the most active catalyst for GSR reaction, as also demonstrated by Hirai et al. [9], the combination of ruthenium with an acid support as Al_2O_3 determines low GSR conversions. Furthermore, the carbon formed during the reaction, settling on the membrane, reduces the hydrogen permeating capacity of Pd–Ag membrane, lowering the hydrogen recovery in the permeate zone.

As illustrated in Fig. 4, CO-free hydrogen recovery (HR) (9) increases with the pressure. As above reported, a higher reaction pressure produces a higher hydrogen permeation driving force that allows, for Fick–Sieverts' law, a higher hydrogen stream to be collected in the permeate side. As best result, at 5.0 bar HR was around 20.0%. Even in this case, the low value of HR may be due to the carbon formed during the reaction and deposited on the membrane, causing the inhibition of the hydrogen permeation and, then, affecting negatively the hydrogen recovery.

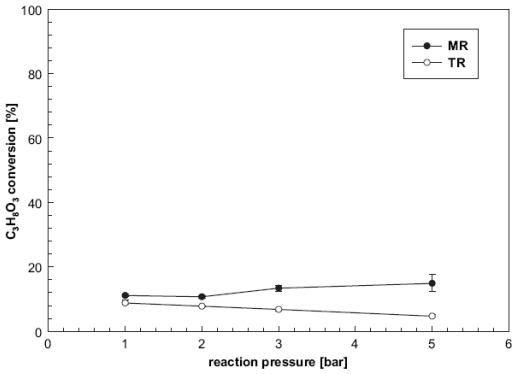

Fig. 3 – Glycerol conversion against reaction pressure for the MR and TR; operative conditions: $T = 400$ °C, $H_2O/C_3H_8O_3 = 6/1$ (mol/mol), WHSV = 1.0 h^{-1}, counter-current flow configuration of sweep-gas, $p_{permeate} = 1.0$ bar and $Q_{sweep-gas}/Q_{C_3H_8O_3-in} = 11.9$.

The hydrogen yield (10) versus reaction pressure is sketched in Fig. 5. At higher pressures, MR hydrogen yield slightly increases. This is due to the positive effect that a higher pressure induces on glycerol conversion. In fact, the higher conversion the higher hydrogen production as well as the higher the pressure the higher the hydrogen stream collected in the permeate side. Nevertheless, as reported in Fig. 3, MR glycerol conversion does not reach great values; as a consequence, low hydrogen yield values are obtained. In details, hydrogen yield is around 5.3% at $p = 1.0$ bar and 7.3%

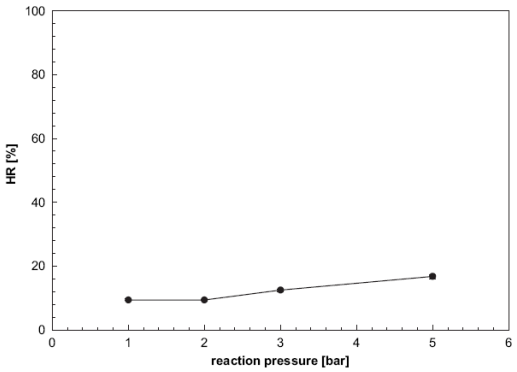

Fig. 4 – CO-free hydrogen recovery (HR) against reaction pressure for the Pd–Ag MR; operative conditions: $T = 400$ °C, $H_2O/C_3H_8O_3 = 6/1$ (mol/mol), WHSV = 1.0 h^{-1}, counter-current flow configuration of sweep-gas, $p_{permeate} = 1.0$ bar and $Q_{sweep-gas}/Q_{C_3H_8O_3-in} = 11.9$.

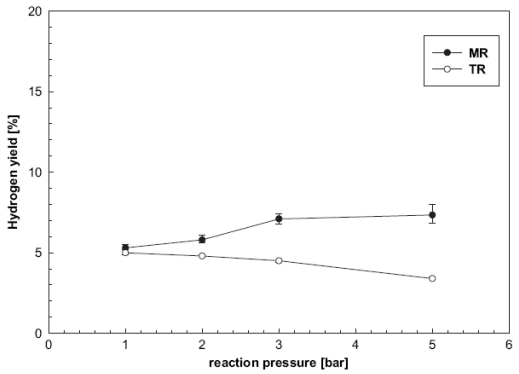

Fig. 5 – Hydrogen yield against reaction pressure for MR and TR; operative conditions: T = 400 °C, $H_2O/C_3H_8O_3$ = 6/1 (mol/mol), WHSV = 1.0 h^{-1}, counter-current flow configuration of sweep-gas, $p_{permeate}$ = 1.0 bar and $Q_{sweep-gas}/Q_{C_3H_8O_3-in}$ = 11.9.

at 5.0 bar. Vice versa, hydrogen yield for TR decreases by increasing the pressure, according to TR conversion trend of Fig. 3. In fact, it is 5.4% at 1.0 bar and around 3.6% at 5.0 bar.

Table 1 reports the MR gas selectivities (8) at different reaction pressures. Relating to CO selectivity, higher pressures act positively on the hydrogen permeation driving force shifting also the water gas shift reaction (2) towards the products, favouring a higher CO consume. In fact, CO selectivity ranges from 51.7% at 1.0 bar to 23.1% at 5.0 bar, whereas CO_2 selectivity increase from 46.2% at 1.0 bar to 72.5% at 5.0 bar. Vice versa, CH_4 selectivity show a constant trend (around to 3.0%).

In conclusion, an increase of the reaction pressure induces an improvement of the MR performances in terms of higher glycerol conversions, hydrogen yields and HRs. Carbon deposition on membrane surface affects negatively the hydrogen permeation through Pd–Ag membrane and combined with the detrimental effect due to the acidic catalyst's support (not very suitable for GSR reaction), represent the main causes of the low MR performances obtained in this work.

However, with respect to the TR operating under the same MR conditions, it was found that the MR offers better performances in terms of glycerol conversion and hydrogen yield.

Table 1 – Gas selectivity against reaction pressure for the Pd–Ag MR; operative conditions: T = 400 °C, $H_2O/C_3H_8O_3$ = 6/1 (mol/mol), WHSV = 1.0 h^{-1}, counter-current flow configuration of sweep-gas, $p_{permeate}$ = 1.0 bar and $Q_{sweep-gas}/Q_{C_3H_8O_3-in}$ = 11.9.

p (bar)	S_{CO}	S_{CO_2}	S_{CH_4}
1	51.7%	46.2%	2.1%
2	32.8%	64.7%	2.5%
3	27.2%	69.6%	3.2%
5	23.1%	72.5%	4.4%

3.3. WHSV effects

Another parameter studied in this work was the WHSV influence on GSR reaction. The reduction of this parameter leads to higher residence time of reactants in the catalytic bed and, thus, higher contact time of them with the catalyst, promoting the conversion. In the first part of this work a WHSV of 1 h^{-1} (corresponding to a feed rate of 0.18 mol/$min_{glycerol}$ $kg_{catalyst}$) was used. This low WHSV value was chosen in order to contain the carbon production during GSR reaction. In fact, Slinn et al. [7] showed, that, carrying out GSR reaction with a platinum alumina catalyst, the best performance was obtained at 0.12 mol/$min_{glycerol}$ $kg_{catalyst}$ as feed rate. In the meanwhile, the authors demonstrated that, at higher feed rate, too consistent carbon formation takes place, causing a fast catalyst degradation. Therefore, we studied the influence of WHSV on GSR reaction working at 400 °C, $H_2O/C_3H_8O_3$ = 6/1 (mol/mol), counter-current flow configuration of sweep-gas and 5.0 bar (best conditions concerning CO-free hydrogen recovery at WHSV = 1 h^{-1}).

Fig. 6 shows glycerol conversion versus WHSV for both MR and TR. MR glycerol conversion results in a higher conversion than the TR owing to the shift effect due to the hydrogen removal through the Pd–Ag membrane. However, in both the reactors, a WHSV decrease acts favorably on glycerol conversion. In fact, the lower the WHSV the higher the residence time of the reactants in the catalytic bed inducing an increase of glycerol conversion. More in details, the conversion reaches 57.0% at WHSV = 0.1 h^{-1} and 12.0% at WHSV = 1.0 h^{-1}, whereas for the TR it is 42.0% at WHSV = 0.1 h^{-1} and 9.0% at WHSV = 1.0 h^{-1}.

Fig. 7 shows the HR trend as a function of WHSV. Also in this case, it was observed that a WHSV decrease produces a positive effect on HR. In fact, a lower WHSV results in a higher hydrogen production. As a consequence, a higher hydrogen partial pressure is realized into reaction side, favouring the hydrogen permeation driving force and, then, collecting a higher CO-free hydrogen stream in the permeate

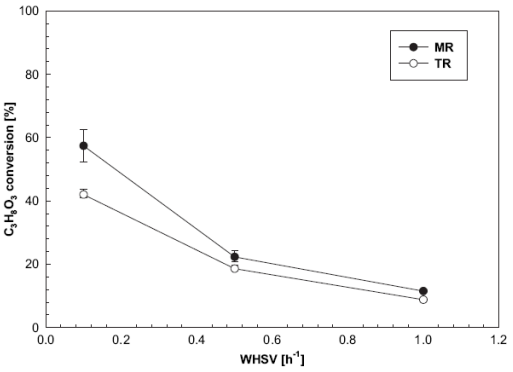

Fig. 6 – Glycerol conversion against WHSV for the MR and TR; operative conditions: T = 400 °C, $H_2O/C_3H_8O_3$ = 6/1 (mol/mol), $p_{reaction}$ = 5.0 bar, counter-current flow configuration of sweep-gas, $p_{permeate}$ = 1.0 bar and $Q_{sweep-gas}/Q_{C_3H_8O_3-in}$ = 11.9.

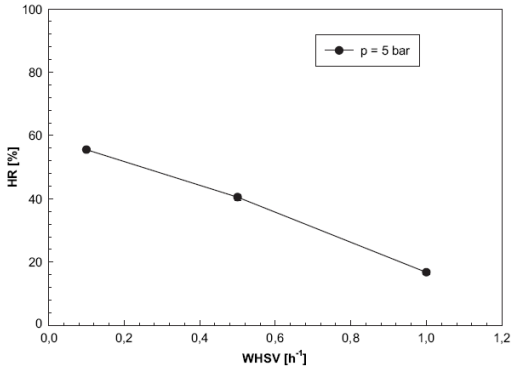

Fig. 7 – CO-free hydrogen recovery (HR) against WHSV for the Pd–Ag MR; operative conditions: $T = 400\ °C$, $p_{reaction} = 5.0$ bar, $H_2O/C_3H_8O_3 = 6/1$ (mol/mol), counter-current flow configuration of sweep-gas, $p_{permeate} = 1.0$ bar and $Q_{sweep-gas}/Q_{C_3H_8O_3-in} = 11.9$.

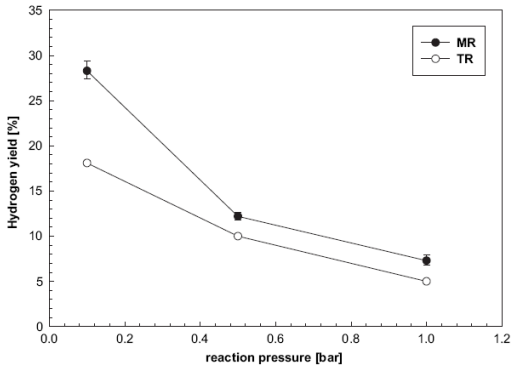

Fig. 8 – Hydrogen yield against WHSV for MR and TR; operative conditions: $T = 400\ °C$, $p_{reaction} = 5.0$ bar, $H_2O/C_3H_8O_3 = 6/1$ (mol/mol), counter-current flow configuration of sweep-gas, $p_{permeate} = 1.0$ bar and $Q_{sweep-gas}/Q_{C_3H_8O_3-in} = 11.9$.

side. In details, HR is around 56.0% at WHSV = 0.1 h^{-1}, whereas it drops to 17.0% at WHSV = 1.0 h^{-1}.

Fig. 8 illustrates the hydrogen yield versus WHSV. Even operating at low WHSV and, hence, high residence times, glycerol conversion still presents low values. In fact, the maximum hydrogen yield obtained in this work was around 28.0% at WHSV = 0.1 h^{-1}.

4. Conclusions

The experimental campaign of this work was focused on GSR reaction performed in a dense Pd–Ag MR packed with a commercial Ru/Al_2O_3 catalyst. Results in terms of glycerol conversion, hydrogen yield and CO-free hydrogen recovery have been deeply discussed and a comparison with a TR, working at the same MR operating conditions, is also proposed. In all cases, it was found that MR seems to be a better choice than the TR. Working at 400 °C, 5.0 bar, $H_2O/C_3H_8O_3 = 6/1$ (mol/mol), $Q_{sweep-gas}/Q_{C_3H_8O_3-in} = 11.9 = 11.9$, WHSV = 0.1 h^{-1} and counter-current flow configuration of sweep-gas, as best result the MR is able to give 57.0% of glycerol conversion, around 60.0% of CO-free hydrogen recovery and 28.0% of hydrogen yield. Carbon formation taking place during the reaction combined with the detrimental effect on GSR reaction due to acidic catalyst's support represent the main problems affecting the whole process. On this basis, it is proposed to continue the work operating at higher temperatures and using another basic catalyst support, more suitable for GSR reaction.

REFERENCES

[1] http://www.epc.eu/TEWN/pdf/309757647_EPC%20Issue%20Paper%2055%2020EU%20energy%20and%20climate%20policy.pdf.
[2] http://www.renewableenergyworld.com/rea/news/home.
[3] Jérôme F, Pouilloux Y, Barrault C. Rational design of solid catalysts for the selective use of glycerol as a natural organic building block. J Chem Sus Chem 2008;7:586–613.
[4] Demirbas A. Biodiesel from waste cooking oil via base-catalytic and supercritical methanol transesterification. Energy Conv Manag 2009;50(4):923–7.
[5] Huber GW, Shabaker JW, Dumesic JA. Raney Ni–Sn catalyst for H_2 production from biomass-derived hydrocarbons. Science 2003;30:2075–7.
[6] Adhikari S, Sandun F, Steven RG, To SDF, Bricka RM, Steele PH, et al. A thermodynamic analysis of hydrogen production by steam reforming of glycerol. Int J Hydrogen Energy 2007;32:2875–80.
[7] Slinn M, Kendall K, Mallon C, Andrews J. Steam reforming of biodiesel by-product to make renewable hydrogen. Bioresour Technol 2008;99:5851–8.
[8] Byrd AJ, Pant KK, Gupta RB. Hydrogen production from glycerol by reforming in supercritical water over Ru/Al_2O_3 catalyst. Fuel 2008;87:2956–60.
[9] Hirai T, Ikenaga N, Miyake T, Suzuki T. Production of hydrogen by steam reforming of glycerin on ruthenium catalyst. Energy Fuels 2005;19:1761–2.
[10] Iriondo A, Barrio VL, Cambra JF, Arias PL, Guëmez MB, Navarro RM, et al. Hydrogen production from glycerol over nickel catalysts supported on Al_2O_3 modified by Mg, Zr, Ce or La. Topics Catal 2008;49:46–58.
[11] Zhang B, Tang X, Li Y, Xu Y, Shen W. Hydrogen production from steam reforming of ethanol and glycerol over ceria-supported metal catalysts. Int J Hydrogen Energy 2007;32:2367–73.
[12] Valliyappan T, Ferdous D, Bakhshi NN, Dalai AK. Production of hydrogen and syngas via steam gasification of glycerol in a fixed-bed reactor. Topics Catal 2008;49:59–67.
[13] Sanchez Marcano JG, Tsotsis ThT, editors. Catalytic membranes and membrane reactors. Wiley-VCH Verlag GmbH; 2002.
[14] Tong J, Matsumura Y. Effect of catalytic activity on methane steam reforming in hydrogen-permeable membrane reactor. Appl Catal A Gen 2005;286. 226–31.
[15] Basile A, Gallucci F, Iulianelli A, Tosti S. CO-free hydrogen production by ethanol steam reforming in a Pd–Ag membrane reactor. Fuel Cells 2008;8:62–8.

[16] Iulianelli A, Longo T, Basile A. CO-free hydrogen production by steam reforming of acetic acid carried out in a Pd–Ag membrane reactor: the effect of co-current and counter-current mode. Int J Hydrogen Energy 2008;33:4091–6.
[17] Iulianelli A, Longo T, Basile A. Methanol steam reforming reaction in a Pd–Ag membrane reactor for CO-free hydrogen production. Int J Hydrogen Energy 2008;33:5583–8.
[18] Velu S, Suzuki K, Kapoor MP, Ohashi F, Osaki T. Selective production of hydrogen for fuel cells via oxidative steam reforming of methanol over CuZnAl (Zr)-oxide catalysts. Appl Catal A Gen 2001;213:47–63.
[19] Lin YM, Rei MH. Study on the hydrogen production from methanol steam reforming in supported palladium membrane reactor. Catal Today 2001;67:77–84.
[20] Tosti S, Bettinali L. Diffusion bonding of Pd–Ag membranes. J Mater Sci 2004;39:3041–6.
[21] Dittmeyer R, Höllein V, Daub K. Membrane reactors for hydrogenation and dehydrogenation processes based on supported palladium. J Mol Catal A Chem 2001;173:135–84.
[22] Iulianelli A, Basile A. An experimental study on bio-ethanolsteam reforming in a catalytic membrane reactor. Part I: temperature and sweep-gasflow configuration effects. Int J Hydrogen Energy 2010;35(7):3170–7.
[23] Basile A, Tosti S, Gallucci F. Synthesis, characterization and applications of palladium membranes. In: Malada R, Menendez M, editors. Inorganic membranes: synthesis, characterization and applications. Membrane science and technology. ISSN0927-5193. Elsevier; 2008. p. 255–323 [chapter 8].
[24] Lin SY, Kim BH, Ha SY. Hydrogen production from ethanol steam reforming over supported cobalt catalysts. Catal Lett 2008;122:295–301.
[25] Davda RR, Shabaker JW, Huber GW, Cortright RD, Dumesic JA. A review of catalytic issues and process conditions for renewable hydrogen and alkanes by aqueous-phase reforming of oxygenated hydrocarbons over supported metal catalysts. Appl Catal B Environ 2005;56:171–86.

Interconnection between Paper 1 & Paper 2

In the paper 1, GSR reaction is carried out in the Pd-Ag MR packed with Ru/A_2O_3 catalyst. The influence of reaction pressure and sweep-gas flow rate on MR performances is studied.

As best result the MR is able to give 57.0% of glycerol conversion, around 60.0% of CO-free hydrogen recovery and 28.0% of hydrogen yield at 400 °C and 5 bar.

An important issue was the carbon formation during the GSR reaction, which was able to negatively affect the performances of the Pd-Ag membrane in terms of a lower hydrogen permeated flux and catalyst deactivation. This drawback is probably due to the effect of low metal content (~ 0.5% of Ru)

So, in the paper II a (15%wt) Co-based catalyst was chosen according to the activity scale towards GSR reaction and the influence of reaction pressure and space velocity on MR performance is analyzed.

ASIA-PACIFIC JOURNAL OF CHEMICAL ENGINEERING
Asia-Pac. J. Chem. Eng. 2010; **5**: 138–145
Published online 20 August 2009 in Wiley InterScience
(www.interscience.wiley.com) DOI:10.1002/apj.365

Curtin University of Technology

Special Theme Research Article

Production of hydrogen via glycerol steam reforming in a Pd-Ag membrane reactor over Co-Al_2O_3 catalyst

*A. Iulianelli, T. Longo, S. Liguori and A. Basile**

Institute on Membrane Technology of Research National Council (ITM-CNR), Via P.Bucci c/o University of Calabria – Cubo 17/C, Rende 87036, Italy

Received 3 December 2008; Revised 8 April 2009; Accepted 15 May 2009

ABSTRACT: Generally, biodiesel fuel, when converted from vegetables oils, produces around 10 wt% of glycerol as a byproduct, which could be used for producing hydrogen by a steam-reforming reaction. Different scientific works have been realized in conventional reactors on the steam reforming of glycerol (GSR) in the aqueous or the gas phase. High reaction pressure and a relatively small catalyst deactivation are noticed when GSR is carried out in an aqueous phase, whereas the catalyst deactivation is the main disadvantage in the gas phase. In this work, GSR reaction was performed in a perm-selective Pd-Ag membrane reactor (MR) packed with a Co-Al_2O_3 commercial catalyst in order to extract a CO-free hydrogen stream and also enhance the performances in terms of glycerol conversion and hydrogen yield with respect to a traditional reactor (TR), both working at weight hourly space velocity (WHSV) = 1.01 h^{-1}, 400 °C and $H_2O/C_3H_8O_3$ = 6/1. In MR, a maximum glycerol conversion of around 45.0% was achieved at 1.0 bar as reaction pressure, whereas it was around 94% at 4.0 bar. Moreover, as best value, more than 60.0% of CO-free hydrogen recovery was achieved in the MR at 4.0 bar and 22.8 of sweep factor (sweep gas to glycerol ratio). © 2009 Curtin University of Technology and John Wiley & Sons, Ltd.

KEYWORDS: membrane reactor; palladium membrane; pure hydrogen; glycerol steam reforming

INTRODUCTION

Air pollution can be due to the presence of solid, liquid, or gaseous substances that are able to alter the natural environmental conditions, with harmful effects on humans. One of the most relevant causes of environmental pollution is represented by the automotive industry and, in particular, by the combustion engines fuelled by derived fossil fuels. One of the possible solutions for limiting the use of derived fossil fuels could be represented by alternative and clean energy sources. For example, biodiesel is a renewable fuel, and it has been gaining much attention in the last few years.

Currently, owing to high cost of vegetable oils,[1] biodiesel is more expensive than the traditional diesel, but in the process of biodiesel production the exploitation of the byproducts could represent an interesting and economical advantage. For instance, when biodiesel is produced through a process of transesterification of vegetable oils, glycerol is produced as a byproduct. The use of glycerol for producing pure hydrogen or synthesis gas by steam-reforming reaction could be particularly interesting. To the best of our knowledge, GSR reaction has been only studied in conventional reactors. In particular, the GSR reaction can be carried out in either the aqueous or the gas phase. When operated in the aqueous phase, its low catalyst deactivation is an advantage, but it has to be operated at high pressures.[2] On the contrary, in the gas phase, it can be carried out at atmospheric pressure, presenting a great catalyst deactivation as a disadvantage.[2]

A reaction kinetics study on the aqueous-phase GSR reaction indicates that Pt and Pd catalysts are selective for producing hydrogen, with Pt showing high catalytic activity.[3]

Metals such as Ni and Ru exhibit good catalytic activity but lead to alkanes formation. Vice versa, Ir, Co, Cu, Ag, Au, and Fe show low catalytic activity.

Huber *et al*.[3] used a heterogeneous catalyst based on Ni, Sn, and Al, active and selective for hydrogen production by aqueous-phase GSR reaction.

Zhang *et al*.[4] studied the hydrogen production by the steam-reforming reaction of ethanol and glycerol over Ir, Co, and Ni-based catalysts, determining that the Ir-based catalyst is significantly more active and selective toward hydrogen production from GSR reaction.

Iriondo *et al*.[5] studied the GSR reaction in both the aqueous and the gas phase over alumina-supported Ni catalysts, modified with Ce, Mg, Zr, and La. For aqueous phase reforming, the addition of Ce, La, and Zr

**Correspondence to*: A. Basile, Institute on Membrane Technology, ITM-CNR, c/o University of Calabria, via P. Bucci, cubo 17/C-87030 Rende (CS), Italy. E-mail: a.basile@itm.cnr.it

to Ni-Al_2O_3 catalyst improves the glycerol conversion with respect to the only one Ni-Al_2O_3 catalyst. The authors suggested that the differences in catalytic activity are related to geometric effects caused by the Ni and La or the close interaction between Ni and Zr. Moreover, this study noted that the catalyst deactivation becomes relevant after few hours under operation, owing to the oxidation of the active catalyst metallic phase. Vice versa, in gas phase, using Ce, La, Mg, and Zr as promoters of Ni-based catalysts, the enhancement of the catalytic activity is noticed, due to the capacity of activating steam (Zr) and the stability of nickel phase under reaction conditions.

Hirai *et al*.[2] proposed the following catalytic activity scale for the gas-phase GSR reaction: Ru ≈ Rh > Ni > Ir > Co > Pt > Pd > Fe. Although a noble metal such as Rh is very effective for the steam reforming of hydrocarbons and less susceptible to carbon formation, Rh-based catalysts are not common in industrial applications owing to their high cost.

The GSR reaction carried out in TRs involves a complex reaction system that produces undesirable byproducts besides hydrogen.[1] Having in mind the CO-free hydrogen production for directly feeding a PEMFC (proton exchange membrane fuel cell), the hydrogen rich-gas stream going out from a conventional reformer needs purification by means of successive purifying steps such as water gas shift reaction, pressure swing adsorption, etc. Therefore, it would be economically advantageous to develop a process that is able to produce a CO-free hydrogen stream in only one system. This can be achieved by means of hydrogen permselective MRs, which are able to both carry out the reaction and remove pure hydrogen in the same device. Unfortunately, scientific studies on GSR reaction in MRs are not present in the literature.

Thus, the aim of this work is to carry out the GSR reaction in a dense Pd-Ag MR for extracting a CO-free hydrogen stream, comparing the experimental results with those of a TR operated under the same MR conditions. Both the TR and the MR are packed with a Co-Al_2O_3 catalyst and work at 400 °C, water/glycerol molar ratio = 6/1 and WHSV = 1.01 h^{-1}.

The Co-Al_2O_3 catalyst was chosen because the analysis of the byproducts took place during the GSR reaction.[1] Among them, the presence of ethanol was noticed. Therefore, as the main purpose of each process is to obtain a total conversion of the reactants with a limited byproducts production, it could be advantageous to choose a selective catalyst that is able to convert such a byproduct as ethanol and catalyze the GSR reaction. As reported in literature, a good compromise can be represented by the use of Co-based catalysts.[2,6,7]

The performances in terms of glycerol conversion, products selectivity, hydrogen yield, and CO-free hydrogen recovery are presented and discussed, paying particularly attention to the effect of the reaction pressure and sweep gas molar rate on the GSR reaction system, when carried out in MR.

EXPERIMENTAL

Experimental details

The scheme of the plant for carrying out the experimental tests on both the MR and TR is represented in Fig. 1, whereas the image of the real plant is reported in Fig. 2. The reaction temperature is set at 400 °C, due to the maximum working temperature of the Pd-Ag membrane (around 450 °C), and the absolute reaction pressure range being between 1.0 and 4.0 bar (abs.), regulated by means of a back pressure controller. A sweep gas (N_2) stream is used in the permeate side of the MR, fed by means of a mass-flow controller (Brooks Instruments 5850S) driven by a computer software furnished by Lira (Italy). In all the experiments, the absolute MR permeate pressure as well as the WHSV (calculated as the ratio between glycerol mass flow rate inlet and mass of catalyst) are kept constant at 1.0 bar and 1.01 h^{-1} respectively. The sweep gas flow rate ranges from 1.42×10^{-3} to 1.25×10^{-2} mol min^{-1}, corresponding to a sweep factor (SF) (defined as the molar ratio within the sweep gas and the feed glycerol flow rates (1)) varying between 2.6 and 22.8.

$$SF = \frac{Q_{SWEEP-GAS,IN}}{Q_{C_3H_8O_3,IN}} \quad (1)$$

where $Q_{SWEEP-GAS,IN}$ and $Q_{C_3H_8O_3,IN}$ are respectively the sweep gas and glycerol flow rates fed to the MR.

A liquid water and glycerol solution with a feed molar ratio $H_2O/C_3H_8O_3 = 6/1$ is fed by means of a HPLC pump (Dionex) into a prereaction zone at 400 °C before coming into the reaction side of the Pd-Ag MR. Moreover, a constant nitrogen molar rate (1.27×10^{-3} mol min^{-1}) is fed as internal standard gas with the reactants into the MR reaction side. The retentate stream is passed over a cold-trap in order to condensate unreacted products (glycerol, water, etc.). Both permeate and retentate stream compositions are analyzed using a temperature-programmed HP 6890 GC with two thermal conductivity detectors at 250 °C and Ar as carrier gas. The GC is equipped by three packed columns: Porapack R 50/80 (8 ft × 1/8 in) and Carboxen™ 1000 (15 ft × 1/8 in) connected in series, and a Molecular Sieve 5Å (6 ft × 1/8 in).

The MR was packed with 3 g of a Co-Al_2O_3 commercial catalyst in pellet form furnished by Johnson Matthey. Before reaction, the catalytic bed was preheated using nitrogen up to 400 °C under atmospheric pressure and, afterward, reduced by using hydrogen

Asia-Pac. J. Chem. Eng. 2010; **5**: 138–145
DOI: 10.1002/apj

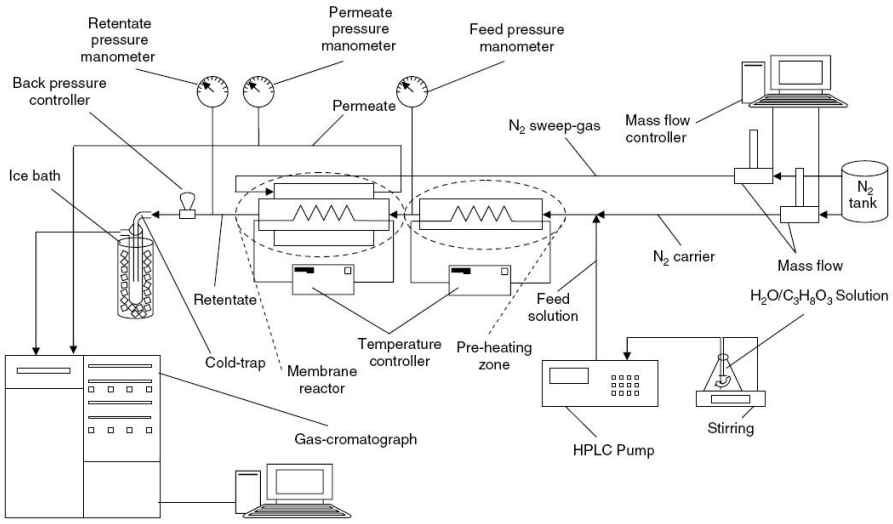

Figure 1. Scheme of the plant for the steam reforming of glycerol carried out in the Pd-Ag membrane reactor.

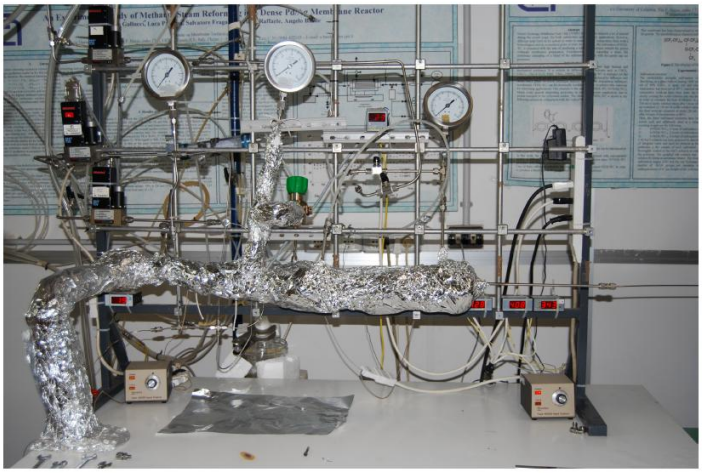

Figure 2. Experimental plant for the glycerol steam-reforming reaction in a Pd-Ag membrane reactor. This figure is available in colour online at www.apjChemEng.com.

(1.80×10^{-3} mol min^{-1}) at the same temperature for 2 h.

Each experimental point obtained in this work is an average value of five experimental points taken in 75 min at steady-state conditions. After each experimental cycle (ranging between 150 and 285 min), the catalyst was regenerated using hydrogen (1.80×10^{-3} mol min^{-1}) for 2 h. A flat temperature profile along the reactor was confirmed during the reaction by means of a three-point thermocouple placed into the reactor.

As already reported by Valliyappan *et al.*,[1] the overall system of reactions, which may take place during GSR reaction at $T < 700\,°C$, can be represented by the following reaction equations:

Steam reforming of pure glycerol:

$$C_3H_8O_3 \xrightarrow{H_2O} 3CO + 4H_2 \qquad (2)$$

Water gas shift reaction (WGS):

$$CO + H_2O \rightleftharpoons CO_2 + H_2 \quad (3)$$

Overall GSR reaction:

$$C_3H_8O_3 + 3H_2O \rightleftharpoons 3CO_2 + 7H_2 \quad (4)$$

The following definitions are used for describing the TR and MR performances:

$$C_3H_8O_3 \text{ conversion (into gas), (\%)} = \frac{CO_{OUT} + CO_{2,OUT} + CH_{4,OUT}}{C_3H_8O_{3,IN}} \times 100 \quad (5)$$

$$X \text{ selectivity, } (S_x, \%) = \frac{X_{OUT}}{H_{2,OUT} + CO_{OUT} + CO_{2,OUT} + CH_{4,OUT}} \times 100 \quad (6)$$

where X is H_2, CO_2, CH_4, and CO, respectively.

$$CO - \text{free } H_2 \text{ recovery, (\%)} = \frac{H_{2,permeate}}{H_{2,permeate} + H_{2,retentate}} \times 100 \text{ (only for the MR)} \quad (7)$$

$$H_2 \text{ yield (\%)} = \frac{H_{2,OUT}}{7\ C_3H_8O_{3,IN}} \times 100 \quad (8)$$

Regarding the MR, the subscript 'OUT' indicates the total (retentate and permeate sides) outlet flow rate of each species, while 'IN' refers to the feed stream.

MR/TR DESCRIPTION

The MR consists of a tubular stainless steel module (length 280 mm, *i.d.* 20 mm) containing a tubular pine-hole free Pd-Ag membrane permeable only to hydrogen (thickness 50 µm, *o.d.* 10 mm, length 145 mm) (Fig. 3). The dense Pd-Ag membrane is produced by cold-rolling and diffusion welding technique[8] and has an upper temperature limit of around 450 °C. It is joined to two stainless steel tube ends for the membrane housing, one of which is closed. In Fig. 4, the scheme of the MR in countercurrent flow configuration is also shown. Catalyst pellets are packed into the lumen of the MR and glass spheres (2 mm diameter) are placed at both the extremities of the membrane. The experimental tests for the TR were performed using the MR with the inlet and outlet permeate side completely closed. Therefore, in this case, only the reformed stream was analyzed by GC.

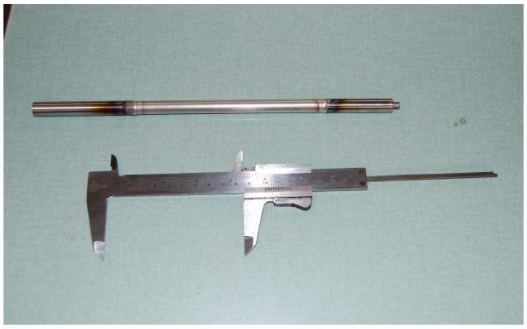

Figure 3. Dense tubular Pd-Ag membrane. This figure is available in colour online at www.apjChemEng.com.

RESULTS AND DISCUSSION

First, the GSR was carried out at a reaction pressure of 1.0 bar (abs.), paying particular attention to stability tests. Figure 5 sketches the glycerol conversion of the MR (operated at SF = 22.8) against time on stream. In the range of 0–100 min, the experimental data can be considered at non-steady-state conditions, whereas between 100 and 180 min the conversion shows a constant trend (standard deviation lower than 4%). At time

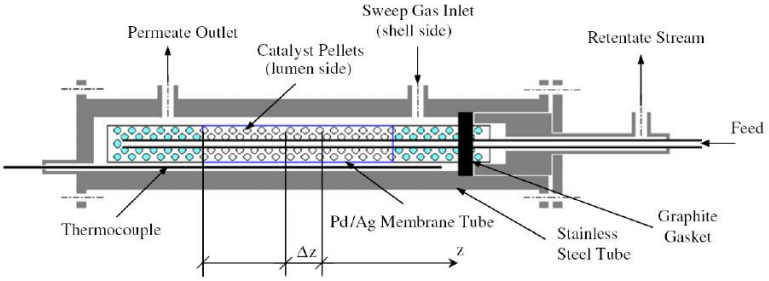

Figure 4. Scheme of the Pd-Ag MR in a countercurrent flow configuration of sweep gas. This figure is available in colour online at www.apjChemEng.com.

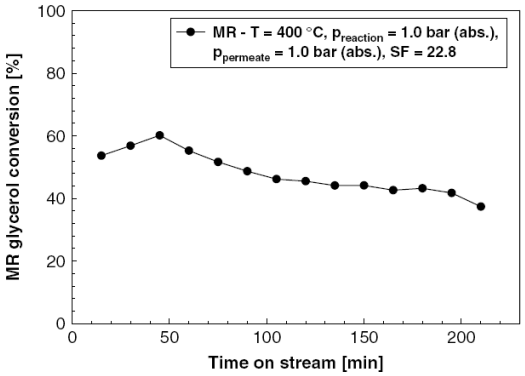

Figure 5. Glycerol conversion *vs* time on stream for the Pd-Ag MR at $T = 400\,°C$, $p_{reaction} = 1.0$ bar, $p_{permeate} = 1.0$ bar, SF = 22.8, and a countercurrent flow configuration.

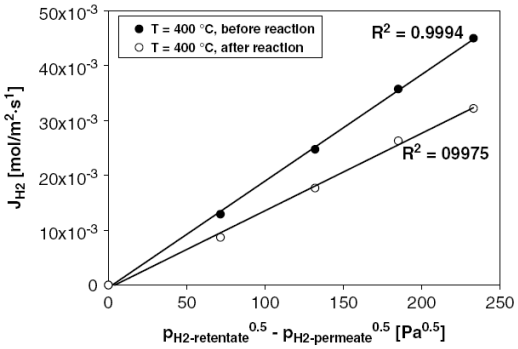

Figure 6. Hydrogen permeating flux *vs* hydrogen partial pressure square root difference between retentate and permeate sides of the Pd-Ag MR before and after reaction at 400 °C.

on stream higher than 180 min, the conversion drops irreversibly due to the catalyst deactivation, probably caused by the carbon formation, which also acts negatively on the Pd-Ag membrane performances, lowering the hydrogen permeating flux through the membrane in particular. In fact, as indicated by Zhang *et al*.[4] using Co-based catalysts, a rapid deactivation is noticeable owing to coke formation during the dehydration of glycerol to ethylene or propylene. Moreover, Iriondo *et al*.[5] also reported that utilizing an acid support such as Al_2O_3, a severe deactivation is observed. Vice versa, when utilizing CeO_2 as support, this phenomenon can be avoided.[4]

Hydrogen permeation experimental tests were carried out before and after the reaction test. Figure 6 clearly illustrates that, in both cases, before and after the reaction tests, the hydrogen flux permeating through the dense Pd-Ag membrane follows a linear trend with the hydrogen partial pressure square root difference between retentate and permeate sides of the MR. This confirms that, in both cases, Sieverts' law (Eqn 9) is followed.

$$J_{H2} = \frac{Pe}{\delta} \cdot (p_{H2-retentate}^{0.5} - p_{H2-permeate}^{0.5}) \qquad (9)$$

where J_{H2} is the hydrogen flux permeating through the membrane, Pe is the hydrogen permeability, δ is the Pd-Ag membrane thickness, $p_{H2-retentate}$ is the hydrogen partial pressure on the retentate side, and $p_{H2-permeate}$ is the hydrogen partial pressure on the permeate side.

It is quite evident that the hydrogen permeating flux decreases after the reaction cycle. This is probably due to the negative effect of carbon formation that, depositing on the membrane surface, does not allow an efficient hydrogen permeation to be realized. Taking into account what is reported in literature,[9] the deactivation of Co-based catalysts due to coke built up on its surface can be recovered under hydrogen treatment with methane formation. Therefore, at least after 200 min on stream, a hydrogen stream was flowed into the catalytic bed for 2 h, even removing the carbon deposited on the membrane surface. In fact, methane formation was noticed during the regeneration procedure.

The trend shown in Fig. 5 was reproduced in all the MR experimental tests. Thus, the experimental data in terms of glycerol conversion, CO-free hydrogen recovery, hydrogen yield, and product selectivities are calculated as the average value of at least five experimental points, taken after transient phenomena (0–100 min on stream) and before the glycerol conversion drop (after 180 min on stream).

The stability tests were also realized on the TR and, in Fig. 7, the glycerol conversion against time on stream is shown. Even in this case, transient phenomena can

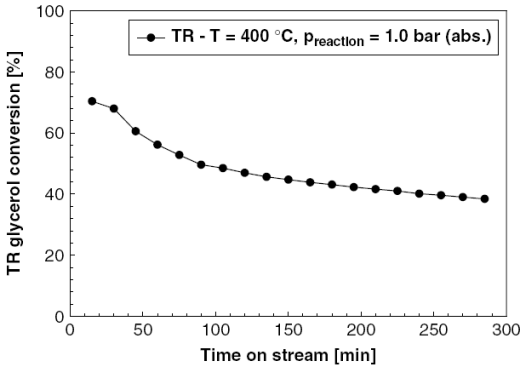

Figure 7. Glycerol conversion *vs* time on stream for the TR at $T = 400\,°C$ and $p_{reaction} = 1.0$ bar, H_2O/glycerol = 6/1, WHSV = 1.01 h^{-1}.

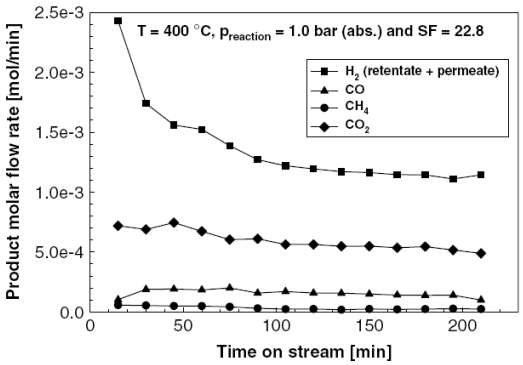

Figure 8. Product molar flow rate *vs* time on stream for Pd-Ag MR at $T = 400\,°C$, $p_{reaction} = 1.0$ bar (abs.), $p_{permeate} = 1.0$ bar (abs.), and SF = 22.8, H_2O/glycerol = 6/1, WHSV = 1.01 h^{-1}.

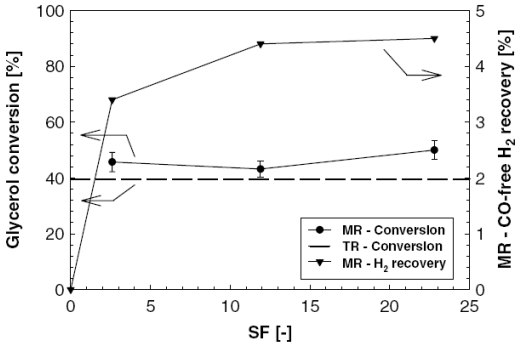

Figure 9. Glycerol conversion and CO-free hydrogen recovery *vs* sweep factor (SF);. Experimental conditions: $T = 400\,°C$, WHSV = 1.01 h^{-1}, H_2O/glycerol = 6/1, $p_{reaction} = 1.0$ bar (abs.), $p_{permeate}$ (only MR) = 1.0 bar (abs.), MR in a countercurrent flow configuration.

be noticed up to around 100 min on stream, whereas successively the glycerol conversion slowly decreases an almost constant trend between 220 and 280 min is achieved, where the average glycerol conversion presents a standard deviation lower than 3%.

In Fig. 8, the molar flow rates of the MR products at 400 °C, reaction pressure of 1.0 bar, and SF = 22.8 against time on stream are reported. It is evident that, overcoming 100 min on stream, the molar flow rates of the products going out from the MR achieve a constant trend, confirming, as previously reported, that the steady-state conditions are reached after 100 min.

The performances of the MR were evaluated in terms of glycerol conversion and hydrogen recovery at 1.0 bar (abs.), 400 °C, and by varying the SF. Figure 9 shows that, by increasing the SF, the conversion slightly increases from around 45.0% at SF = 2.6 to 50.0% at SF = 22.8. A higher sweep gas acts positively on the hydrogen permeating flux through the membrane, decreasing the hydrogen partial pressure on the permeate side and improving the hydrogen permeation driving force. Consequently, a higher hydrogen stream is removed from the reaction to the permeate side, favoring the shift of the GSR reaction toward the products and, then, a higher glycerol consume. However, this positive effect is limited at the operating conditions considered in this work because, as also shown in Fig. 9, the hydrogen recovery does not overcome 5%, although it increases at higher SFs. Moreover, SFs higher than 22.8 were not used during the MR experimental tests due to the pressure drops in the permeate side. Therefore, with respect to the TR, the advantage of the MR in terms of a higher glycerol conversion is quite limited at ambient pressure. In fact, the conversion value of the TR working at 400 °C and 1.0 bar was around 40.0%.

Having in mind to mainly produce pure or, at least, CO-free hydrogen stream by GSR reaction in a Pd-Ag MR, it was necessary to investigate the MR performances by increasing the reaction pressure. Figure 10 shows that, by increasing the pressure from 1.0 to 4.0 bar, the glycerol conversion enhances in the overall range of SF. Generally, two opposite effects on the MR system occur by increasing the pressure. On the one hand, a pressure increase induces a positive effect in terms of a higher hydrogen permeation driving force (membrane effect). In fact, a higher pressure increases the hydrogen partial pressure on the reaction side, resulting in a higher hydrogen flux permeated through the membrane that favors the shift of the GSR reaction toward the products, allowing a higher glycerol conversion to be reached. On the other hand, as the GSR (4) is a reaction presenting an increase in the moles number, a pressure increase gives a detrimental

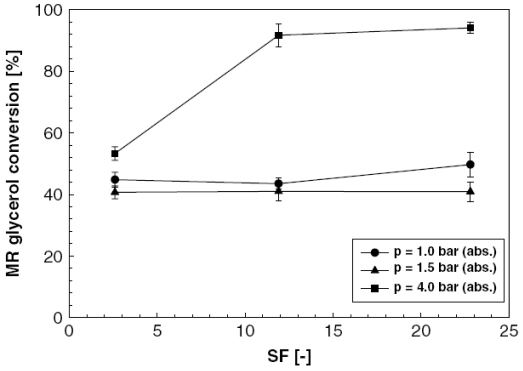

Figure 10. Glycerol conversion *vs* sweep factor (SF) for the Pd-Ag MR at different reaction pressure, WHSV = 1.01 h^{-1}, $T = 400\,°C$ and H_2O/glycerol = 6/1.

effect on the equilibrium of the glycerol conversion (thermodynamic effect).

At 4.0 bar, clearly, the selective removal of hydrogen from the reaction medium compensates and overcomes the detrimental effect of the thermodynamics. Moreover, at 4.0 bar, by increasing the SF from 2.6 to 11.9, the glycerol conversion enhances from around 55.0 to 92.0%. On the contrary, a great improvement of conversion is not noticed at a higher SF (94.0% at SF = 22.8) because a further increase in the sweep gas flow rate does not induce an increase of the hydrogen permeation driving force.

At 1.5 bar, the detrimental effect due to the thermodynamics is prevalent on the membrane effect and, thus, in the whole range of SFs considered the glycerol conversion is lower than that at 1.0 bar.

Moreover, as already seen in Fig. 9, the higher the SF the higher is the conversion due to the positive effect of the SF on the hydrogen permeation driving force that, owing to the hydrogen removal from the reaction zone to the permeation side, favors the shift of the glycerol conversion toward the products.

Although the glycerol conversion increases from 1.0 to 4.0 bar, the hydrogen yield shows a slight decreasing trend by increasing the pressure and SF (Table 1). On the one hand, a higher pressure favors the formation of methane,[10] as confirmed by the increase in methane selectivity with the pressure (Table 2); on the other hand, Co-based catalysts do not effectively catalyze the reaction of methane steam reforming.[4] Therefore, both effects negatively affect the hydrogen production as well as the hydrogen selectivity with a consequent decrease in the hydrogen yield. However, at 1.0 bar, the MR hydrogen yield is higher than that of the TR (~30.0%) in the whole range of SFs investigated (Table 1).

Taking into account that the main aim of this work is the pure (or at least CO-free) hydrogen production, particular attention was paid to CO-free hydrogen recovery. By increasing both the reaction pressure and the SF, the hydrogen permeation driving force is enhanced, more hydrogen can be removed from the reaction side toward the permeate side, and a higher CO-free hydrogen recovery can be reached. This is illustrated in Fig. 11, where the hydrogen recovery

Table 1. Hydrogen yield for MR and TR.

		$Yield_{H2}$ (%)		
	SF	$p = 1.0$ bar	$p = 1.5$ bar	$p = 4.0$ bar
MR	2.6	34.5	31.6	30.3
	11.9	34.8	31.2	33.3
	22.8	38.7	31.4	26.3
TR	–	30.5	–	–

Operating conditions: $T = 400\,°C$, H_2O/glycerol = 6/1, WHSV = 1.01 h^{-1}.

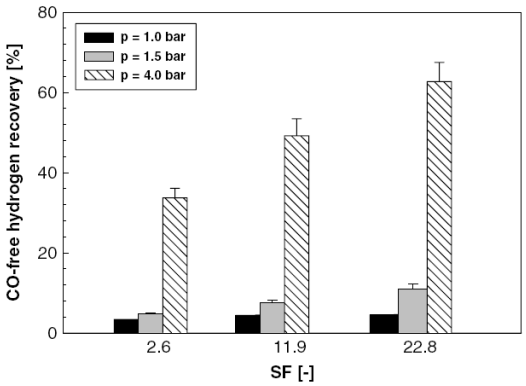

Figure 11. CO-free hydrogen recovery *vs* sweep factor (SF) at a different reaction pressure; MR conditions: $T = 400\,°C$, H_2O/glycerol = 6/1, WHSV = 1.01 h^{-1}.

increases with the pressure and the SF. In particular, the best recovery of around 63.0% is obtained at the highest SF and pressure considered in this work (SF = 22.8 and 4.0 bar of pressure). Moreover, it is quite evident that, operating at relatively low pressure, the detrimental effect of the thermodynamics and/or the limited membrane effect allow a lower CO-free hydrogen recovery to be achieved (at SF = 22.8, 5.0% at 1.0 bar 11.0% at 1.5 bar). Related to the TR, no experiments were carried out at higher pressures because the glycerol conversion is not favored at higher pressures due to the detrimental effect that a pressure > 1.0 bar induces on the thermodynamics of the GSR reaction.

Table 2 resumes the gas selectivity of the MR at 400 °C, and a different reaction pressure and SF. As already mentioned, the hydrogen selectivity slightly decreases by increasing the pressure. For instance, at SF = 22.8, the hydrogen selectivity drops from around 64.0% at 1.0 bar to 39.4% at 4.0 bar, whereas the methane selectivity shows a great increase from 1.4–1.7% in the pressure range of 1.0 and 1.5 bar to 24.0% at 4.0 bar. This result can be explained taking into account that from a thermodynamic point of view, an increase in reaction pressure favors the formation of methane, whereas hydrogen production is reduced.[10] Relating to CO selectivity, although Co-based catalysts are not very active for catalyzing the WGS reaction,[4,10] both higher pressures and SFs act positively on the hydrogen permeation driving force and, then, a higher hydrogen stream is recovered in the permeate side, shifting the WGS reaction toward the products and favoring a higher CO consume. In fact, as shown in Table 2, CO selectivity in the MR decreases by increasing the pressure and the SF.

Another important issue of this work was the carbon formation. The carbon deposition was probably the

Table 2. MR gas selectivity *vs* sweep factor (SF) at different reaction pressure (TR gas selectivity only at 1.0 bar).

$p = 1.0$ bar					$p = 1.5$ bar					$p = 4.0$ bar				
SF	S_{H2}	S_{CO}	S_{CO2}	S_{CH4}	SF	S_{H2}	S_{CO}	S_{CO2}	S_{CH4}	SF	S_{H2}	S_{CO}	S_{CO2}	S_{CH4}
2,6	63.9	5.6	30.0	1.5	2.6	64.4	3.5	30.6	1.8	2.6	57	3.0	30.9	8.6
11,9	64.1	5.3	29.1	1.5	11.9	63.9	3.3	31.0	1.8	11.9	45.9	1.9	34.5	17.7
22,8	64.0	5.1	29.3	1.4	22.8	64.2	3.1	29.3	1.7	22.8	39.4	0.7	35.8	24.0
TR	54.6	22.4	17.9	5.1	–	–	–	–	–	–	–	–	–	–

Operating conditions: $T = 400\,°C$, H_2O/glycerol = 6/1, WHSV = 1.01 h^{-1}.

main cause of the decrease in the Pd-Ag membrane performances in terms of the hydrogen permeated flux. In particular, methane formation was noticed when a hydrogen stream was used for regenerating the catalytic bed of the MR. Moreover, the hydrogen permeation behaviors of the Pd-Ag membrane were reestablished after the catalyst regeneration. Therefore, in a next work, the carbon deposition and its influence on the Pd-Ag membrane will be deeply investigated.

CONCLUSION

The GSR reaction was carried out in a perm-selective Pd-Ag MR packed with a Co-Al_2O_3 catalyst for producing a CO-free hydrogen stream. The MR was operated at 400 °C, H_2O/Glycerol molar ratio = 6/1, WHSV = 1.01 h^{-1}, and in a countercurrent flow configuration of sweep gas, whereas the reaction pressure and the SF were varied in the range of 1.0–4.0 bar (abs.) and 2.6–22.8 respectively. At ambient pressure and SF = 22.8, the maximum MR glycerol conversion of around 50.0% and a CO-free hydrogen recovery lower than 5.0% were achieved. However, at 1.0 bar, the Pd-Ag MR presented a better glycerol conversion than the TR working at the same MR conditions. Vice versa, at a relatively high pressure (4.0 bar), the MR showed a conversion of 94.0% and a CO-free hydrogen recovery higher than 60.0% at the maximum SF considered in this work. An important issue was the carbon formation during the GSR reaction, which was able to negatively affect the performances of the Pd-Ag membrane in terms of a lower hydrogen permeated flux and catalyst deactivation. This issue will be studied in depth in a next work, paying particular attention to the effect of the catalyst regeneration cycles on the hydrogen permeation performances of the Pd-Ag membrane.

REFERENCES

[1] T. Valliyappan, D. Ferdous, N.N. Bakhshi, A.K. Dalai. *Top. Catal.,* **2008;** *49*, 59–67.
[2] T. Hirai, N. Ikenaga, T. Miyake, T. Suzuki. *Energy Fuels,* **2005;** *19*, 1761–1762.
[3] G.W. Huber, J.W. Shabaker, J.A. Dumesic. *Science,* **2003;** *30*, 2075–2077.
[4] B. Zhang, X. Tang, Y. Li, Y. Xu, W. Shen. *Int. J. Hydrogen Energy,* **2007;** *32*, 2367–2373.
[5] A. Iriondo, V.L. Barrio, J.F. Cambra, P.L. Arias, M.B. Guëmez, R.M. Navarro, M.C. Sánchez-Sánchez, J.L.G. Fierro. *Top. Catal.,* **2008;** *49*, 46–58.
[6] M.S. Batista, R.K.S. Santos, E.M. Assaf, J.M. Assaf, E.A. Ticianelli. *J. Power Sour.,* **2003;** *124*, 99–103.
[7] A. Kaddouri, C. Mazzocchia. *Catal. Commun.,* **2004;** *5*, 339–345.
[8] S. Tosti, L. Bettinali. *J. Mater. Sci.,* **2004;** *39*, 3041–3046.
[9] S.S.Y. Lin, D.H. Kim, S.Y. Ha. *Catal. Lett.,* **2008;** *122*, 295–301.
[10] S. Adhikari, S. Fernando, S.R. Gwaltney, S.D. Filip To, R.M. Bricka, P.H. Steele, A. Haryanto. *Int. J. Hydrogen Energy,* **2007;** *32*, 2875–2880.

Asia-Pac. J. Chem. Eng. 2010; **5**: 138–145
DOI: 10.1002/apj

Conclusion to Chapter 2

In this chapter, the Pd-Ag based MR technology has been used for producing a pure hydrogen stream by exploiting glycerol as a renewable source. Therefore, the main aim was to analyze the influence of some operative conditions as reaction pressure, sweep gas flow rate, catalyst and space velocity on MR performances carrying out GSR reaction.

In the open literature only few works are focused on this reaction and in all studies a conventional reactor is employed.

Therefore, from my best knowledge, these works can be considered as the first studies in which GSR reaction takes place in a Pd-based MR.

In the first study, MR is packed with Co/Al_2O_3 catalyst, the reaction pressure and the SF (sweep-gas to glycerol ratio) were varied in the range of 1.0–4.0 bar (abs.) and 2.6-22.8 respectively, whereas in the second study, a Ru-based catalyst is used, the reaction pressure and space velocity were changed from 1.0 bar to 5.0 bar and from 0.1 h^{-1} to 1.0 h^{-1}, respectively.

Moreover, in both studies the main issue was the carbon formation during the GSR reaction, which was able to negatively affect the performances of the Pd-Ag membrane in terms of a lower hydrogen permeated flux and catalyst deactivation.

Moreover, it is evident that the Co-based catalyst is more active towards GSR reaction than Ru-based one. Indeed, the Table 3.2 shows the MR performances in terms glycerol conversion, hydrogen recovery and yield obtained performing the GSR reaction.

	Co/Al_2O_3 ($p_{reaction}$ = 4.0 bar)	Ru/Al_2O_3 ($p_{reaction}$ = 5.0 bar)
Glycerol conversion	90 %	22 %
hydrogen recovery	60 %	20 %
hydrogen yield	33 %	10 %

Table 3.2 Performances of Pd-Ag MR carrying out GSR reaction at 400 °C, WHSV = 1.0 h-1, water/glycerol = 6/1, SF = 11.9.

Probably, the lower MR performances obtained with Ru-based catalyst are probably due to the combination of low ruthenium content (0.5%) with an acid support as Al_2O_3.

Therefore, higher temperatures and basic catalyst support, more suitable for GSR reaction, could be used in order to avoid the detrimental effect due to carbon deposition.

References

Adhikari S, Fernando S, Gwaltney SR, To SDF, Bricka RM, Steele PH, Haryanto A, "A thermodynamic analysis of hydrogen production by steam reforming of glycerol", Int. J. Hydrogen En, 32 (2007) 2875-2880.

Adhikari, S.; Fernando, S.D.; Haryanto, A. Hydrogen production from glycerin by steam reforming over nickel catalysts. Renew. Energy, 2008, 33, 1097-1100.

Batista M.S., R.K.S. Santos, E.M. Assaf, J.M. Assaf, E.A. Ticianelli, Characterization of the activity and stability of supported cobalt catalysts for the steam reforming of ethanol, J. Power Sou., 124 (2003) 99-103.

Breen J.P., R. Burch, H.M. Coleman, Metal-catalysed steam-reforming of ethanol in the production of hydrogen for fuel cell applications, Appl. Catal., 39 (2002) 65-74.

Demirbas A, "Progress and recent trends in biofuels", Prog Energy Comb Sci, 33 (2007) 1-18

Haga F., T. Nakajima, K. Yamashita, S. Mishima, Effect of crystallite size on the catalysis of alumina-supported cobalt catalyst for steam reforming of ethanol, React. Kinet. Catal. Lett., 63 (1998) 253-259.

Haryanto A., S. Fernando, N. Murali, S. Adhikari, Current status of hydrogen production techniques by steam reforming of ethanol: a review, En. Fuels, 19 (2005) 2098-2106.

Jefferson M. Sustainable energy development: performance and prospects. Renew Energy 2006;31:571–82

Kaddouri A., C. Mazzocchia, A study of the influence of the synthesis conditions upon the catalytic properties of Co/SiO2 or Co/Al2O3 catalysts used for ethanol steam reforming, Catal. Comm., 5 (2004) 339-345.

Llorca J., N. Homs, J. Sales, P.R. de la Piscina, Efficient production of hydrogen over supported cobalt catalysts from ethanol steam reforming, J. Catalysis, 209 (2002) 306-317.

Maggio G, Freni S, Cavallaro S, "Light alcohols/methane fuelled molten carbonate fuel cells: a comparative study", *J Power Sou*, 74 (1998) 17-23.

Ni M., D.Y.C. Leung, M.K.H. Leung, A review on reforming bio-ethanol for hydrogen production, Int. J. Hydrogen En., 32 (2007) 3238-3247.

Ozcimen D, Karaosmanoglu F. Production and characterization of bio-oil and biochar from rapeseed cake. Renew Energy 2004;29:779–87.

Pfeffer M., W. Wukovits, G. Beckmann, A. Friedl, Analysis and decrease of the energy demand of bioethanol-production by process integration, Appl. Thermal Eng., 27 (2007) 2657-2664.

Song H., L. Zhang, R.B. Watson, D. Braden, U.S. Ozkan, Investigation of bio-ethanol steam reforming over cobalt-based catalysts, Catal. Today, 129 (2007) 346-354.

Xuan J, Michael K.H. Leung , Dennis Y.C. Leung, Meng Ni, "A review of biomass-derived fuel processors for fuel cell systems", Renewable and Sustainable Energy Reviews 13 (2009) 1301–1313

Hirai T, Ikenaga N, Miyake T, Suzuki T, "Production of hydrogen by steam reforming of glycerin on ruthenium catalyst", Energy Fuels, 19 (2005) 1761–1762.

Iriondo, A.; Barrio, V.L.; Cambra, J.F.; Arias, P.L.; Güemez, M.B.; Navarro, R.M.; Sánchez-Sánchez, M.C.; Fierro, J.L.G. Hydrogen production from glycerol over nickel catalysts supported on Al_2O_3 modified by Mg, Zr, Ce or La. Top. Catal., 2008, 49, 46-58.

Zhang, B.C.; Tang, X.L.; Li, Y.; Xu, Y.D.; Shen, W.J. Hydrogen production from steam reforming of ethanol and glycerol over ceria-supported metal catalysts. Int. J. Hydrogen Energy, 2007, 32, 2367-2373.

Part IV

Water gas shift Reaction

Introduction to *Part IV*

The WGS reaction is a well-known step for upgrading carbon monoxide to hydrogen in the production of synthesis gas. For more than 90 years after its first industrial application, many issues in respect of the catalyst, process configuration, reactor design, reaction mechanisms and kinetics have been investigated.

By the beginning of the 20th century and because the major source of synthesis gas production was from coal and coke, the WGS reaction was used as a stand-alone process. By that time, the most common and economical design was to conduct the reaction in a single stage, at temperatures around 450 – 600 °C, and using Fe-Cr based catalyst. Over the years now, a second-stage is introduced, operating around 320 – 360 ◦C and using a Cu-based catalyst.

More recently, a growing interest in the WGS reaction carried out in hydrogen perm-selective membrane reactors (MRs) has been observed because of the rising use of PEMFCs that operate using high-purity hydrogen.

Moreover, MRs are viewed as an interesting technology in order to overcome the equilibrium conversion limitations in conventional reactors. In particular, the selective permeation of hydrogen towards the permeate side of a Pd-Ag MR enables the WGS reaction to proceed towards completion, making possible to achieve:

a) higher conversion than conventional reactor working under the same operating conditions, or

b) the same conversion of a conventional reactor, but working under milder operative conditions.

In this *Part IV*, firstly, an overview on the impact of the MR in the field of WGS reaction is given, paying attention to the benefits and the drawbacks of this technology. Afterwards, the WGS reaction is carried out in a Pd-based supported MR for analyzing the effect of syngas mixture characterized by low CO content on the MR performances.

The papers are reported hereunder:

Paper 1: A. Basile, P. Pinacci, S. Tosti, M. De Falco, C. Evangelisti, T. Longo, ***S. Liguori****, A. Iulianelli, Water gas shift reaction in Pd-based membrane reactors, Advances in Science and Technology, 72 (****2010****) pp 99-104.*

Paper 2: S ***Liguori S****, PK Seelam, P. Pinacci, F. Drago A.Basile A Iulianelli Syngas stream upgrading through water gas shift reaction in a PSS supported Pd based membrane reactor submitted to Catalysis Today, (****2011****)*

Chapter 1

Overview on WGS reaction in MR

Introduction to paper 1

Conventionally, the WGS reaction is limited by thermodynamic constrains: its conversion may be closer to the thermodynamic predictions, depending on the suitable choice of catalyst. In other words, the laws of thermodynamics set a rigid limit for the conversion achievable in conventional reactors in which this reaction proceeds only to partial completion. As a consequence, the interest of scientists seems quite justified on searching for alternatives to conventional reactors. Among different technologies, the membrane one seems to be very promising. In particular, due to the attractive possibility of realizing both reaction and gas separation/purification in the same device, MRs are currently considered as good candidates for replacing conventional reactors. With respect to a classic configuration of a conventional system consisting of a reactor unit in series with a separation unit, a MR represents a modern solution having many potential advantages: reduced capital and downstream separation costs as well as enhanced yields and selectivities. From the viewpoint of the WGS process in an MR, a reaction product (e.g. hydrogen, in the case of Pd membranes) moves to the permeate side, enabling the WGS reaction to proceed toward completion with the advantages previously illustrated.

In fact, great interest toward WGS reaction assisted by MRs has been evidenced in the literature and many studies are focused on hydrogen recovery from MRs, either using Pd-based [Basile *et al* (1996), (2001), Brunetti *et al* (2007), Iyoha *et al* (2007)] or silica membranes[Giessler *et al* (2003) Battersby *et al* (2008)]. In the following, the effects of the main process variables on the operation of Pd-based WGS MRs will be analyzed.

Advances in Science and Technology Vol. 72 (2010) pp 99-104
© (2010) Trans Tech Publications, Switzerland
doi:10.4028/www.scientific.net/AST.72.99

Water gas shift reaction in Pd-based Membrane Reactors

A. Basile[1, a], P. Pinacci[2,b], S. Tosti[3,c], M. De Falco[4,d], C. Evangelisti[5,e], T. Longo[1,f], S. Liguori[1,g], A. Iulianelli[1,h]

[1] Institute on Membrane Technology of National Research Council (ITM-CNR), Via P. Bucci Cubo 17/C c/o University of Calabria, Rende (CS) – 87036 – Italy

[2] Erse S.p.A., via Ribattino 54, 20134 Milano, Italy

[3] ENEA, Unità Tecnico Scientifica Fusione, C.R. ENEA Frascati, via E. Fermi 45, Frascati, 00044 Roma, Italy

[4] Department of Chemical Engineering, University of Rome "La Sapienza", via Eudossiana, 18-00184 Rome, Italy

[5] Department of Chemistry and Industrial Chemistry, University of Pisa, via Risorgimento 35, 56126 Pisa, Italy

[a] a.basile@itm.cnr.it, [b]pietro.pinacci@erse-web.it, [c]tosti@frascati.enea.it, [d]marcello.defalco@uniroma1.it, [e]claudio@dcci.unipi.it, [f]t.longo@itm.cnr.it, [g]s.liguori@itm,cnr.it, [h]a.iulianelli@itm.cnr.it

Keywords: water gas shift reaction, membrane reactor, hydrogen production, PEM fuel cell.

Abstract. Water-gas shift reaction is an important industrial reaction, used for producing synthesis gas and ammonia as well as pure hydrogen for supplying at PEM fuel cells. In this work, an overview on water gas shift reaction performed in Pd-based membrane reactors is shown, paying particular attention to the influence on the performances of some operating variables such as reaction temperature, reaction pressure, H_2O/CO molar ratio and sweep gas.

Introduction

Water-gas shift reaction (WGS) (Eq. 1) is a chemical reaction in which carbon monoxide reacts with water vapor to form carbon dioxide and hydrogen:

$$CO + H_2O \rightarrow CO_2 + H_2 \qquad \Delta H^\circ_{298\,K} = -41.1\ kJ/mol. \qquad (1)$$

It is an important industrial reaction mainly used in fixed bed reactors (FBRs) for producing synthesis gas [1] and also in the Haber–Bosch process of ammonia manufacture [2] for reducing the CO concentration, which deactivates the Fe-based catalyst used in this process.
Generally, the reformed stream coming out from a conventional reformer is composed by hydrogen and other by-products such as CO, CO_2, H_2O and small amounts of unconverted reactants. These compounds need to be separated from hydrogen, in order to use it for supplying a PEM fuel cell system. In particular, CO concentration of this stream must be reduced (CO concentration < 10 ppm) in order to avoid the anode poisoning of PEM fuel cells [3].
Moreover, after the economic boom of the 1990s and the inherent increased energy demand coupled with growing concerns about environmental issues, high emphasis has been given to pure hydrogen production for fuel cell technology able to convert the chemical energy directly into electric power at moderate temperatures [4,5].
Hydrogen can be purified using different processes, such as pressure swing adsorption (PSA), cryogenic distillation (CD) or membrane separation, as reported in Table 1, where the comparative characteristics and performances of these technologies are summarized.

Table 1 – Comparison of hydrogen purification technologies.

Characteristic	PSA	CD	Membranes [a]
H_2 purity / vol. %	≥ 99.9	95-99	< 95
H_2 recovery / vol.%	75-90	90-98	< 90
H_2 product pressure	Feed Pressure	Variable	<< Feed pressure
Byproducts available	No	Yes	No
Feed Pressure / bar	10-50	15-35	15 -125
Capital Cost	High	Very High	Low
Energy Consumption	Intensive	Very Intensive	Low
Flexibility to expansion	Very Good	Good	Limited
Reliability	High	Moderate	High

[a] – Values based on the systems typically used in refineries [6]

Actually, Pd-Ag MRs are considered to be the most promising technologies for the production of pure hydrogen, owing to the infinite hydrogen perm-selectivity of these membranes with respect to all other gases [7-12]. With respect to a classic configuration of a FBR, consisting of a reactor unit in series with a separation unit, a MR represents a modern solution, able to simultaneously perform a chemical reaction and a mixture gas separation in the same physical device. For this reason, it presents many potential benefits: reduced capital and downstream separation costs as well as enhanced yields and selectivities. For these reasons, a great interest was ascribed in the specialized literature to WGS reaction assisted by MRs and many studies were focused on hydrogen recovery from MRs [7-33]. In particular, the selective permeation of hydrogen towards the permeate side of a Pd-Ag MR enables the WGS reaction to proceed towards completion, making possible to achieve: a) higher conversion than FBR working under the same operating conditions, or b) the same conversion of a FBR, but working under milder operative conditions.
In this work, an overview on the impact of the MR in the field of WGS reaction is given, paying attention to the benefits and the drawbacks of this technology.

Discussions

Temperature effect

WGS reaction is slightly exothermic and strongly controlled by the chemical equilibrium. The laws of thermodynamics set a rigid limit for the FBRs in which this reaction proceeds only to partial completion. As a consequence, it seems quite justified the interest of scientists on searching for alternatives to the traditional systems as MRs.
Generally, the temperature influence on CO conversion shows two opposite effects on the Pd-Ag MR system. On one hand, a temperature increase induces a positive effect in terms of a higher hydrogen permeability. In fact, a higher temperature enhances the hydrogen permeating flux from the reaction side to the permeation side, resulting in a shift of the WGS thermodynamic equilibrium towards the reaction products, which allows to reach higher CO conversion. In the meanwhile, since the WGS reaction is an exothermic reaction, a temperature increase gives a detrimental effect on the CO equilibrium conversion.
Figure 1 sketches the CO conversions obtained by using different Pd-based MRs:

1. a MR composed by Pd-Ag rolled membrane (thickness: 50 μm): in this case, the reaction was carried out at 1.0 bar, H_2O/CO = 1/1 and by using nitrogen as a sweep gas in co-current configuration, obtaining 93% CO conversion at around 330 °C [8];
2. a MR composed by an ultra-thin palladium film (~ 0.1 μm) coated by co-condensation technique on the inner surface of a porous ceramic support (γ-Al_2O_3): taking into account that at around 320 °C the thermodynamic equilibrium of CO conversion is ~ 70%, a 96%

CO conversion was obtained with the MR working at 1.1 bar and $H_2O/CO = 2/1$ at the same temperature [9];

3. a MR composed by a composite membrane with a Pd film of 10 μm coated on a ceramic support: around 98% CO conversion was reached at around 320 °C [10];
4. a MR composed by an ultra-thin Pd film (~ 0.2 μm) coated on a ceramic support (α-Al_2O_3/γ-Al_2O_3), by co-condensation technique [12]: the tests were carried out at $H_2O/CO = 0.98/1$ in order to reduce the energy consumption due to the excess of water vapour at ratios > 1/1. In this case, as shown in Fig. 1, the CO conversion increases by increasing the temperature up to achieving a maximum around 92% at ~ 330 °C, as a compromise between the kinetic rate of the reaction and permeation and the thermodynamic considerations of the WGS reaction. On the contrary, the thermodynamic equilibrium shows a continuous decreasing trend by increasing the temperature.

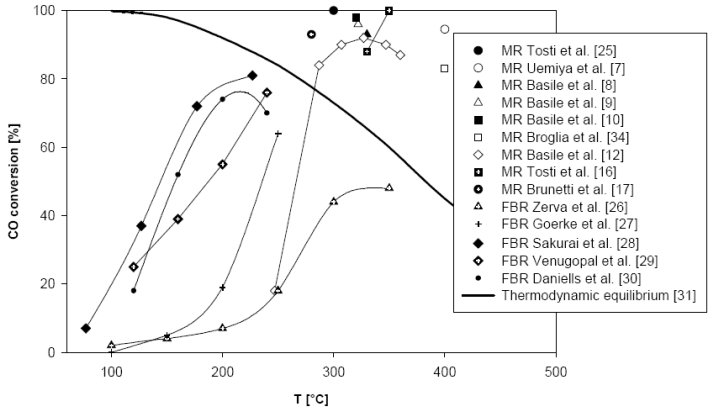

Figure 1 - CO conversion vs reaction temperature of different MRs and FBRs from specialized literature [21].

Moreover, in the temperature range of 50 – 400 °C, other literature data concerning a few FBRs as well as the thermodynamic equilibrium conversion and CO conversions of few FBRs are reported. Unfortunately, it is not possible to directly compare the results due to the different operating conditions (pressure, catalyst type, H_2O/CO feed molar ratio, etc.) used for the experimental data illustrated in Fig. 1. In all cases, the MRs showed CO conversions overcoming the thermodynamic equilibrium due to the permeation of hydrogen through the membrane that shifts the WGS reaction towards the products, allowing a higher CO conversion to be achieved. Moreover, at temperatures higher than 300 °C, it is evident that CO conversions obtained in the MRs are higher than the thermodynamic equilibrium conversion, which is the limit for the FBRs. This result can be explained by considering that, as already said, the selective removal of hydrogen from the reaction medium compensates the detrimental effect of the thermodynamics due to the increase of temperature.

Sweep-gas effect

A sweep-gas stream can be used into the permeate side of MRs for improving the hydrogen permeation driving force. In fact, referring to Pd-based membranes only selective to hydrogen, the sweep-gas acts positively on the hydrogen permeation through the membrane by decreasing the hydrogen partial pressure in the permeate side (increasing the driving force), allowing thus a higher hydrogen permeating flux through the membrane (Sieverts-Fick's law - Eq. 2).

$$J_{H_2} = Pe_{H_2} (p^{0.5}_{H_2,ret} - p^{0.5}_{H_2,perm})/\delta. \quad (2)$$

where J_{H2} is the hydrogen flux permeating through the membrane, Pe the hydrogen permeability, δ the membrane thickness, $p_{H2\text{-}ret}$ and $p_{H2\text{-}perm}$ the hydrogen partial pressures in the retentate (reaction side) and permeate sides (volume in which the hydrogen permeating through the membrane is collected), respectively.
As a result, the WGS chemical equilibrium is shifted towards the products, resulting so in a higher CO conversion.
The CO conversion of different MRs working at almost the same operating conditions (reaction pressure, H_2O/CO feed ratio and reaction temperature) and at different sweep-gas flow rates is presented in Table 2.
In the case of no full perm-selective membranes towards hydrogen, a higher sweep-gas flow rate does not improve significantly CO conversion. In fact, Giessler et al. [32] demonstrated that the conversion of CO was not increased in a MR using a molecular sieve silica membrane when the sweep-gas flow rate was increased from 50 cm^3/min to 300 cm^3/min (at normal conditions).
On the contrary, by using a MR allocating a membrane selective only to hydrogen, the CO conversion enhances from 84.0 % to 100 % when the sweep-gas flow rate is increased from 230 cm^3/min to 470 cm^3/min [16]. Hence, it is possible to point out that the use of a sweep-gas plays an important role for improving CO conversion, particularly when the MR allocates a membrane completely perm-selective towards hydrogen.

Table 2. Influence of the sweep-gas flow rates on the CO conversion in MRs from literature [21].

Membrane type	T [°C]	$p_{reaction}$ [bar]	$CO_{conversion}$ [%]	Reference	Sweep-gas flow-rate (N_2) [cm^3/min]	H_2O/CO
Silica supported on α-Al_2O_3	250	1.0	99.5 99.1	Giessler et al. [32]	50.0 300.0	1.00
Pd/γ-Al_2O_3/-αAl_2O_3	322	1.1	94.0 92.0	Basile et al. [12]	28.2 -	0.96
Pd/Ag-ceramic support	330	1.0	98.5 94.0	Basile et al. [8]	515.0 250.0	1.00
Pd-ceramic support	350	1.1	~100 ~100 84.0	Tosti et al. [16]	470.0 340.0 230.0	1.00

H_2O/CO molar ratio effect

Table 3 illustrates the influence of H_2O/CO molar ratio on CO conversion in a Pd-Ag MR and other literature data.

Table 3. Influence of the H_2O/CO molar ratios on the CO conversion in MRs from literature [21].

Membrane type	T [°C]	$p_{reaction}$ [bar]	$CO_{conversion}$ [%]	Reference	H_2O/CO	Sweep-gas	Sweep-gas flow-rate [cm^3/min]
Pd (20μm)on porous glass support	400	0.48-2.9	94.0 97.0 98.0	Uemiya et al. [7]	1.00 2.00 5.00	argon	300.0
Hydrophobic silica membrane	250	1	85.0 95.0 98.0	Giessler et al. [32]	0.90 1.50 2.50	nitrogen	20.0-60.0
Pd/γ-Al_2O_3/-αAl_2O_3	322	1.14 1.1 1.1	94.3 97.2 98.0	Basile et al. [12]	0.96 2.10 3.00	nitrogen	7.1
Silica membrane	250	1	65.0 88.0 92.0	Battersby et al.[33]	1.00 2.00 3.00	-	-

In general, a H_2O/CO molar ratio > 1/1 affects positively the CO conversion (limiting reactant), since the water excess shifts the WGS reaction towards the products; however, the benefit in terms of higher CO conversions by using H_2O/CO > 1/1 could be not so consistent to balance the economical disadvantage due to the water excess. Hence, from an economical point of view, the optimum could be represented by a MR able to achieve high CO conversions working at

stoichiometric or H_2O/CO molar ratio < 1/1, ambient pressure, relatively low temperature and without using sweep-gas [12].

Reaction pressure effect

A total pressure increase could act positively on the Pd-based MR performance in terms of higher conversion, when the hydrogen permeating flux through Pd-Ag membranes follows the Sieverts-Fick's law (Eq. 2). Therefore, the higher the driving force the higher the permeation of hydrogen through the membrane. As a result, WGS equilibrium is shifted towards the reaction products, favouring higher CO consumption, as reported in Table 4. Besides, before reaching equilibrium conditions, reaction kinetics is also favoured by increasing the total pressure. Nevertheless, the thermodynamic of WGS reaction is not affected by the pressure since the reaction proceeds with no variation of the total moles number.

Table 4. Influence of the total pressure on the CO conversion in MRs from literature [21].

Membrane type	T [°C]	$p_{reaction}$ [bar]	$CO_{conversion}$ [%]	Reference	H_2O/CO	Sweep-gas	Sweep-gas flow-rate [cm^3/min]
Pd/Ag rolled membrane	331	1.00	93.5	Basile et al. [8]	1.0	nitrogen	440.0
		1.50	95.0				
		1.75	97.0				
Pd/γ-Al_2O_3/-αAl_2O_3	322	1.10	99.2	Basile et al. [12]	1.0	nitrogen	28.2
		1.15	99.6			nitrogen	28.2
		1.20	99.9			nitrogen	28.2
		1.20	99.7			-	-
Silica supported on PSS[a]	280	3.20	91.0	Brunetti et al. [17]	1.0	-	-
		4.00	95.5			nitrogen	
		6.00	92.5			nitrogen	

[a] PSS = porous stainless stell

Conclusions

In this work, an overview on the study concerning WGS reaction performed in Pd-based membrane reactors was presented, paying particular attention to the effect of the Pd-based membrane on the shift effect of the thermodynamic equilibrium of the WGS reaction as well as the effect of temperature, pressure, H_2O/CO molar ratio and sweep gas on MRs performances.
As future trends, the WGS MR technology developments should have in mind many challenges, namely to improve the preparation of low cost, defect-free and homogeneous membranes able to work for a long period at high temperatures and pressures. In fact, more experimental studies on the life time of the MRs should be realized in order to validate them as good candidate to substitute the conventional systems at larger scales.

References

[1] A. Basile, A. Criscuoli, F. Santella and E. Drioli: Gas Sep. Purif. Vol. 10 (1996), pp. 243-254.
[2] C. Bosch and W. Wild, Canadian Patent 153,379 (1914).
[3] J.H. Wee: Renew. Sustain. En. Reviews Vol. 11 (2007), pp. 1720-1738.
[4] J.O.M. Bockris: Environment Vol. 13 (1971), p. 51.
[5] B.C.H. Steele and A. Heinzel: Nature Vol. 414 (2001), pp. 345-352.
[6] N. Patel, K. Ludwig and P. Morris in: Insert flexibility into your hydrogen network - Part 1. *Hydrocarbon Process.,* Int. Ed., 84 (2005).
[7] S. Uemiya, N. Sato, H. Ando and E. Kikuchi: Ind. Eng. Chem. Res. Vol. 30 (1991), pp. 585-589.
[8] A. Basile, G. Chiappetta, S. Tosti and V. Violante: Sep. Pur. Techn. Vol. 25 (2001), pp. 549-571.

[9] A. Basile, E. Drioli, F. Santella, V. Violante and G. Capannelli: Gas Sep. Purif. Vol 10 (1996), pp. 53-61.
[10] A. Basile, V. Violante, F. Santella and E. Drioli: Catal. Today Vol. 25 (1995), pp. 321-326.
[11] E. Kikuchi, S. Uemiya, N. Sato, H. Inoue, H. Ando and T. Matsuda: Chem. Lett. Vol. 18 (1989), pp. 489-492.
[12] A. Basile, A. Criscuoli, F. Santella and E. Drioli: Gas Sep. Purif. Vol. 10 (1996), pp. 243-254.
[13] H. Yoshida, H. Takeshita, S. Konishi, H. Ohno, T. Kurasawa and H. Watanabe: Nucl. Tech. Fusion Vol 5 (1984), pp. 178-188.
[14] C. Hsu and R.E. Buxbaum: J. Nucl. Mater. Vol. 141 (1986), pp. 238-243.
[15] V. Violante, E. Drioli and A. Basile: Fusion Eng. Des. Vol. 22 (1993), pp. 257-263.
[16] S. Tosti, V. Violante, A. Basile, G. Chiappetta, S. Castelli, M. De Francesco, S. Scaglione and F. Sarto: Fusion Eng. Des. Vol. 49-50 (2000), pp. 953-958.
[17] A. Brunetti, G. Barbieri, E. Drioli, K.H. Lee, B. Sea and D.W. Lee: Chem. Eng. Proc. Vol. 46 (2007), pp. 119-126.
[18] O. Iyoha, R. Enick, R. Killmeyer, B. Howard, B. Morreale and M. Ciocco: J. Membrane Sci. Vol. 298 (2007), pp. 14-23.
[19] E. Xue, M. O'Keeffe and J.R.H. Ross: Catal. Today Vol. 30 (1996), pp. 107-118.
[20] L. Lloyd, D.E. Ridler and M.V. Twigg in: Catalyst Handbook, 2nd edition, edited by M.V. Twigg, Wolfe, London (1989), p. 283.
[21] D. Mendes, A. Mendes, L.M. Madeira, A. Iulianelli, J.M. Sousa1 and A. Basile: Asia-Pac. J. Chem. Eng. (2009), in press, DOI:10.1002/apj.364.
[22] J. Sun, J. DesJardins, J. Buglass, and K. Liu: Int. J. Hydrogen En. Vol. 30 (2005), pp. 1259-1264.
[23] Y.S. Cheng, M.A. Pena, J.L. Fierro, D.C.W. Hui and K.L. Yeung: J. Membrane Sci. Vol. 204 (2002), pp. 329-340.
[24] J.R. Ladebeck and J.P. Wang, in: Catalyst development for water-gas shift. *Handbook of Fuel Cells, Fuel Cell Technology and Applications*, edited by John Wiley & Sons, England (2003), Vol. 3, pp. 190-201
[25] S. Tosti, A. Basile, G. Chiappetta, C. Rizzello and V. Violante: Chem. Eng. J. Vol. 93 (2003), pp. 23-30.
[26] C. Zerva and C.J. Philippopoulos: Appl. Catal. B: Env. Vol 67 (2006), pp. 105-112.
[27] O. Goerke, P. Pfeifer and K. Schubert: Appl. Catal. A: Gen. Vol. 263 (2004), pp. 11-18.
[28] H. Sakurai, T. Akita, S. Tsubota, M. Ciuchi and M. Haruta: Appl. Catal. A: Gen. Vol. 291 (2005), pp. 179-187.
[29] A. Venugopal and M.S. Scurrell: Appl. Catal. A: Gen. Vol. 245 (2003), pp. 137-147.
[30] S.T. Daniells, M. Makkee and J.A. Moulijn: Catal. Lett. Vol. 100 (2005), pp. 39-47.
[31] T. Utaka, T. Okanishi, T. Takeguchi, R. Kikuchi and K. Eguchi: Appl. Catal. A. Vol 245 (2003), pp. 343-351.
[32] S. Giessler, L. Jordan, J.C. Diniz da Costa and G.Q. Lu: Sep. Pur. Techn. Vol. 32 (2003), pp. 255-264.
[33] S. Battersby, M.C. Duke, S. Liu, V. Rudolph and J.C. Diniz da Costa: J. Membrane Sci. Vol. 316 (2008), pp. 46-52.
[34] M. Broglia. P. Pinacci, C.Valli in: Proc. of ICCMR9, Lyon (Fr) June 28-July 2, 2009.

Chapter 2

WGS reaction in Pd/PSS MR

Introduction to paper 2

In the following paper, WGS reaction of a syngas mixture has been carried out in a tubular palladium-based membrane reactor. In particular, a composite palladium-porous stainless steel membrane, obtained by electroless plating is used. This kind of membrane combines the benefits of dense metallic Pd-based membranes, which offer an infinite H_2 perm-selectivity with respect to other gases, and porous membranes, which exhibit relatively high H_2 permeability, resulting available at moderate cost.

Concerning the syngas mixture, it has been assumed that the syngas produced in IGCC plant was already treated in order to reduce the CO concentration from around 40% to below 8% and to minimize the CO poisoning effects on the membrane surface.

Thus, the influence of feed conditions (H_2O/CO ratio, feed flow rate and different feed mixtures) and reaction pressure (7.0 – 11.0 bar) on the MR performance in terms of CO conversion, H_2 recovery and H_2 permeate purity is studied.

The following paper is *submitted to Catalysis Today*

Syngas stream up-grading through WGS reaction in a PSS supported Pd-based membrane reactor

S. Liguori[1,2], P. Pinacci[3], P.K. Seelam[4], R. Keiski[4], F. Drago[3], V. Calabrò[1], A. Basile[2*], A. Iulianelli[1]

[1]Dept. of Modeling Engineering, via P. Bucci Cubo 39/C University of Calabria, Rende (CS) – 87036 – Italy
[2]Institute on Membrane Technology of Italian National Research Council (ITM-CNR), c/o University of Calabria Cubo 17/C, Rende (CS) – 87036, Italy.
[3]RSE S.p.A., Via Rubattino 54, Milano (MI) – 20134, Italy.
[4]Dept. of Process and Environmental Engineering, Mass and Heat Transfer Process Laboratory, University of Oulu, P.O. Box 4300, FI-90014 Oulu, Finland.

Abstract

In this work, the performance of WGS reaction carried out in a porous stainless steel (PSS) supported Pd-based membrane reactor (MR) have been experimentally investigated in terms of conversion, hydrogen recovery and hydrogen purity of permeate stream. A 20 μm thick Pd - membrane obtained by electroless plating and a high temperature Fe-Cr based WGS catalyst have been used during the experimental campaign. Influence of parameters such as reaction pressure (from 7 to 11 bar) and gas space hourly velocity, GHSV, (from 3450 to 14000 h^{-1}) at different steam to carbon ratio (from 1/1 to 4/1) have been investigated at the reaction temperature of 390 °C. As a best result, while feeding a syngas mixture, 8% CO, 32% H_2O, 24% CO_2, 36% H_2, at GHSV = 3450 h^{-1} and reaction pressure of 11 bar, almost 80% CO conversion, 70% hydrogen recovery with a permeate hydrogen purity around 97% have been obtained. Membrane fouling due to coke deposition has been proven to be fully reversible: after 700 hours of tests in WGS mixtures, H_2 permeation and ideal selectivity remained unchanged.

Keywords: water gas shift, high purity hydrogen, PSS support Pd-based membrane reactor

* Corresponding author: a.basile@itm.cnr.it

1. Introduction

The majority of hydrogen produced industrially comes from natural gas via reforming reactions performed in conventional reactors. The reformed stream leaving the conventional reformer is constituted mainly by H_2, CO, CO_2, H_2O and small amounts of unconverted reactants [1]. Commonly, the up-grading of this hydrogen-rich gas stream is devoted to reduce the CO concentration up to a specified level, having in mind two main goals: to increase the hydrogen production rate and to purify the reformate stream. To these ends, WGS reaction is widely used. In small-scale processes such as the fuel processing for fuel cells (e.g., PEM fuel cells), usually WGS reaction is performed in a single fixed bed reactor (FBR) at an intermediate temperature. An interesting alternative for increasing CO conversion is the MR utilization, in which some reaction products (e.g., H_2) are selectively removed from the reaction side and collected in the permeate side via permeation through the membrane, shifting the reaction towards further products formation and, consequently, increasing the conversion. Therefore, MRs have deserved considerable attention in the scientific literature and particular attention has been paid towards the H_2 removal performed by using selective dense Pd-based membranes or its alloys [2-10]. Indeed, owing to the full hydrogen perm-selectivity of this kind of membranes, the continuous removal of hydrogen promotes the reaction conversion shifting also beyond the thermodynamic equilibrium of a FBR exercised at the same MR operating conditions. Nevertheless, dense Pd-based membranes show two main drawbacks: low permeation fluxes and high cost. Both these problems can be reduced considering composite Pd-based membranes characterized by a selective metallic layer deposited on a substrate having high porosity. In particular, composite Pd-based membranes can be realized depositing a small Pd-based layer onto porous support obtaining, contemporary, cost reduction and increasing of mechanical resistant. On this route, many studies has been focused on the development of thin Pd film deposited onto porous supports [11-16]. Among the different porous supports (ceramic, glass, metallic), stainless steel sintered porous support is particularly suitable for the integration with Pd-based layers owing to its easy welding with dense metallic materials. PSS supports show also other

benefits such as the high mechanical strength, a linear coefficient of thermal expansion close to that of palladium and the relatively low price [17].

In the recent past, most of the works on WGS reaction in MR, housing dense Pd-based and its alloy or microporous amorphous silica-based membranes, was conducted at relatively low temperatures (<350 °C) [18-24]. Nevertheless, both these kind of membranes have issues of material instability in the WGS environment. In particular, Pd-based membranes, in addition to the aforementioned drawbacks, are vulnerable to surface carbonization, sulphur-poisoning and embrittlement phenomenon [25-28], while the amorphous silica-based membranes degrade due to the condensation reaction of silanol in hydrothermal conditions [29-34].

To the best of our knowledge, only a few works are focused on WGS reaction performed at 400 °C using composite MRs [8,35-36]. In particular, Uemiya et al. [35] and Bi et al. [8] have dealt with a syngas stream, produced by steam reforming of natural gas, using Pd-based membranes supported onto ceramic support obtaining complete CO conversion at 400 °C and low gas hourly space velocity (GHSV), while Pinacci et al. [36] studies the H_2 purification of a syngas stream, produced in integrated gasification combined cycle (IGCC) plants, employing a PSS supported Pd-based MR realizing 85% CO conversion and around 80% H_2 recovery at 6.0 bar.

The aim of the present study is to use a PSS supported Pd-based membranes, characterized by 20 μm as layer, for the up-grading of a typical industrial syngas stream via WGS reaction performd at 390 °C. In detail, it has been assumed that the syngas produced in IGCC plant was already treated in order to reduce the CO concentration from around 40% to below 8% and to minimize the CO poisoning effects on the membrane surface.

Thus, the influence of feed conditions (H_2O/CO ratio, feed flow rate and different feed mixtures) and reaction pressure (7.0 – 11.0 bar) on the MR performance in terms of CO conversion, H_2 recovery and H_2 permeate purity is studied.

2. Experimental

2.1 Membrane preparation and membrane reactor setup

The electroless plating technique has been used for preparing at RSE laboratories a 20 μm thick composite Pd membrane onto a stainless steel tubular macroporous support. The support is supplied by Mott Metallurgical Corporation and it is characterized by a 10 mm O.D. AISI 316L porous tube, with a nominal pore size of 0.1 μm. Nominal pore size is determined by the manufacturer based on a 95% rejection of particles with size greater than 0.1 μm. The actual pore size is however much larger: a mean and a maximum value of about 2 and 5 μm, respectively, have been determined by mercury intrusion measurements [37].

Figure 1. Pd-based membrane supported onto porous stainless steel.

The porous support was welded to two non porous AISI 316 L tubes for the membrane housing, one of which is closed (Figure 1). The total length of the support is 21 cm and the active length of the porous support is 7.7 cm. The active area of the membrane is 23.2 cm^2. The membrane preparation has been performed according to the procedure described elsewhere [36, 38].

The MR consists of a tubular stainless steel module (length 280 mm, i.d. 20 mm) containing the above described tubular membrane, Figure 2. A commercial Fe-Cr based catalyst in pellet form was packed in the annulus of the MR within glass spheres (2 mm diameter) to avoid catalyst dispersion.

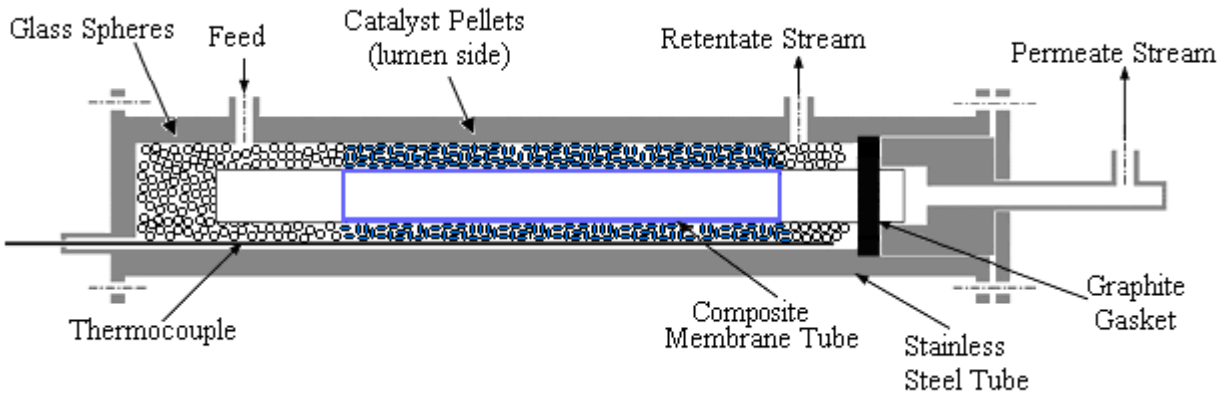

Figure 2. MR scheme.

2.2 Experimental details

The scheme of the experimental plant used for performing the WGS reaction is represented in Figure 3. In detail, the MR is heated by means of a heating tape connected to a temperature-controller.

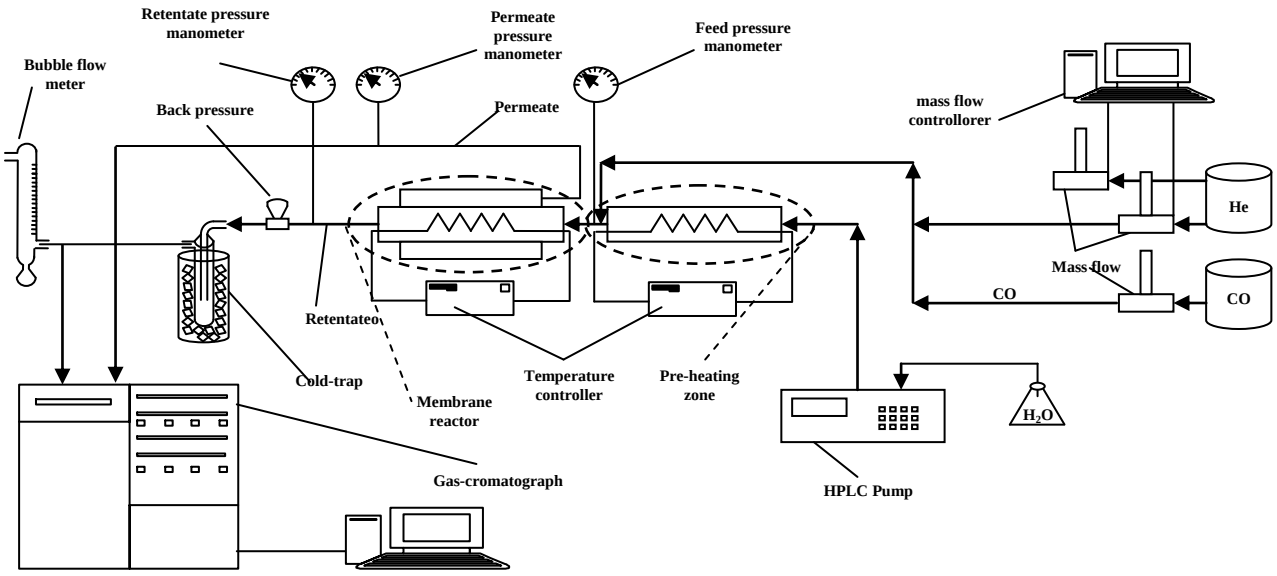

Figure 3. Scheme of the experimental plant.

The operating temperature is measured by a thermocouple inserted into the MR module.

The experimental setup is constituted of: a P680 HPLC pump (Dionex) used for supplying liquid distilled water, which is vaporized into the preheating zone, Brooks Instruments 5850S mass-flow controllers, which regulate the gases feed flow, cold trap for condensing the water vapour fraction

of retentate streams, on-line gas chromatograph (HP 6890 GC) for the analysis of dry gases. The Absolute Calibration Curve Method [38] was used for calculating the molar compositions of both retentate and permeate streams.

Table 1 shows the overall tests (permeation and reaction) performed with the palladium composite membrane. The membrane has operated at temperatures ranging for 300 up to 410 °C for more for a total of ~ 4170 h and for 9 thermal cycles. In each thermal cycle, the membrane has been heated up to the operative temperature at a rate of 1 °C/min with inert gas (He); at the end of the cycle, before cooling down the system to room temperature, the membrane has been purged with He at pressure of 3.0 bar for about 2 h, to purge any H_2 trapped in the palladium lattice.

Thermal cycle	Description	Length of time [h]
I	Permeation tests pure gas: He	268
II	Permeation tests pure gas: He and H_2	800
III	Permeation tests pure gas: He and H_2	1290
IV	Permeation tests pure gas N_2 and H_2	48
V	Permeation tests pure gas (N_2, He, H_2) and gaseous mixture	776
VI	WGS reaction tests (H_2O/CO = 1/1)	240
VII	WGS reaction tests (H_2O/CO = 4/1, 3/1)	504
VIII	WGS reaction tests (mix syngas)	168
IX	WGS reaction tests for repeatability	72
Total		**4166**

Table 1. Permeation and reaction tests performed using the Pd-based supported onto PSS membrane.

The stability to the permeation the gases of interest for this membrane has been first evaluated at RSE laboratories using pure gases (H_2 and He) at 300 – 400 °C. In particular, during the III thermal cycle, the membrane has been exposed to a H_2 flux for about 1200 hours at 400 °C and a pressure drop across the membrane at 1.5 bar, without any degradation of its performance. The membrane has been, then, sent to ITM-CNR for further tests. During IV thermal cycle, permeation tests with pure gases (N_2, He and H_2) have been carried out to measure H_2 permeance and the ideal selectivity $\alpha_{H2/He}$ and $\alpha_{H2/N2}$ (5) at 390 °C.

During the V cycle, the permeation tests with one binary mixture and two gas mixtures simulating synthesis gas compositions (Table 2) are carried out to evaluate the effect of gases such as CO,

CO_2, He, H_2O on H_2 permeation. From VI to IX thermal cycles, WGS reaction tests were performed for evaluating the influences of different operative conditions on the MR performance in terms of CO conversion, H_2 recovery and H_2 purity in the permeate stream, as reported below.

Mixtures type	Gas mixture fed in MR	Gaseous composition [%]
Binary Mix	H_2/He	45/55
Mix 1	H_2/CO/CO_2/H_2O	45/8/31/16
Mix 2	H_2/He/CO_2/H_2O	45/8/31/16

Table 2. Mixtures type supplied in Pd-PSS MR at 390 °C for performing permeation test.

During each reaction test, 3 g of commercial Fe-Cr catalyst is packed into the MR, the reaction temperature is kept constant at 390 °C as well as permeate pressure at 1.0 bar, without using any sweep gas into the permeate side.

During VI thermal cycle, the reaction pressure was varied from 7.0 to 11.0 bar, by supplying a stoichiometric feed stream of H_2O and CO and using GHSV equal to 5750 h^{-1}.

Afterwards, during the VII thermal cycle, the influence of GHSV, in the range of 3450 ÷ 14000 h^{-1} at different feed molar ratio (H_2O/CO = 3/1, 4/1) was studied, keeping constant the reaction pressure at 11.0 bar.

In the VIII thermal cycle, different syngas mixtures corresponding to various steam to carbon feed molar ratio are considered for performing the WGS reaction in Pd-based MR.

At the last thermal cycle, some reaction tests are performed for evaluating the repeatability of the results realized in the previous experimental tests. In particular, WGS reaction is carried out at 390 °C, feed molar ratio equal to H_2O/CO = 4/1, reaction pressure 11.0 bar and varying the GHSV from 3450 ÷ 14000 h^{-1}.

Concerning the description of the MR performance, some equations are defined as reported below:

$$\text{CO Conversion (\%)} = \frac{(\text{CO})_{\text{in}} - (\text{CO})_{\text{out}}}{(\text{CO})_{\text{in}}} \cdot 100 \qquad (2)$$

$$H_2\text{ - Permeate purity}(\%) = \frac{H_{2,\,permeate}}{(H_2 + CO + CO_2)_{permeate}} \cdot 100 \qquad (3)$$

$$H_2\text{ Recovery }(\%) = \frac{H_{2,\,permeate}}{H_{2,\,permeate} + H_{2,\,retentate}} \cdot 100 \qquad (4)$$

$$(\text{Ideal selectivity})\,\alpha_{H_2/Gas\_i} = \frac{\text{Permeance}_{H_2}}{\text{Permeance}_{Gas\_i}}, \qquad Gas\_i = N_2 \text{ or He} \qquad (5)$$

where the subscript "OUT" indicates the total (retentate and permeate sides) outlet flow rate of each species, while "IN" refers to the feed stream.

Each experimental point obtained in this work is an average value of 6 experimental tests taken in 90 min. After each experimental cycle (90 min), the catalyst is regenerated using H_2 ($1.8 \cdot 10^{-3}$ mol/min).

Moreover, coke is detected and calculated. The coke measurement is realized supplying H_2 into the reactor and analyzing with GC the methane formation obtained by methanation reaction (6).

$$C + H_2 \rightarrow CH_4 \qquad \Delta H°_{298\,K} = -75.0 \text{ kJ/mol.} \qquad (6)$$

No oxygen was used for regenerating the catalyst and eliminate the carbon deposition, essentially, owing to two effects: higher temperature should be required (~ 600 °C) and, secondly, to avoid the formation of palladium oxides, which could damage the Pd-layer and its performance.

3. Results and discussion

3.1 Permeation tests

Permeation tests with pure gases (H_2, N_2, He) and gas mixtures (Table 2) in the range of 1.8 – 10.0 bar and at 390 °C have been performed during I, II, III, IV and V thermal cycles.

In particular, He and N_2 permeation tests were performed in order to verify the presence of any defect in the palladium layer and, consequently, to calculate the ideal selectivities (5) $\alpha_{H2/He}$ and $\alpha_{H2/N2}$.

In Table 3, the permeance of each pure gas and the ideal selectivity as a function of the pressure drop across the Pd-based membrane is reported. As shown, ideal selectivity decreases while increasing pressure drop across the membrane. Such a trend has also been reported by Rothenberger et al. [39] for two composite Pd-porous stainless steel membranes similar to the one tested in this work, and can be attributed to the viscous flow component through the defects in the Pd layer, as discussed in reference [40].

Δp	**Permeance H_2**	**Permeance N_2**	**Permeance He**	**$\alpha_{H2/He}$**	**$\alpha_{H2/N2}$**
[kPa]	[mol/m^2·s·Pa]	[mol/m^2·s·Pa]	[mol/m^2·s·Pa]	[-]	[-]
80	$4.343 \cdot 10^{-07}$	$1.432 \cdot 10^{-09}$	$2.368 \cdot 10^{-09}$	183.4	303.4
100	$4.331 \cdot 10^{-07}$	$1.512 \cdot 10^{-09}$	$2.362 \cdot 10^{-09}$	183.3	286.4
170	$4.246 \cdot 10^{-07}$	$1.699 \cdot 10^{-09}$	$2.847 \cdot 10^{-09}$	149.2	249.8
200	$4.190 \cdot 10^{-07}$	$1.737 \cdot 10^{-09}$	$3.031 \cdot 10^{-09}$	138.3	241.3
260	$4.043 \cdot 10^{-07}$	$1.938 \cdot 10^{-09}$	$3.603 \cdot 10^{-09}$	112.2	208.7
300	$3.954 \cdot 10^{-07}$	$2.035 \cdot 10^{-09}$	$3.689 \cdot 10^{-09}$	107.2	194.3
360	$3.816 \cdot 10^{-07}$	$2.199 \cdot 10^{-09}$	$3.742 \cdot 10^{-09}$	102.0	173.5

Table 3. H_2, N_2, He permeances and ideal selectivity at different pressure drop through the Pd/PSS membrane at 390°C.

3.1.1 Stability of membrane permeation characteristics

The long-term stability of Pd/PSS membrane permeation characteristics has been examined at 390 °C as a function of both pressure and thermal cycles. In particular, during the III cycle, H_2 has been supplied to the membrane module and pressure drop across the membrane was kept constant at 1.5 bar. Every week, H_2 and He permeances have been measured for verifying if any variation in the membrane permeation characteristics is happened. Constant hydrogen flux has been detected up to 1000 h and, at the end of the test (1200 h), is slightly decreased of about 8%. Moreover, He permeance remained unchanged until the end of the test.

The stability of membrane permeative characteristics has been also verified during thermal cycles. In particular, in Figure 4 is reported the N_2 permeance calculated during two different thermal cycles (IV and V). As shown, no variation in the membrane permeation characteristics was found.

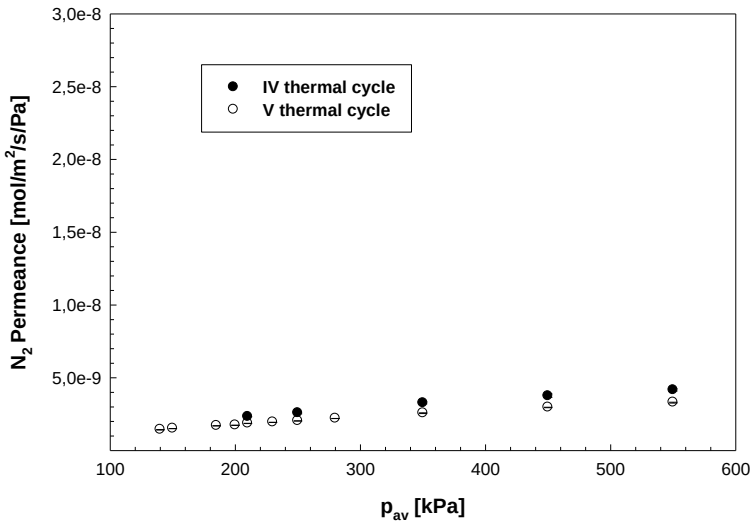

Figure 4. N_2 permeance vs pressure drop across the Pd/PSS membrane during the IV and V thermal cycles.

3.1.2 Hydrogen permeation performance

The Pd/PSS composite membrane was characterized in terms of H_2 permeation. Usually, at constant temperature, H_2 permeation through dense palladium membranes occurs via solution/diffusion mechanism. This transport can be described by the following general expression [41]:

$$J_{H2} = Pe\left(p^{n}_{H2-retentate} - p^{n}_{H2-permeate}\right) \qquad (7)$$

where: J_{H2} is the H_2 flux permeating through the Pd-based membrane, Pe the H_2 permeance, $p_{H2\text{-}retentate}$ and $p_{H2\text{-}permeate}$ the H_2 partial pressure in the retentate and permeate sides, respectively, and "n" the dependence factor of H_2 partial pressure, in the range 0.5 – 1.0, used as an indicator for the rate-controlling step of the permeation [41]. Therefore, by considering the H_2 flux permeating through the membrane against H_2 permeation driving force, the linear regression factor (R^2) was calculated at different "n" values. Figure 5 shows the H_2 permeation flux versus H_2 partial pressure drop across the membrane varying the "n" value. As shown, the highest linear regression value (R^2) corresponded to n = 0.7, used to describe the H_2 permeation through the Pd/PSS composite membrane of this work.

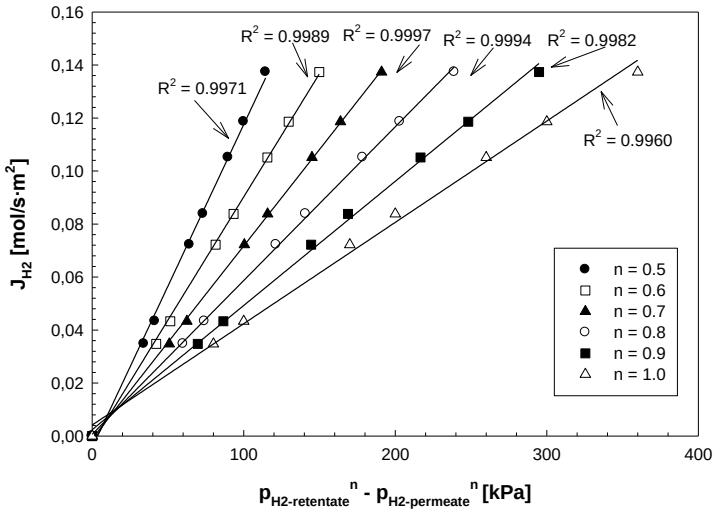

Figure 5. Hydrogen flux permeating through the membrane by varying "n" values, at 390 °C.

3.1.3 The effect of the He, CO , CO_2 and steam addition on hydrogen permeation

The hydrogen permeating flux through the membrane, taking place when a mixture of hydrogen is supplied to a membrane module, is influenced by several factors, such as hydrogen dilution owing to the presence of other gaseous components [42], hydrogen depletion [43] or possible competitive adsorption of other gas components on the membrane surface [44-46]. For this reason, during the V thermal cycle, three different gaseous mixtures have been considered (Table 2) and the H_2 permeation characteristic were evaluated for understanding the relative importance of the effects previously mentioned.

In Figure 6, the hydrogen permeating flux through the Pd-based composite membrane realized by supplying pure H_2 has been compared with the one obtained by feeding Mix 1 (H_2/CO/CO_2/H_2O). It is evident a detrimental effect on the hydrogen permeating flux owing to the addition of other gaseous compounds. In particular, this negative effect is probably due to the presence of CO and steam in the mixture. Indeed, several studies [26,42,47] have found that the presence of CO could cause a decrease in the hydrogen permeating flux owing to its competitive adsorption with H_2 on Pd surface, whereas, concerning the steam, the formation of adsorbed O atoms, via H_2O decomposition/recombination mechanism, could poison the surfaces of Pd-based membrane [48].

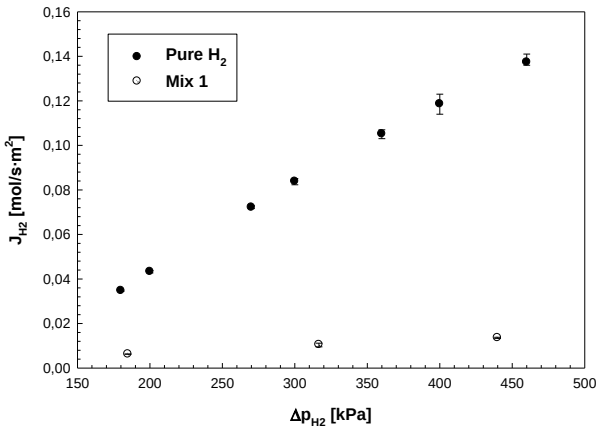

Figure 6. Hydrogen permeating flux vs hydrogen partial pressure difference between retentate and permeate side at 390 °C by supplying pure H_2 and Mix 1 (H_2/CO/CO_2/H_2O).

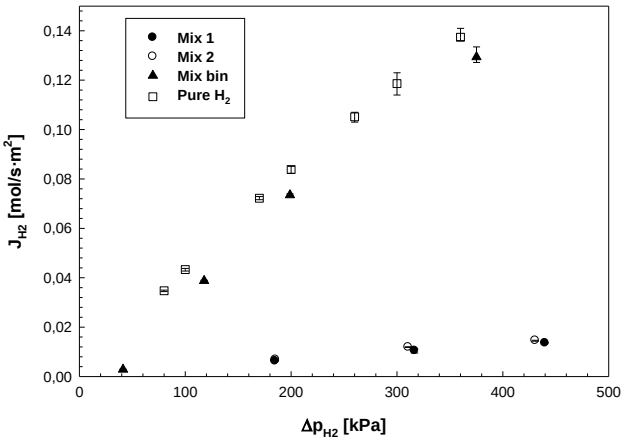

Figure 7. Hydrogen permeating flux vs hydrogen partial pressure difference, at 390 °C feeding pure H_2 and various gas mixtures (Table 2).

Obviously, the process of H_2O decomposition/recombination could be more complex than the adsorption of CO on the Pd surface. Moreover, the adsorbed steam molecules have, probably, a more negative effect on hydrogen permeation into the Pd film compared to the adsorbed CO. This prevalent effect caused by steam has been verified by performing H_2 permeation tests using also the Mix 2 and by comparing the overall results (Figure 7). As shown, the detrimental effect of both mixture (Mix 1 and Mix 2) on H_2 permeating flux is almost similar. Nevertheless, both Mix 1 and Mix 2 present 16% steam content, whereas CO is contained only in Mix 1, with 8% content (Table 2). As a consequence, it can be concluded that the presence of steam and CO_2 has a more detrimental effect than carbon monoxide. Furthermore, the binary mixture (H_2/He) has been also used for carrying out the H_2 permeation tests (Figure 7). The reduction in hydrogen permeating flux realized when the binary mixture is used instead of pure H_2 is probably due to the dilution and depletion effect [49].

3.2 Reaction tests

3.2.1 Reaction test using CO and H_2O

After permeation test, the WGS reaction was performed in the Pd/PSS MR packed with 3 g Fe-Cr catalyst, operated at 390 °C from 7.0 to 11.0 bar and supplied by stoichiometric steam to carbon feed ratio as a first approach.

Figure 8 shows the conversion and hydrogen recovery trends by increasing the reaction pressure. As expected, hydrogen recovery is emphasized at higher reaction pressures because of the improved hydrogen permeation driving force. As a consequence, the higher the pressure the higher the hydrogen removal from the reaction to the permeation side. On the contrary, the conversion follows a constant trend because the positive effect of the selective permeation of hydrogen is counterbalanced by the negative effect due to the loss of part of CO as a reactant, passing through the defects of the membrane. As a result, at 11 bar, CO conversion is 80%, hydrogen recovery around 60% and the permeate purity is around 95% in all pressure investigated.

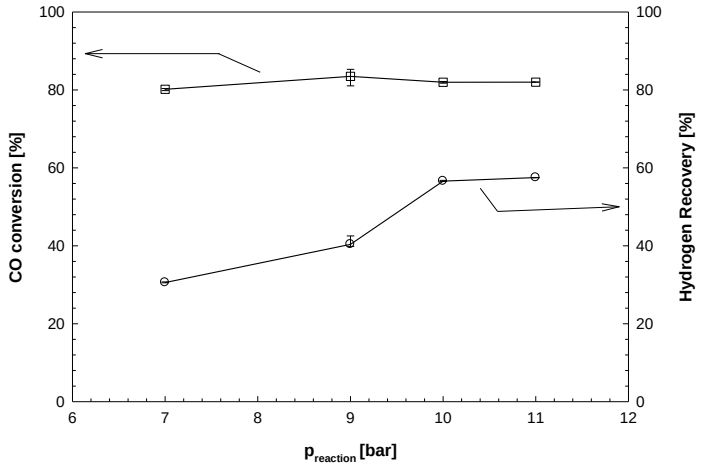

Figure 8. CO conversion and hydrogen recovery vs reaction pressure, at 390 °C, CO/H_2O = 1/1, permeate pressure = 1.0 bar and GHSV = 5750 h^{-1}.

Therefore, taking into account that the best results in terms of CO conversion and H_2 recovery have been obtained at 11.0 bar, the experimental campaign was direct to realized other reaction tests varying GHSV between 3450 ÷ 14000 h^{-1} at different feed molar ratio ranging from 3/1 to 4/1.

Figure 9 depicts the CO conversion against the GHSV at two different feed molar ratio H_2O/CO. As shown, at constant GHSV, the CO conversion is improved by increasing the feed molar ratio. In particular, at 3450 h^{-1} the CO conversion is enhanced from 85.0% to 97% by increasing the H_2O/CO ratio from 3/1 to 4/1. This effect is due to the water excess that shifts WGS reaction towards a further products formation favoring a higher CO consume. However, a GHSV decrease acts favorably on CO conversion. Indeed, the reduction of this parameter leads to higher residence time of reactants in the catalytic bed and, thus, higher contact time of them with the catalyst, promoting the conversion. As a consequence, the GHSV decrease produces a positive effect on hydrogen recovery (Figure 10). In particular, the H_2 recovery is around 83.0% at GHSV = 3450 h^{-1}, whereas it drops to 31.0% at GHSV = 13984 h^{-1}.

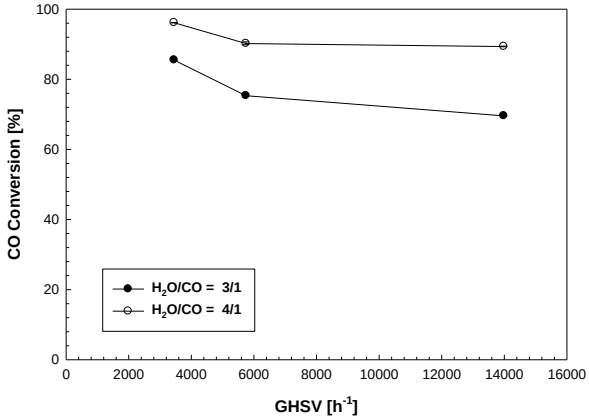

Figure 9. CO conversion vs GHSV at different feed molar ratio, T = 390 °C, reaction pressure = 11.0 bar and permeate pressure = 1.0 bar.

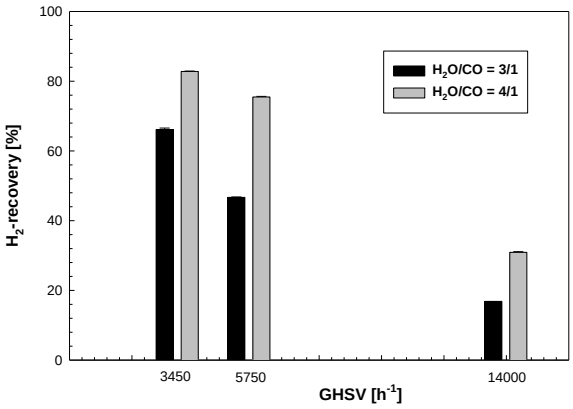

Figure 10. Hydrogen recovery against GHSV at feed molar ratio at T = 390 °C, reaction pressure = 11.0 bar and permeate pressure = 1.0 bar.

Moreover, as shown in Table 4, the hydrogen permeate purity is higher than 90% in each experimental results.

	Hydrogen permeate purity [%]	
GHSV [h^{-1}]	H_2O/CO = 3/1	H_2O/CO = 4/1
3450	93.8	94.6
5750	95.9	94.7
14000	92.2	90.0

Table 4. Hydrogen purity in the permeate stream at different GHSV and feed molar ratio, at reaction pressure = 11.0 bar, T = 390 °C and permeate pressure = 1.0 bar.

However, after each reaction test, carbon deposition was detected. In particular, a H_2 stream has been supplied into the MR and methane formation was observed and analyzed by GC. Therefore, the carbon content has been calculated considering the methanation reaction (6). Table 5 reports the carbon amount deposited on the membrane surface. It is evident that the carbon deposits decrease by increasing feed molar ratio and decreasing GHSV. In particular, the increase of steam as well as the decrease of GHSV, probably, shift WGS reaction towards further H_2 and CO_2 production, thus minimizing carbon formation owing to the Boudouard reaction [50].

	Coke [g/h]	
GHSV [h^{-1}]	$H_2O/CO = 3/1$	$H_2O/CO = 4/1$
3450	0.141	0.071
5750	0.260	0.100
14000	0.590	0.273

Table 5. Carbon amount deposited during WGS reaction at 390 °C and 11.0 bar of reaction pressure.

3.2.2 Reaction test using syngas compositions

Table 6 shows three feeds representing different compositions of syngas, in which CO concentration has been kept constant, while steam to carbon ratio has been varied between 2/1 and 4/1. These feeds were used for performing the WGS reaction tests in Pd/PSS MR.

	Composition %				
Feed	CO	H_2	CO_2	H_2O	H_2O/CO
Feed 1	0.08	0.45	0.31	0.16	2/1
Feed 2	0.08	0.405	0.275	0.24	3/1
Feed 3	0.08	0.36	0.24	0.32	4/1

Table 6. Various syngas mixtures fed into MR.

In Figure 11, the CO conversion and H_2 recovery against the three feeds are illustrated. It is evident, that changing the syngas compositions from Feed 1 to Feed 3, corresponding to an increase of the feed molar ratio from 2/1 to 4/1, the CO conversion is improved. In particular, it is enhanced from 67% to 77%, while H_2 recovery shows a decreasing trend. This is probably due to two effects: the first is the carbon deposition on the membrane surface, which, as previously said, affects negatively

the hydrogen permeation through the Pd/PSS membrane; the second is the lower hydrogen permeating driving force realized during WGS reaction using the different syngas compositions (Table 7). However, in each reaction test performed, the hydrogen purity in the permeate stream is superior at 97%.

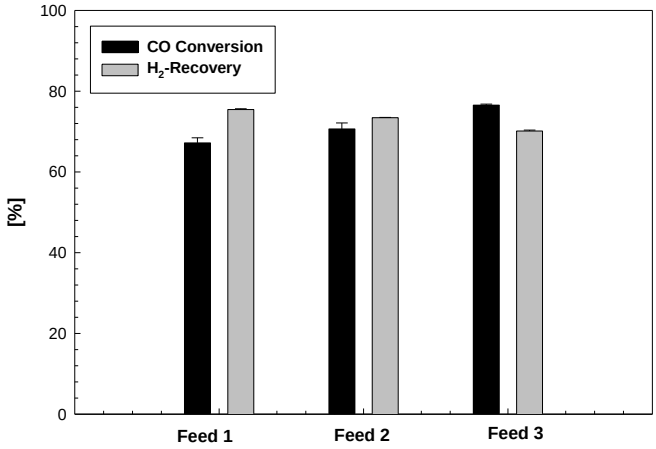

Figure 11. CO conversion and H_2 recovery against the three syngas compositions (Table 7) used for performing WGS reaction at 390 °C, GHSV = 3450 h^{-1}, reaction pressure = 11.0 bar and permeate pressure = 1.0 bar.

Alimentazione	Δp_{H2} [bar]
Feed 1 (H_2O/CO = 2/1)	5.85
Feed 2 (H_2O/CO = 3/1)	5.60
Feed 3 (H_2O/CO = 4/1)	5.36

Table 7. Hydrogen partial pressure driving force for each feed during WGS reaction.

As a conclusion, some reaction tests have been repeated for verifying if any change in the Pd/PSS MR performance in terms of CO conversion, H_2 recovery and H_2 permeate purity happened. Therefore, after ~ 700 h, the WGS reaction has been performed for a second time at 390°C, 11.0 bar, H_2O/CO = 4/1 varying the GHSV from 3450 to 14000 h^{-1}.

In Table 8, a comparison between the "original" and "repeated" reaction tests are reported. As shown, the variations in the MR performance can be considered negligible. This data indicates that membrane fouling due to coke deposition can be considered as completely reversible.

	CO conversion		H_2 recovery		H_2 permeate purity	
GHSV [h^{-1}]	"Original"	"Repeated"	"Original"	"Repeated"	"Original"	"Repeated"
3450	96.1	94.8	82.8	80.2	94.6	94.2
5750	90.2	89.7	75.5	73.6	94.7	93.5
14000	89.3	88.6	30.9	28.9	90.0	89.8

Table 8. Comparison of Pd/PSS MR performances between "original" and "repeated" reaction tests.

This finding has been also confirmed by permeation measurements with single gases made at the end of the experimental campaign: H_2 permeance and ideal selectivity of the membrane exhibit the same values obtained at the beginning of tests (see Table 3).

Conclusion

In this experimental work, a PSS supported palladium membrane, obtained by electroless plating, has been, firstly, tested with pure gases (H_2, He, N_2) at 390 °C and in the 1.8 – 10.0 bar pressure range. Long-term stability of the membrane permeative characteristics has also been tested by supplying H_2 at 390 °C over a period of 1200 h. Moreover, the permeation tests with one binary mixture and two gas mixtures simulating synthesis gas compositions were performed to evaluate the effect of gases such as CO, CO_2, He, H_2O on H_2 permeation characteristic through the Pd/PSS membrane. The experimental results have showed a detrimental effect on H_2 permeating flux, probably, caused by CO and steam presences.

After permeation tests, the membrane has been used for performing WGS reaction tests. The Pd/PSS MR was packed with a Fe-Cr catalyst and operated at 390 °C from 7.0 to 11.0 bar and from 3450 to 13984 h^{-1}, at different steam to carbon molar ratio. CO conversion showed a constant trend around 80% when a steam to carbon stoichiometric feed ratio was supplied to the MR. On the contrary, H_2 recovery varied from 35% to 60% in the reaction pressure range from 7.0 to 11.0 bar.

Afterwards, the influence of GHSV and feed molar ratio (H_2O/CO) has been studied keeping constant reaction temperature and pressure, 390 °C and 11 bar, respectively. Under these operative

conditions, the PSS supported Pd-based MR made possible to achieve almost 85% of CO conversion, 66% of hydrogen recovery with a permeate hydrogen purity around 95%.

Furthermore, the WGS reaction was carried out in the MR supplying three different compositions of syngas, characterized by a constant CO concentration and diverse steam to carbon ratio. As best result, the MR was able to achieve up to 76% of CO conversion and 75% of hydrogen recovery with a H_2 permeate purity exceeding the 97%.

As a last aspect, the membrane fouling due to coke deposition has been proven to be fully reversible: after 700 hours of tests in WGS mixture membrane H_2 permeation and ideal selectivity remained unchanged.

Acknowledgements

This work has been financed by the Research Fund for the Italian Electrical System under the Contract Agreement between RSE (formerly known as ERSE) and the Ministry of Economic Development - General Directorate for Nuclear Energy, Renewable Energy and Energy Efficiency stipulated on July 29, 2009 in compliance with the Decree of March 19, 2009.

References

[1] D. Mendes. A. Mendes, L.M. Madeira, A. Iulianelli, J.M. Sousa, A. Basile, The water-gas shift reaction: from conventional catalytic systems to Pd-based membrane reactors – a review, Asia Pac. J. Chem. Eng., 5 (2010) 111-137.
[2] A. Basile, G. Chiappetta, S. Tosti, V. Violante, Experimental and simulation of both Pd and Pd/Ag for a water gas shift membrane reactor, Sep. Purif. Technol., 25 (2001) 549-571.
[3] A. Basile, E. Drioli, F. Santella V. Violante, G. Capannelli, G. Vitulli, A study on catalytic membrane reactors for water gas shift reaction, Gas. Sep. Purif., 10 (1996) 53-61.
[4] A. Basile, A. Criscuoli, F. Santella, E. Drioli, Membrane reactor for water gas shift reaction, Gas. Sep. Purif., 10 (1996) 243-254.
[5] A. Criscuoli, A. Basile, E. Drioli, An analysis of the performance of membrane reactors for the water-gas shift reaction using gas feed mixtures, Catal. Today, 56 (2000) 53-64.
[6] O. Iyoha, R. Enick, R. Killmeyer, B. Howard, B. Morreale, M. Ciocco, Wall-catalyzed water-gas shift reaction in multi-tubular Pd and 80 wt%Pd-20 wt%Cu membrane reactors at 1173 K, J. Membrane Sci., 298 (2007) 14-23.
[7] O. Iyoha, R. Enick, R. Killmeyer, B. Howard, M. Ciocco, B. Morreale, H_2 production from simulated coal syngas containing H_2S in multi-tubular Pd and 80 wt% Pd-20 wt% Cu membrane reactors at 1173 K, J. Membrane Sci., 306 (2007) 103-115.
[8] Y. Bi, H. Xu, W. Li, A. Goldbach, Water-gas shift reaction in a Pd membrane reactor over $Pt/Ce0.6Zr0.4O_2$ catalyst, Int. J. Hydrogen En., 34 (2009) 2965-2971.
[9] A. Brunetti, G. Barbieri, E. Drioli, Upgrading of a syngas mixture for pure hydrogen production in a Pd-Ag membrane reactor, Chem. Eng. Sci., 64 (2009) 3448-3454.
[10] A. Brunetti, G. Barbieri, E. Drioli, Pd-based membrane reactor for syngas upgrading, Energy Fuels, 23 (2009) 5073-5076.
[11] Y. Huang, R. Dittmeyer, Preparation of thin palladium membranes on a porous support with rough surface, J. Membrane Sci., 302 (2007) 160-170.
[12] K.R. Patil, Y.K. Hwang, M.J. Kim, J.S. Chang, S.E. Park, Preparation of thin films comprising palladium nanoparticles by a solid–liquid interface reaction technique, J. Colloid Interface Sci., 276 (2004) 333-338.
[13] K. Zhang, H. Gao, Z. Rui, Y. Lin, Y. Li, Preparation of thin palladium composite membranes and application to hydrogen/nitrogen separation, Chinese J. Chem. Eng., 15 (2007) 643-647.
[14] N. Itoh, T. Akiha, T. Sato, Preparation of thin palladium composite membrane tube by a CVD technique and its hydrogen permselectivity, Catal. Today, 104 (2005) 231-237.
[15] E. Kikuchi, S. Uemiya, Preparation of supported thin palladium-silver alloy membranes and their characteristics for hydrogen separation, Gas Sep. Pur., 5 (1991) 261-266.
[16] C. Chen, E. Gobina, Ultra-thin palladium technologies enable future commercial deployment of PEM fuel cell systems, Membrane Tech., 2010 (2010) 6-13.
[17] J. Shu, B.P.A. Grandjean, S. Kaliaguine, Asymmetric Pd-Ag/stainless steel catalytic membranes for methane steam reforming, Catal Today, 25 (1995) 327-332.
[18] A. Brunetti, G. Barbieri, E. Drioli, T. Granato, K.-H. Lee, A porous stainless steel supported silica membrane for WGS reaction in a catalytic membrane reactor, Chem. Eng. Sci., 62 (2007) 5621- 5626.
[19] S. Giessler, K. Jordan, J.C. Diniz da Costa, G.Q.(M.) Lu, Performance of hydrophobic and hydrophilic silica membrane reactors for the water gas shift reaction, Sep. Purif. Technol., 32 (2003) 255-264.
[20] S. Battersby, M.C. Duke, S. Liu, V. Rudolph, J.C. Diniz da Costa, Metal doped silica membrane reactor: Operational effects of reaction and permeation for the water gas shift reaction, J. Membrane Sci., 316 (2008) 46-52.

[21] S. Battersby, S. Smart, B. Ladewig, S. Liu, M.C. Duke, V. Rudolph, J.C. Diniz da Costa, Hydrothermal stability of cobalt silica membranes in a water gas shift membrane reactor, Sep. Purif. Technol., 66 (2009) 299-305.
[22] Z. Tang, S.J. Kim, G.K. Reddy, J. Dong, P. Smirniotis, Modified zeolite membrane reactor for high temperature water gas shift reaction, J. Membrane Sci., 354 (2010) 114-112.
[23] J.C. Diniz da Costa, G.P. Reed, K. Thambimuthu, High Temperature Gas Separation Membranes in Coal Gasification, Energy Procedia 1 (2009) 295-302.
[24] G. Barbieri, A. Brunetti, G. Tricoli, E. Drioli, An innovative configuration of a Pd-based membrane reactor for the production of pure hydrogen. Experimental analysis of water gas shift, J. Power Sou., 182 (2008) 160-167.
[25] N.W. Ockwig, T.M. Nenoff, Membranes for hydrogen separation, Chem. Rev., 107 (2007) 4078-4110.
[26] H. Gao, Y.S. Lin, B. Zhang, Chemical stability and its improvement of palladium based metallic membranes, Ind. Eng. Chem. Res., 43 (2004) 6920-6930.
[27] L. Yang, Z. Zhang, B. Yao, X. Gao, H. Sakai, T. Takahashi, Hydrogen permeance and surface states of Pd–Ag/ceramic composite membranes, AIChE J., 52 (2006) 2783-2791.
[28]O. Iyoha, B. Howard, B. Morreale, R. Killeyer, R. Enick, The effects of H_2O, CO and CO_2 on the H_2 permeance and surface characteristics of 1mm thick $Pd_{80\ wt\%}$ Cu membranes, Top. Catal., 49 (2008) 97-107.
[29] J. Dong, Y.S. Lin, M. Kanezashi, Z. Tang, Microporous inorganic membranes for high temperature hydrogen purification, J. Appl. Phys., 104 (2008) 121301-121318.
[30] K. Yoshida, Y. Hirano, H. Fujii, T. Tsuru, M. Asaeda, Hydrothermal stability and performance of silica–zirconia membranes for hydrogen separation in hydrothermal conditions, J. Chem. Eng. Jpn., 34 (2001) 523-530.
[31] M. Kanezashi, M. Asaeda, Hydrogen permeation characteristics and stability of Ni-doped silica membranes in steam at high temperature, J. Membrane Sci., 271(2006) 86-93.
[32] V. Boffa, D.H.A. Blank, J.E. ten Elshof, Hydrothermal stability of microporous silica and niobi–silica membranes, J. Membrane Sci., 319 (2008) 256-263.
[33] M. Asaeda, Y. Sakou, J. Yang, K. Shimasaki, Stability and performance of porous silica–zirconia composite membranes for pervaporation of aqueous organic solutions, J. Membrane Sci., 209 (2002) 163-175.
[34]Y. Gu, S.T. Oyama, High molecular permeance in a pore less ceramic membrane, Adv. Mater., 19 (2007) 1636-1640.
[35] S. Uemiya, N. Sato, H. Ando, E. Kikuchi, The water gas shift reaction assisted by a palladium membrane reactor, Ind. Eng. Chem. Res., 30 (1991) 589-591.
[36] P. Pinacci, M. Broglia, C. Valli, G. Capannelli, A. Comite, Evaluation of the water gas shift reaction in a palladium membrane reactor, Catal. Today, 156 (2010) 165-172.
[37] I.P. Mardilovich, E. Engwall, Y.H. Ma Dependence of hydrogen flux on the pore size and plating surface topology of asymmetric Pd-porous stainless steel membranes, Desalination, 144 (2002) 85-89.
[38] A. Basile, P. Pinacci, A. Iulianelli, M. Broglia, F. Drago, S. Liguori, T. Longo, V. Calabrò, Ethanol steam reforming reaction in a porous stainless steel supported palladium membrane reactor, Int. J. Hydr. En., 36 (2011) 2029-2037.
[39] K.S. Rothenberger, A.V. Cugini, B.H. Howard, R.P. Killemeyer, M.V. Ciocco, B.D. Morreale, et al. High pressure hydrogen permeance of porous stainless steel coated with a thin palladium film via electroless plating. J. Memb. Sci., 244 (2004) 55-68.
[40] I.P. Mardilovich, Y. She, Y.H. Ma, M.H. Rei. Defect-free palladium membranes on porous stainless-steel support, AIChE J., 44 (1998) 310-322.
[41] R. Dittmeyer, V. Höllein, K. Daub, Membrane reactors for hydrogenation and dehydrogenation processes based on supported palladium, J. Molecular Catal. A: Chem., 173 (2001) 135–184.

[42] A. Li, W. Liang, R. Hughes, The effect of carbon monoxide and steam on the hydrogen permeability of a Pd/stainless steel membrane, J. Membrane Sci. 165 (2000) 135-141.
[43] W.P. Wang, S. Thomas, X.L. Zhang, X.L. Pan, W.S. Yang, G.X. Xiong, H_2/N_2 gaseous mixture separation in dense Pd/α-Al_2O_3 hollow fiber membranes: experimental and simulation studies, Sep. Purif. Technol. 52 (2006) 177-185.
[44] K. Hou, R. Hughes, The effect of external mass transfer, competitive adsorption and coking on hydrogen permeation through thin Pd/Ag membranes, J. Membrane Sci. 206 (2002) 119-130.
[45] H. Amandusson, L.G. Ekedahl, H. Dannetun, Hydrogen permeation through surface modified Pd and PdAg membranes, J. Membrane Sci., 193 (2001) 35-47.
[46] A.S. Augustine, Y.H. Ma, N.K. Kazantzis, High pressure palladium membrane reactor for the high temperature water-gas shift reaction, Int J Hydrogen En., 36 (2011) 5350-5360.
[47] H. Amandusson, L.G. Ekedahl, H. Dannetun, The effect of CO and O_2 on hydrogen permeation through a palladium membrane, Appl. Surf. Sci., 153 (2000) 259-267.
[48] J.M. Heras, G. Estiu, L. Viscido, The interaction of water with clean palladium films: A thermal desorption and work function study, Appl. Surf. Sci., 108 (1997) 455-464.
[49] T.A. Peters, M. Stange, H. Klette, R. Bredesen, High pressure performance of thin Pd–23%Ag/stainless steel composite membranes in water gas shift gas mixtures; influence of dilution, mass transfer and surface effects on the hydrogen flux, J. Membrane Sci., 316 (2008) 119-127.
[50] D. Shekhawat, D.A. Berry, T.H. Gardner, J.J. Spivey, in Catalysis, edited by J.J. Spivey and K.M. Dooley, 19 (2006) 184-244

Conclusion to Part IV

In this *Part IV,* an extensive overview was presented concerning the WGS reaction carried out in Pd-based MRs, paying particular attention to the effect of the membrane in shifting the reaction toward the products. Therefore, the influence of some operative conditions such as reaction temperature and pressure, feed molar ratio and sweep-gas flow rate on MR performances have been analyzed.

As a result, high sweep gas and high feed molar ratio ($H_2O/CO > 1/1$) affect positively the MR performances. Concerning the pressure, a total pressure increase could act positively on the Pd-based MR performance in terms of higher conversion, when the hydrogen permeating flux through Pd-Ag membranes follows the Sieverts-Fick's law. Nevertheless, the thermodynamic of WGS reaction is not affected by the pressure since the reaction proceeds with no variation of the total moles number. Regarding the temperature effect, this parameter involves two opposite effects on Pd-based MR: on one hand, a temperature increase induces a positive effect in terms of a higher hydrogen flux permeating through the membrane, on the other hand a temperature increase gives a detrimental effect on the CO equilibrium conversion owing to the reaction exothermicity.

So, WGS reaction was carried out in Pd-based supported MR and the influence of feed conditions and reaction pressure on the MR performance in terms of CO conversion, H_2 recovery and H_2 permeate purity is studied. As best result, at GHSV ~ 3500 h^{-1} and reaction pressure of 11 bar, the MR was able to achieve up to 76% of CO conversion and 75% of hydrogen recovery with a H_2 permeate purity exceeding the 97%.

References

Basile A, Chiappetta G, Tosti S, Violante V, "Experimental and simulation of both Pd and Pd/Ag for a water gas shift membrane reactor", *Sep Purif Technol*, 25, (2001) 549-571.

Basile A, Drioli E, Santella F, Violante V, Capannelli G, "A study on catalytic membrane reactors for water gas shift reaction", *Gas Sep Purif*, 10 (1996) 53-61.

Brunetti A, Barbieri G, Drioli E, Lee KH, Sea B, Lee DW, "WGS reaction in a membrane reactor using a porous stainless steel supported silica membrane", *Chem Eng Prog*, 46 (2007) 119-126.

Iyoha O, Enick R, Killmeyer R, Howard B, Morreale B, Ciocco M, "Wall-catalyzed water-gas shift reaction in multi-tubular Pd and 80 wt%Pd–20 wt%Cu membrane reactors at 1173 K", *J Memb Sci*, 298 (2007) 14-23.

Giessler S, Jordan L, Diniz da Costa JC, Lu GQ, "Performance of hydrophobic and hydrophilic silica membrane reactors for the water gas shift reaction ", *Sep Purif Technol*, 32 (2003) 255-264.

Battersby S, Duke MC, Liu S, Rudolph V, Diniz da Costa JC, "Metal doped silica membrane reactor: Operational effects of reaction and permeation for the water gas shift reaction", *J Memb Sci*, 316 (2008) 46-52.

Conclusion & Recommendations

In this final part of the thesis, a summary of the main innovations obtained during the PhD course is given. Moreover, recommendations for future research is also provided.

The main objective of this PhD course was to produce a pure or, at least, a high purity hydrogen stream for supplying a PEM fuel cell by reforming reactions of bio-sources and using Pd-based MRs.

This work was conducted using tubular, inorganic Pd-based supported and self-supported MRs in which reforming reactions of bio-sources such as: bio-ethanol and bio-glycerol were carried out. So, the influence of such operative conditions as reaction temperature and pressure, feed molar ratio, space velocity on MR performances was analyzed.

The studies showed that, by using Pd-based MRs, is possible to realize higher bio-sources conversion than the one obtained in the conventional reactor and, at the same time, to collect a pure or highly pure H_2 stream.

Indeed, it has been illustrated that, working with high steam to bio-sources feed molar ratio and at relatively low reaction temperature (400 - 500 °C), the self supported Pd-Ag and Pd/PSS supported MRs realizes better performances, in terms of bio-fuels conversion, hydrogen yield than fixed bed reactor.

In particular, as a best result of the work, by using a simulated bio-ethanol mixture (without impurities), the Pd-Ag self-supported MR has been able to give: 100% ethanol conversion (~85.0% for the conventional reactor), around 95.0% hydrogen recovery and ~60.0% hydrogen yield, at 400 °C, 3.0 (abs) bar of reaction pressure, SF = 25.2.

By adding such impurities to simulated bio-ethanol mixture as glycerol and acetic acid, and using Pd/PSS MR, the best results has been realized working at 12.0 bar of reaction pressure reaching 94% of bio-ethanol conversion, hydrogen recovery around 40% with a hydrogen permeate purity of 95% and a hydrogen yield of around 40%. Nevertheless, during this study, it has been observed that

the permeating flux of H_2 through the membrane was declining after each reaction test, thus resulting in decreasing in the overall efficiency of MR due to coke deposition on the membrane surface, causing, consequently, a decrease of the MR performance, particularly the hydrogen recovery. The coke formation has been, probably, due to the acidic support of catalyst but also to the impurities presence, which are the major precursors for the carbon coke formation.
The coke formation has been also the main drawback during glycerol steam reforming reaction performed in Pd-Ag MR. Indeed, it was able to negatively affect the performances of the Pd-Ag membrane in terms of a lower hydrogen permeated flux and catalyst deactivation.

Moreover, during the PhD course, simulation tests on methane steam reforming in the membrane reactor were realized and compared with the experimental results obtained by validating the mathematical model.

Therefore, this thesis has dealt with the combination of two distinct sciences such as catalysis and membrane technology. At scientific level, it is difficult to consider which of them is more prevalent in MR development. Nevertheless, it is clear that the exploitation of renewable sources represents a key factor for hydrogen production via reforming reactions by MR technology, particularly to improve the hydrogen production units. Rarely, in the open literature this concept is emphasized: while natural gas (and more in general derived fossil fuels) is preferentially used for stationary applications, it is expected that renewable feedstocks such as, for example, ethanol will play a more important role in the future non-stationary applications. Concerning the reforming reactions performed in MRs, a problem afflicting several studies present in the specialized literature consists of the impossibility to compare the performances in terms of conversion, hydrogen yield and hydrogen recovery because of the not equal operating conditions used in the experimental tests. Furthermore, there is a lack of information regarding the cost analysis for the MRs. This is because MR technology still presents some limits to be overcome before its implementation at larger scales.

Future efforts should be done for preparing defect-free inorganic membranes able to work for long periods at hard operating conditions as well as to develop membrane systems not based on palladium or with low palladium content. By solving these problems (i.e. synthesis of defect-free, stable and impurity-resistant membranes, no- and/or low-palladium content membranes development), the benefits resulting from the use of MRs at industrial scale rather than FBRs for performing reforming reactions to produce hydrogen could become more realistic. More consistent economic analyses based on the combination of renewable sources and MR technology would be necessary for stimulating improvements on this research contest.

In summary, the future perspectives on performing the reforming reactions of renewable sources via inorganic MRs are described as in the following:

• Scale-up of MRs for reforming reactions is one of the most important issues. The development of low-cost, defect-free, effective membranes could represent a chance for realistic application of MRs at industrial scale.

• Many efforts should be pursued for improving the membrane mechanical resistance during the reaction processes, both at relatively high reaction temperatures and pressures.

• More experimental analyses on the lifetime of MRs utilized to perform reforming reactions for hydrogen production should be realized to validate them as a possible alternative to the conventional systems at larger scales.

Acknowledgements

Three years are over – the thesis is written and now it’s time to say Thank to the people who contributed to this work.

I wish to express my gratitude to Dr Ing Angelo Basile and Prof. Vincenza Calabrò for giving me the opportunity to realize this work and for all their scientific-support in the last three years.

Adolfo, thanks for everything. I enjoy a lot working with you and due to you I really improved my “technical” skills ☺...!!!

During these three years I shared the room with a wonderful girl: Tiziana... Thanks a lot for the time that we spent together and... with the mouse... ☺ I miss you so much!

I do not only have roommates, I also have office “neighbours”. In particular, I would like to mention Adele. I am very happy that we shared the final moment of my PhD-journey. Thanks for all your endless help!!

During my time at the University of Oulu I met several people, without whom it would have been a boring time. Thanks very much to Prem and Jasy... Moreover, thanks to my Indian friends.

The world is not only University and Research; so, I also would like to thank all my friends from outside the University.

I would like to dedicate a deep and big thanks to my parents (Santo and Virginia), my sisters (Manuela, Zenice, Maria) and my brothers in law for their support during these last years.

Doing a PhD is like a trip with a rollercoaster, with a lot of ups and downs.
At my deepest point there were *you* who helped me up again. Thanks to Vincenzo, for all your support!

Ringraziamenti

Tre anni sono passati – la tesi è scritta, per cui è arrivata l'ora di ringraziare le persone che hanno contribuito a realizzare questo lavoro.

Inizio con il ringraziare il Dr Ing Angelo Basile e la Prof.ssa Vincenza Calabrò per avermi dato l'opportunità di realizzare questo lavoro e per il supporto scientifico offertomi.

Ado, la frase non la traduco… fa più effetto in inglese, soprattutto quel "technical" skills ☺!!! Anyhow, grazie mille.

Tì… sei una persona a me molto cara, cos'altro dire se non: grazie per tutto!!!

Ade… grazie per aver condiviso con me il viaggio finale di questo percorso! Grazie per i tuoi consigli e suggerimenti!!!

Un ringraziamento particolare va a Jasy e Prem, i miei amici indiani conosciuti in Finlandia. Vi sarò infinitamente grata per avermi fatto sentire a casa pur essendo lontana 4000 km dalla mia famiglia. Un grazie va anche ai tutti gli "indian-friends" incontrati in questi tre anni.

Ed a proposito di "casa", non possono mancare i ringraziamenti alla mia famiglia (cognati inclusi) per il loro supporto.

Ovviamente, il ringraziamento più grande va a Colui che ha retto e supportato/sopportato tutti i miei "bassi": Grazie Amore mio.